TISSUE ENGINEERING OF CO-CULTURED SKIN SUBSTITUTES USING BIOCOMPOSITE MEMBRANES BASED ON COLLAGEN AND POLYCAPROLACTONE

NIANN-TZYY DAI

Doctor of Philosophy

ASTON UNIVERSITY

August 2006

Aston University

Tissue engineering of co-cultured skin substitutes using biocomposite membranes based on collagen and polycaprolactone

Niann-Tzyy DAI Doctor of Philosophy, 2006

Summary

The preparation and characterisation of collagen:PCL, gelatin:PCL and gelatin/collagen:PCL biocomposites for manufacture of tissue-engineered skin substitutes are reported. Films of collagen:PCL, gelatin:PCL (1:4, 1:8 and 1:20 w/w) and gelatin/collagen:PCL (1:8 and 1:20 w/w) biocomposites were prepared by impregnation of lyophilised collagen and/or gelatin mats by PCL solutions followed by solvent evaporation. *In vitro* assays of total protein release of collagen:PCL and gelatin:PCL biocomposite films revealed an expected inverse relationship between the collagen release rate and the content of synthetic polymer in the biocomposite samples that may be exploited for controlled presentation and release of biopharmaceuticals such as growth factors. DSC analysis for all protein:PCL biocomposites revealed the characteristic melting point of PCL at around 60°C and a tendency for the protein component to impede crystallinity development within the PCL phase. Fibrous porous structures were shown in all biocomposite groups by SEM, and a relatively smooth surface was observed in the samples with higher PCL content indicating the more coverage of PCL phase. Good biocompatibility of all biocomposite groups was proven by interaction with 3T3 fibroblasts, normal human epidermal keratinocytes (NHEK), and primary human epidermal keratinocytes (PHEK) & dermal fibroblasts (PHDF) *in vitro* respectively. The 1:20 collagen:PCL materials exhibiting good cell growth curves and mechanical characteristics were selected for engineering of skin substitutes in this work. A 55.3% increase in cell number was measured in the designed co-culture system when 3T3 fibroblasts were seeded on both sides of a biocomposite film compared with cell culture on one surface of the biocomposite in the feasibility study. The tissue-engineered skin model based on single-donor PHEK and PHDF with differentiated confluent epidermal layer and fibrous porous dermal layer was then developed successfully *in vitro* proven by SEM and immunohistochemistry assay. The following *in vivo* animal study on athymic mice revealed early complete wound healing in 10 days and good integration of co-cultured skin substitutes with adjacent mice skin structures proven by clinical evaluation and histological studies based on H & E and Gomori's trichrome staining methods. Thus the co-cultured skin substitutes based on 1:20 collagen:PCL biocomposite membranes was proven in principle. The approach to skin modeling reported here may find application in wound treatment, gene therapy and screening of new pharmaceuticals.

Keywords: Collagen:PCL biocomposite, Gelatin/collagen:PCL biocomposite, Gelatin:PCL biocomposite, Co-culture, Keratinocyte, Fibroblast, Athymic mice.

DEDICATION

To my beloved wife, Wan-Ju Nancy Lee, for her everlasting love and support.

ACKNOWLEDGEMENTS

Writing this thesis has been a great personal achievement for me and I would like to take this opportunity to express my warmest gratitude to the following people without whom my accomplishment would not have been possible. Firstly, I would like to thank my prior internal supervisor, Professor Allan Coombes in Kingston University, whose supervision, comprehensive academic insight and continuos support have been invaluable. More over, his indefatigability in the face of my relentless contact should be commended and will never be forgotten.

My research would not have been possible without the inspiration and motivation of the unsurpassable internal supervisor of mine, Dr. Eric Adams. His expert teaching style motivated me to learn throughout the past few years and his guidance are always an unrelenting source of inspiration for me.

I would like to thank my external supervisor, Dr. Ming-Kung Yeh in Tri-Service General Hospital, for his help and guidance. His supervision has been valuable and his guidance has been most constructive during my studies with him.

Thanks to Dr. Ann Vernallis, Dr. Nancy Khammo, Dr. Matthew Williamson, Mr. Chris Bache and Mr. James Duggins in U.K. for their enthusiasm and help.

I would cordially like to give thanks to Professor Hsian-Jenn Wang and Dr. Tim-Mo Chen for their instructions on my clinical practice in Plastic Surgery and the fully supports of my research works.

Thanks to Professor Chiao-Hsi Chiang, Chung-Yang Yen, Chien-Ming Shih and Huey-Kang

Sytwu, Dr. Demeral David Liu, Dr. Jiin-Long Chen, Dr. Ke-Chi Chen, Mr. Tsung-Hsun Liu, Miss Li-Lien Chao, Miss Yi-Wen Wang, and Miss Wen-Gen Guo in National Defense Medical Center, ROC for their help and supports of my research works.

Thanks to Professor Po-Da Hong in National Taiwan University of Science and Technology, and Dr. Feng-Jiin Liu in National United University, ROC for their enthusiasm and help.

This study was supported in part by National Science Council (NSC 92-2314-B-016-069; NSC 93-2314-B-016-024; NSC 94-2314-B-016-010), Childhood Burn Foundation, National Defense Medical Center (DOD-94-1-14), Tri-Service General Hospital (TSGH-95-57) and C Y Foundation for Advancement of Education, Sciences and Medicine, ROC. Thanks for their enthusiasm and financial supports.

I would like to thank my parents for their fully supports and for making me confident whenever I encounter problems.

Lastly, I am indebted to my heroic wife, Wan-Ju Nancy Lee, for her benevolent encouragement that has given me the confidence to strive for achievement in whatever I choose to do. Her constant backing, moral support is what motivates me to have the enthusiasm to pursuit success. Let us not forget to thank my lovely children, Sasha Dai and Alex Dai, for sacrificing their play time in these years.

LIST OF CONTENTS

LIST OF TABLES

LIST OF FIGURES

ABBREVIATIONS

BPE	Bovine pituitary extract
DMEM	Dulbecco's modified eagle's medium
DMSO	Dimethylsulfoxide
DSC	Differential scanning calorimetry
ECM	Extracellular matrix
EDTA	Diamenoethanetetra-acetic acid
EGF	Epidermal growth factor
ELISA	Enzyme-linked immunosorbant assay
FCS	Fetal calf serum
FN	Fibronectin
GAG	Glycosaminoglycan
hEGF	Human recombinant epidermal growth factor
IFN	Interferon
Ig	Immunoglobulin
IL	Interleukin
KGF	Keratinocyte growth factor
MEM	Modified eagle's medium
MMP	Matrix matalloproteinase
Mn	Number average molecular weight
NHEK	Normal human epidermal keratinocytes
NP-40	Octylphenyl-polyethylene glycol
PBS	Phosphate buffered saline
PBT	Polybutylene terephthalate
PCL	Poly-ε-caprolactone
PDGF	Platelet-derived growth factor
PDLLACL	Poly(DL-lactic acid-co-ε-caprolactone)
PDLLGA	Poly(DL-lactic-co-glycolic acid)
PEG	Polyethylene glycol
PEO	Polyethylene oxide
P(EO-BTP)	Poly(ethylene oxide-co-butylene terephthalate)
PGA	Poly(glycolic acid)
PHDF	Primary human dermal fibroblasts
PHEK	Primary human epidermal keratinocytes
PLGA	Poly(lactic-co-glycolic acid)
PLLA	Poly(L-lactic acid)

PLLACL	Poly(L-lactic acid-co-ε-caprolactone)
PPF	Poly(propylene fumarate)
P(PF-co-EG)	Poly(propylene fumarate-co-ethylene glycol)
PVA	Polyvinyl alcohol
RGD	Arginine-glycine-aspartic acid
RPM	Revolution per minute
TCP	Tissue culture plastics
β-TCP	β-tricalcium phosphate
TGF	Tumor growth factor
VN	Vitronectin

CHAPTER ONE

INTRODUCTION

1.1 Overview

Patients suffering from deep and extensive burns need the affected area covered as early as possible in order to survive. The conventional treatment for wound coverage uses autologous split-thickness skin grafts. Patients with acute wounds, in general, do not have healing impairment, but may not have sufficient donor sites to cover their wounds if a large total body surface area (TBSA) is involved. In addition to burns, other wounds involving a large TBSA, such as excised burn scars and congenital cutaneous anomalies (i.e. giant nevus) also require skin grafting as well. Despite refinements in burn shock resuscitation, improvements in surgical techniques, advances in intensive care medicine and the presence of very expert surgeons in recent years, the treatment of patients with acute wounds exceeding 60% TBSA remains a major challenge. On the other hand, morbidity from grafting of autologous split-thickness skin [1] can also occur at both the treatment site and the donor site [2].

Cultured human keratinocytes have added a valuable new perspective to treat extensive burn wounds since the investigation by Rheinwald and Green in 1979 [3, 4]. Clinical trials have shown the feasibility of using sheets of multilayered autologous cultured keratinocytes (cultured epithelial autografts [CEA]) to resurface large areas of skin loss [5-8]. Although initial studies with CEA reported some success, these tissue-engineered grafts never performed as well as standard split-thickness skin. Extremely uncertain and variable graft acceptance was described. Initially slow in forming strong epidermal-dermal junctions, the cultured sheet grafts were subject to physical stress resulting in early graft loss, blistering, and scarring. These problems were most likely related to the lack of a dermal component [8-10]. Furthermore, enough keratinocytes need to be cultivated from a single autologous skin biopsy measuring 2 x 3 cm to cover the entire body of an adult in 3 to 4 weeks. As a consequence, under the therapeutic policy of burns treatment with early debridement and early grafting, a pretreatment of full-thickness wounds by initial grafting of allogenic cadaver skin, followed

by removal of the epidermis after engraftment and subsequent replacement with CEA was developed to overcome such problems [9-11]. The latter technique appears to produce better results than CEA alone, as evidenced by more stable wound closure and decreased scarring [8-10]. Unfortunately, the current temporary human skin substitutes – allografts – have a number of disadvantages, including antigenicity, limited availability, high cost and a limited shelf life. If fresh allografts are used, the risk of transmission of life threatening diseases such as HIV and hepatitis from the donor has to be considered. The lack of clear success in the use of simple methods of keratinocyte sheet application and the drawbacks of two-stage skin grafting involving CEA and cadaver skin suggest that the production of laboratory-based skin-substitutes consisting of a sheet of keratinocytes, fibroblasts or both attached to a bio-compatible carrier would be of value as an extension to the technique. This would provide a suitable environment for laying down new fibrous tissue in the wound and a close supply of epithelium.

Skin tissue engineering provides a prospective source of advanced therapies for treatment of acute and chronic skin wounds. Theoretically, engineering of skin substitutes can allow deliberate fabrication of biomaterials with properties that address specific patho-biologic conditions (e.g., burns, scar, cutaneous ulcers, congenital anomalies). By design and incorporation of specific therapeutic factors in skin substitutes, promotion of wound healing and reduction of morbidity and mortality from large wounds may be achieved.

1.2 Normal skin structure

The skin, a complex organ responsible for numerous physiologic and immunologic functions, is arguably the largest organ in the body [12]. An average human adult's skin weights 3 to 4 kg, constitutes 6% to 7% body weight, and measures about 2 square meters [13, 14]. The skin's principal duty is to serve as a barrier to harmful exogenous substances, chemicals, and

pathogens while retaining water and endogenous proteins. The skin also regulates body temperature, is a sensory organ, protects against physical injury, has psychosocial and aesthetic importance, and is an important component of the immune system. Human skin consists of three layers: [1] the epidermis composed of keratinocytes, melanocytes, Merkle cells, skin pigmentation; [2] the dermis composed of fibroblasts, collagen, elastic fibers, ground substance, blood and lymphatic vessels, nerves; and [3] the subcutaneous fat (Figure 1). In addition, the dermoepidermal junction - basement membrane, and the adnexal structures – hair follicles and sebaceous, apocrine, and eccrine glands play an important role in the normal skin functions as well.

Figure 1: Cross section of human skin. (Based on data from the illustration of skin. In: Nemours Foundation, KidsHealth®. Retrieved 00:10, August 1, 2006, from http://kidshealth.org/kid/body/images_45364/skin325.gif)

Epidermis

The epidermis is an integrated epithelium consisting of several zones, or strata from the dermis to the skin surface, including the basal, squamous, granular and cornified layers. The basal layer consists of cuboidal or columnar cells, one to three layers in thickness, comprising the main proliferative compartment of the epidermis. The epidermis replaces itself every 12 to

14 days. Within the epidermis, proliferation takes place in the basal layer of keratinocytes that are attached to the underlying basement membrane, and cells undergo terminal differentiation as they migrate through the suprabasal layers, finally being shed from the tissue surface as dead, cornified squames [15].

Three subpopulations of basal keratinocytes have been defined by cell kinetic analysis: stem cells, transit-amplifying cells, and committed cells [16]. Stem cells retain a high capacity for self-renewal throughout adult life and are ultimately responsible for epidermal maintenance and repair. The daughters of stem cells can either be stem cells themselves or cells known as transit-amplifying cells, which divide a small number of times, but have a high probability of producing daughters that withdraw irreversibly from the cell cycle and are committed to differentiate terminally. Committed cells detach from the basement membrane and move upward from the basal layer via a mechanism that involves inactivation of β_1 integrin extracellular matrix receptors on the cell surface [17]. In cultures of human epidermal keratinocytes, cells with characteristics of stem and transit-amplifying cells can be identified and isolated on the basis of their adhesive properties [18]. Stem cells express high levels of three of the β_1 family of integrins ($\alpha_2\beta_1$, receptor for collagen and laminin; $\alpha_3\beta_1$, receptor for laminin and epiligrin/ kalinin; and $\alpha_5\beta_1$, fibronectin receptor) and adhere rapidly to type IV collagen, fibronectin, and extracellular matrix deposited by cultured keratinocytes.

Suprabasal keratinocytes within the spinous layer are polygonal in appearance with numerous delicate "spiny" projections – desmosomes for intercellular attachments, spanning the intercellular spaces to adjacent keratinocytes. Langerhans cells, dendritics, immunomodulating cells, are scattered throughout the spinous layer and function in delayed hypersensitivity reactions, allograft rejection and graft-versus-host disease.

The granular layer composed of keratinocytes replete with keratohyalin granules comprises two to three cell layers between the spinous and cornified layers. Lamellar bodies found in granular layer keratinocytes participate in the cornification process by discharging their lipid components into intercellular spaces, enhancing the skin's barrier function as well as aiding intercellular cohesion within the stratum corneum. Protein envelopes also develop within the stratum corneum influenced by filaggrin, a protein component of the keratohyalin granules, which causes keratin filament aggregation [19]. Furthermore, the formation of cornified envelop was catalysed by a Ca^{2+}-dependent enzyme - transglutaminase.

The major barrier function of skin is provided by the thin stratum corneum. Cornification results from a sequence of events including the synthesis and assembly of a series of keratins; the addition of filaggrin; and, ultimately the synthesis and assembly of the cornified envelope [15]. Similarly, the protection function of skin is dependent on the integrity of the epidermis and its attachment to the dermis, which is maintained by elaborate intercellular adhesion structures (desmosomes) and by strong and ordered intracellular intermediate filaments, predominately keratin, as well as other intracellular structural proteins, actin-containing microfilaments, and tubulin-containing microtubules [20].

Formation of keratin fibres is one of the major functions of epidermal keratinocytes. The keratins are a family of approximately 20 intermediate-filament proteins that have a molecular mass ranging from 40 to 70 [21]. Keratin 5 and 14 are synthesised in the undifferentiated basal layer, while keratins 1 and 10 are synthesised in the more differentiated spinous and granular layers [22, 23]. Each keratin pair assembles to form intermediate filaments that with tubulin and actin form the cytoskeleton of keratinocytes [24]. The major function of keratin appears to be to maintain the three-dimensional architecture of the epidermis by providing an intracellular skeleton for the keratinocyte.

Skin colour is determined by the amount of melanin present in the skin and the way in which it is distributed. Melanin is produced in pigment granules known as melanosomes, which are synthesised in melanocytes and passed to epidermal cells in the lower layers of the epidermis.

Dermoepidermal junction

The dermoepidermal junction (DEJ) is a large, specialised attachment site that forms an extensive interface between the epidermis and papillary dermis and is continuous with the analogous junction between epithelial appendages and their periadnexal dermis. The major function of the DEJ is to keep the epidermis firmly attached to the dermis, while other functions include support, regulation of permeability across the dermoepidermal interface, and a role in embryonic differentiation. The attachment function of the DEJ is accomplished through a series of interacting filamentous molecules that exist in hemidesmosomes, anchoring filaments, lamina densa, anchoring fibrils and other fibrous dermal elements causing strong adhesion of basal keratinocytes to dermal interstitial collagen. Anchoring filaments, consisting of laminin 5 (kalinin, nicein) connect hemidesmosomes to the lamina densa, which is composed of type IV collagen, nidogen/ entactin, laminins 1, 6 and 7, and heparan sulfate proteoglycan (perlecan). Type IV collagen has a unique structure, which aggregates into a lattice-like network that is believed to act as a scaffold providing structure and tensile strength to the basement membrane. Anchoring fibrils, which are located in papillary dermis and are made up predominantly of type VII collagen, form a bridge between the lamina densa and anchoring plaques located in the papillary dermis. Type VII collagen binds to fibronectin, a major dermal glycoprotein. Basal layer keratinocytes and dermal fibroblasts each contribute dermoepidermal junction components, including types IV and VII collagen and laminin. Laminin 5 appears to primarily be a product of the epithelium and may serve as a nidus for basement membrane formation [24].

Dermis

The dermis consists primarily of connective tissues – collagen, elastic tissue and ground substance (they provide protection against trauma and envelop the body in a strong and flexible wrap), and blood vessels, lymphatics, nerves and epithelial adnexa – hair follicles and sebaceous, apocrine, and eccrine glands.

Collagen is the major structural component of the dermis, which is seen as fibres measuring from 2 to 15 μm under conventional microscopy. In the adventitial and papillary dermis, collagen forms a finely woven meshwork of fibers, while in the reticular dermis collagen fibres form thick bundles. So far there have been about 27 types of collagen identified. Among them, there are at least 9 types of connective tissue collagen detected in human skin. The two major types of collagen are types I and III. Type I collagen, which accounts for 80% of total collagen in human skin, is present throughout the entire dermis, imparting to it tensile strength. Type III collagen constitutes approximately 15% of dermal collagen and is localised mainly in the adventitial dermis, including beneath the epidermal basement membrane where it plays an important role in anchoring the epidermis to the dermis. Type IV collagen is a major component of the basement membrane of vessels, nerves, adnexa, and DEJ. Type V collagen is localised to surfaces of dermal cells at the interface between the cells and their immediate environment of collagen fibres. Type VI collagen is concentrated around nerves, blood vessels, and adipocytes and may serve to anchor these structures into the surrounding connective tissue. Type VII collagen is the major component of the anchoring fibrils and is found beneath the basal lamina of the DEJ. It helps anchor the DEJ to the adjacent dermis [24].

Elastic fibres constitute approximately 3% of the dermis by dry weight, measure 1 to 3 μm in diameter, and play a major role in skin elasticity and resilience. Three types of fibers can be identified: oxytalan, elaunin, and elastic fibres. Elaunin fibres form a plexus in the papillary dermis, oriented parallel to the DEJ. Oxytalan fibres, oriented perpendicular to the DEJ, connect elaunin to the DEJ. Elastic fibres, arranged parallel to the epidermis, are thickest and are confined to the lower portion of the dermis.

Ground substance, an amorphous material that fills spaces between the fibrillar components of the dermis imparting turgidity and resilience, is composed of water, electrolytes, plasma proteins, and mucopolysaccharides. Mucopolysaccharides are constructed of long chains of aminated sugars to form glycosaminoglycans, and can be linked covalently to polypeptides to form proteoglycans as well. In the dermis, the most common glycosaminoglycans are hyaluronic acid and dermatan sulfate. Small amounts of chondroitin-6-sulfate, heparan sulfate, and heparin are also found [24]. They play an important role in the maintenance of the homeostatic balance of salt and water and, because of their high viscosity, serve as humectins, lubricants, anticoagulants and adhesion molecules and as support for the other components of the dermis. Sequestering cytokines and acting as signal-transducing molecules are further functions of proteoglycans. Fibronectin, another important component of ground substance, are high molecular weight glycoproteins present on the surfaces of cells, in extracellular fluid, and in connective tissue matrices. In skin, fibronectin is found within the lamina lucida of the basement membrane and at the DEJ, as well as bound to type III collagen fibres. The most important function of fibronectin is to facilitate the attachment of fibroblasts, macrophages, and keratinocytes to cell membranes, basement membranes, glycosaminoglycans, collagen, and fibrin or fibrinogen. The interactions between cells and extracellular substrate mediated by fibronectin are stabilised by glycosaminoglycans such as heparan sulfate [24].

Vasculature, nerves and subcutaneous fat

The blood supply of the dermis originates from a plexus located in the reticular dermis that connects via communicating vessels to three more superficial plexuses. The three superficial plexuses are the subpapillary plexus, and plexuses around hair follicles and around eccrine glands. Lymphatics in the skin form a complex network following the distribution of arterioles and venules.

The skin is richly innervated. Cutaneous nerves, which contain both sensory and motor fibers forming plexuses in the subcutaneous tissue and in the dermis, supply overlapping, contiguous regions of the skin.

Subcutaneous fat serves as a shock absorber protecting vital structures, maintaining body heat, and storing energy. The basic unit of the subcutaneous fat is the microlobule, which is composed of collection of adipocytes. Aggregations of primary microlobules form secondary lobules that are separated by connective tissue septa containing nerves, vessels, and lymphatics. The blood supply to and from the subcutaneous tissue is carried by arteries and veins located in the fibrous septa [24].

Adnexal structures

Longitudinal sections of hair follicles reveals three zones: the infundibulum, extending from the ostium (opening) of the follicle to the opening of the sebaceous duct; the isthmus, extending from the opening of the sebaceous duct to the insertion of the arrector pili muscle; and the inferior segment, which extends from the site of insertion of the pili muscle to the base of the hair follicle.

Sebaceous glands, which develop from a column of undifferentiated cells (mantle) that later differentiates into one or several lobules, are present in all cutaneous areas except palms, soles, and the dorsal feet. A sebaceous lobule consists of a peripheral rim of undifferentiated germinative cells surrounding maturing sebaceous cells that gradually accumulate cytoplasmic lipid, filling and surrounding the centrally placed nucleus [24].

Apocrine glands consist of a coiled secretory gland, present in the lower dermis or subcutaneous fat, leading to a straight excretory duct. A viscous, milky, odorless substance is produced and stored by apocrine glands, and then is released intermittently with intervening longer refractory periods. Apocrine glands do not participate in heat regulation and therefore are not sweat glands, although they may function in humans as scent glands, their primary function in other mammals [24].

Eccrine glands, which are the only true sweat gland in humans, are tubular glands that develop from buds of embryonic epidermis independent of the primary epithelial germ, and then descend to the dermo-subcutaneous junction. The major function of eccrine glands is to produce the hypotonic solution known as sweat, which facilitates evaporative cooling [24].

1.3 Inflammation and wound healing

Wound healing process

The wound healing process in the skin has been the subject of much study, primarily in animal model situations. Perhaps the most recent extensive review of the wound healing process is that of Clark and Henson [25], which reviews all aspects of wound healing. The subject is complicated but it can be considered that wound healing occurs in four stages. The first stage is regarded as a damage limitation stage, conventionally in which hemorrhage into the wound

occurs with clotting [26]. This acts not only to prevent further blood loss but also to generate a temporary wound infill and to import the first wave of responding cells into the wound area which act to promote the next, the inflammatory stage of wound repair. This second stage is characterised by increased blood flow to the wounded area and ingress into the wound of leukocytes of various classes which act to remove irreparably damaged tissue, reclaim salvageable tissue and protect against wound colonisation by micro-organisms. When the wound environment is sufficiently 'prepared' by the inflammatory cells the process moves to the third, proliferative stage. In this stage there is an ingrowth of blood vessels into the area delimited by the original haematogenous infill accompanied by fibroblasts which serve to lay down a fibrous infill, granulation tissue, to the wound. At the same time there is a stimulation of growth activity of epithelial cells at the edges of the wound area and in deep epidermal appendages, which process functions to supply epithelial cell cover thereby bridging the wound to provide closure. When closure of the wound is achieved the wound may be regarded conventionally as healed, but this point really only marks the commencement of the longest and least understood stage, which may continue for months after closure has been achieved, the fibrous tissue infill laid down in the wound area is modified, presumably by the action of fibroblasts to give the final outcome of the process of wound healing, the scar. This scar may be indistinguishable macroscopically from the surrounding skin (an atrophic scar), elevated above the level of the surrounding skin within the bounds of the original wound (a hypertrophic scar) or elevated above and overgrowing the original lesion (a keloid scar). The hypertrophic scar is, regrettably, a very familiar sight to all involved in treating burn-injured patients [27].

The influence of depth upon healing can be thought about in terms of profound influences upon supply and demand for particular cell populations and activities, and for the necessity to regulate the activities of these cells. In superficial and partial thickness wounds there is an ample supply of new epithelium throughout the wounded area from the undamaged hair

follicles, sweat and sebaceous glands. Healing in these wounds does not involve replacement of damaged structural matrix and proceeds spontaneously to a good outcome. In deep partial thickness and full thickness wounds the supply of new epithelium may be effectively restricted to the edges of the wound since the deep structures which furnish epithelial cells in superficial wounds are, by definition, destroyed. Damaged structured matrix may require clearance and replacement. Under these circumstances wound closure may only occur from the edge of the wound and the time taken may be so long as to be effectively immeasurable and surgical intervention will be necessary to ensure that the wound is healed by grafting with split thickness skin grafts [27].

Wound healing to tissue engineering

Resolution or repair of injury and altered homeostatic mechanisms occurs *via* the distinct processes of [A] regeneration of tissue-specific parenchymal cells and restitution of the normal tissue structure or [B] reorganisation and replacement of the injured tissue with newly synthesised fibrovascular connective tissue. These processes are generally controlled by either the proliferative capacity of the cells in the tissue or organ receiving the implant, or the extent of injury and persistence of the tissue framework of the implant site. Cells in the body can be classified into three groups based on their regenerative capacity: labile cells that continue to proliferate throughout life, stable cells that retain this capacity but do not normally replicate, and permanent cells that cannot reproduce themselves after birth. The ideal repair situation is the restitution of normal tissue structure. Restitution of the tissue following injury is possible only in tissue consisting of stable cells (e.g. parenchymal cells of the liver, kidney and pancreas), labile cells (e.g. epithelial cells, and lymphoid and hematopoetic cells), mesenchymal cells (e.g. fibroblasts, smooth muscle cells, osteoblasts and chondroblasts) and vascular endothelial cells. Partial or complete fibrosis is also a possible pathway of inflammation resolution with these regenerative cell types if the injury is severe enough to

disrupt the framework for normal tissue structure restitution. Wound healing in tissues comprised of permanent cells (e.g. nerve cells, skeletal and cardiac muscle cells) results in fibrosis with very little restitution of the normal tissue or organ structure. The goal or purpose of tissue-engineered devices is typically the restitution of tissue structure and function. However, some degree of reorganisation of the tissue because of the wound healing response to device implantation, the presence of a biomaterial and/ or cells causing an inflammatory or immune response, often results in fibrovascular tissue generation or fibrous encapsulation. The functional success of the device may be impacted to varying degrees by the host response [28].

1.4 Biomaterials applied for tissue engineering

Tissue engineering studies are beginning to lead to development of devices that promise to be effective in restoring or replacing diseased organ or tissue function. The two main components of a tissue engineered device are the transplanted cells and the biomaterial, creating a device with living, three-dimensional cellular constructs that can be used not only as clinical replacements of damaged tissues and organs but also as research tools to study cell and matrix interactions that occur in higher-order systems [28, 29].

As a definition, a tissue engineered implant is a biologic-biomaterial combination in which some component of tissue has been combined with a biomaterial to create a device for the restoration or modification of tissue or organ function [30]. Concomitant with this definition is the objective of inducing a desirable host response depending on the application. The devices important in tissue engineering include:

A. Polymer matrices to control and guide wound healing and tissue regeneration, to elicit specific cellular interactions, functions and tissue responses and to serve as scaffolds to support cell transplantation;

B. Controlled growth factor/ cytokine release from devices or transplanted cells to control tissue regeneration;

C. Immobilised bioactive ligands on materials (biomimetic materials) for receptor-mediated control of single and multiple cell morphology and function; and

D. Biomaterial barriers to block the molecular signals that stimulate scar formation and immune rejection [28].

Porous polymer scaffolds are widely used in tissue engineering for cellular incorporation by the following mechanisms:

A. Polymer scaffolds are seeded with cells *in vitro* and implanted.

B. Polymer scaffolds are implanted and infiltrated by host tissue.

C. Tissue induction occurs *via* the release of incorporated chemotactic agents that attract the desired cells into the porous scaffold [28].

Cells attached to the polymer scaffold proliferate and secrete matrix and growth factors, while the polymer scaffold provides structural and mechanical form. Fibrovascular inflammatory tissue infiltrates the scaffold pores and cells reorganise into functional tissue as the polymer scaffold degrades. The polymer scaffold helps to determine the three-dimensional morphology, increases cell survival, provides initial mechanical stability, supports tissue ingrowths, aids in the formation of tissue structure and should be ultimately replaced by a regenerated extracellular matrix to form normal, completely natural tissue. Biodegradable polymers for these scaffolds can be designed to resorb over controllable periods of time and to degrade into metabolites of limited toxicity. They are not permanent and hence the long-term complications of a foreign body may be avoided, although several aspects concerning the biodegradation of the scaffolds are important issues. Cell adhesive ligands derived from cell binding regions of extracellular matrix proteins, can be incorporated into synthetic, resorbable scaffolds to mediate selective control of cell adhesion and behavior [31-33].

Scaffolds of natural polymers and synthetic polymers have been used to facilitate tissue regeneration (Table 1). Synthetic polymer scaffolds for cell seeding and tissue regeneration have focused on the poly(α-hydroxy acid) family of polymers. Other synthetic polymers that have been used are also listed in Table 1.

Table 1: Scaffolds of natural and synthetic polymers used to facilitate tissue regeneration.

Polymers	**Tissue regeneration**	**References**
Collagen	Cartilage and wound healing	[34-37]
Collagen-GAG	Nerve, skin and tendon	[38-40]
Collagen-laminin-fibronectin	Nerve	[41]
Hyaluronic acid	Nerve	[42]
Fibrin	Wound healing	[43]
PLLA	Bone and cartilage	[44-46]
PGA	Cartilage, tendon, urothelium, intestine, liver, bone, transplanting islets and genetically modified cells	[46-55]
PDLLGA	Bone, cartilage and urothelium	[56-60]
PVA-PLLA	Hepatocyte transplantation	[61]
Collagen-PLLA	Hepatocyte transplantation	[62]

PLGA-PEG	Soft tissue and tubular tissue	[63]
PLLACL	Meniscal tissue	[64]
PDLLACL	Nerve guides	[65]
Polyphosphazenes	Skeletal tissue and nerve	[66, 67]
PPF/ β-TCP	Bone applications	[68]
P(PF-co-EG)	Cardiovascular applications	[69]
Bi-layered matrix [PLLA/ P(EO-BTP) + P(EO-BTP)]	Skin substitute	[70, 71]
Gelatin-resorcinol-formaldehyde glue	Wound healing in experimental rabbit lungs	[72]

GAG: glycosaminoglycan; PLLA: poly(L-lactic acid); PGA: poly(glycolic acid); PDLLGA: poly(DL-lactic-co-glycolic acid); PVA: polyvinyl alcohol; PLGA: poly(lactic-co-glycolic acid); PEG: polyethylene glycol; PLLACL: poly(L-lactic acid-co-ε-caprolactone); PDLLACL: poly(DL-lactic acid-co-ε-caprolactone); PPF: poly(propylene fumarate); β-TCP: β-tricalcium phosphate; P(PF-co-EG): poly(propylene fumarate-co-ethylene glycol); P(EO-BTP): poly(ethylene oxide-co-butylene terephthalate).

Collagen

Collagen is the main protein found in the skin, ligament, tendon, bone, cartilage, teeth, and other connective tissues in animals and the most abundant protein in mammals, making up about 40% of the total. So far there have been about 27 types of collagen identified. As one of the long, fibrous structural proteins, the functions of collagen are quite different from those of globular proteins such as enzymes. Along with soft keratin, collagen is responsible for skin strength and elasticity, and its degradation leads to wrinkles that accompany aging. It

strengthens blood vessels and plays a role in tissue development. Furthermore, the crystalline form of collagen is present in the cornea and lens of the eye.

A distinctive feature of collagen is the regular arrangement of amino acids in each of the three left-handed polyproline II-like chains wrapped around each other to form a triple helical conformation. The sequence often follows the pattern Gly-X-Pro or Gly-X-Hypro, where X may be any of various other amino acid residues. This packing requires glycine (Gly) as the every third residue. Proline (Pro) and hydroxyproline (Hypro) often appear in the X and Y position respectively. The substitution of the Gly residues by any other amino acids often lead to diseases such as osteogenesis imperfecta, Ehlers-Danlos syndorme, and Alport syndrome as well as others[73-76]. Prolines and lysines at specific locations relative to glycine are modified post-translationally by different enzymes, both of which require vitamin C as a cofactor. Vitamin C deficiency causes scurvy, a serious and painful disease in which defective collagen prevents the formation of strong connective tissue[77].

Gly-Pro-Hypro occurs frequently. This kind of regular repetition and high glycine content is found in only a few other fibrous proteins, such as silk fibroin. 75-80% of silk is (approximately) -Gly-Ala-Gly-Ala- with 10% serine and elastin is rich in glycine, proline, and alanine (Ala), whose side group is a small, inert methyl. Such high glycine and regular repetitions are never found in globular proteins. Chemically-reactive side groups are not needed in structural proteins as they are in enzymes and transport proteins. The high content of Pro and Hypro rings, with their geometrically constrained carboxyl and (secondary) amino groups, accounts for the tendency of the individual polypeptide strands to form left-handed helices spontaneously, without any intrachain hydrogen bonding. The triple helix tightens under tension, resisting stretching, making collagen inextensible.

Because glycine is the smallest amino acid, it plays a unique role in fibrous structural proteins. In collagen, Gly is required at every third position because the assembly of the triple helix puts this residue at the interior (axis) of the helix, where there is no space for a larger side group than glycine's single hydrogen atom. For the same reason, the rings of the Pro and Hypro must point outward. These two amino acids thermally stabilize the triple helix - Hypro even more so than Pro - and less of them are required in animals such as fish, whose body temperatures are low.

The three peptide chains are first produced in the endoplasmic reticulum (ER), then the C-propeptides come together and the three chains start twist together (a process called propagation), with N-propeptides at the end of the chain. This molecule is the procollagen. Cleavage then occurs, where the propeptides are cut off. The resulting collagen will assemble with other collagens, forming fibrils[73-76].

The tropocollagen subunit is a rod about 300 nm long and 1.5 nm in diameter, made up of three polypeptide strands, each of which is a left-handed helix. They are twisted together into a right-handed coiled coil, a triple helix, a cooperative quaternary structure stabilized by numerous hydrogen bonds. Tropocollagen subunits spontaneously self-assemble, with regularly staggered ends, into even larger arrays in the extracellular spaces of tissues. There is some covalent crosslinking within the triple helices, and a variable amount of covalent crosslinking between tropocollagen helices, to form the different types of collagen found in different mature tissues — similar to the situation found with the α-keratins in hair. Collagen's insolubility was a barrier to study until it was found that tropocollagen from young animals can be extracted because it is not yet fully crosslinked.

In bone, entire collagen triple helices lie in a parallel, staggered array. 40 nm gaps between the ends of the tropocollagen subunits probably serve as nucleation sites for the deposition of long, hard, fine crystals of the mineral component, which is (approximately) hydroxyapatite, $Ca_5(PO_4)_3(OH)$, with some phosphate. It is in this way that certain kinds of cartilage turn into bone through the calcification process. Collagen gives bone its elasticity and contributes to fracture resistance[77].

Collagen has been widely used is cosmetic surgery and certain skin substitutes for burns patients. The cosmetic use of collagens is declining because of a fairly high rate of allergic reactions causing prolonged redness; the risk of transmitting prion diseases like BSE for the bovine-origin collagen; and the development of alternatives using the patient's own fat or hyaluronic acid. On the other hand, collagens are still employed in the construction of artificial skin substitutes used in the management of severe burns. These collagens may be bovine or porcine and are used in combination with silicones, glycosaminoglycans, fibroblasts, growth factors and other substances[77].

Gelatin

Gelatin is a protein product produced by partial hydrolysis of collagen extracted from skin, bones, cartilage, ligaments, etc. The natural molecular bonds between individual collagen strands are broken down into a form that rearranges more easily. Gelatin melts when heated and solidifies when cooled again. Together with water it forms a semi-solid colloidal gel. The raw materials are prepared by different curing, acid, and alkali processes which are employed to extract the dried collagen hydrolysate and which may take several weeks.

Gelatin typically constitutes the shells of pharmaceutical capsules in order to make their contents easier to swallow. Hypromellose is the vegetarian counterpart to gelatin, but is more expensive to produce. Animal glues such as hide glue are essentially unrefined gelatin. Cosmetics may contain a non-gelling variant of gelatin under the name "hydrolyzed collagen".

Although gelatin is 98–99% protein by dry weight, it has less nutritional value than many other protein sources. Gelatin is unusually high in the non-essential amino acids glycine and proline, (i.e., those produced by the human body), while lacking certain essential amino acids (i.e., those not produced by the human body). It contains no tryptophan and is deficient in isoleucine, threonine, and methionine[78].

The approximate amino acid composition of gelatin is: glycine 21 %, proline 12 %, hydroxyproline 12 %, glutamic acid 10 %, alanine 9 %, arginine 8%, aspartic acid 6 %, lysine 4 %, serine 4 %, leucine 3 %, valine 2 %, phenylalanine 2 %, threonine 2 %, isoleucine 1 %,hydroxylysine 1 %, methionine and histidine <1% and tyrosine < 0.5 %. These values vary, especially the minor constituents, depending on the source of the raw material and processing technique[79].

Due to Bovine spongiform encephalopathy (BSE), also known as "mad cow disease", and its link to the Creutzfeldt-Jakob disease (CJD), there has been much concern about using gelatin derived from possibly infected animal parts. One study released in 2004, however, demonstrated that the gelatin production process destroys most of the BSE prions that may be present in the raw material [80]. However, more detailed recent studies regarding the safety of gelatin in respect to mad cow disease have prompted the U.S. Food and Drug Administration to re-issue a warning and stricter guidelines for The Sourcing and Processing of Gelatin to Reduce the Potential Risk Posed by Bovine Spongiform Encephalopathy from 1997.

Poly(ε-caprolactone)

Polycaprolactone (PCL) is the biodegradable polyester with a low melting point of around 60°C and a glass transition temperature of about −60°C. PCL can be prepared by ring opening polymerization of ε-caprolactone using a catalyst such as stannous octanoate (Figure 2).

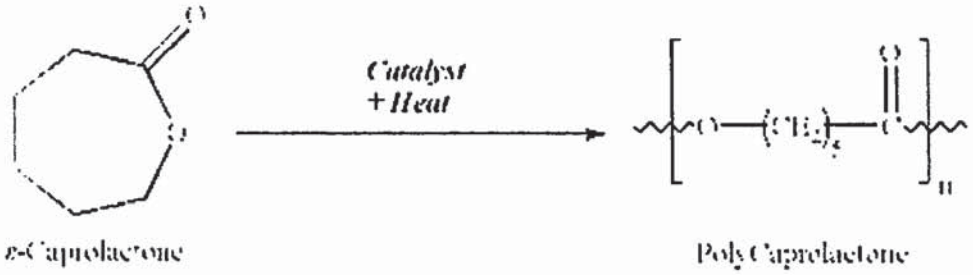

Figure 2: Ring opening polymerization of ε-caprolactone to polycaprolactone

This polymer is often used as an additive for resins to improve their processing characteristics and their end use properties (e.g.: impact resistance). Being compatible with a range of other materials, PCL can be mixed with starch to lower its cost and increase biodegradability or it can be added as a polymeric plasticizer to PVC.

Poly-ε-caprolactone (PCL) is a biodegradable, biocompatible and semicrystalline polymer having a very low glass transition temperature. The *in vitro* degradation process of PCL has been studied and it revealed a bulk process that can be divided into two phases: (1) molecular weight (Mn) loss up to 5000 due to chain scission (2) onset of weight loss. The kinetic patterns of PCL degradation are consistent with an autocatalytic process, whereby the liberated carboxylic acid end groups catalyse the hydrolysis. No weight loss is observed during the initial phase of the biodegradation process, which covers an Mn range of 200,000

to 5000. The second phase of polymer degradation is characterised by a decrease in the rate of chain scission and the onset of weight loss. Weight loss has been attributed to an increased probability that chain scission of a low molecular weight polymer will produce a fragment small enough to diffuse out of the polymer bulk and the break up of the polymer mass will produce smaller particles with an increased probability of phagocytosis. The decrease in the rate of chain scission is associated with an increase in crytallinity, since cleavage takes place in the amorphous region of the polymer. Due to its slow degradation, PCL is ideally suitable for long-term delivery extending over a period of more than one year. This has led to its application in the preparation of different delivery systems in the form of microspheres, nanospheres and implants. On the other hand, the *in vivo* degradation process was also investigated by implanting low molecular weight PCL in rats, and it was observed that absorption was complete in 60 days. The ε-hydroxycaproic acid, derived from complete hydrolysis of the polymer, and tritiated water were the only metabolites detected. Electron microscopic examination revealed the presence of intracellular polymer particles and demonstrated the role of phagocytosis in the final stage of polymer degradation[81].

PCL is degraded by hydrolysis of its ester linkages in physiological conditions (such as in the human body) and has therefore received a great deal of attention for use as an implantable biomaterial. In particular it is especially interesting for the preparation of long term implantable devices, owing to its degradation which is even slower than that of polylactide. PCL is an FDA approved material that is used in the human body as (for example) a drug delivery device, suture, adhesion barrier and is being investigated as a scaffold for tissue repair via tissue engineering. A variety of drugs have been encapsulated within PCL beads for controlled release and targeted drug delivery which have been peer reviewed[82].

1.5 Principles of tissue engineering of human skin

The ultimate objective for skin substitutes is restoration of the anatomy and physiology of uninjured skin after treatment and healing of the wound [83]. Hypothetically, color, texture, pliability, tensile strength, barrier, matrix or cytokine expression may be altered by modification of the composition of engineered skin [84, 85].

Cells, biopolymer and soluble mediators constitute the anatomy and physiology of human skin. Definitive to wound closure is restoration of the epidermal barrier to provide protection from fluid loss and infection. This barrier is synthesised by the parenchymal cells of the epidermis, the keratinocytes [86]. Sheets of cultured keratinocytes were studied by many investigators for treatment of excised, full-thickness burns [6, 87-90], and a consensus was reached that replacement of connective tissue - dermis layer, was also required [11, 91]. Fibrovascular tissue restores the mechanical strength and blood supply to attach and nourish the epidermis. Therefore, repopulation of fibroblasts, endothelial cells and smooth muscle is required to form stable skin. Connective tissue cells may repopulate grafts from the wound bed but engineered skin can also include cultured fibroblasts to facilitate repair [92-95]. Pigment cells, the melanocytes, have also been cultured and transplanted for treatment of vitiligo [96] and burn scar [97] and added into cell-polymer constructs [98, 99]. Nerve cells may extend dendrites into healing grafts of engineered skin, but full restoration of skin sensation has not been demonstrated either with split-thickness skin graft or engineered skin [100, 101]. Glands (sweat, sebaceous) and hair follicles have been transplanted experimentally as well [102, 103], but neither engineered skin nor skin autografts restore these structures at present. Consequently, thermal regulation after healing of wounds treated with engineered skin is also deficient. However, these deficiencies do not reduce the importance of engineered skin for definitive closure of wounds and therapeutic benefits to patients [83].

1.6 Biocompatibility of skin substitutes

The two main components of a tissue-engineered device are the polymer membrane or scaffold and the transplanted cells which may be of autologous, isogeneic, allogeneic, or xenogeneic origin. Evaluation of the biocompatibility of a tissue-engineered implant includes the determination of the host response to the biomaterial component, the tissue component, and the combination of biomaterial and tissue components (the device) [30]. The host response to the biomaterial can impact the immune response towards transplanted cells and *vice versa*. The implantation of a biomaterial (without transplanted cells) initiates a sequence of events akin to a foreign body reaction starting with an acute inflammatory response and leading in some cases to a chronic inflammatory response and/ or granulation tissue development, a foreign body reaction and fibrous capsule development [104]. The duration and intensity of each of these is dependent upon the extent of injury created in the implantation, biomaterial chemical composition, surface free energy, surface charge, porosity, roughness, and implant size and shape [105]. For biodegradable materials, such as those used in many polymer scaffold constructs for cell transplantation, the intensity of these responses may be modulated by the biodegradation process which may lead to shape, porosity and surface roughness changes, release of polymeric oligomer and monomer degradation products [106], and formation of particulates [106-108]. It is the extent and duration of the deviation from the optimal wound healing condition that determines the biocompatibility of the material [30].

Biocompatibility is the key to successful development of tissue-engineered skin. Materials must be able to support and maintain the activity of the proliferating cells involved in the repair of wounds. Thus they must allow angiogenesis to support viability and activity of cells involved in repair and also anchorage and migration of keratinocytes to achieve wound

closure [109]. All these processes are essential to the healing of burn wounds [109, 110].

1.7 Clinical considerations

Currently available skin substitutes are avascular, slower to heal than skin autografts and may be mechanically fragile. Among the factors that influence the outcome with engineered skin are wound bed preparation, control of microbial contamination, dressings and nursing care and survival of transplanted cells during vascularisation of grafts [83]. Clinical complications with engineered skin result predominantly from anatomic and physiological deficiencies that compromise responses to the wound healing process. Split-thickness skin graft contains a vascular plexus and adheres to debrided wounds by coagulum, followed by inoculation of vessels in the graft to vessels in the wound within 2-5 days. Although healing is not complete within one week, native skin is engrafted and reperfused. In comparison, engineered skin substitutes with dermal and epidermal components are avascular, and reperfusion results from *de novo* angiogenesis. If the rate of vascularisation is considered constant, then the time required for reperfusion is directly proportional to the thickness of the dermal component of the skin substitute, and is longer than reperfusion of split-thickness skin. The additional time required for vascularisation may cause epithelial loss from microbial destruction and/or nutrient deprivation [83]. In the former case, topical antimicrobial agents have been shown to be more effective for control of wound contamination than parenteral antimicrobials [111]. Requirements for any topical antimicrobial include effective coverage of a broad spectrum of gram-negative and gram-positive bacteria as well as common fungal organisms. In burns, these groups are represented most frequently by Pseudomonas aeruginosa, Staphylococcus aureus, and Candida albicans.

Mechanical fragility of cultured skin grafts is an important source of failure from shear and maceration. For friable grafts, mechanical reinforcement may be added with a backing

material that allows convenient handling and stapling to the wound. Cultured epithelial autografts are routinely attached to petrolatum-impregnated gauze for surgical application [8], but this material is not compatible with wet dressings.

The high costs of culture of skin substitutes remain a practical factor for clinical use. Estimates of cost of keratinocyte sheets range from $1,000 - $13,000/ % body surface area covered [5, 112]. Those costs can approximately double if a dermal substitute is also used [113, 114]. Therefore, costs can become limiting for treatment of large (60 - 90%) total body surface area burns with cultured skin substitutes. For contemporary treatment of burns, cultured skin substitutes remain an important adjunct to conventional skin grafting [91] but are not a primary modality of wound closure except in extreme cases.

1.8 Production of novel skin substitutes

The design concept for the tissue engineered skin equivalent described in the present work was based on existing models comprising a stratified squamous epithelium grown on a collagen-containing matrix populated with dermal fibroblasts. It is envisaged that the tissue-like character of this construct would generate a three-dimensional and organotypic culture, demonstrating correct epithelial differentiation, morphology, and proliferation rates similar to that found in skin [115, 116]. The biomaterials selected for supporting skin cell growth in the present study were biocomposites comprising collagen and the synthetic α-polyester, poly(ε-caprolactone).

Collagen is currently one of the most popular materials for scaffold production in soft tissue repair and reconstruction such as Apligraf ® tissue engineered human skin equivalent [115, 117]. The advantages of biocompatibility and cell adhesion of collagen are however offset by possible toxicity caused by residual catalysts, initiators and un-reacted or partially reacted

chemical cross-linking agents that are generally employed to improve stability and mechanical properties [118]. Biocomposites of synthetic polymers and natural polymers benefit from the wide range of physicochemical properties and processing techniques applicable to synthetic polymers and the cell adhesion properties of natural polymers. Biocomposite films comprising non-crosslinked collagen and PCL have been produced previously by impregnation of lyophilised collagen mats with a solution of PCL followed by solvent evaporation. This approach avoids the toxicity problems associated with chemical cross-linking of collagen whilst retaining the advantages associated with use of synthetic polymers. Changes in film morphology, from virtually pore-free coatings to open porous format, were achieved by variation of the collagen:PCL w/w ratio [86]. An investigation of human osteoblasts interaction with collagen:PCL biocomposites in cell culture revealed higher numbers of attached cells on collagen:PCL biocomposites in comparison with PCL films.

1.9 Aims and objectives

The overall aim of the work reported in this thesis was to develop improved skin substitutes based on a collagen:PCL biocomposite scaffold. Alternatives of gelatin:PCL and gelatin/collagen:PCL biocomposites were also developed on the purpose to refine the collagen:PCL materials. Four distinct areas are covered:

A. The preparation and characterisation of collagen:PCL, gelatin:PCL and gelatin/collagen:PCL biocomposites.
B. Investigation of biocompatibility of biocomposites *in vitro* by growth of fibroblasts and keratinocytes respectively.
C. The design of a co-culture system for fibroblasts and keratinocytes.
D. Investigation of biocompatibility of co-cultured skin models *in vivo*.

CHAPTER TWO

MATERIALS AND METHODS

2.1 Materials

Poly(ε-caprolactone) (PCL, MW 50,000; CAPA® 6500) was obtained from Solvay Interox, Warrington, UK. Type I acid-soluble collagen from calf skin (Cat No.C-3511), gelatin from bovine skin (Cat No.G9382, Type B), NP-40 (non-ionic detergent, I-3021, Lot 51k0084), and phosphate buffered saline (PBS) (Cat No.P-4417) were obtained from Sigma Chemicals Company, UK. Fisher Scientific, UK provided 7ml clear (CLR) glass shell vials (Cat No.4100-1545), 25ml CLR glass shell vials, glacial acetic acid and dichloromethane (HPLC grade). Sodium hydroxide was bought from BDH Chemicals Ltd, England. Bicinchoninic acid solution (BCA) (Cat No.B9643), phosphate buffered saline (PBS) (Cat. No.P-4417), and copper (II) sulfate petahydrate 4% solution (Cat No.C2284) were obtained from Sigma Chemicals Company, UK. Cuvettes (UV absorbance) (Cat No.FB55143), acetone (HPLC grade) and dichloromethane (HPLC grade) were obtained from Fisher Scientific, UK. Dimethyl Sulfoxide (DMSO) (Cat No.D-8418), HEPES (Cat No.H-4034, Lot 89H5431), Minimum Essential Medium Eagle (10x) with Hanks' salts without L-glutamine and $NaHCO_3$ (Cat No.M9288), and Fetal Bovine Serum (Cat No.F7524, Lot 70K3355) were obtained from Sigma Chemicals Company, UK. GIBCOBRL Company supplied 7.5% sodium bicarbonate (Cat No.25080-060), EDTA disodium salt (Cat No.15706-021), MEM (100x) Non-Essential Amino Acids (Cat No.11140-035), Trypsin-EDTA solution (10x) (Cat No.35400), DMEM (Cat No.12430), Fetal Bovine Serum (Cat No.10437-028) and Penicillin-Streptomycin (10000 units/ml penicillin G sodium, 10000ug/ml streptomycin sulfate in 0.85% saline, Cat No.15140-122). Tissue culture flasks (25cm^2, Cat No.9025) were bought from TPP®, Europe/Switzerland. Tissue culture flasks (75cm^2, Cat No. 2010200) were supplied by Orange Scientific Ltd. 24 Well Cell Culture Clusters, Costar® (Cat No. 3526) were obtained from Appleton Woods Ltd. Isoton II (Azide-free balanced electrolyte solution, Cat No. 24820) was bought from Beckman Coulter Ltd. The 3T3 fibroblasts were supplied by Dr E. F. Adams in Aston University. The cryopreserved adult Normal Human Epidermal Keratinocyte (NHEK)

(single donor) (CC-2501) and the Keratinocyte Growth Medium Bulletkit® (KBM®-2 BulletKit) (CC-3107), were bought from BioWhittaker, Inc. The KBM®-2 BulletKit medium contains a 500 ml bottle of Keratinocyte Basal Medium (KBM®-2), at a 0.15mM calcium concentration and all the supplements (CC-4152) listed below, conveniently packaged as single-use aliquots called SingleQuot®: BPE (Bovine Pituitary Extract) (2.0ml), hEGF-B (human recombinant Epidermal Growth Factor) (0.5ml), insulin (0.5ml), hydrocortisone (0.5ml), transferrin (0.5ml), epinephrine (0.5ml), and GA-1000-Gentamicin/ Amphotericin-B. The EpiLife® HKM (Human keratinocyte culture medium) (Cat No.M-EPI-012-5; Cat No.M-EPIcf-500 with addition of 0.06mM calcium chloride and HKGS kit: Cat No.S-001-5) was obtained from Cascade Biologics®, Inc., USA.

2.2 Study on collagen:PCL biocomposites

2.2.1 Preparation of collagen:PCL biocomposites

Collagen solution (0.25% w/v) was prepared by dissolving collagen in 1% acetic acid. In order to eliminate pH changes during incubation of biocomposites in PBS or cell culture medium, the pH of the collagen solution (pH 2.7) was adjusted with 4M NaOH solution to achieve a pH of 7.4 for some preparations. The dissolution of collagen was facilitated by stirring with a magnetic stirrer in a 25ml glass shell vial overnight at room temperature. After complete dissolution, aliquots (0.25ml) of the collagen solution were added to 4ml glass vials followed by elimination of air bubbles and frozen at –20°C for approximately 45-50 minutes. In the second stage, samples were transferred to a freezer at –72°C for 35 minutes. Finally, the frozen samples were placed in a freeze dryer (Edwards Modulyo®) at -44°C under 42 mbar vacuum for 24 hours. Aliquots (0.5ml) of 0.5%, 1%, 2.5% w/v PCL/dichloromethane (DCM) solution were added carefully to the freeze dried collagen mats to prepare 1:4, 1:8, 1:20 collagen:PCL biocomposites respectively. The vials were kept stopped for 30 minutes before

removing the lids to allow solvent evaporation overnight.

2.2.2 Analysis of pH changes on incubation of collagen:PCL biocomposites in PBS

Collagen was dissolved in 1% acetic acid during biocomposite preparation. The purpose of these experiments was to determine whether the residual acid content of the biocomposites could affect the pH of PBS buffer media and thus influence the interaction between cells and biocomposite films. A pH meter (Mettler Toledo® Ltd, MP230) was used to measure the pH value of PBS (1.5ml) containing collagen:PCL biocomposite samples over 14 days at room temperature. The pH was measured every two days. Collagen:PCL samples of various collagen:PCL ratios were used in the analysis. In addition, biocomposite samples prepared using 0.25% collagen solution with the pH adjusted to 7.4 were also investigated in this assay.

2.2.3 BCA assay for estimation of collagen release in collagen:PCL biocomposites incubated in PBS at 37°C

To determine the protein release from the collagen:PCL biocomposites, the bicinchoninic acid (BCA) was chosen for total protein assay. The principle of the BCA assay relies on the formation of a Cu^{2+}-protein complex under alkaline conditions, followed by reduction of the Cu^{2+} to Cu^{1+}. The amount of reduction is proportional to the protein present. It has shown that cysteine, cystine, tryptophan, tyrosine, and the peptide bond are able to reduce Cu^{2+} to Cu^{1+} [120]. BCA forms a purple-blue complex with Cu^{1+} in alkaline environments, thus providing a basis to monitor the reduction of alkaline Cu^{2+} by proteins [120].

The BCA total protein assay was used to estimate the amount of collagen release in 1:4, 1:8 and 1:20 collagen:PCL biocomposites after incubation in PBS at 37°C for 12 days. Individual samples of collagen:PCL biocomposites were added to 7ml glass shell vials containing 1ml

PBS, and incubated at 37°C in a water bath. The release media was replaced completely by fresh PBS periodically and analysed for collagen content using the BCA total protein assay.

Calibration samples of collagen solution were prepared fresh before use in the BCA assay. A collagen stock solution of concentration 1mg/ml was prepared in advance by magnetic stirring overnight, and serial dilutions were carried out by mixing 750µl, 500µl, 400µl, 300µl, 200µl, and 100µl of collagen stock solution (1mg/ml) with 250µl, 500µl, 600µl, 700µl, 800µl, and 900µl of PBS respectively resulting in calibration samples of 1000µg/ml, 750µg/ml, 500µg/ml, 400µg/ml, 300µg/ml, 200µg/ml and 100µg/ml in concentration.

The BCA working reagent was prepared by mixing 50 parts of bicinchoninic acid solution (Cat. No.B9643; Sigma®) containing bicinchoninic acid, sodium carbonate, sodium tartrate, and sodium bicarbonate in 0.1N NaOH (final pH 11.25) with 1 part of copper (II) sulfate pentahydrate 4% solution (Cat No.C2284; Sigma®). The mixture of BCA working reagent will show light green in color. For the BCA assay, a 96-well plate was used in this study, and the BCA working reagent 200µg were mixed with 25µg of a protein sample for each well. The study samples and standards were arranged in triplicate. Test and calibration samples were then placed in a water bath at 37°C for 40 minutes. The absorbance of the calibration samples measured at 562nm was used to produce a calibration curve of collagen concentration that was subsequently used to calculate the protein concentration of the test samples.

2.2.4 BCA assay for estimation of residual collagen content in collagen:PCL biocomposites incubated in PBS at 37°C

The BCA total protein assay was used to estimate the amount of residual collagen in 1:4, 1:8 and 1:20 collagen:PCL biocomposites after incubation in PBS at 37°C for 12 days. Individual samples of collagen:PCL biocomposites were collected at the end of the release study described in Section 2.2.3, and added to 25ml glass shell vials containing 2ml PBS/ 2ml

acetone/ 2ml DCM and stirred using a magnetic stirrer overnight. The PCL component of the biocomposites dissolved in the solvent initially and formed solid precipitates on the bottom of vials when the solvent evaporated. The residual collagen solution in PBS was collected and analysed for collagen content using the BCA assay. The preparation for the calibration samples of collagen solution and the protocol for BCA assay were the same as described in Section 2.2.3.

2.2.5 BCA assay for estimation of residual collagen content in collagen:PCL biocomposites during fibroblast culture

The residual amount of collagen in 1:4, 1:8 and 1:20 collagen:PCL biocomposites post-culture with 3T3 fibroblasts on 1, 8 and 11 days was also estimated by using the BCA assay. The biocomposite samples were collected after cell detachment using 0.25% trypsin-EDTA and cell counting using the haemocytometer. The biocomposite substrates were washed three times in 2ml PBS, and then added to 25ml glass shell vials containing 2ml PBS/ 2ml acetone/ 2ml DCM. Samples were stirred using a magnetic stirrer overnight. The collagen was extracted and analysed as described in Section 2.2.4.

2.2.6 Differential Scanning Calorimetry (DSC)

Differential scanning calorimetry (DSC) is frequently a preferred thermal analytical technique because of its ability to provide detailed information about both the physical and energetic properties of a substance. There are two main types of thermal analysis instruments commercially available, differential thermal analysers (DTA) and differential scanning calorimeters (DSC). These instruments provide quantitative information about exothermic, endothermic and heat capacity changes as a function of temperature and time (such as melting, purity and glass transition temperature). Both techniques consist of a two-pan configuration

(sample and reference). The basic difference between DTA and DSC is that the former measures temperature differences between the sample and reference pan whereas DSC measures energy differences [121]. That means the DSC measures the difference in heat flow from a sample and a reference material as a function of time and temperature [122].

The thermal characteristics of 1:4, 1:8 and 1:20 collagen:PCL biocomposites and PCL films (prepared by solvent casting from a 2.5% w/v PCL/DCM solution) with weight between 2-10 mg were recorded using a Perkin-Elmer Pyris Diamond differential scanning calorimeter. All the samples were lightly pressed into the bottom of the pan to ensure good thermal contact. Sealed DSC pans were used in the study. Triplicate samples were heated at a rate of 10°C/min from 10°C to 100°C. Peak melting temperature (Tm) and heat of fusion data for the PCL component of the materials were determined using the software facility of the DSC. The latter measurement was subsequently used to estimate the percentage crystallinity of PCL in the composites from the reported heat of fusion of 139.5J/g for fully crystalline PCL [123]. Indium was used as a standard.

2.2.7 Scanning electron microscopy (SEM)

The scanning electron microscope was used to evaluate the surface morphology of biocomposites and the condition of cell adhesion, growth and distribution on the surface of biocomposite membranes.

SEM of collagen:PCL biocomposites

Collagen:PCL biocomposites (1:4, 1:8 and 1:20) incubated in PBS at 37°C for 0, 3 and 7 days were examined by using SEM. Samples were attached to aluminum SEM stubs using carbon tabs (Agar Scientific). Specimens were sputter coated with gold prior to examination using a

Cambridge® Stereoscan 90 Scanning Electron Microscope.

SEM of cell growth on collagen:PCL biocomposites

The growth of 3T3 fibroblasts, NHEK, PHEK and PHDF on gelatin:PCL biocomposites respectively were also investigated by using SEM. The materials and methods for sample preparation needed to preserve and fix the cells were described as below.

The Sucrose Buffer (0.33M Sucrose in 0.1M Cacodylate Buffer) was prepared by mixing 11g Sucrose (Cat No.S-9378; Sigma), 50 ml 0.2 M Sodium Cacodylate Buffer, and 50ml Distilled Water. The Cacodylate Buffer Stock Solution (0.2M Sodium Cacodylate Buffer) was prepared by adding 8.5612 g Dimethylarsinic acid sodium salt (Cat No.103256; Merck, Inc.) in 200ml Double distilled water, and adjust pH value to 7.2 - 7.4 with HCl. The working solution of 2.5 % Glutaraldehyde Solution was prepared by mixing 10 ml 25% Glutaraldehyde (Cat No.50-746; Ferak, Inc.), 50 ml 0.2 M Sodium Cacodylate Buffer, and 40 ml Distilled Water. The 1% Osmium Tetroxide (Adjust pH to 7.4) was also prepared by mixing 1gm Osmium Tetroxide, 50ml 0.2M Sodium Cacodylate Buffer, and 50 ml Distilled Water. Firstly, the sample of collagen:PCL biocomposite seeded with cells was removed from the culture system, washed in phosphate buffer 2 to 3 times, then fixed with 2.5% glutaraldehyde for 3 hours, and washed in 0.33M sucrose buffer for 10 minutes twice in 4℃ afterwards. Next, the sample was transferred to a shell glass vial and soaked in 1% osmium tetroxide for 1 hour in 4℃, then washed twice in 0.33M sucrose buffer again for 10 minutes each and washed again in distilled water for 10 minutes in 4℃ afterwards. Lastly, the sample was dehydrated in gradient ethanol (from 60%, 65%, 70%, 75%, 80%, 90%, 95%, 100% to 100%), then in a mixture of 100% ethanol (1/2) and isoamylacetate (1/2) followed by isoamylacetate alone for 10 minutes each in 4℃, and finally soaked in isoamylacetate overnight in 4℃ for critical point drying the next day. After the process of critical point drying, sample was attached to aluminum SEM stubs

using carbon tabs (Agar Scientific), and then was sputter coated with gold prior to examination using either Cambridge® Stereoscan 90 or HITACHI® S-3000N Scanning Electron Microscope.

2.2.8 Capillary Flow Analysis

The porosity of 1:8 and 1:20 (w/w) gelatin:PCL biocomposites (n=3) was investigated using the Automated Capillary Flow Porometer (PMI®, CFP-1200-A, Porous Materials, Inc.). The 1:4 collagen:PCL biocomposite was excluded in this study due to the characteristics of poor mechanical strength and easy-broken during taking off from the glass vial. In the analysis, the fully wetted biocomposite film is firstly placed in the sample chamber and the chamber is sealed. Gas is then allowed to flow into the chamber behind the sample. When the pressure reaches a point that can overcome the capillary action of the fluid within the largest pore, the bubble point has been found. After determination of the bubble point, the pressure is increased and the flow is measured until all pores are empty, and the sample is considered dry. Gas pressure and flow rates through the dry sample are also measured. Bubble point pore diameter was measured as the maximum pore size of the biocomposite film.

2.2.9 Immunohistochemistry Assay

The adhesion, growth and distribution of cells seeded on collagen:PCL biocomposites were investigated by using the immunohistochemistry assay in a certain period of time. The protocol for immunohistochemistry assay was described in brief as below. First, samples were fixed using 4% formalin for 30 min, washed in PBS twice afterwards, then NP-40 (0.05%) was added and they were incubated at room temperature for 30 min, and it was removed afterwards. Next, 2% FCS/PBS was added for 30 min, it was removed and then primary antibody (1:200) 200μl was added and incubated at 25℃ for 3 hours (or 4℃ overnight).

Lastly, samples were washed twice in PBS, then secondary antibody (1:100) 200μl was added, and it was stored in the dark for fluorescence microscopy in one hour.

Immuno-staining for 3T3 fibroblasts

Mouse 3T3 fibroblasts were seeded on the top surface of type I & IV collagen:PCL biocomposites and TCP (24-well tissue culture plastics) at a cell density of $3.5x10^4$ per cm^2 for time intervals up to 12 days. The growth and distribution of 3T3 fibroblasts on collagen:PCL biocomposites (1:4, 1:8 and 1:20) on day 4 at an initial cell seeding density of $3.5x10^4$ cells per cm^2 were examined using fluorescence microscopy by labeling with the (primary) monoclonal mouse anti-vimentin IgG 1:200 (Cat No.MAB3400; Chemicon® International, Inc.), and the (secondary) fluorescein (FITC)-conjugated polyclonal goat anti-mouse IgG 1:100 (Lot No.62686; Jackson ImmunoResearch Laboratories, Inc., USA) respectively.

Immuno-staining for PHEK

Primary human epidermal keratinocytes (PHEK; child foreskin; P4) were seeded on the top surface of collagen:PCL biocomposites (1:8 and 1:20) and TCP (24-well tissue culture plastics) at a cell density of $1.7x10^5$ cells per cm^2 for time intervals up to 9 days. The growth and distribution of PHEK on 1:8 & 1:20 collagen:PCL biocomposites on day 1 and 6 at an initial cell seeding density of $1.7x10^5$ cells per cm^2 were examined using fluorescence microscopy by labeling with the (primary) monoclonal mouse anti-human involucrin antibody 1:200 (Cat No.I8447-25; United States Biological, Inc.), and the (secondary) rhodamine-conjugated polyclonal goat anti-mouse IgG 1:100 (Cat No.I1903-08C, United States Biological, Inc.) respectively.

Immuno-staining for PHDF

Primary human dermal fibroblasts (PHDF; adult foreskin; P3) were seeded on the top surface of collagen:PCL biocomposites (1:8 and 1:20) and TCP (24-well tissue culture plastics) at a cell density of $2.0x10^4$ cells per cm^2 for time intervals up to 10 days. The growth and distribution of PHDF on 1:8 & 1:20 collagen:PCL biocomposites on day 1 and 7 at an initial cell seeding density of $2.0x10^4$ cells per cm^2 were examined using fluorescence microscopy by labeling with the (primary) monoclonal mouse anti-human α tubulin antibody 1:200 (Cat No.sc-5286; Santa Cruz Biotechnology, Inc.), and the (secondary) fluorescein (FITC)-conjugated polyclonal goat anti-mouse IgG 1:100 (Lot No.62686; Jackson ImmunoResearch Laboratories, Inc., USA) respectively.

2.2.10 Mouse 3T3 fibroblast growth on collagen:PCL biocomposites in cell culture

Fibroblast culture medium was prepared using double-distilled water (400ml), 10% Fetal Calf Serum (FCS), MEM (10x) 50ml with Hanks' salt without L-glutamine and $NaHCO_3$, 7.5% sodium bicarbonate 5ml, 5M HEPES 5ml, 1% (v/v) Non-Essential Amino Acids 5ml, 5M sodium hydroxide 2ml, L-glutamine 5ml and 5ml penicillin/streptomycin (100U/ml and 100mg/ml, respectively).

Thawing of cryopreserved 3T3 fibroblasts

Primary mouse 3T3 fibroblasts were obtained from cryopreserved stock maintained in 10% DMSO-containing fibroblast culture medium at –76°C. The thawing method used was the direct plating method. Cryopreserved cells were first removed from storage and thawed quickly in a 37°C water bath. The cells were plated directly with complete growth medium by

using10 to 20ml of 10% FCS/ MEM medium per 1ml of frozen cells. Vital cell counting was performed and cell inoculum should be at least $3x10^5$ viable cells/ml. The original culture medium was replaced with fresh complete growth medium after 12 to 24 hours to remove the cryopreservative.

Cell expansion and passage

The incubated cell culture in tissue culture plastic flasks ($75cm^2$) was checked under a microscope every day. Cell attachment, growth, morphological changes and confluence were evaluated. The procedure of cell passage and expansion was performed at 80-90% confluence in the laminar airflow cabinet as described below. First, using stock cell culture flasks from incubator, the medium was removed and cells were washed in 5ml sterile PBS once or twice. PBS was removed and 2ml 0.25% trypsin-EDTA solution was added to each flask, then incubated at 37°C for 5 minutes and the flask was shaken gently to check whether trypsinisation has been completed (If trypsinisation is complete, the suspension should be cloudy). Trypsin was inactivated by adding 10ml 10% serum medium in each flask afterwards. The suspension was dispensed into centrifuge tube and centrifuged at 1200 rpm for 5 min, the suspension fluid removed and the cell pellet re-suspended with 10% FCS/ MEM fibroblast culture medium afterwards. Lastly, living cells were counted with Weber's haemocytometer, and the cell suspension dispensed into tissue culture flasks to obtain an average cell density of $3x10^5$ viable cells per ml, and incubate at 37°C and change medium every other day. If a cell culture study was planned, the seeding density and aliquots of cell suspension used for the experiment should be selected at this stage.

Cell detachment and cell counting

A comparison of both the trypsinisation and zypocyte cytolysis methods for cell detachment and cell counting in preliminary experiments revealed that the trypsinisation method gave the

most reproducible results (data not shown in this report). Therefore, 0.25% trypsin-EDTA solution was chosen for cell detachment. In addition, the haemocytometer was selected for cell counting as the results obtained using the Coulter Counter® Z1 particle counter were also unreliable due to the relatively small cell numbers in the study. The procedures for cell detachment and cell counting are described below. First, medium was removed from sample vials and TCP plates, and then the biocomposite and PCL film samples with attached cells were washed once or twice in sterile PBS. Next, samples were transferred to sterile 24-well plates, then 0.25% trypsin-EDTA solution (0.5 ml) added into each sample well, and incubated at 37°C for 5 min afterwards. Trypsin was inactivated by adding 10% FCS/ MEM fibroblast medium (0.5 ml). Last, samples were pipetted up and down several times to assist cell detachment from the biocomposite and PCL substrates, and cells counted with the haemocytometer.

Interaction of 3T3 fibroblasts with collagen:PCL biocomposites

Mouse 3T3 fibroblasts ($7.1x10^4$ cells per cm^2) were seeded in 7ml glass shell vials containing collagen:PCL biocomposites (1:4, 1:8 and 1:20), PCL films (made by solvent evaporation from 2.5% w/v PCL/DCM solution) and collagen-coated PCL films [made by 0.25 ml collagen solution (0.25% w/w) dried on the top surface of PCL film at 37°C overnight]. Cells were also seeded in 24-well tissue culture plastic plates (TCP) as controls. All the materials used were sterilised in advance by UV irradiation for one hour. Samples of each substrate type were seeded in triplicate for each time point measure of cell number. Cell numbers were counted at day 1, 8 and 11 (mean±SE) to enable construction of a cell growth curve.

2.2.11 Normal human epidermal keratinocyte (NHEK) growth on collagen:PCL biocomposites in cell culture

The cryopreserved adult Normal Human Epidermal Keratinocytes (NHEK) from single donor

and KBM®-2 medium with supplements were obtained from BioWhittaker, Inc. On arrival, the supplements were added to KBM®-2 in a laminar airflow cabinet. The medium was warmed to the amount needed in water bath at 37°C.

Thawing of cryopreserved NHEK

Primary human keratinocytes were obtained from cryopreserved stock maintained in liquid nitrogen. The thawing method used was the direct plating method [125]. A cryovial of NHEK was first removed from storage and thawed quickly in a 37°C water bath. The cells were plated directly with complete growth medium by using 10 to 20 ml of KBM®-2 BulletKit medium per 1 ml of frozen cells. The cell suspensions were dispensed to two vented T-25 (25 cm^2) tissue culture plastic (TCP) flasks and then transferred to a 37°C, 5% CO_2, humidified incubator. The original culture medium was replaced with fresh complete growth medium after 12 to 24 hours to remove the cryopreservative.

Cell expansion and passage

The incubated cell culture in T-25 flask was checked under a microscope every day. Cell attachment, growth, morphological changes and confluence were evaluated. The procedure of cell passage and expansion was performed at 70-80% confluence in the laminar airflow cabinet. Trypsin-EDTA solution (0.05%) was used for cell detachment, and was neutralised using 10% MEM/ FCS fibroblast medium. The other procedures for passage are the same as that used for 3T3 mouse fibroblasts described in Section 2.2.10.

Cell detachment and cell counting

The trypsinisation method and haemocytometer were used for NHEK detachment and cell counting respectively. The procedures are the same as those described for 3T3 mouse

fibroblasts in Section 2.2.10.

2.2.11.1 Interaction of NHEK with collagen:PCL biocomposites

NHEK ($3.5x10^4$ cells per cm^2) were seeded in 4 ml glass shell vials containing collagen:PCL biocomposites (1:4, 1:8 and 1:20) and also 24-well TCP as a control. All the materials used were sterilised in advance by UV irradiation for one hour. Samples of each substrate type were seeded in triplicate for each time point measurement of cell number. Submerged growth of NHEK was allowed for 6 days. Cell numbers were counted at day 1, 4 and 6 to enable construction of a cell growth curve.

2.2.12 Primary human epidermal keratinocyte (PHEK) growth on collagen:PCL biocomposites in cell culture

Primary human epidermal keratinocytes (PHEK) were isolated and primarily cultured from the donated human foreskin samples after the surgery of circumcision in the study.

2.2.12.1 Primary culture of PHEK

Collection of samples

The sample should be placed in sterile skin transport medium containing Leibovitz medium with 10% serum and antibiotics. This should be stored at 4℃ and has a shelf life of 6 months.

Sample treatment

All tissue and cell culture manipulations were carried out under aseptic conditions, and the procedures were described in brief as below. First, the skin sample was washed with sterile

PBS once/twice in a universal and then transferred to a sterile universal containing 10ml of 0.2% Dispase II in Leibovitz solution and incubated at room temperature overnight. Last, the contents of the universal were transferred to a petri-dish and the epidermis separated from the dermis with sterile forceps.

Isolation of keratinocytes

First, the epidermis sheet was tarnsferred to a Petri-dish (10 ml per Petri-dish) or bijoux containing 0.025% Trypsin-EDTA, and incubated for possibly 10-15 minutes. Next, it was triturated with a pipette to see whether trypsinisation has completed or not. In general, the process of trypsinisation was thought to be complete if the suspension appeared very cloudy. If it requires further incubation then it was replaced into the incubator for a further 5-10min. Once the trypsinisation process was complete, aan equal volume of fibroblast culture medium was added to inactivate the trypsin, and the keratinocyte cell suspension was transferred into a universal and the cells centrifuged (5 minutes and 1300RPM). Lastly, the base of the flask was coated with fibronectin/collagen coating solution (this coating is only necessary for primary isolation), then the cells were gently seeded onto the coated flask, and the medium changed after 12 hours and every other day.

Culture expansion for proliferating keratinocytes

The cell culture needs to be expanded at 70-80% confluence. First, the culture was washed twice with PBS, and 0.05% Trypsin-EDTA solution added for 5 min (5ml regardless of size of flask) until the cultures dispersed. Next, an equal volume of fibroblast culture medium was added and centrifuged as mentioned previously. Last, the cell pellet was re-suspended in keratinocyte culture medium and cultured to requirements.

Cell expansion and passage

The incubated cell culture in T-25 flask was checked under a microscope every day. Cell attachment, growth, morphological changes and confluence were evaluated. The procedure of cell passage and expansion was performed at 70-80% confluence in the laminar airflow cabinet. Trypsin-EDTA solution (0.05%) was used for cell detachment, and was neutralised using 10% MEM/ FCS fibroblast medium. The other procedures for passage are the same as that used for 3T3 mouse fibroblasts described in Section 2.2.10.

Cell detachment and cell counting

The trypsinisation method and haemocytometer were used for NHEK detachment and cell counting respectively. The procedures are the same as those described for 3T3 mouse fibroblasts in section 2.2.10.

2.2.12.2 Interaction of PHEK with collagen:PCL biocomposites

Primary human epidermal keratinocytes (PHEK; child foreskin; P4) were seeded on the top surface of collagen:PCL biocomposites (1:8 and 1:20) and TCP (24-well tissue culture plastics) at a cell density of 1.7×10^5 cells per cm^2 for time intervals up to 9 days. Trypsin-EDTA solution was used for cell detachment followed by cell counting at day 1, 3, 6 and 9 using a Weber's haemocytometer.

2.2.13 Primary human dermal fibroblast (PHDF) growth on collagen:PCL biocomposites in cell culture

Primary human dermal fibroblasts (PHDF) were isolated and primarily cultured from the donated human foreskin samples after the surgery of circumcision in the study.

2.2.13.1 Primary culture of PHDF

The procedures for collection of skin samples and treatment of sample were the same as that described in Section 2.2.12.1.

Isolation of fibroblasts

First, the dermal piece of skin sample was rinsed in a sterile PBS petri-dish containing 10ml of 0.05% collagenase solution in fibroblast culture medium and incubated in 5% CO_2 for 24 hours. Next, p the contents of the bijoux were pipetted for 1 to 2 minutes and transferred to a universal and centrifuged for 5 minutes at 1300 RPM, then the pellet re-suspended in fibroblast culture medium and seeded into a suitable tissue culture treated dish, and incubated in 5% CO_2 afterwards. Last, the culture medium was changed at 2 to 24 hours and every other day until confluent.

Fibroblasts culture expansion

First, the culture medium was aspirated from the confluent layer in cell culture and washed with PBS. Next, trypsin (0.05%)-EDTA (0.02%) solution was added and incubated for 2 to 3

minutes. An equal volume of fibroblast culture medium was then added to inactivate the trypsin and the suspension centrifuged for 5 minutes at 1300RPM. Last, the pellet was re-suspended in a known quantity of culture medium depending on ratio of expansion.

Cell expansion and passage

The incubated cell culture in T-25 flask was checked under a microscope every day. Cell attachment, growth, morphological changes and confluence were evaluated. The procedure of cell passage and expansion was performed at 70-80% confluence in the laminar airflow cabinet. Trypsin-EDTA solution (0.05%) was used for cell detachment, and was neutralised using 10% MEM/ FCS fibroblast medium. The other procedures for passage are the same as that used for 3T3 mouse fibroblasts described in Section 2.2.10.

Cell detachment and cell counting

The trypsinisation method and haemocytometer were used for PHDF detachment and cell counting respectively. The procedures are the same as those described for 3T3 mouse fibroblasts in Section 2.2.10.

2.2.13.2 Interaction of PHDF with collagen:PCL biocomposites

Primary human dermal fibroblasts (PHDF; adult foreskin; P3) were seeded on the top surface of collagen:PCL biocomposites (1:8 and 1:20) and TCP (24-well tissue culture plastics) at a cell density of 2.0×10^4 cells per cm^2 for time intervals up to 10 days. Trypsin-EDTA solution was used for cell detachment followed by cell counting at day 1, 4, 7 and 10 using a Weber's haemocytometer.

2.2.14 Statistical analysis

The data were analysed using the **ANOVA** two-factor with replication test, and the variances are further investigated by using the **Student Newman-Keuls** test. The data are shown as "**Mean** ± Standard Error (SE)" when sample numbers (**n**) are not less than three. The result is statistically significant when the **P value** is less than 0.05 ($P<0.05$).

2.3 Study on gelatin:PCL biocomposites

2.3.1 Preparation of gelatin:PCL biocomposites

Gelatin (type B) solution (0.1% w/v) was prepared by dissolving gelatin in double distilled water. The dissolution of gelatin was facilitated by stirring using a heating magnetic stirrer in a 25ml glass shell vial at the temperature greater than 40°C. After complete dissolution, aliquots (0.25ml) of the gelatin solution were added to 7ml glass vials followed by elimination of air bubbles and frozen at –20°C for approximately 45-50 minutes. In the second stage, samples were transferred to a freezer at –72°C for 35 minutes. Finally, the frozen samples were placed in a freeze dryer (Edwards Modulyo®) at -44°C under 42 mbar vacuum for 24 hours. Aliquots (0.5ml) of 0.4%, 0.8%, 2% w/v PCL/dichloromethane (DCM) solution were added carefully to the freeze dried gelatin mats to prepare 1:4, 1:8, 1:20 w/w gelatin:PCL biocomposites respectively. The vials were kept stopped for 30 minutes before removing the lids to allow solvent evaporation overnight.

2.3.2 BCA assay for estimation of gelatin release from gelatin:PCL biocomposites incubated in PBS at 37°C

To determine the protein release from biocomposites, the BCA total protein assay was used to estimate the amount of gelatin release in 1:4, 1:8 and 1:20 gelatin:PCL biocomposites after incubation in PBS at 37°C for 12 days. Individual samples of gelatin:PCL biocomposites were added to 7ml glass shell vials containing 1ml PBS, and incubated at 37°C in a water bath. The release media was replaced completely by fresh PBS periodically and analysed for gelatin content using the BCA total protein assay.

Calibration samples of gelatin solution were prepared fresh before use in the BCA assay. A gelatin stock solution of concentration 1mg/ml was prepared in advance by magnetic stirring at the temperature of 80℃, and serial dilutions were carried out by mixing 750µl, 500µl, 400µl, 300µl, 200µl, and 100µl of gelatin stock solution (1mg/ml) with 250µl, 500µl, 600µl, 700µl, 800µl, and 900µl of PBS respectively resulting in calibration samples of 1000µg/ml, 750µg/ml, 500µg/ml, 400µg/ml, 300µg/ml, 200µg/ml and 100µg/ml in concentration.

The BCA working reagent was prepared as the same as that described in Section 2.2.3. For the BCA assay, a 96-well plate was used in this study, and the BCA working reagent 200µg were mixed with 25µg of a protein sample for each well. The study samples and standards were arranged in triplicate. Test and calibration samples were then placed in a water bath at 37°C for 40 minutes. The absorbance of the calibration samples measured at 562nm was used to produce a calibration curve of gelatin concentration that was subsequently used to calculate the protein concentration of the test samples.

2.3.3 Differential Scanning Calorimetry (DSC)

The thermal characteristics of 1:4, 1:8 and 1:20 gelatin:PCL biocomposites with weight between 2-10 mg were recorded using a Perkin-Elmer Pyris Diamond differential scanning calorimeter. All the samples were lightly pressed into the bottom of the pan to ensure good

thermal contact. Sealed DSC pans were used in the study. Triplicate samples were heated at a rate of 10°C/min from 10°C to 100°C. Peak melting temperature (Tm) and heat of fusion data for the PCL component of the materials were determined using the software facility of the DSC. The latter measurement was subsequently used to estimate the percentage crystallinity of PCL in the composites from the reported heat of fusion of 139.5J/g for fully crystalline PCL [123]. Indium was used as a standard.

2.3.4 Scanning electron microscopy (SEM)

The scanning electron microscope was used to evaluate the surface morphology of gelatin:PCL biocomposites and the condition of cell adhesion, growth and distribution on the surface of biocomposite membranes.

SEM of gelatin:PCL biocomposites

Gelatin:PCL biocomposites (1:4, 1:8 and 1:20 w/w) were examined by using SEM. Samples were attached to aluminum SEM stubs using carbon tabs (Agar Scientific). Specimens were sputter coated with gold prior to examination using a HITACHI® S-3000N Scanning Electron Microscope (Magnification: x5 to x300,000; Accelerating voltage: 0.3 to 30kV; Variable pressure range: 1 to 270Pa; Specimen size: 150mm diameter in maximum; Secondary electron image: 3.0nm at 25 kV and high vacuum mode).

SEM of cell growth on gelatin:PCL biocomposites

The growth of PHEK and PHDF on gelatin:PCL biocomposites were also investigated using SEM. The methods for sample preparation for SEM were the same as that described in Section 2.2.7.

2.3.5 Immunohistochemistry Assay

The adhesion, growth and distribution of cells seeded on gelatin:PCL biocomposites were investigated by using the immunohistochemistry assay. The protocol for immunohistochemistry assay was the same as described in Section 2.2.9.

Immuno-staining for PHEK

Primary human epidermal keratinocytes (PHEK; child foreskin; P4) were seeded on the top surface of gelatin:PCL biocomposites (1:8 and 1:20), collagen:PCL biocomposites (1:8 and 1:20) and TCP (24-well tissue culture plastics) at a cell density of $1.7x10^5$ cells per cm^2 for a time intervals up to 9 days. The growth and distribution of PHEK on gelatin:PCL biocomposites (1:8 and 1:20) on day 1 and 6 at an initial cell seeding density of $1.7x10^5$ cells per cm^2 were examined under fluorescent microscope by labeling with the (primary) monoclonal mouse anti-human involucrin antibody 1:200 (Cat No.I8447-25; United States Biological, Inc.), and the (secondary) rhodamine-conjugated polyclonal goat anti-mouse IgG 1:100 (Cat No.I1903-08C, United States Biological, Inc.) respectively.

Immuno-staining for PHDF

Primary human dermal fibroblasts (PHDF; adult foreskin; P3) were seeded on the top surface of gelatin:PCL biocomposites (1:8 and 1:20) and TCP (24-well tissue culture plastics) at a cell density of $2.0x10^4$ cells per cm^2 for a time intervals up to 10 days. The growth and distribution of PHDF on gelatin:PCL biocomposites (1:8 and 1:20) on day 1, 7 and 10 at an

initial cell seeding density of $2.0x10^4$ cells per cm^2 were examined under fluorescent microscope by labeling with the (primary) monoclonal mouse anti-human α tubulin antibody 1:200 (Cat No.sc-5286; Santa Cruz Biotechnology, Inc.), and the (secondary) fluorescein (FITC)-conjugated polyclonal goat anti-mouse IgG 1:100 (Lot No.62686; Jackson ImmunoResearch Laboratories, Inc., USA) respectively.

2.3.6 Mouse 3T3 fibroblast growth on gelatin:PCL biocomposites in cell culture

Fibroblast culture medium was prepared using 10% Fetal Calf Serum (FCS), DMEM (1x) 500ml and penicillin/streptomycin 5ml (100U/ml and 100mg/ml respectively). The methods for thawing of cryopreserved 3T3 fibroblasts, cell expansion, and cell counting were the same as that described in Section 2.2.10.

2.3.6.1 Interaction of 3T3 fibroblasts with gelatin:PCL biocomposites

Mouse 3T3 fibroblasts were seeded on the top surface of type I collagen:PCL & gelatin:PCL biocomposites (1:4, 1:8 and 1:20) and TCP (24-well tissue culture plastics) at a cell density of $3.5x10^4$ per cm^2 for time intervals up to 12 days. Trypsin-EDTA solution was used for cell detachment followed by cell counting at day 1, 4, 8 and 12 using a Weber's haemocytometer.

2.3.7 PHEK growth on gelatin:PCL biocomposites in cell culture

Primary human epidermal keratinocytes (PHEK) were isolated and primarily cultured from the donated human foreskin samples after the surgery of circumcision in the study. EpiLife® keratinocyte culture medium was used for keratinocyte culture. The methods for treatment of skin samples, cell expansion and cell counting were the same as that described in Section 2.2.12.1.

2.3.7.1 Interaction of PHEK with gelatin:PCL biocomposites

Primary human epidermal keratinocytes (PHEK; child foreskin; P4) were seeded on the top surface of gelatin:PCL biocomposites (1:8 and 1:20), collagen:PCL biocomposites (1:8 and 1:20) and TCP (24-well tissue culture plastics) at a cell density of $1.7x10^5$ cells per cm^2 for a time intervals up to 9 days. Trypsin-EDTA solution was used for cell detachment followed by cell counting at day 1, 3, 6 and 9 using a Weber's haemocytometer.

2.3.8 PHDF growth on gelatin:PCL biocomposites in cell culture

Primary human dermal fibroblasts (PHDF) were isolated and primarily cultured from the donated human foreskin samples after the surgery of circumcision in the study. The methods for treatment of sample, cell expansion and cell counting were the same as that described in Section 2.2.13.1.

2.3.8.1 Interaction of PHDF with gelatin:PCL biocomposites

Primary human dermal fibroblasts (PHDF; adult foreskin; P3-4) were seeded on the top surface of gelatin:PCL and collagen:PCL biocomposites (1:8 and 1:20) and TCP (24-well tissue culture plastics) at a cell density of $2.0x10^4$ cells per cm^2 for a time intervals up to 10 days. Trypsin-EDTA solution was used for cell detachment followed by cell counting at day 1, 4, 7 and 10 using a Weber's haemocytometer.

2.3.9 Statistical analysis

The data were analysed using the **ANOVA** two-factor with replication test, and the variances were further investigated by using the **Student Newman-Keuls** test. The data are shown as **mean±standard error (SE)** when sample numbers (**n**) are not less than three. The result is statistically significant when the **P value** is less than 0.05 ($P<0.05$).

2.4 Study on gelatin/collagen:PCL biocomposites

To decrease the amount of collagen used for the preparation of collagen:PCL biocomposites and improve the mechanical strength of gelatin:PCL biocomposites, the mixture of collagen and gelatin solutions was used to prepare the brand-new gelatin/collagen:PCL biocomposites.

2.4.1 Preparation of gelatin/10% collagen:PCL biocomposites

Aliquots of gelatin/10% collagen solution was prepared by dissolving 0.2% w/v gelatin 0.2ml in double distilled water followed by mixing 0.25% w/v collagen 0.025ml (10% of the amount of collagen used for preparation of collagen:PCL biocomposites). The dissolution of gelatin/ collagen was facilitated by stirring using a heating magnetic stirrer in a 25ml glass shell vial at the temperature of 80°C. After complete dissolution, aliquots (0.2ml) of the gelatin/ collagen solution were added to 7ml glass vials followed by elimination of air bubbles and frozen at –20°C for approximately 45-50 minutes. In the second stage, samples were transferred to a freezer at –72°C for 35 minutes. Finally, the frozen samples were placed in a freeze dryer (Edwards Modulyo®) at -44°C under 42 mbar vacuum for 24 hours. Aliquots (0.5ml) of 0.74% and 1.85% w/v PCL/dichloromethane (DCM) solution were added carefully to the freeze dried gelatin/collagen mats to prepare 1:8 and 1:20 w/w gelatin/10% collagen:PCL biocomposites respectively. The vials were kept stopped for 30 minutes before removing the lids to allow solvent evaporation overnight.

2.4.2 Preparation of gelatin/25% collagen:PCL biocomposites

Aliquots of gelatin/25% collagen solution were prepared by dissolving 0.2% w/v gelatin (0.2ml) in double distilled water followed by mixing 0.25% w/v collagen (0.062ml) (25% of the amount of collagen used for preparation of collagen:PCL biocomposites). The dissolution of gelatin/ collagen was facilitated by stirring using a heating magnetic stirrer in a 25ml glass shell vial at the temperature of 80°C. After complete dissolution, aliquots (0.2ml) of the gelatin/ collagen solution were added to 7ml glass vials followed by elimination of air bubbles and frozen at –20°C for approximately 45-50 minutes. In the second stage, samples were transferred to a freezer at –72°C for 35 minutes. Finally, the frozen samples were placed in a freeze dryer (Edwards Modulyo®) at -44°C under 42 mbar vacuum for 24 hours. Aliquots (0.5ml) of 0.89% and 2.23% w/v PCL/dichloromethane (DCM) solution were added carefully to the freeze dried gelatin/ collagen mats to prepare 1:8 and 1:20 w/w gelatin/25% collagen:PCL biocomposites respectively. The vials were kept stopped for 30 minutes before removing the lids to allow solvent evaporation overnight.

2.4.3 BCA assay for estimation of total protein release from gelatin/collagen biocomposites incubated in PBS at 37°C

To determine the total protein release from biocomposites (n=3), the BCA assay was used to estimate the amount of gelatin/ collagen release in 1:8 & 1:20 gelatin/10% collagen:PCL and gelatin/25% collagen:PCL biocomposites after incubation in PBS at 37°C for 12 days. Individual samples of gelatin/collagen:PCL biocomposites were added to 7ml glass shell vials containing 1ml PBS, and incubated at 37°C in a water bath. The release media was replaced completely by fresh PBS periodically and analysed for total protein content using the BCA assay.

Calibration samples of collagen and gelatin solution were prepared fresh before use respectively in the BCA assay. The collagen and gelatin stock solutions of concentration

1mg/ml were prepared separately in advance by magnetic stirring, and serial dilutions were carried out by mixing 750µl, 500µl, 400µl, 300µl, 200µl, and 100µl of collagen/gelatin stock solution (1mg/ml) with 250µl, 500µl, 600µl, 700µl, 800µl, and 900µl of PBS respectively resulting in calibration samples of 1000µg/ml, 750µg/ml, 500µg/ml, 400µg/ml, 300µg/ml, 200µg/ml and 100µg/ml in concentration.

The BCA working reagent was prepared as the same as that described in Section 2.2.3. For the BCA assay, a 96-well plate was used in this study, and the BCA working reagent 200µg were mixed with 25µg of a protein sample for each well. The study samples and standards were arranged in triplicate. Test and calibration samples were then placed in a water bath at 37°C for 40 minutes. The absorbance of the calibration samples measured at 562nm was used to produce a calibration curve of collagen concentration that was subsequently used to calculate the protein (gelatin/collagen) concentration of the test samples. In comparing data sets, the similarity of the variance of the sets was determined using the F-test, and the sets were then compared by paired t-test using equal or unequal variances as appropriate. Error bars and tolerances represent 95% confidence limits.

2.4.4 Differential Scanning Calorimetry (DSC)

The thermal characteristics of 1:8 and 1:20 (w/w) gelatin/10% collagen:PCL and gelatin/25% collagen:PCL biocomposites with weight between 2-10 mg were recorded using a Perkin-Elmer Pyris Diamond differential scanning calorimeter. All the samples were lightly pressed into the bottom of the pan to ensure good thermal contact. Sealed DSC pans were used in the study. Triplicate samples were heated at a rate of 10°C/min from 10°C to 100°C. Peak melting temperature (Tm) and heat of fusion data for the PCL component of the materials were determined using the software facility of the DSC. The latter measurement was subsequently used to estimate the percentage crystallinity of PCL in the composites from the reported heat of fusion of 139.5J/g for fully crystalline PCL [123]. Indium was used as a

standard.

2.4.5 Scanning electron microscopy (SEM)

The scanning electron microscope was used to evaluate the surface morphology of gelatin/collagen:PCL biocomposites and the condition of cell adhesion, growth and distribution on the surface of biocomposite membranes.

Gelatin/10% collagen:PCL and gelatin/25% collagen:PCL biocomposites (1:4, 1:8 and 1:20 w/w) were examined by using SEM respectively. Samples were attached to aluminum SEM stubs using carbon tabs (Agar Scientific). Specimens were sputter coated with gold prior to examination using a HITACHI® S-3000N Scanning Electron Microscope.

2.4.6 Immunohistochemistry Assay

The adhesion, growth and distribution of cells seeded on gelatin/collagen:PCL biocomposites were investigated by using the immunohistochemistry assay. The protocol for immunohistochemistry assay was the same as described in Section 2.2.9.

Immuno-staining for PHEK

Primary human epidermal keratinocytes (PHEK; child foreskin; P4) were seeded on the top surface of gelatin/10% collagen:PCL biocomposites (1:8 and 1:20), gelatin/25% collagen:PCL biocomposites (1:8 and 1:20), collagen:PCL biocomposites (1:8 and 1:20) and TCP (24-well tissue culture plastics) at a cell density of 1.7×10^5 cells per cm^2 for time intervals up to 9 days. The growth and distribution of PHEK on gelatin/10% collagen:PCL and gelatin/25% collagen:PCL biocomposites (1:8 and 1:20) on day 1, 3 and 6 at an initial cell seeding density of 1.7×10^5 cells per cm^2 were examined under fluorescent microscope by labeling with the

(primary) monoclonal mouse anti-human involucrin antibody 1:200 (Cat No.I8447-25; United States Biological, Inc.), and the (secondary) rhodamine-conjugated polyclonal goat anti-mouse IgG 1:100 (Cat No.I1903-08C, United States Biological, Inc.) respectively.

Immuno-staining for PHDF

Primary human dermal fibroblasts (PHDF; adult foreskin; P3-4) were seeded on the top surface of 1:8 and 1:20 (w/w) gelatin/10% collagen:PCL, gelatin/25% collagen:PCL and collagen:PCL biocomposites and TCP (24-well tissue culture plastics) at a cell density of $2.0x10^4$ cells per cm^2 for time intervals up to 10 days. The growth and distribution of PHDF on gelatin/10% collagen:PCL and gelatin/25% collagen:PCL biocomposites (1:8 and 1:20) on day 1, 7 and 10 at an initial cell seeding density of $2.0x10^4$ cells per cm^2 were examined under fluorescent microscope by labeling with the (primary) monoclonal mouse anti-human α tubulin antibody 1:200 (Cat No.sc-5286; Santa Cruz Biotechnology, Inc.), and the (secondary) fluorescein (FITC)-conjugated polyclonal goat anti-mouse IgG 1:100 (Lot No.62686; Jackson ImmunoResearch Laboratories, Inc., USA) respectively.

2.4.7 PHEK growth on gelatin/collagen:PCL biocomposites in cell culture

Primary human epidermal keratinocytes (PHEK) were isolated and primarily cultured from the donated human foreskin samples after the surgery of circumcision in the study. EpiLife® HKM (Cat No.M-EPIcf-500 with addition of 0.06mM calcium chloride and HKGS kit: Cat No.S-001-5) was used for keratinocyte culture. The methods for treatment of skin samples, cell expansion and cell counting were the same as that described in Section 2.2.12.1.

2.4.7.1 Interaction of PHEK with gelatin/collagen:PCL biocomposites

Primary human epidermal keratinocytes (PHEK; child foreskin; P4) were seeded on the top surface of gelatin/10% collagen:PCL biocomposites (1:8 and 1:20), gelatin/25% collagen:PCL biocomposites (1:8 and 1:20), collagen:PCL biocomposites (1:8 and 1:20) and TCP (24-well

tissue culture plastics) at a cell density of $1.7x10^5$ cells per cm^2 for time intervals up to 9 days. Trypsin-EDTA solution was used for cell detachment followed by cell counting at day 1, 3, 6 and 9 using a Weber's haemocytometer.

2.4.8 PHDF growth on gelatin/collagen:PCL biocomposites in cell culture

Primary human dermal fibroblasts (PHDF) were isolated and primarily cultured from the donated human foreskin samples after the surgery of circumcision in the study. The methods for treatment of sample, cell expansion and cell counting were the same as that described in Section 2.2.13.1.

2.4.8.1 Interaction of PHDF with gelatin/collagen:PCL biocomposites

Primary human dermal fibroblasts (PHDF; adult foreskin; P3-4) were seeded on the top surface of 1:8 and 1:20 (w/w) gelatin/10% collagen:PCL, gelatin/25% collagen:PCL and collagen:PCL biocomposites and TCP (24-well tissue culture plastics) at a cell density of $2.0x10^4$ cells per cm^2 for time intervals up to 10 days. Trypsin-EDTA solution was used for cell detachment followed by cell counting at day 1, 4, 7 and 10 using a Weber's haemocytometer.

2.4.9 Statistical analysis

The data were analysed using the **ANOVA** two-factor with replication test, and the variances were further investigated by using the **Student Newman-Keuls** test. The data are shown as "**mean±SE**" when sample numbers (**n**) are not less than three. The result is statistically significant when the **P value** is less than 0.05 ($P<0.05$).

CHAPTER THREE

DESIGN OF A CO-CULTURED SKIN MODEL *IN VITRO*

3.1 Introduction

Conceptually, skin substitutes are either permanent or temporary; epidermal, dermal or composite; and biologic or synthetic. Biologic components are either autogenous, allogeneic, or xenogeneic. For treatment of deep or full-thickness wounds in a large body surface area, autogenous biosynthetic skin substitutes will be needed for permanent wound coverage and healing. To achieve the goal of epithelialisation and mimic the normal skin epidermal-dermal structures, composite skin substitutes were considered to be the best choice for the design of a tissue-engineered skin. Moreover, the fact that fibroblast proliferation is increased in an *in vitro* co-culture model, compared with a fibroblast monolayer alone, implicates that keratinocytes and fibroblasts are not isolated in the skin tissue but their activity is influenced by each other [125]. Therefore, an *in vitro* skin model designed by the co-culture of keratinocytes and fibroblasts to mimic the normal skin tissue would be more realistic for possible clinical applications.

Currently commercially available or marketed co-cultured skin substitutes include Apligraf® or Graftskin® (Organogenesis, Inc., Canton, MA, USA) prepared by co-culture of allogeneic human neonatal keratinocytes and fibroblasts on type I bovine collagen gel; Comp Cult Skin® or OrCel® (Ortec International, Inc., NY, USA) prepared by co-culture of allogeneic human keratinocytes and fibroblasts on type I bovine collagen sponge; and Polyactive® (HC Implants, Inc.) prepared by co-culture of autologous human keratinocytes and fibroblasts on PEO/PBT materials. All of these skin substitutes serve as an absorbable biocompatible matrix that provides a favorable environment for host cell migration and have been shown to contain many cell-expressed cytokines and growth factors produced by seeded cells themselves; however, they do not contain Langerhans cells, melanocytes, macrophages, lymphocytes, blood vessels or hair follicles. Up to date, no tissue-engineered skin substitutes could be designed and consist of the full characteristics seen in the normal skin structures *in vitro*.

Furthermore, most of the skin substitutes based on the collagen gel or sponge are keen to shrink in the early stage of wound healing process due to the rapid degradation rate of collagen matrix and the contraction force generated by fibroblasts. Biosynthetic scaffolds such as collagen:PCL biocomposites consisting of a polyester component exhibit much stronger mechanical strength than pure collagen materials and are thought to be more resistant to the contraction force caused by fibroblasts during wound healing process. Therefore, among the 1:4, 1:8 and 1:20 w/w collagen:PCL biocomposites developed in this work, 1:20 w/w collagen:PCL material was finally chosen and used for the design of a co-cultured skin substitute due to its characteristics of good biocompatibility in both keratinocyte and fibroblast culture *in vitro*, and that of much stronger mechanical strength in observation than the other materials allowing for easy manipulation and transfer during preparation process.

Serum-free culture media were chosen for the culture of human keratinocytes in this work; however, many culture systems are commercially available up to date. Rheinwald and Green improved keratinocyte growth and colony formation by plating cells on lethally irradiated 3T3 fibroblasts and adding Epidermal Growth Factor (EGF) and hydrocortisone to the medium, which required serum-supplementation such as Medium 199 and NCTC 168 [3]. Serum-free cultivation of human keratinocytes without 3T3 fibroblast feeder layers became widely used with the development of MCDB-153 that included trace elements, ethanolamine, phosphoethanolamine, hydrocortisone, EGF and bovine pituitary extract (BPE) [126]. Even though serum-free culture in medium containing BPE as the primary mitogen has several drawbacks such as that the undefined composition of BPE may complicate experimental models and interpretation of results, and sustain limited stability in medium for about four weeks, it is still widely used for human keratinocyte culture *in vitro*. Up to date, the keratinocyte culture medium has been subject to several enhancements and, in general, the supplements contain BPE, hEGF (human recombinant Epidermal Growth Factor), insulin, hydrocortisone, transferrin, L-glutamine, cholera toxin, adenine, and epinephrine.

To achieve the goal of co-culture of keratinocytes and fibroblasts on 1:20 w/w collagen:PCL materials *in vitro*, specific culture medium should be chosen or developed to establish a suitable environment for both of these two distinct types of skin cells. In a pilot test on different types of medium (KBM®-2 BulletKit medium, fibroblast culture medium, mixed medium with 1:1 KBM®-2 BulletKit medium and fibroblast culture medium, and EpiLife® human keratinocyte culture medium) for growth of NHEK and 3T3 fibroblasts respectively in this work, best cell growth numbers for both human keratinocytes (NHEK) and 3T3 fibroblasts were observed in the study group of EpiLife® human keratinocyte culture medium (Data not shown). Therefore, EpiLife® human keratinocyte culture medium was finally chosen for co-culture study in this work. Furthermore, the co-cultured construct is submerged in EpiLife® human keratinocyte culture medium with addition of 0.06mM calcium chloride and HKGS (human keratinocyte growth factors) kit to allow cells to spread and cover the surface of the dermal lattices. Instead of raising the Ca^{2+} concentration of the medium to a high level of 1.8mM, differentiation of the overlying epidermis was finally achieved by lifting the co-cultured construct at the air-liquid interface for about 10 days to enable for generation of a protective cornified layer.

3.2 Design of the co-culture device for preparation of skin substitutes *in vitro*

The ultimate aim of the research on skin substitutes was to prepare a co-cultured skin model using collagen:PCL biocomposite membranes to support the growth of keratinocytes and fibroblasts on either side of the membrane. Cells could not be seeded simultaneously because of the need for cell settling under gravity onto the membrane. Therefore, two-stage cell seeding was used to allow cell attachment on either side of the membrane. A special co-culture device was designed to hold the biocomposite film between open chambers, which allowed the culture medium to contact both sides of the membrane to allow cell seeding. A

sterilising filter holder, Swinnex (13mm) (Cat No.FDR-355-010C) with a diameter of 13 mm was obtained from the Fisher Company for feasibility studies and modified manually for this purpose (Figure 3). In addition, 40 ml sterile Universals, 18# long needles and 5 ml syringes were used.

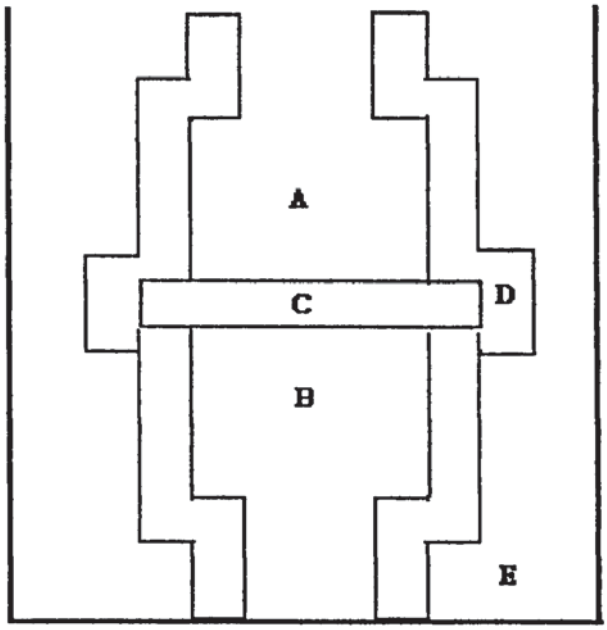

Figure 3: Schematic illustration of the co-culture device.
A sterilizing filter holder (D), Swinnex (13 mm) with a diameter of 13 mm, placed in a Universal (E) was used for the design of a special co-culture device to hold the biocomposite film (C) between open chambers (A and B) that allowed the culture medium to contact both sides of the membrane to allow cell seeding.

3.3 Feasibility study: Co-culture of 3T3 fibroblasts on both surfaces of collagen:PCL biocomposite membranes separately

Preliminary investigations carried out to establish the design of the co-culture device and the cell seeding technique were based on two-stage cell seeding of 3T3 fibroblasts on either side of a 1:20 collagen:PCL biocomposite membrane. This biocomposite was chosen because of the good cell growth characteristics obtained in cell culture studies. A total of 8 samples of 1:20 collagen:PCL biocomposites were used for the co-culture experiment. All the samples were seeded with 3T3 fibroblasts on the upper surface of the biocomposite membrane using a

cell density of $1.0x10^5$ cells per cm^2 on day 0, and incubated for 6 days. Three samples were counted on day 3, and two samples were counted on day 6 as controls. Two samples were used for a co-culture experiment on day 3, in which cells were seeded on the reverse side of the biocomposite membrane and were counted on day 6 as a study group. Only one sample was used as a control for day 1 counting because cell attachment was known from earlier studies to be very low at this time point.

The co-culture procedure is described in brief as below. Firstly, the 1:20 collagen:PCL biocomposite membranes were sterilised by UV irradiation for one hour before use and the instruments used including co-culture devices were autoclaved in advance. Sterile sample of biocomposite (1.2 cm in diameter) was then rinsed in 1 ml sterile PBS once, and was transferred onto the filter-holding area of the co-culture device using sterile forceps. After that, both sections of the co-culture device were screwed tightly together to fix the biocomposite membrane in the central portion of the filter holder. The co-culture device was subsequently transferred into a sterile 40 ml Universal with fibroblast culture medium (10% FCS/ MEM) added to the outer space of co-culture device until level with the surface of the biocomposite. Finally, the 3T3 fibroblasts were seeded onto the upper surface of the biocomposite using a cell density of $1.0x10^5$ cells per cm^2 on day 0. Culture medium on both outer and inner spaces was changed every 2 to 3 days. On day 3, the co-culture device was turned upside down, and 3T3 fibroblasts were seeded onto the upper surface of biocomposite with the same cell density of $1.0x10^5$ cells per cm^2.

3.4 Co-culture of NHEK and 3T3 fibroblasts

After proving the feasibility of the co-culture system based on two-stage cell seeding procedure by co-culture of 3T3 fibroblasts on both sides of 1:20 collagen:PCL biocomposite successfully, co-culture of normal human epidermal keratinocytes (NHEK) and 3T3 fibroblasts on either side of the membrane was subsequently performed using the same

co-culture system. In the early stages of the study, the design of a co-cultured skin model was based on the successful seeding, adherence and growth of both NHEK and 3T3 fibroblasts on either side of the membrane separately. The co-culture procedure is similar to that described above in Section 3.3. In brief, 1:20 collagen:PCL biocomposite film was transferred to the co-culture system firstly. Secondly, 3T3 fibroblasts ($8.0x10^4$ cells per cm^2) were seeded on one side of the 1:20 collagen:PCL biocomposite in the co-culture system for 3 days. Finally, the co-culture device was turned upside down, and NHEK ($4.0x10^4$ cells per cm^2) were then seeded on the top surface of the biocomposite film in culture for another 3 days in submerged culture.

3.4.1 Scanning electron microscopy (SEM)

In order to prove whether NHEK and 3T3 fibroblasts could successfully adhere and grow on either side of the biocomposite membrane separately or not, the surface morphologic change of co-cultured skin models was investigated by using SEM. The protocol for sample preparation was the same as that described in Section 2.2.7. Samples were finally attached to aluminum SEM stubs using carbon tabs (Agar Scientific), and then sputter coated with gold prior to examination using a Cambridge® Stereoscan 90 Scanning Electron Microscope.

3.5 Co-culture of PHEK and 3T3 fibroblasts

In the next stage of the study, a co-cultured skin model was designed by growing a confluent keratinocyte sheet on the biocomposite film upwards with a populated 3T3 fibroblast layer underneath using the same co-culture system. Primary human epidermal keratinocytes (PHEK) at passage 2-4 isolated and cultured from the epidermal layer of human foreskin, the waste tissue of circumcision surgery, were used in the following study to mimic the normal clinical condition. Co-culture of PHEK and 3T3 fibroblasts on either side of the membrane was

subsequently performed and a co-cultured skin model was developed by growing a confluent PHEK sheet on the biocomposite film upwards with a populated 3T3 fibroblast layer underneath followed by lifting the co-cultured membrane onto the air-fluid level for another 10 days to enhance keratinocyte differentiation. The co-culture procedure was modified and described as below briefly. Firstly, PHEK (1.7×10^5 cells/cm^2; child foreskin) at passage 4 were seeded on one side of the biocomposite film for about 14 days to achieve 80% to 90% confluence compared to the control group of growing PHEK with the same seeding density on polystyrene in 24-well tissue culture plastics (TCP). Secondly, biocomposite film containing sub-confluent keratinocytes were turned upside down and transferred to the co-culture system. Then, 3T3 fibroblasts (2.0×10^4 cells per cm^2) were seeded on the other side (top surface) of biocomposite film for another 3 days (to achieve 100% confluence in keratinocyte culture on TCP). Finally, biocomposite films were turned upside down again, and lifted onto the air-fluid level for another 10 days to enable keratinocyte differentiation.

The surface morphologic change of co-cultured skin model in terms of cell growth and distribution on each side of the biocomposite membrane were investigated using SEM and immunohistochemistry assay.

3.5.1 Scanning electron microscopy (SEM)

Co-cultured skin models based on PHEK and 3T3 fibroblasts were investigated by using SEM. The protocol for sample preparation was the same as that described in Section 2.2.7. Samples were finally attached to aluminum SEM stubs using carbon tabs (Agar Scientific), and then sputter coated with gold prior to examination using a HITACHI® 3000N Scanning Electron Microscope.

3.5.2 Immunohistochemistry assay

The growth and distribution of PHEK and 3T3 fibroblasts alone on either surface of the 1:20 collagen:PCL biocomposite membranes were ascertained by immunohistochemistry assay. Double labeling of PHEK and 3T3 fibroblasts with the (primary) monoclonal mouse anti-cytokeratin 19 IgG 1:200 (Cat No.NCL-CK 19; Novocastra®, Inc.), and mouse anti-vimentin IgG 1:200 (Cat No.MAB3400; Chemicon® International, Inc.). The secondary antibodies used for detection of cytokeratin 19 and vimentin were rhodamine-conjugated polyclonal goat anti-mouse IgG 1:100 (Cat No.I1903-08C, United States Biological, Inc.), and the fluorescein (FITC)-conjugated polyclonal goat anti-mouse IgG 1:100 (Lot No.62686; Jackson ImmunoResearch Laboratories, Inc., USA) respectively. Thus, the keratinocytes will show in red fluorescent staining, and populated fibroblasts will show in green fluorescent staining in the co-cultured skin model.

3.6 Co-culture of single-donor PHEK and PHDF

To increase the resources of human keratinocyte and fibroblast cells, and mimic the normal clinical condition, primary human epidermal keratinocytes (PHEK) and primary human dermal fibroblast (PHDF) were isolated and cultured from the epidermal and dermal layers of single-donor human foreskin respectively in the this study. Co-culture of PHEK and PHDF on either side of the membrane was subsequently performed using the same co-culture system. The design of a novel co-cultured skin model was achieved by growing a confluent PHEK sheet on the biocomposite film upwards with a populated PHDF layer underneath followed by lifting the co-cultured membrane onto the air-fluid level for another 10 days to enhance keratinocyte differentiation. The co-culture procedure was therefore modified and described below briefly. PHEK (1.7×10^5 cells/cm^2; child foreskin) at passage 4 were firstly seeded on one side of the biocomposite film for about 6 days to achieve 80% to 90% confluence

compared to the control group of growing PHEK with the same seeding density on polystyrene in 24-well tissue culture plastics (TCP). Biocomposite film containing sub-confluent keratinocytes were then turned upside down and transferred to the co-culture system. PHDF (2×10^4 cells/cm^2; child foreskin) at passage 4 were thereby seeded on the other side (top surface) of biocomposite film for another 3 days (to achieve 100% confluence in keratinocyte culture on TCP). Finally, biocomposite films were turned upside down again and kept in submerge culture for another 6 days, and then lift onto the air-fluid level for another 10 days to enable keratinocyte differentiation.

3.6.1 Scanning electron microscopy (SEM)

Co-cultured skin models based on PHEK and PHDF were investigated by using SEM. The protocol for sample preparation was the same as that described in Section 2.2.7. Samples were finally attached to aluminum SEM stubs using carbon tabs (Agar Scientific), and then sputter coated with gold prior to examination using a HITACHI® 3000N Scanning Electron Microscope.

3.6.2 Immunohistochemistry assay

The growth and distribution of PHEK and PHDF alone on either surface of the biocomposite membranes were ascertained by immunohistochemistry assay. Double labeling of PHEK and PHDF with monoclonal mouse anti-human involucrin antibody 1:200 (Cat No.I8447-25; United States Biological, Inc.), and monoclonal mouse anti-human α tubulin antibody 1:200 (Cat No.sc-5286; Santa Cruz Biotechnology, Inc.) respectively. The secondary antibody used for detection of involucrin was rhodamine-conjugated goat anti-mouse IgG 1:100 (Cat No.I1903-08C, United States Biological, Inc.), and for the detection of α Tubulin was fluorescein (FITC)-conjugated goat anti-mouse IgG 1:100 (Lot No.62686; Jackson

ImmunoResearch Laboratories, Inc., USA). Thus, the keratinocytes will show in red fluorescent staining, and populated fibroblasts will show in green fluorescent staining in the co-cultured skin model.

3.7 Interaction of PHEK and PHDF in the co-culture system *in vitro*

Subepithelial fibroblasts in adult tissues, such as the oral mucosa and the skin, have shown their influence on both normal epithelial growth and regeneration during wound healing [127-131]. To investigate the interaction between skin keratinocytes and fibroblasts in the co-cultured skin mode based on 1:20 collagen:PCL biocomposites, we compared the keratinocyte growth factor (KGF) production (as a model) of fibroblast populations after co-culture with keratinocytes and after stimulation with the proinflammatory cytokine IL-1β. Differences in production of KGF may further help explain the obscure differences in epithelial cell kinetics and elucidate the significant characteristics of the co-cultured skin model.

3.7.1 Assays

In this study, fibroblasts were stimulated to produce KGF by co-culture with keratinocytes and IL-1β respectively. PHDF (adult foreskin) at passage 4-6 were seeded on polystyrene in 24-well plates, on 1:20 collagen:PCL biocomposites in 7 ml glass vials, or in the co-cultured skin model with the same cell seeding number of 2.4×10^4 cells in 3ml DMEM/0.5% FCS culture medium. The fibroblasts were cultured in DMEM/10% FCS culture medium for 3 days, and then serum-starved for 3 days in DMEM/0.5% FCS culture medium. Keratinocytes from the same donor at passage 2-4 were firstly seeded on 1:20 collagen:PCL biocomposites with the cell seeding density of 1.7×10^5 cells/cm^2 in serum-free EpiLife® medium (M-EPI-012-5; Cascade Biologicals, Inc.) for 3 days, and then the biocomposite membranes

were turned upside down and seeded with PHDF (2.4×10^4 cells in total) on the top surface of membranes to serve as the study group of co-cultured skin model. At the time of stimulation, fresh DMEM containing 0.5% FCS was added to all fibroblast cultures including the co-culture system. Cytokine stimulation of the fibroblast cultures was performed by addition of 10 ng/ml recombinant human IL-1β (R & D System, Oxford, UK). Cultures without keratinocytes and cytokine stimulation served as controls. The culture medium was not changed during the experiment, and collected after 24, 48 hours and stored at -80℃. KGF proteins in the supernatants from the above study groups were determined by ELISA and the values compared.

3.7.2 KGF ELISA

Human KGF sandwich ELISA was performed using standards and matched cytokine antibody pairs (R & D System) according to the manufacturer's protocol. These assays recognize both natural and recombinant KGF, with no significant cross-reactivity or influence with other cytokines, as described by the manufacturer. In brief, microtitre plates were coated with 5μg/ml anti-KGF monoclonal antibody in PBS overnight and blocked with PBS containing 5% sucrose, 1% BSA and 0.05% NaN_3 for 1 hour. These and all other incubations were performed at room temperature. Between each of the described steps in the procedure the plates were washed three times with PBS (pH 7.4) containing 0.5% Tween 20. Standards and samples diluted in Tris-buffered saline (pH 7.3) containing 0.1% BSA and 0.05% Tween 20 were dispensed into each well and the plates were incubated for 2 hours. Biotinylated polyclonal goat anti-human antibody at a concentration of 50μg/ml for KGF was added and the plates were incubated for 2 hours. Following incubation with Streptavidin HRP solution for 20 minutes the color reagent tetramethylbenzidine (TMB) was added for 30 minutes to develop a blue color. The reaction was stopped with 1M H_2SO_4. Absorbance was read at 450 nm by an automatic plate reader with a reference wavelength of 570 nm.

3.7.3 Statistical analysis

In comparing data sets, the similarity of the variance of the sets was determined using the F-test, and the sets were then compared by paired t-test using equal or unequal variances as appropriate. Error bars and tolerances represent 95% confidence limits.

CHAPTER FOUR

IN VIVO ANIMAL STUDY FOR THE CO-CULTURED SKIN MODEL

4.1 Experimental design

To investigate the biocompatibility of co-cultured skin model based on 1:20 collagen:PCL biocomposites *in vivo*, grafting of co-cultured skin substitute to athymic mice was performed under aseptic conditions. For all experiments reported here, tissue-engineered co-cultured skin model (n=3), biocomposite only (without cell seeding) group (n=3), and sustained open wound group (n=3) were included in this study. A preliminary *in vivo* study was conducted to evaluate the biocompatibility of co-cultured skin model grafted to athymic mice.

4.2 Preparation of co-cultured skin substitutes

Tissue-engineered skin models were prepared from PHEK and PHDF sequentially inoculated onto 1:20 collagen:PCL biocomposite substrates. There was a 3- to 6-days interval between keratinocyte and fibroblast inoculation, with the latter identified as culture day 0. On day 3, the co-cultured skin models were turned upside down to keep the keratinocyte layer on the top and then were incubated (5% CO_2, 37℃, saturated humidity) at the air-liquid interface of the culture medium for another 10 more days to enable the differentiation of keratinocytes. Nutrient media were changed every other day throughout *in vitro* culture. The confluence of epidermal layer was proven by SEM and immunohistochemistry assay. All co-cultured skin models in round shape with 1.2 cm in diameter were prepared for grafting to athymic mice without meshing or pretreatment with any other agents.

4.3 Animal surgery

All animals were acquired, housed and studied under a protocol approved by the Institutional Animal Care and Use Committee of National Defense Medical Center, R.O.C. Grafting of co-cultured skin model to athymic mice was performed under aseptic conditions using

procedures described below. Skin substitutes were grafted orthotopically to full-thickness skin wounds (in round shape with 1.2cm in diameter) surgically created to the depth of the panniculus carnosus on the flanks of athymic mice. Grafts were attached with 4 stent-sutures at the wound margin, and then were covered with gel-type medium containing DMEM/gelatin/agarose/10% FCS covered with Tagaderm® transparent film, and finally sealed and fixed with elastic Omnifix® non-woven retention tapes (Hartmann Inc., Spain) to the surrounding murine skin. No gauzes were used as dressings and no post-operative treatments were given in this study. At 1 week after surgery, all dressings and sutures were removed, data were collected, and the healing wounds were left open to the air. The data of clinical evaluation of graft taking and surface area were collected at weekly intervals for the remainder of the *in vivo* study periods.

4.4 Assessment of biocompatibility of co-cultured skin model *in vivo*

The *in vivo* biocompatibility of co-cultured skin substitutes was investigated by grafting onto a surgical wound of athymic mice in this work. Evaluation was based on the clinical inspection and histological studies.

4.4.1 Clinical evaluation of graft taking

The wound healing process was recorded by photography periodically in a certain period of time. Furthermore, the wound size and clinical appearance were evaluated by the main investigator.

4.4.2 Histological study with frozen section and immunohistochemistry

The athymic mice were sacrificed and the specimen including biocomposite and adjacent normal mouse tissue were widely excised for histological study periodically in a certain period of time. Frozen section of the specimen was performed and the immunohistochemistry assay was used to evaluate the biocompatibility of grafts.

The growth and distribution of PHEK and PHDF on 1:20 collagen:PCL biocomposite membranes engrafted on the back skin defect of athymic mice for a certain period of time were ascertained by immunohistochemistry assay. PHEK was labeled with monoclonal mouse anti-human involucrin antibody 1:200 (Cat No.I8447-25; United States Biological, Inc.). The secondary antibody used for detection of involucrin was rhodamine-conjugated goat anti-mouse IgG 1:100 (Cat No.I1903-08C, United States Biological, Inc.). On the other hand, the survival of human-origin fibroblasts/epithelial cells in graft was further confirmed by labeling PHEK and PHDF with monoclonal mouse anti-human D7-FIB antibody 1:200 (Cat No.NB 600-777; Novus® Biologicals, Inc.) that will not cross-react with mouse or rat, and the secondary antibody of rhodamine-conjugated goat anti-mouse IgG 1:100 (Cat No.I1903-08C, United States Biological, Inc.). Thus, the human-origin fibroblasts/epithelial cells will show in red fluorescent staining alone in the co-cultured skin model *in vivo*.

4.4.3 Histological study with paraffin wax-embedded H & E staining method

To distinguish the nuclei (blue-black) and cytoplasm (pink) in terms of the status of cell attachment, growth and distribution on the surface of the co-cultured skin model engrafted on the back wound of athymic mice *in vivo*, the specimen was investigated using the H & E (Harris hematoxylin and Eosin-Y) staining method with paraffin wax embedding procedure. The protocol for paraffin wax-embedded H & E staining method was described in detail as

below. The samples of co-cultured skin model engrafted on athymic mice *in vivo* were firstly obtained and fixed in 10% formalin. Samples were then embedded in wax and stored in fridge at – 20℃. A slice machine (Microm® HM 400) was used for cross resection of the samples with 10μm in thickness. The slice of samples were transferred into a flotation bath (Fisher® Tissue Prep™ Flotation Bath Model 134) at 30℃, and then were transferred to water bath at 25℃ for cooling, and onto glass slides afterwards. After that, the slides were placed in an oven at 56℃ for 15 to 20 minutes for dewaxing. In the following processing, the slides were firstly soaked in Xylene solution for 5 minutes twice, and then were washed in 99% Ethanol for 1 to 3 minutes once. Tap water irrigation was performed on the beneath side of slides for 30 seconds. Then, the slides were soaked in Harris hematoxylin for another 1 to 5 monutes followed by the same procedure of tape water irrigation for 30 seconds. After that, the slides were washed in 50% and 70% Ethanol for 1 minute respectively, and were soaked in 1% Eosin Y for 5 to 10 minutes. In the final stage, the slides were washed in a serial increasing concentration of Ethanol (75%, 80%, 90% and 95%) and 99% Ethanol/ Xylene (1:1) for 1 minute respectively, and then were soaked in Xylene solution for 5 minutes twice. The slides were finally inspected using light microscopy after mounting and drying in hood for 4 hours.

4.4.4 Histological study with frozen section and Gomori's trichrome staining

Gomori's trichrome is a staining procedure that combines the plasma stain (chromotrope 2R) and connective fiber stain (light green SF) in a phosphotungstic acid solution to which glacial acetic acid has been added. The staining method was selected to distinguish the nuclei (blue-black), cytoplasm (red) and collagen (green) in terms of the status of cell attachment, growth and distribution on the surface of the co-cultured skin model.

To evaluate the histological change of the co-cultured biocomposite membrane by using the Gomori's trichrome staining method, the frozen section of the skin specimen of athymic mice was performed firstly followed by fixing in methanol/acetone (1:1) solution for 30 minutes at 4℃, and then was rehydrated in descending alcohol solutions (100% x 2, 90%, 80% and 70%) for 5 minutes each followed by rinsing with tap water. The sample was then immersed in Harris Hematoxylin for 5 minutes followed by washing in tap water until the water is clear. Thereafter, the sample was placed in Gomori's trichrome stain (solution A) for 25 minutes and then quickly rinsed with distilled water followed by rinsing in solution B for 5 seconds. Finally the sample was dehydrated in ascending alcohol solutions (95% x 2, 100% x 2) for 5 minutes each, and then was placed onto a glass slide to be investigated using light microscopy. Xylene was not used here due to adverse effect on the structure of collagen:PCL biocomposite film during staining procedure in this study.

CHAPTER FIVE

RESULTS

5.1 Study on collagen:PCL biocomposites

5.1.1 Analysis of pH changes due to incubation of collagen:PCL biocomposites in PBS

Collagen:PCL biocomposites (1:4, 1:8 and 1:20) prepared from collagen solution of pH 2.7 were used in this experiment. Collagen solution with a pH of 7.4 will gel in about one hour at room temperature. Collagen:PCL biocomposites prepared from 0.25% collagen solution (pH 7.4) and gel respectively with ratios of 1:4, 1:8 and 1:20 were also included. No significant variations of pH value were found between the biocomposites having varying collagen:PCL ratio.

The purpose of monitoring pH changes due to incubation of collagen:PCL biocomposites in PBS was to predict the pH trends in the cell culture environment due to concerns over the effect of the acidic properties of the biocomposites on cell attachment and growth. The acid content of the biocomposite depends on the acid strength used to dissolve the collagen initially. Volatile acids are removed to some extent during freeze-drying, while solid acids remain completely in the dry product. Acetic acid evaporates partially during freeze-drying [130]. The 0.25% collagen solution used for preparation of biocomposite films had a pH value of 2.7 before freeze-drying. Thus it was necessary to check the pH value induced in PBS incubation media containing collagen:PCL biocomposite material. The results in Figure 4 revealed that the pH of PBS media containing collagen:PCL biocomposites prepared using 0.25% collagen solution of pH 2.7 varied between 7.16 and 7.32 over 14 days. A low pH value of 7.16 was recorded on day 1, but the pH increased rapidly and reached a plateau ranging from 7.23 to 7.31 by day 3 (Figure 4). On the other hand, collagen:PCL biocomposites prepared using both 0.25% collagen solution and collagen gel respectively with a pH value of 7.4 resulted in similar pH values ranging from 7.2 to 7.33 over 14 days (Figure 5 and 6). A higher pH around 7.4 was recorded for the 1:20 biocomposite on day 1.

The pH trends in all study groups are similar although a small decrease in pH 7.16 was recorded on day 1 for collagen:PCL biocomposites prepared from 0.25% collagen solution of pH of 2.7 (Figure 4). A change of culture medium during cell culture after day 1 could be carried out to resolve this problem, if necessary.

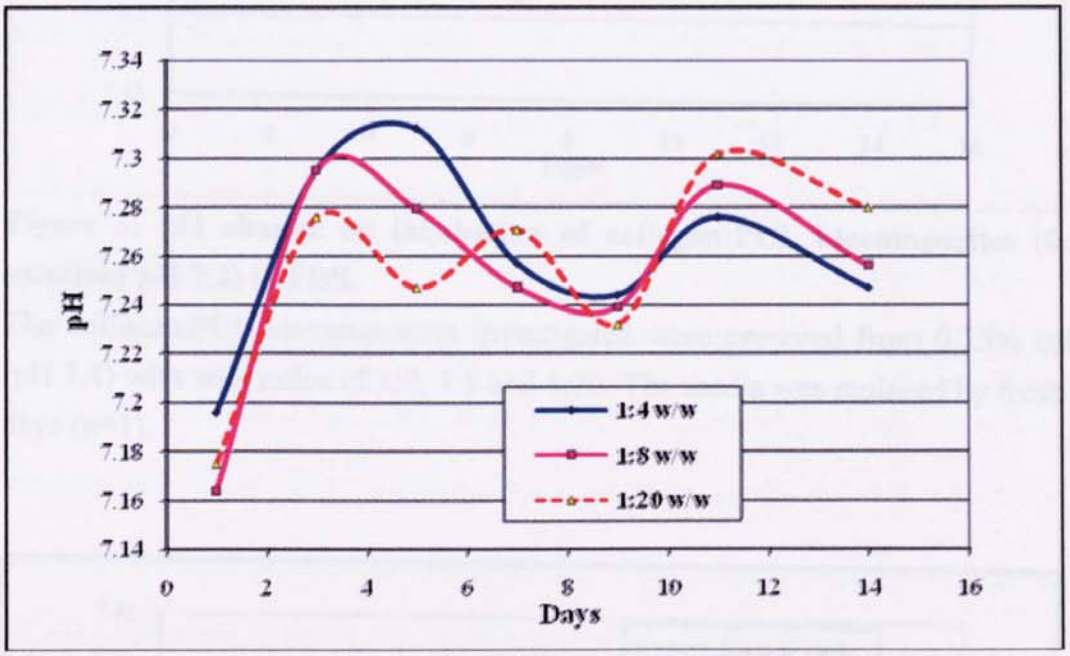

Figure 4: pH change on incubation of collagen:PCL biocomposites (0.25% collagen solution; pH 2.7) in PBS.

The collagen:PCL biocomposites investigated were prepared from 0.25% collagen solution (pH 2.7) with w/w ratios of 1:4, 1:8 and 1:20. The media was replaced by fresh PBS every 2-3 days (n=1).

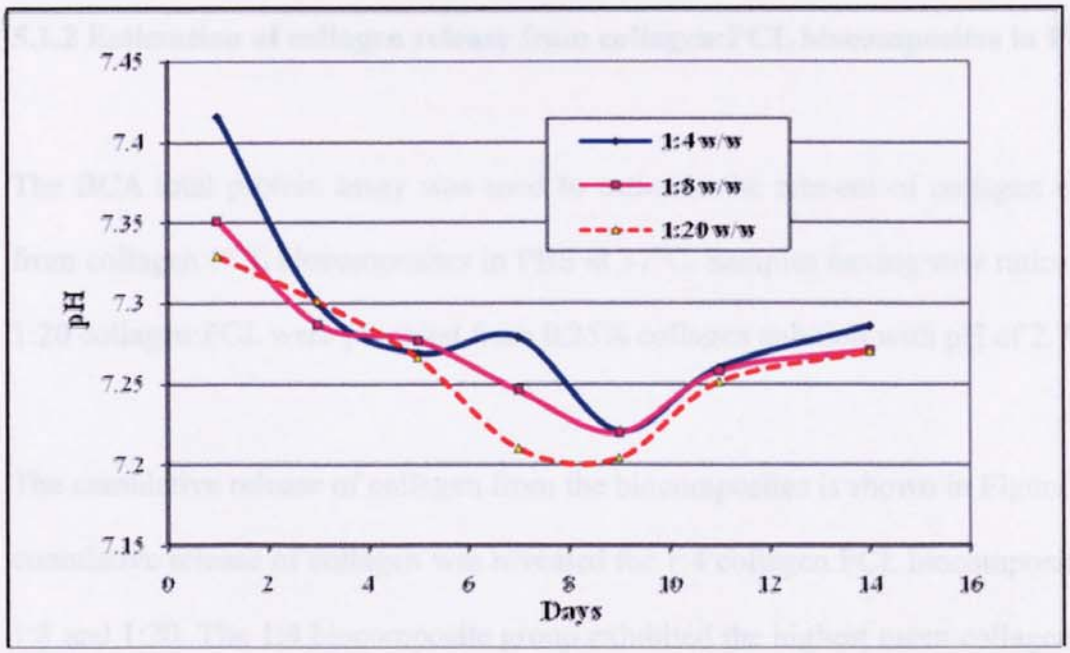

Figure 5: pH change on incubation of collagen:PCL biocomposites (0.25% collagen solution; pH 7.4) in PBS.

The collagen:PCL biocomposites investigated were prepared from 0.25% collagen solution (pH 7.4) with w/w ratios of 1:4, 1:8 and 1:20. The media was replaced by fresh PBS every 2-3 days (n=1).

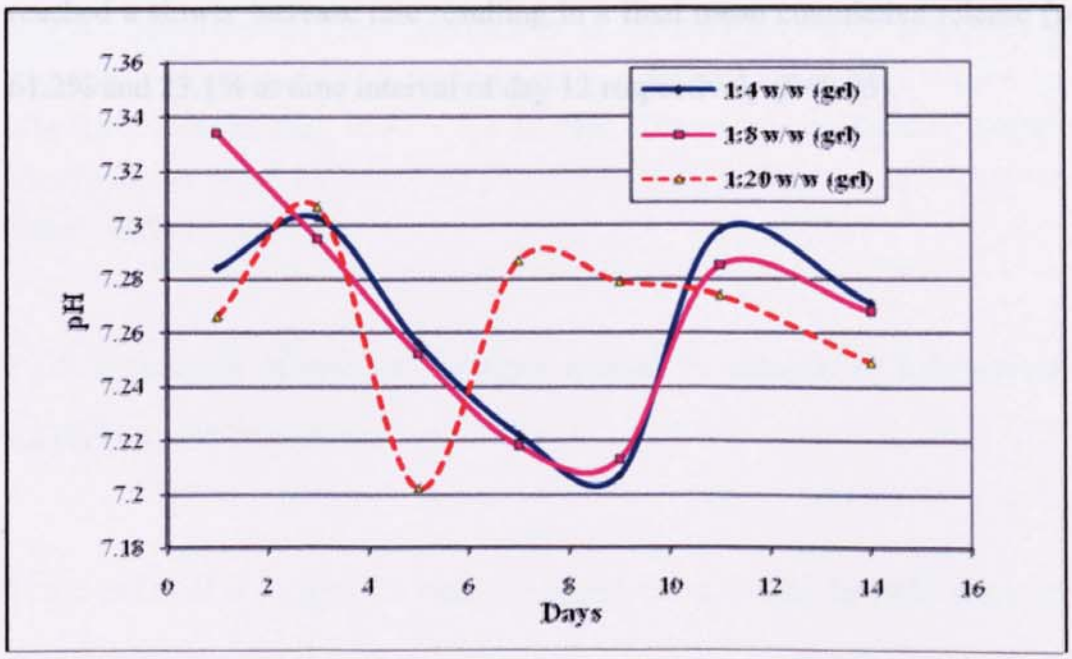

Figure 6: pH change on incubation of collagen:PCL biocomposites (0.25% collagen gel; pH 7.4) in PBS.

The collagen:PCL biocomposites investigated were prepared from 0.25% collagen gel (pH 7.4) with w/w ratios of 1:4, 1:8 and 1:20. The media was replaced by fresh PBS every 2-3 days (n=1).

5.1.2 Estimation of collagen release from collagen:PCL biocomposites in PBS at 37°C

The BCA total protein assay was used to estimate the amount of collagen content released from collagen:PCL biocomposites in PBS at 37°C. Samples having w/w ratios of 1:4, 1:8 and 1:20 collagen:PCL were prepared from 0.25% collagen solution with pH of 2.7.

The cumulative release of collagen from the biocomposites is shown in Figure 7. The highest cumulative release of collagen was revealed for 1:4 collagen:PCL biocomposite, followed by 1:8 and 1:20. The 1:4 biocomposite group exhibited the highest mean collagen release rate at 6 hours with about 40.1% of the original collagen content being released into PBS, while 16% and 6.2% were released from 1:8 and 1:20 biocomposites respectively ($P<0.05$). The amount of collagen released significantly increased within 24 hours for all the biocomposites investigated. After 24 hours, the release of collagen in 1:4, 1:8 and 1:20 biocomposites reached a slower increase rate resulting in a final mean cumulative release (w/w) of 86.8%, 61.2% and 23.1% at time interval of day 12 respectively ($P<0.05$).

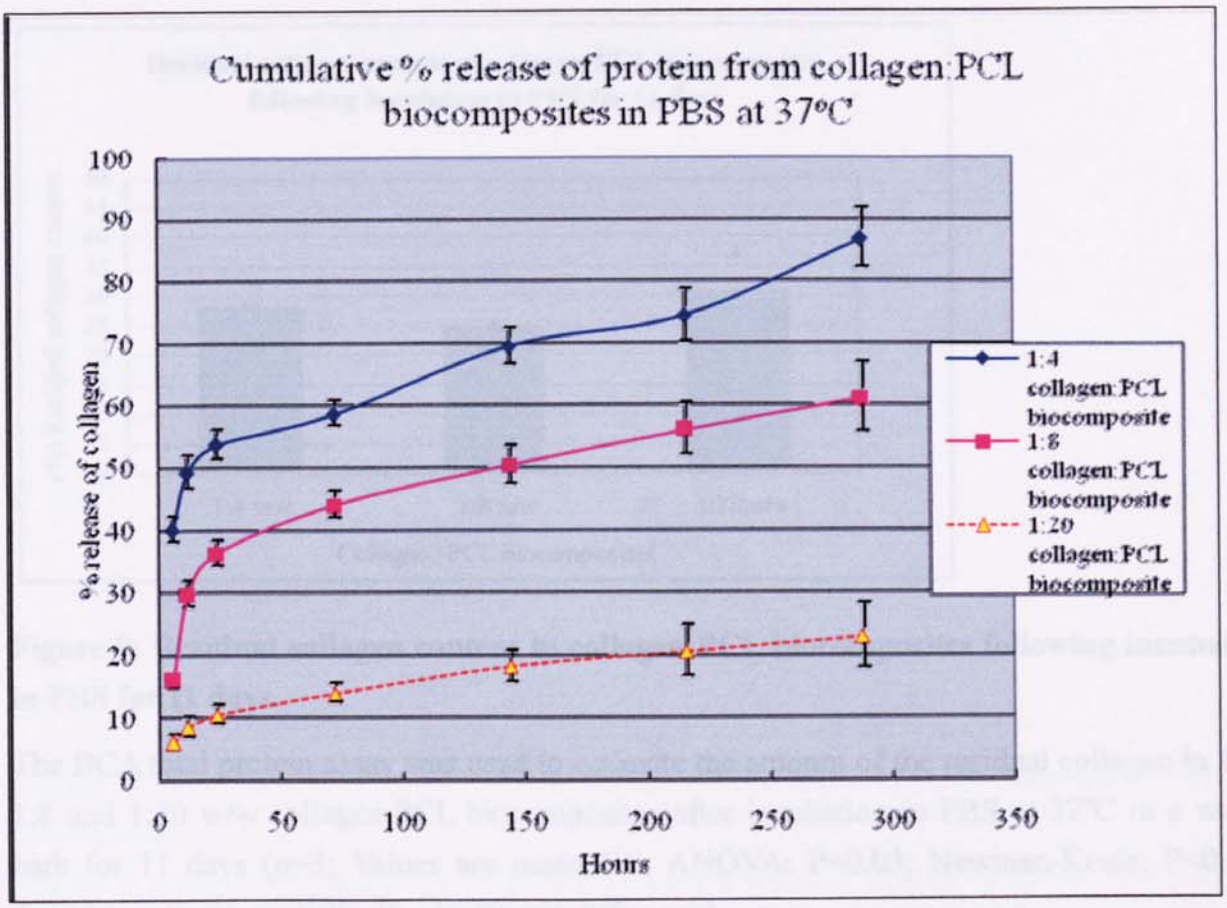

Figure 7: Cumulative release of collagen from collagen:PCL biocomposites in PBS at 37°C.

The BCA total protein assay was used to estimate the amount of collagen release in 1:4, 1:8 and 1:20 w/w collagen:PCL biocomposites (prepared by 0.25% collagen solution; pH 2.7) after incubation in PBS at 37°C for 12 days. The release media were analysed for collagen content and replaced by fresh PBS periodically (n=3; Values are mean±SE; ANOVA: $P<0.05$; Newman-Keuls: $P<0.05$).

5.1.3 Estimation of residual collagen content of collagen:PCL biocomposites following incubation in PBS at 37°C

The samples of collagen:PCL biocomposites were collected for BCA assay after incubation in PBS for 11 days and the residual collagen content was analyzed as described in Section 2.2.3. Collagen:PCL biocomposite with a w/w ratio of 1:20 displayed the highest residual collagen content of 30.5±0.3%, followed by 27.8±0.6% in 1:4 biocomposite samples and 24.4±0.7% in the 1:8 materials (n=3; Values are mean±SE; ANOVA: $P<0.05$; Newman-Keuls: $P<0.05$). The results are shown in Figure 8.

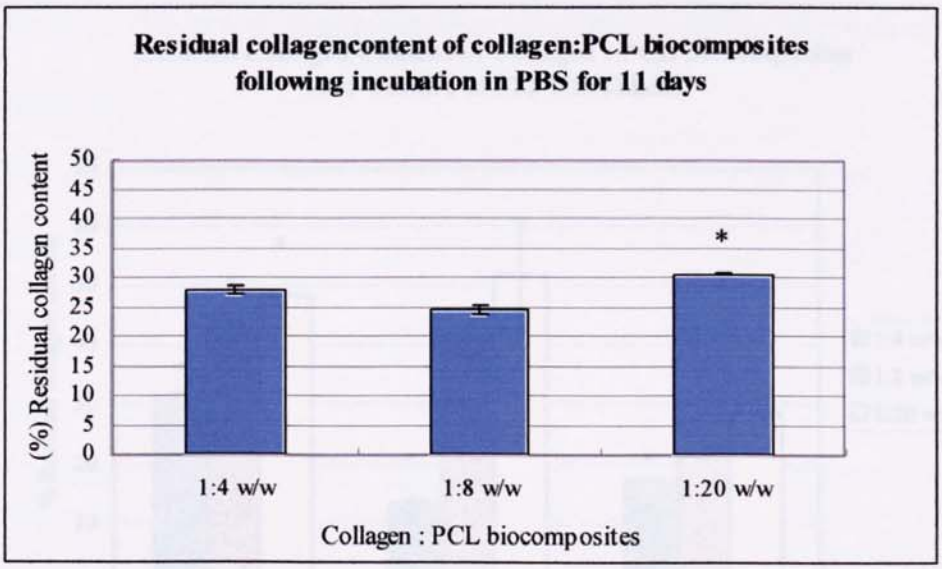

Figure 8: Residual collagen content in collagen:PCL biocomposites following incubation in PBS for 11 days.

The BCA total protein assay was used to estimate the amount of the residual collagen in 1:4, 1:8 and 1:20 w/w collagen:PCL biocomposites after incubation in PBS at 37°C in a water bath for 11 days (n=3; Values are mean±SE; ANOVA: $P<0.05$; Newman-Keuls: $P<0.05$; Asterisk indicates statistically significant difference).

5.1.4 Estimation of residual collagen content of collagen:PCL biocomposites following fibroblast cell culture

In order to investigate the possible association between the residual collagen content of collagen:PCL biocomposites and cell growth characteristics, the BCA assay for estimation of residual collagen content was performed on biocomposite samples following cell culture using 3T3 fibroblasts on day 1, 8 and 11. The results are shown in Figure 9. On day1, 1:20 collagen:PCL biocomposite exhibited the highest amount of residual collagen of 48.2±0.1%, followed by 43.7±0.5% for 1:8 and 31.3±0.7% for 1:4 collagen:PCL samples. On day 11, the 1:20 biocomposite exhibited the highest residual collagen content of 28.5±0.6%, followed by 21.1±0.9% for 1:8 and 17.3±0.1% for 1:4 samples (n=3; Values are mean±SE; ANOVA: $P<0.05$; Newman-Keuls: $P<0.05$).

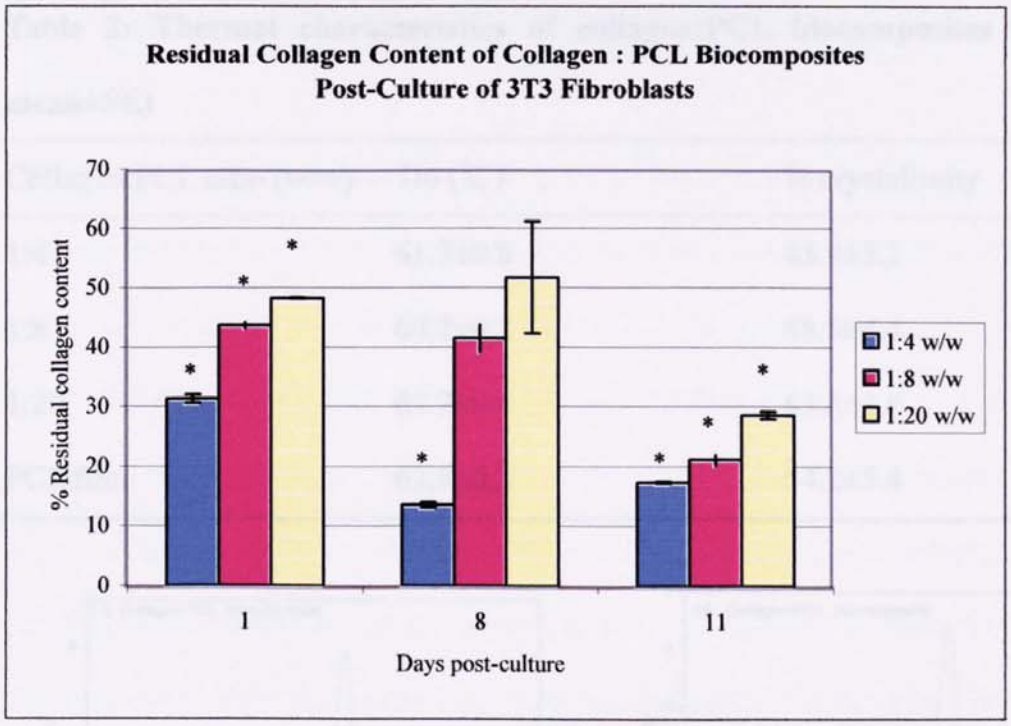

Figure 9: Residual collagen content in collagen:PCL biocomposites post-culture of 3T3 fibroblasts.

The BCA total protein assay was used to estimate the residual amount of collagen in 1:4, 1:8 and 1:20 collagen:PCL biocomposites post-culture with 3T3 fibroblasts on consecutive days. The biocomposite samples were collected after cell detachment and cell counting (n=3; Values are mean±SE; ANOVA: $P<0.05$; Newman-Keuls: $P<0.05$; Asterisk indicates statistically significant differences).

5.1.5 Differential Scanning Calorimetry (DSC) for collagen:PCL biocomposites

The thermal analysis of collagen:PCL biocomposites (n=3) is shown in Table 2. The melting point of the PCL phase was close to the value of 60℃ normally quoted for PCL. The mean percentage crystallinity of the PCL phase in the high collagen content (1:4 and 1:8 w/w) materials tended to be lower than that of solvent cast films. A reduction in crystallinity of around 20% was measured in the case of the highest collagen loaded (1:4 w/w) materials. In contrast the average % crystallinity of the PCL phase in the lowest collagen content (1:20 w/w) composite was found to increase by almost 18% relative to the solvent cast films. The DSC scan of 1:4, 1:8 and 1:20 w/w collagen:PCL biocomposites was shown in Figure 10.

Table 2: Thermal characteristics of collagen:PCL biocomposites (n=3; Values are mean±SE)

Collagen:PCL ratio (w/w)	Tm (°C)	% crystallinity
1:4	61.7±0.8	43.4±5.2
1:8	60.7±0.2	48.5±4.4
1:20	63.7±0.4	63.5±3.8
PCL film	62.8±0.2	54.2±5.4

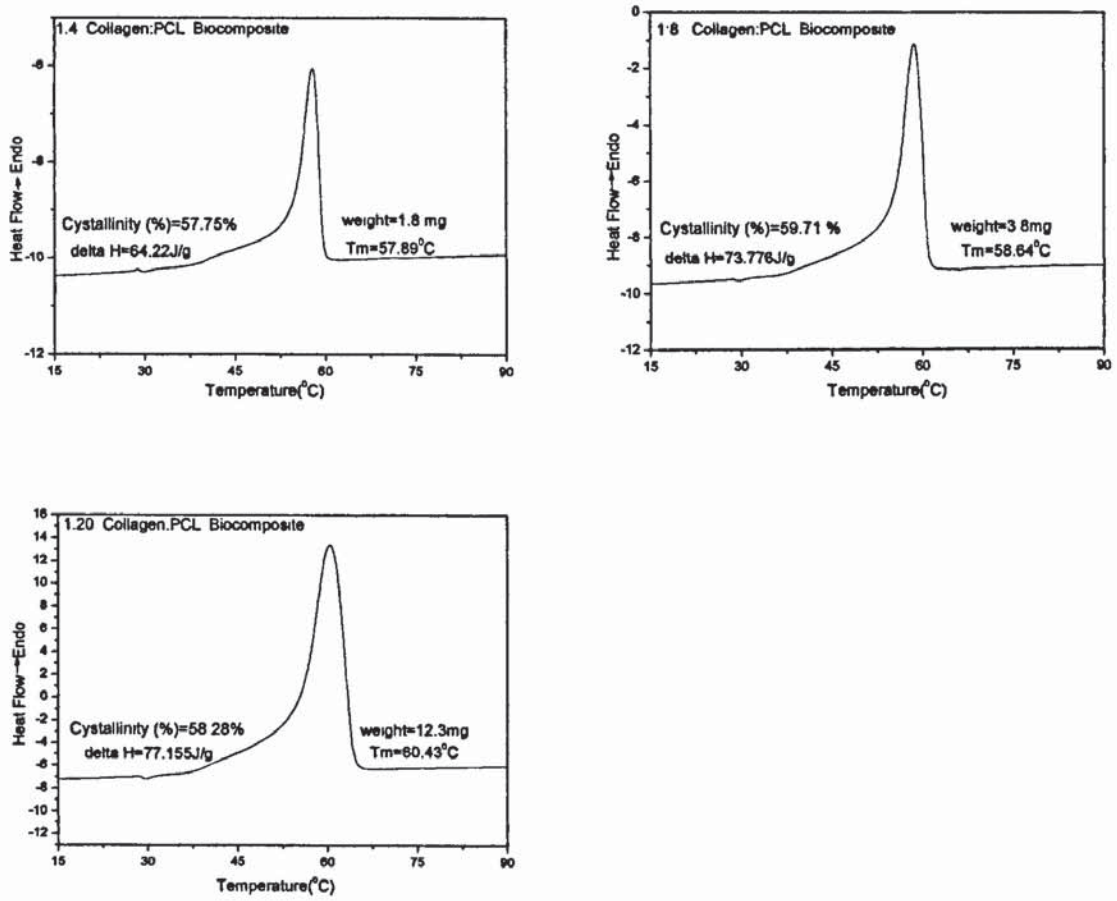

Figure 10: Differential scanning calorimetry scan of 1:4, 1:8 and 1:20 w/w collagen:PCL biocomposites. (Tm: melting temperature; Endo: endothermic; data H: enthalpy)

5.1.6 Scanning electron microscopy (SEM)

The morphology of collagen:PCL biocomposites before and after incubation in PBS was investigated using SEM to identify the changes due to collagen release, which could influence cell attachment and growth (Figures 11 to 13). The 1:4 biocomposites before incubation in PBS exhibit a rough, fibrous surface due to the collagen mat structure and smooth overlying areas that could be formed by the PCL phase. Little differences in morphology were apparent after incubation for seven days in PBS at 37°C. The 1:8 biocomposites exhibited a greater masking or coating effect of the fibrous structure to produce a smoother surface than the 1:4 biocomposites. Pore formation was more pronounced in 1:8 samples that had been incubated for 3 and 7 days. The 1:20 biocomposites were characterised by a roughened dimpled surface texture and separated pores with sizes ranging from approximately 20 to 60 μm in diameter. More pores are present in the micrograph of samples incubated for 7 days but further analysis is requested to establish whether or not this is representative of the total sample area.

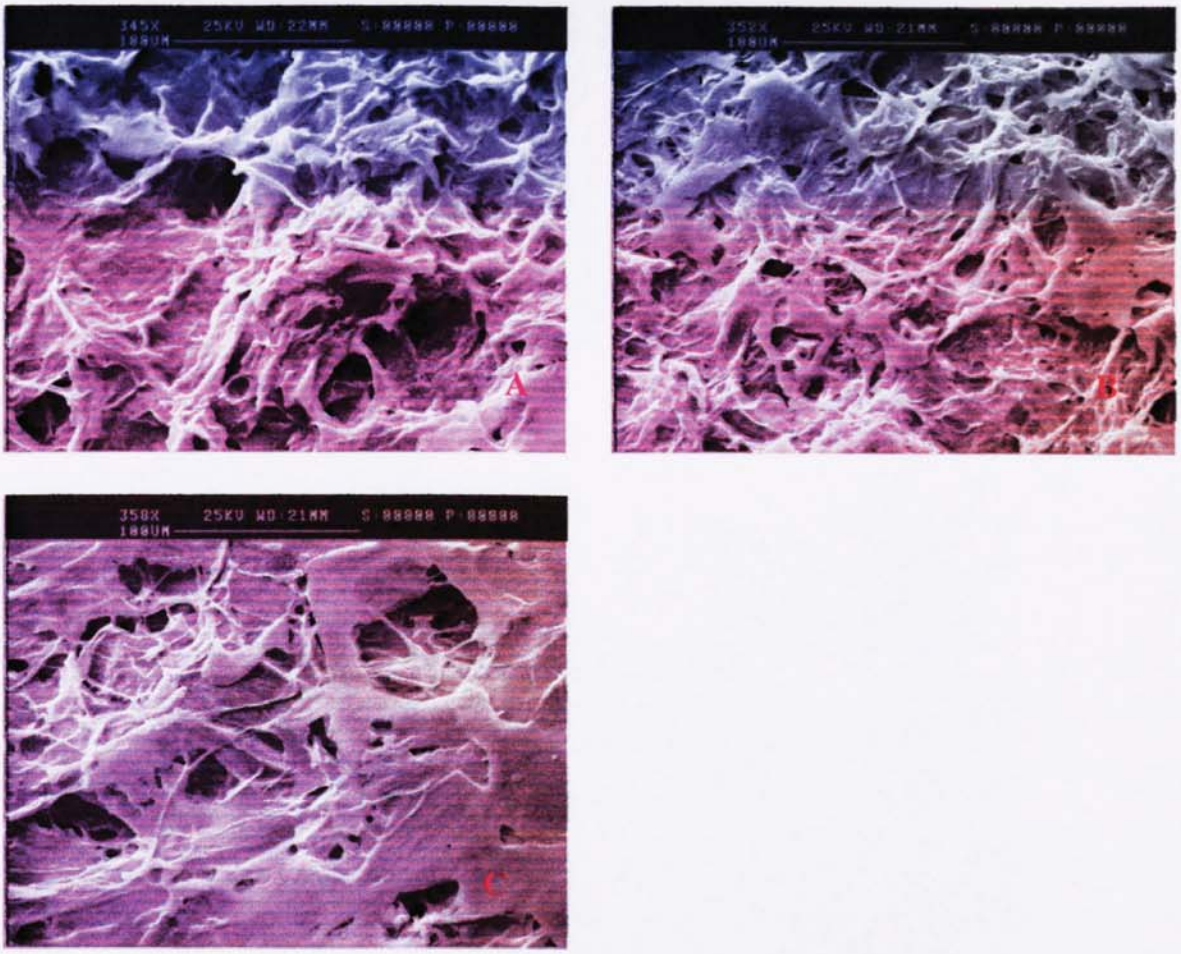

Figure 11: SEM of 1:4 w/w collagen:PCL biocomposites before (A) and after incubation in PBS at 37°C for 3 (B) and 7 (C) days.

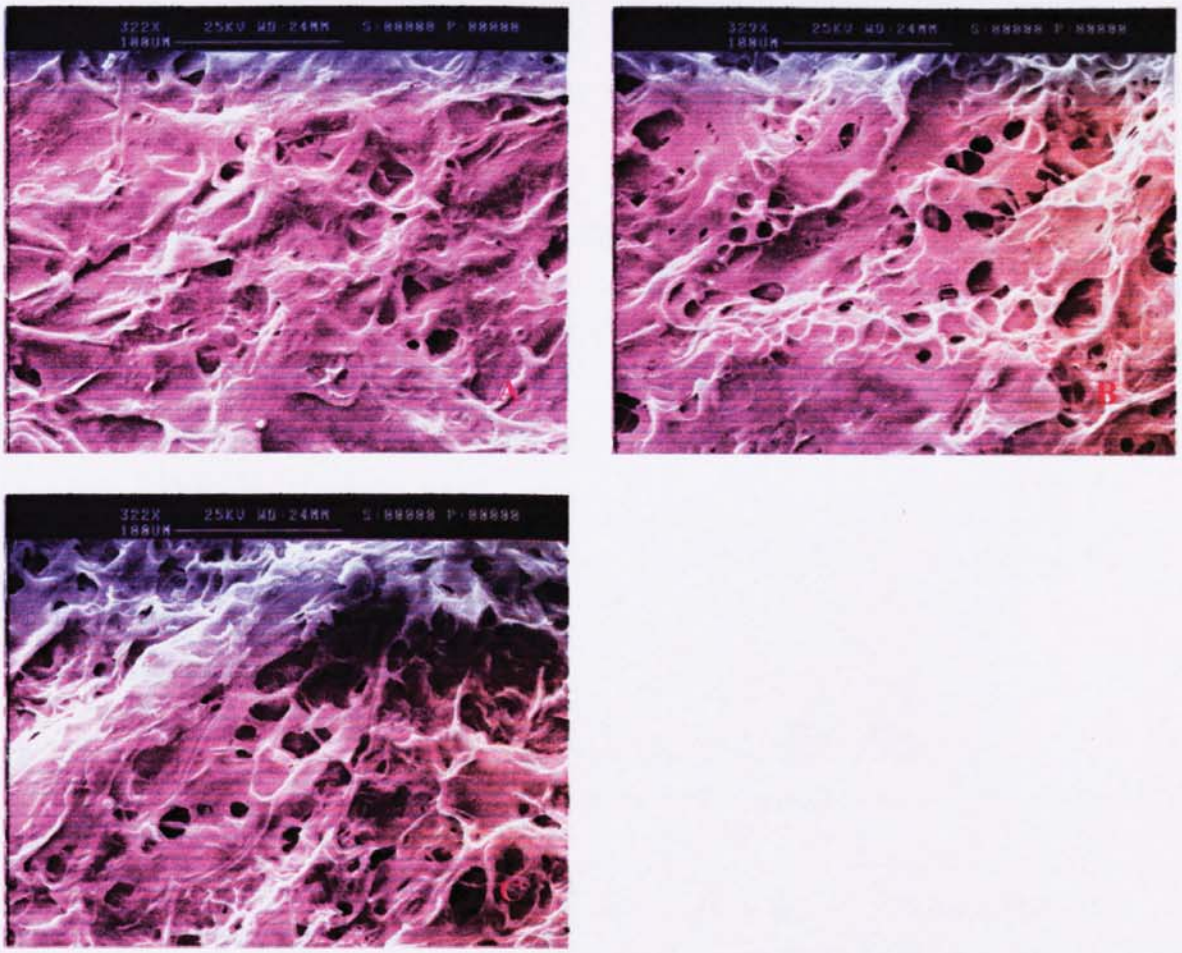

Figure 12: SEM of 1:8 w/w collagen:PCL biocomposites before (A) and after incubation in PBS at 37°C for 3 (B) and 7 (C) days.

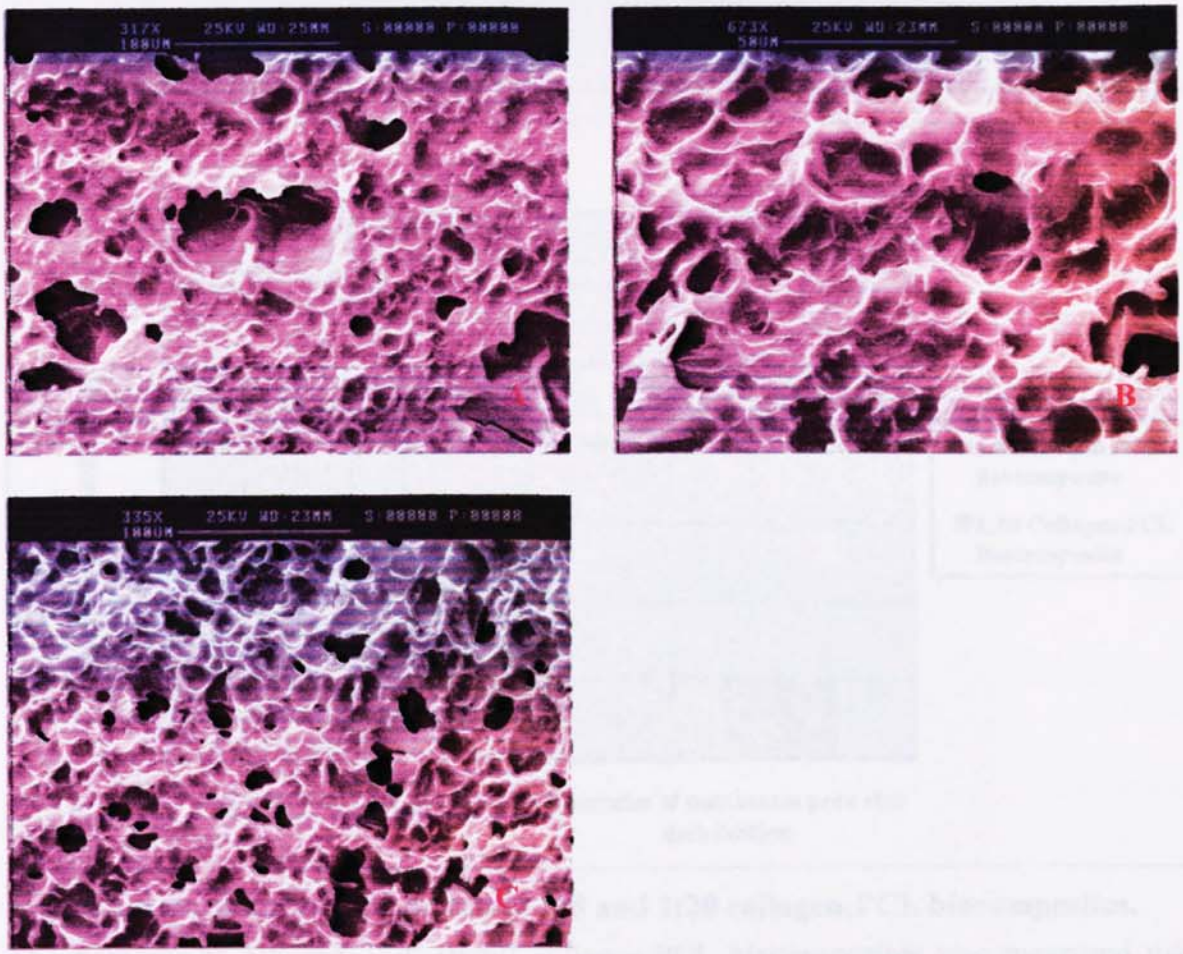

Figure 13: SEM of 1:20 w/w collagen:PCL biocomposites before (A) and after incubation in PBS at 37°C for 3 (B) and 7 (C) days.

5.1.7 Capillary Flow Analysis

The porosity of 1:4, 1:8 and 1:20 (w/w) collagen:PCL biocomposites was measured using the Automated Capillary Flow Porometer (PMI®, CFP-1200-A, Porous Materials, Inc.). The study group of 1:4 collagen:PCL biocomposite films were finally excluded in the study due to the early tearing of the membranes during processing (data was not shown in here). Therefore, only the 1:8 and 1:20 groups were included in this study, and the results were shown in Figure 14. Higher mean bubble point pore size in diameter, in terms of the maximum pore size, was measured as 47.1 ± 11.5μm (n=3) in the 1:8 group (ranged from 22.18 to 77.63μm) compared to that of 28.8 ±16.1μm (n=3) in the 1:20 group (ranged from 5.6 to 75.41μm); however, no significant differences were apparent (P=0.391). Furthermore, both 1:8 and 1:20 groups exhibited the similar pore size of 9 to 10μm in diameter at the maximum pore size distribution (P=0.739).

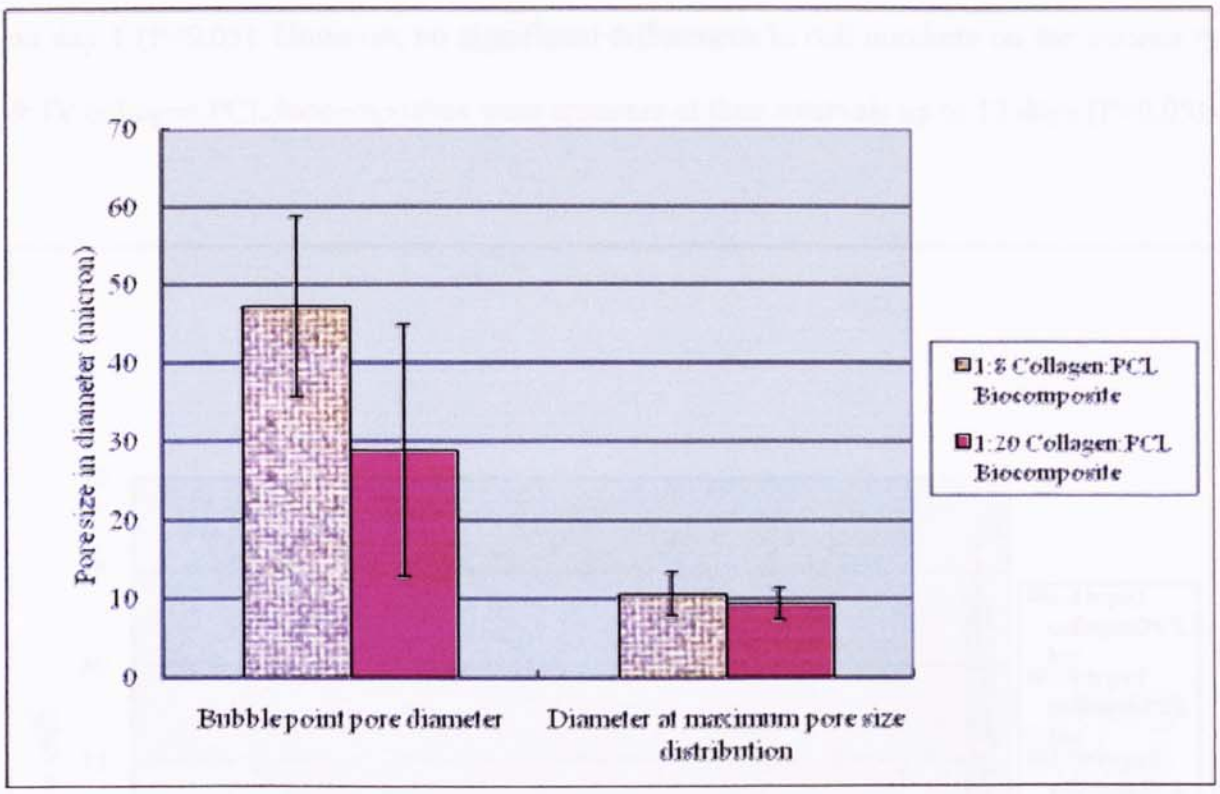

Figure 14: Porosity measurements of 1:8 and 1:20 collagen:PCL biocomposites.
The porosity of 1:8 and 1:20 (w/w) collagen:PCL biocomposites was measured using the Automated Capillary Flow Porometer (n=4; Values are mean±SE; Paired t-test: $P>0.05$).

5.1.8 Interaction of 3T3 fibroblasts with collagen:PCL biocomposites

Mouse 3T3 fibroblasts were seeded on the top surface of type I & IV collagen:PCL biocomposites and TCP (24-well tissue culture plastics) at a cell density of $3.5x10^4$ per cm^2 for time intervals up to 12 days. Trypsin-EDTA solution was used for cell detachment followed by cell counting at day 1, 4, 8 and 12 using a Weber's haemocytometer.

The proliferation rates of 3T3 fibroblasts on type I & IV collagen:PCL biocomposites (1:4, 1:8 and 1:20), and TCP surfaces are shown in Figure 15. The TCP surface showed the best cell attachment on day 1, 8 and 12 ($P<0.05$), and a better cell growth was shown in TCP group ($1.0x10^5$ per cm^2) compared to the groups of 1:20 (type I) collagen:PCL, and 1:8 & 1:20 (type IV) collagen:PCL biocomposites ($P<0.05$) on day 4. The 1:8 (type I) collagen:PCL

biocomposite group has the better cell attachment compared to the other biocomposite groups on day 1 ($P<0.05$). However, no significant differences in cell numbers on the various type I & IV collagen:PCL biocomposites were apparent at time intervals up to 12 days ($P>0.05$).

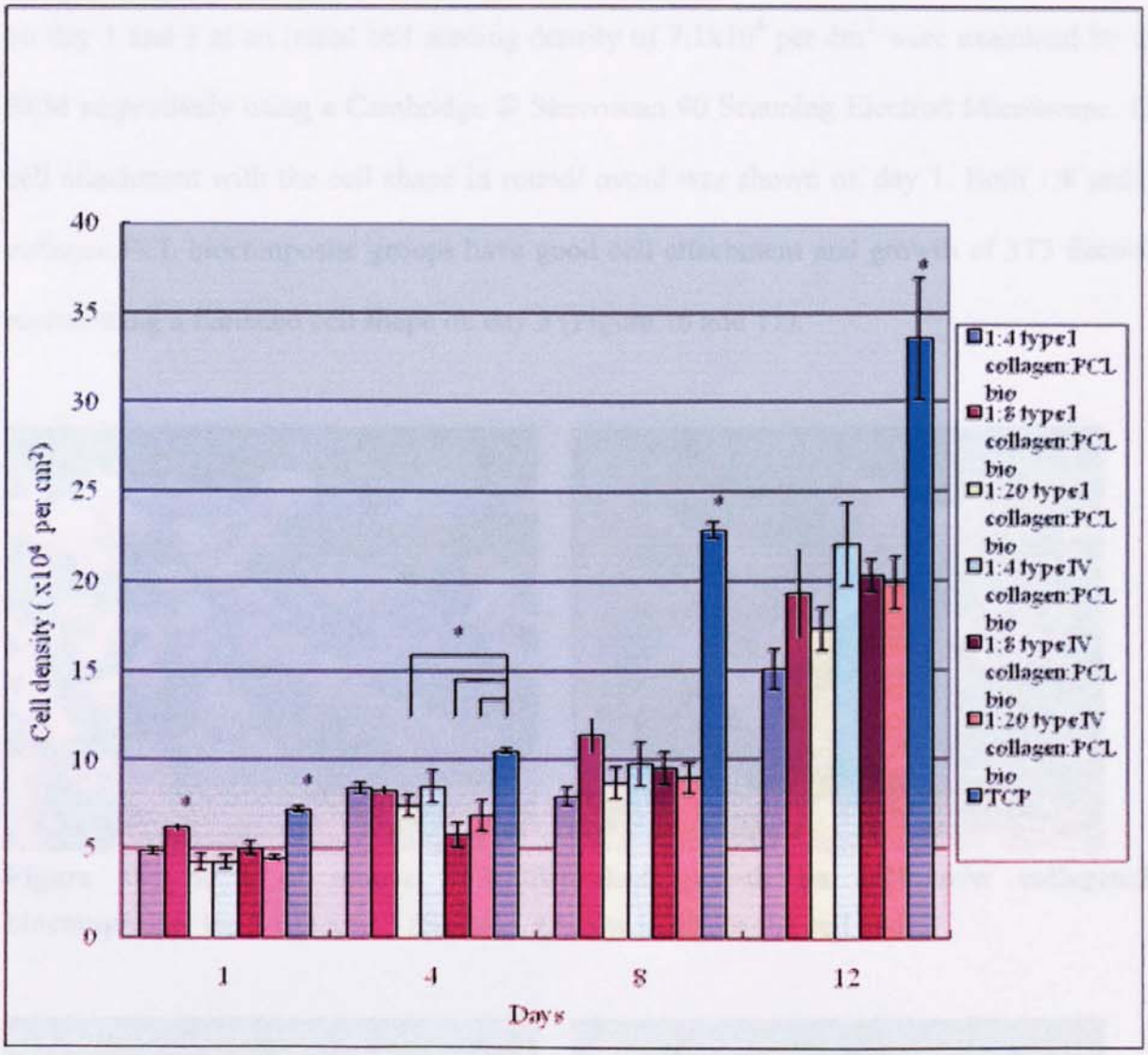

Figure 15: Comparison of 3T3 fibroblast growth on 1:4, 1:8 and 1:20 w/w type I & IV collagen:PCL biocomposites and TCP.

Mouse 3T3 fibroblasts ($3.5x10^4$ cells per cm^2) were seeded in 7 ml glass shell vials containing 1:4, 1:8 and 1:20 w/w type I (S1) & type IV (S2) collagen:PCL biocomposites and TCP over 12 days. Cell counting was performed at day 1, 4, 8 and 12 (n=4; Values are mean±SE; ANOVA: $P<0.05$; Newman-Keuls: $P<0.05$; Asterisk indicates statistically significant difference).

5.1.8.1 Scanning electron microscopy (SEM)

The growth and distribution of 3T3 fibroblasts on collagen:PCL biocomposites (1:8 and 1:20) on day 1 and 3 at an initial cell seeding density of $7.1x10^4$ per cm^2 were examined by using SEM respectively using a Cambridge ® Stereoscan 90 Scanning Electron Microscope. Good cell attachment with the cell shape in round/ ovoid was shown on day 1. Both 1:8 and 1:20 collagen:PCL biocomposite groups have good cell attachment and growth of 3T3 fibroblasts representing a flattened cell shape on day 3 (Figure 16 and 17).

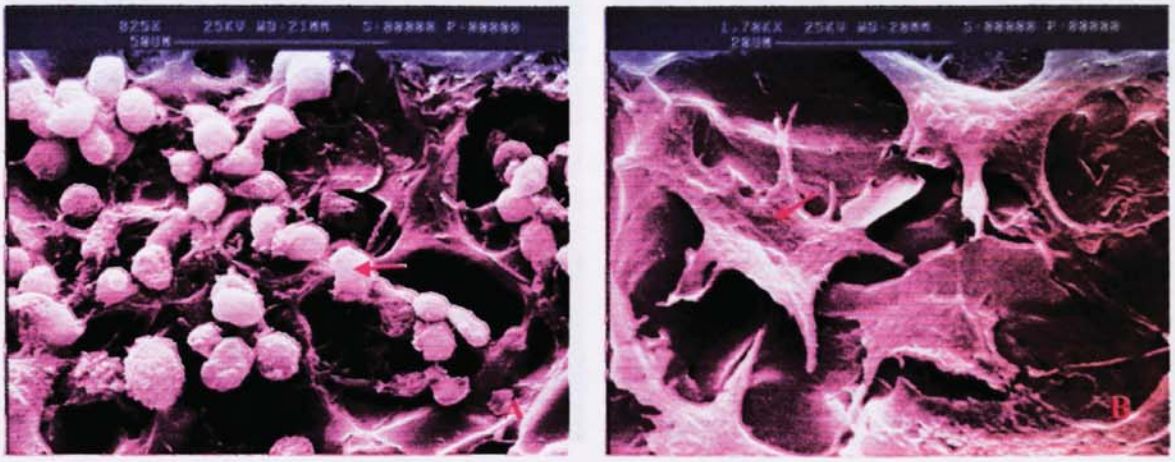

Figure 16: SEM of mouse 3T3 fibroblast growth on 1:20 w/w collagen:PCL biocomposites for 1 (A) and 3 (B) days. (Arrow indicates the cell body.)

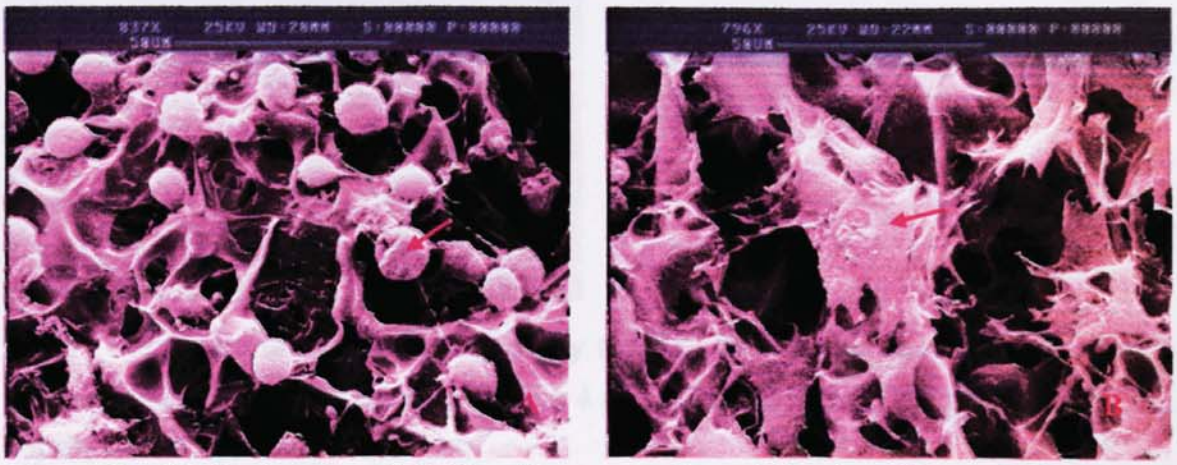

Figure 17: SEM of mouse 3T3 fibroblast growth on 1:8 w/w collagen:PCL biocomposites for 1 (A) and 3 (B) days. (Arrow indicates the cell body.)

5.1.8.2 Immunohistochemistry assay

The growth and distribution of 3T3 fibroblasts on collagen:PCL biocomposites (1:4, 1:8 and 1:20) on day 4 at an initial cell seeding density of $1.0x10^4$ cells per cm^2 were examined under fluorescent microscope by labeling with the primary monoclonal mouse anti-mouse vimentin antibody 1:200 (Cat No.MAB 3400; CHEMICON® International, Inc., USA), and the secondary fluorescein (FITC)-conjugated polyclonal goat anti-mouse IgG 1:100 (Lot No.62686; Jackson ImmunoResearch Laboratories, Inc., USA) respectively (Figure 18).

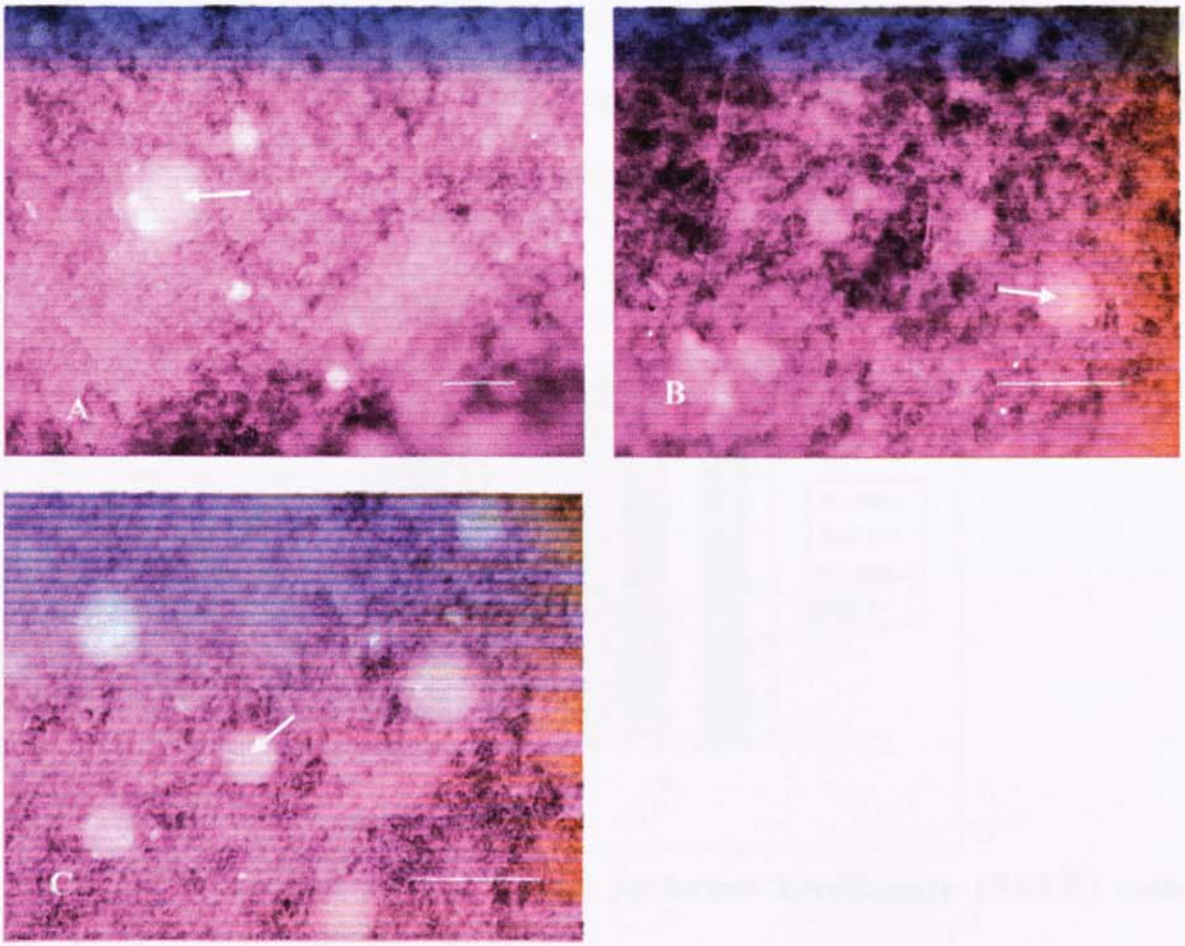

Figure 18: Immunohistochemistry assay for 3T3 fibroblast growth on 1:4, 1:8 and 1:20 w/w collagen:PCL biocomposite on day 4 (A: 100x, scale bar: 100μm; B: 400x, scale bar: 50μm; C: 400x; scale bar: 50μm).

Mouse 3T3 fibroblasts ($1.0x10^4$ cells per cm^2) were seeded on 1:4, 1:8 and 1:20 w/w collagen:PCL biocomposite on day 0. The primary antibody used for labeling of vimentin was monoclonal mouse anti-mouse vimentin antibody 1:200, and the secondary antibody used was fluorescein (FITC)-conjugated goat anti-mouse IgG 1:100. Green fluorescence (arrow)

indicates positive cell staining.

5.1.9 Interaction of NHEK with collagen:PCL biocomposites

Normal human epidermal keratinocytes (NHEK) were seeded on the top surface of collagen:PCL biocomposites (1:4, 1:8 and 1:20) and TCP (24-well tissue culture plastics) at a cell density of $3.5x10^4$ cells per cm^2 for time intervals up to 6 days. Trypsin-EDTA solution was used for cell detachment followed by cell counting at day 1, 4 and 6 using a Weber's haemocytometer. The submerged proliferation rates of NHEK on biocomposites and TCP are shown in Figure 19. Cell confluence was observed in TCP control groups at a cell density of $6.0x10^4$ cells per cm^2 on day 6. No significant differences in cell numbers on the various collagen:PCL biocomposites were apparent, the measurements being within the range of standard error. The keratinocyte density (cells/ unit area) was higher on the biocomposites than TCP at time intervals up to 4 days and equivalent at 6 days.

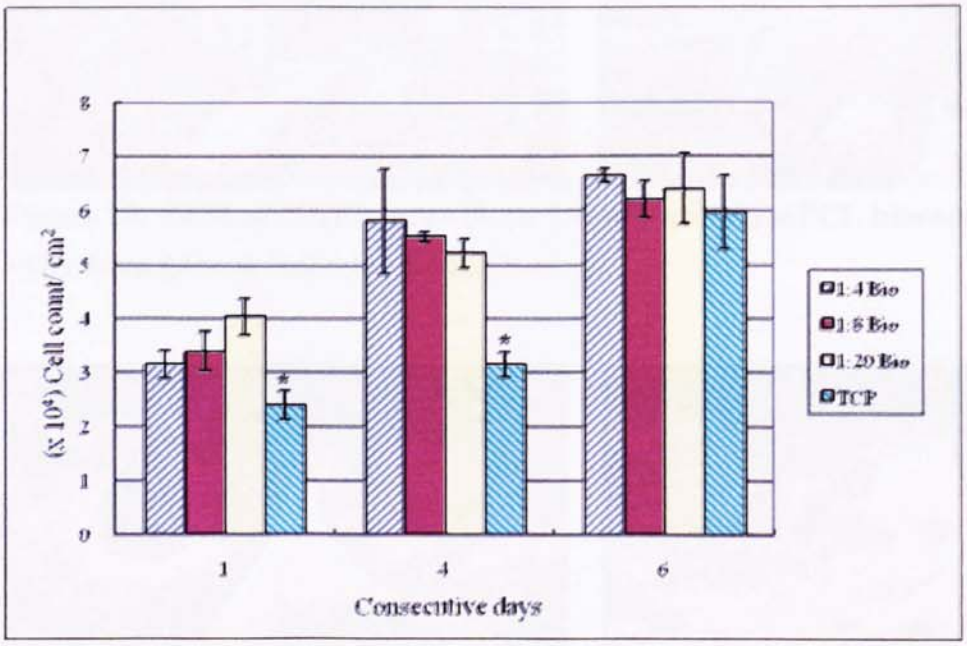

Figure 19: Submerged normal human epidermal keratinocyte (NHEK) culture on collagen:PCL biocomposites and TCP.

Normal human epidermal keratinocytes (NHEK) were seeded on the top surface of collagen:PCL biocomposites (1:4, 1:8 and 1:20) and TCP at a cell density of $3.5x10^4$ cells per cm^2 (passage 2). The keratinocyte density (cells/ unit area) was higher on the biocomposites than TCP at time intervals up to 4 days and equivalent at 6 days (n=3; Values are mean±SE; ANOVA: $P<0.05$; Newman-Keuls: $P<0.05$; Asterisk indicates statistically significant difference).

5.1.9.1 Scanning electron microscopy (SEM)

The growth and distribution of NHEK on collagen:PCL biocomposites (1:4, 1:8 and 1:20) on day 1 and 3 at an initial cell seeding density of 1.0 x 10^4 per cm^2 were examined by using SEM (Cambridge® Stereoscan 90 Scanning Electron Microscope) respectively. The pictures were shown in Figure 20 and 21. Increased cell growth numbers and good cell attachment represented by the change of cell shapes were observed in the cell culture on day 3 compared to that shown on day 1.

Figure 20: SEM of NHEK growth on 1:8 w/w collagen:PCL biocomposites for 1 (A) and 3 (B) days. (Arrow indicates the cell body.)

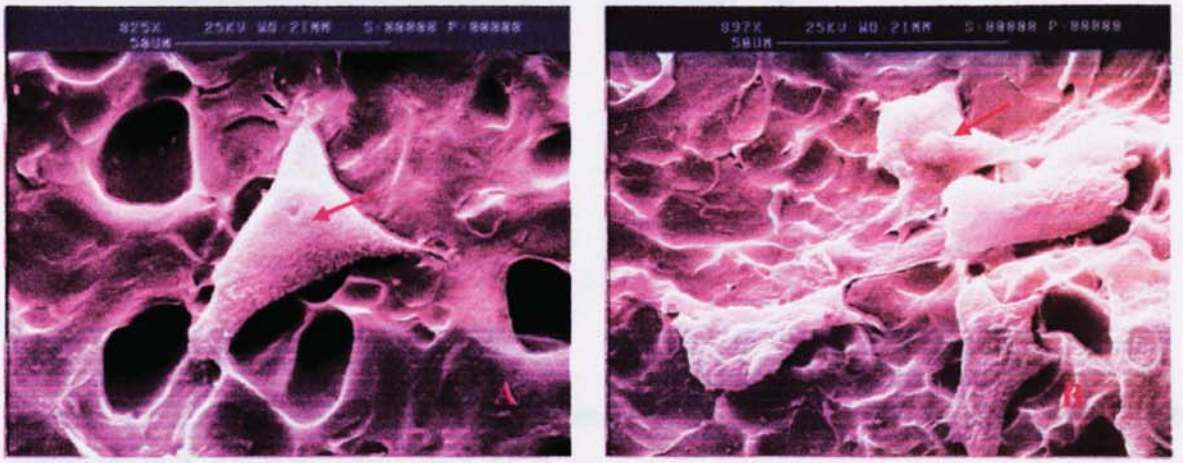

Figure 21: SEM of NHEK growth on 1:20 w/w collagen:PCL biocomposites for 1 (A) and 3 (B) days. (Arrow indicates the cell body.)

5.1.10 Interaction of PHEK with collagen:PCL biocomposites

Primary human epidermal keratinocytes (PHEK; child foreskin; P4) were seeded on the top surface of collagen:PCL biocomposites (1:8 and 1:20) and TCP (24-well tissue culture plastics) at a cell density of $1.7x10^5$ cells per cm^2 for time intervals up to 9 days. Trypsin-EDTA solution was used for cell detachment followed by cell counting at day 1, 3, 6 and 9 using a Weber's haemocytometer.

The submerged proliferation rates of PHEK on biocomposites and TCP are shown in Figure 22. Best cell growth was observed in TCP control group at time intervals up to 9 days ($P<0.05$), cell confluence was achieved at a cell density of $4.1x10^5$ cells per cm^2 on day 9. The mean keratinocyte density (cells per cm^2) seemed to be higher on the 1:8 collagen:PCL biocomposite group than 1:20 group at time intervals up to 9 days; however, there is no statistical significance ($P>0.05$).

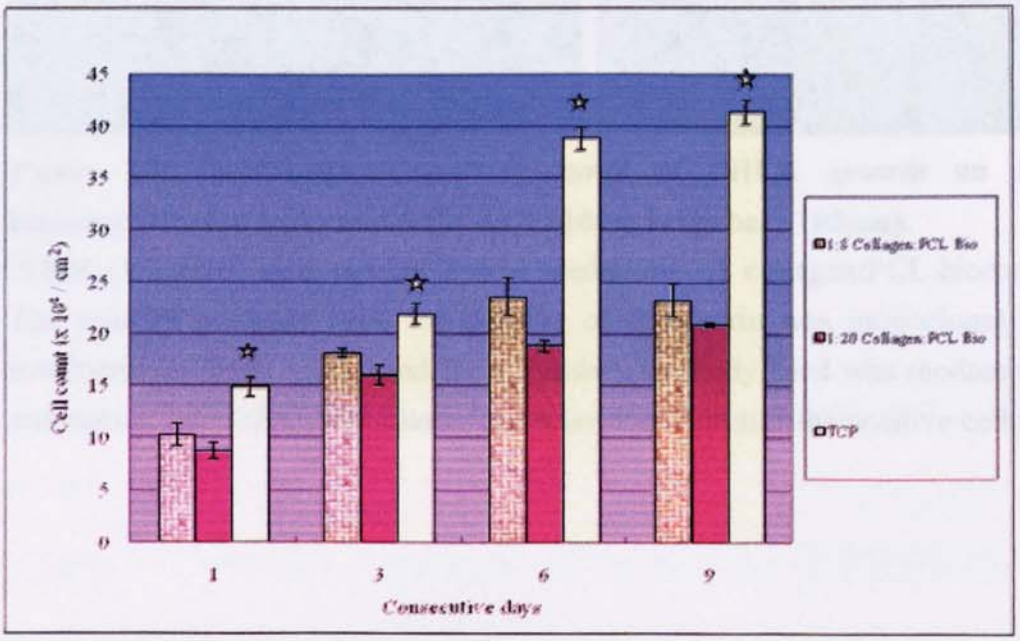

Figure 22: Comparison of primary human epidermal keratinocyte (PHEK) culture on collagen:PCL biocomposites and TCP.

PHEK (1.7×10^5 cells per cm^2; child foreskin; P4) were seeded in 7 ml glass shell vials containing collagen:PCL biocomposites (1:8 and 1:20) and TCP. Submerged growth of PHEK was allowed for 9 days. Cell confluence was observed in the TCP control group at day 9. Cell counting was performed at day 1, 3, 6 and 9. (n=4; Values are mean±SE; ANOVA: $P<0.05$; Newman-Keuls: $P<0.05$; Asterisk indicates statistically significant difference).

5.1.10.1 Immunohistochemistry assay

The growth and distribution of PHEK (adult foreskin; P4) on collagen:PCL biocomposites (1:8 and 1:20) on day 1 and 6 at an initial cell seeding density of 2.0 x 10^4 cells per cm^2 were examined using fluorescence microscopy by labeling with the primary monoclonal mouse anti-human involucrin antibody 1:200 (Cat No.I8447-25; United States Biological, Inc.) and the secondary rhodamine-conjugated polyclonal goat anti-mouse IgG 1:100 (Cat No.I1903-08C, United States Biological, Inc.) respectively (Figure 23 and 24). More distribution and better growth numbers of cells were observed at time intervals up to 6 days.

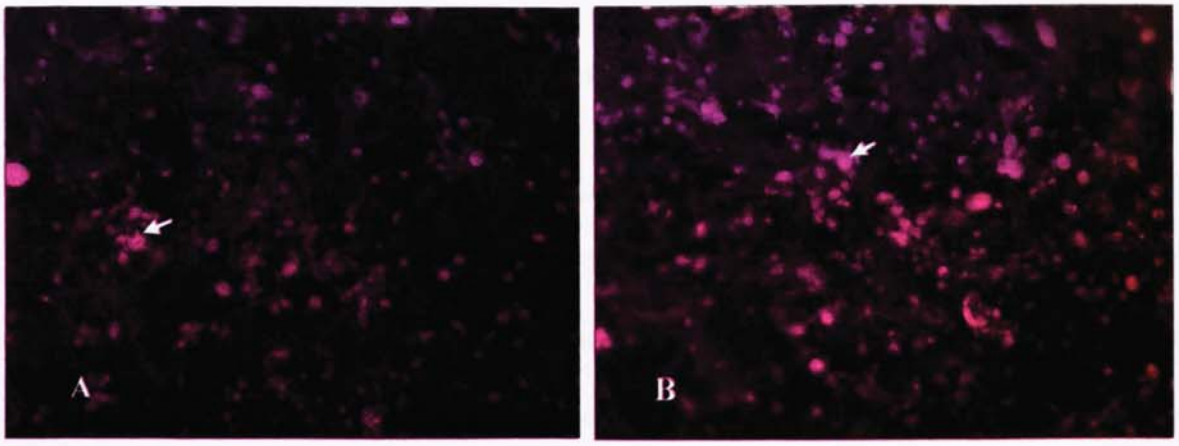

Figure 23: Immunohistochemistry assay of PHEK growth on 1:8 collagen:PCL biocomposite for 1 (A) and 6 (B) days (100x; scale bar: 100μm).
PHEK (1.7 x 10^5 cells per cm^2) were seeded on 1:8 collagen:PCL biocomposites on day 0. The primary antibody used for labeling of involucrin was monoclonal mouse anti-human involucrin antibody 1:200, and the secondary antibody used was rhodamine-conjugated goat anti-mouse IgG 1:100. Red fluorescence (arrow) indicates the positive cell staining.

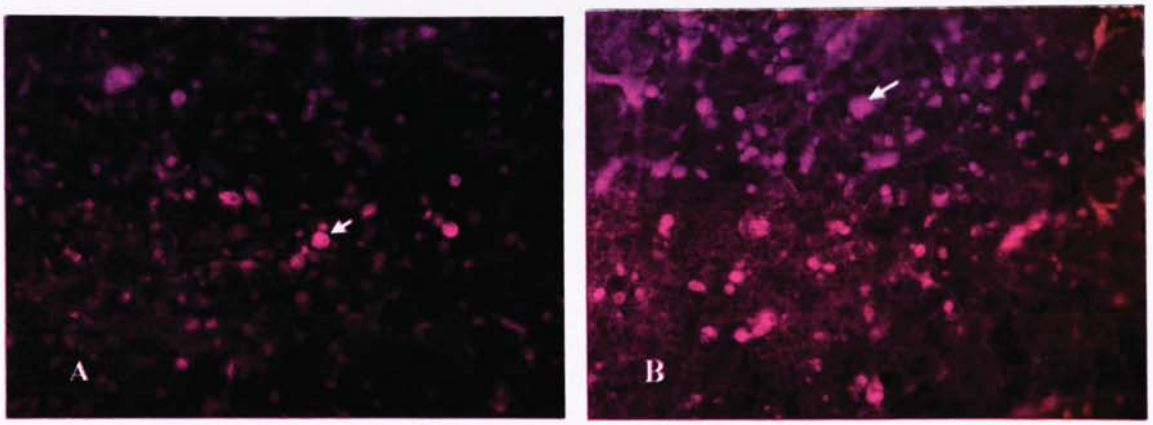

Figure 24: Immunohistochemistry assay of PHEK growth on 1:20 collagen:PCL biocomposite for 1 (A) and 6 (B) days (100x; scale bar: 100μm).
PHEK (1.7 x 10^5 cells per cm^2) were seeded on 1:20 collagen:PCL biocomposites on day 0. The primary antibody used for labeling of involucrin was monoclonal mouse anti-human involucrin antibody 1:200, and the secondary antibody used was rhodamine-conjugated goat anti-mouse IgG 1:100. Red fluorescence (arrow) indicates the positive cell staining.

5.1.11 Interaction of PHDF with collagen:PCL biocomposites

Primary human dermal fibroblasts (PHDF; adult foreskin; P3) were seeded on the top surface of collagen:PCL biocomposites (1:8 and 1:20) and TCP (24-well tissue culture plastics) at a cell density of $2.0x10^4$ cells per cm^2 for time intervals up to 10 days. Trypsin-EDTA solution was used for cell detachment followed by cell counting at day 1, 4, 7 and 10 using a Weber's haemocytometer.

The submerged proliferation rates of PHDF on biocomposites and TCP are shown in Figure 25. The best cell growth was observed in TCP control group at a cell density of $3.4x10^5$ cells per cm^2 on day 10 ($P<0.05$). The fibroblast density (cells per cm^2) was higher on the 1:8 collagen:PCL biocomposite group than 1:20 group at day 10 ($P<0.05$) and almost equivalent at time intervals up to 7 days ($P>0.05$).

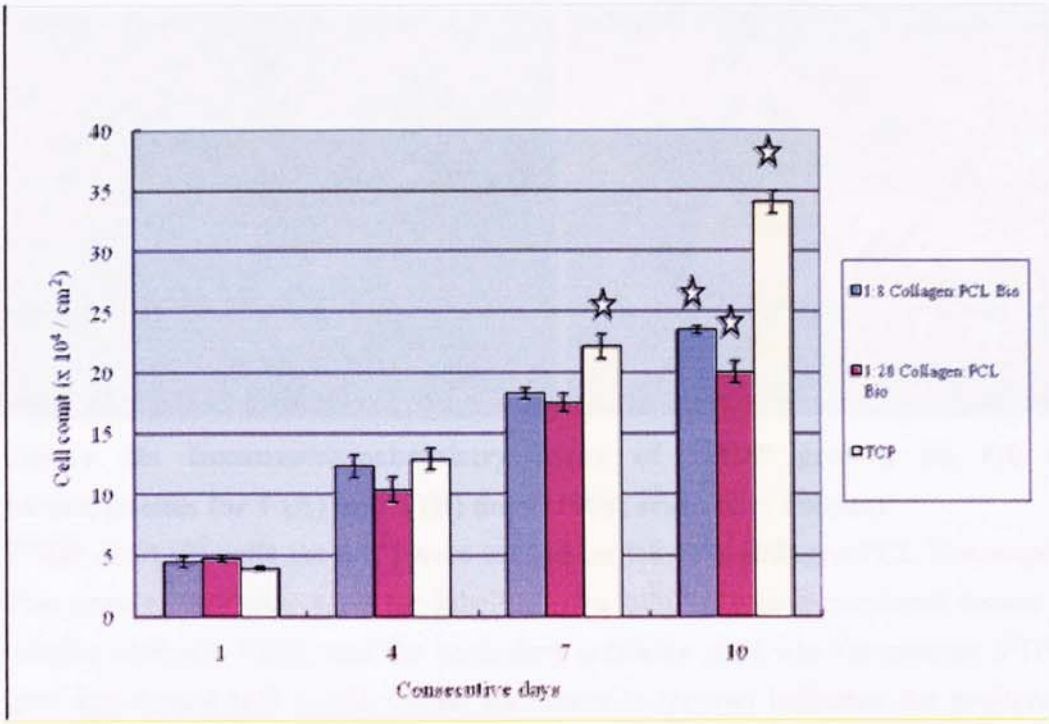

Figure 25: Growth curves of primary human dermal fibroblasts (PHDF) culture on collagen:PCL biocomposites and TCP.

PHDF ($2.0x10^4$ cells per cm^2; adult foreskin; P3) were seeded in 7 ml glass shell vials containing collagen:PCL biocomposites (1:8 and 1:20) and TCP. Submerged growth of PHDF was allowed for 10 days. Cell counting was performed at day 1, 4, 7 and 10. (n=4; Values are mean±SE; ANOVA: $P<0.05$ & Newman-Keuls: $P<0.05$ except on day 1 and 4; Asterisk indicates statistically significance).

5.1.11.1 Immunohistochemistry assay

The growth and distribution of PHDF (adult foreskin; P3) on collagen:PCL biocomposites (1:8 and 1:20) on day 1 and 7 at an initial cell seeding density of $2.0x10^4$ cells per cm^2 were examined using fluorescence microscopy by labeling with the primary monoclonal mouse anti-human α tubulin antibody 1:200 (sc-5286; Santa Cruz Biotechnology, Inc.), and the secondary fluorescein (FITC)-conjugated polyclonal goat anti-mouse IgG 1:100 (Lot No.62686; Jackson ImmunoResearch Laboratories, Inc., USA) respectively (Figure 26 and 27).

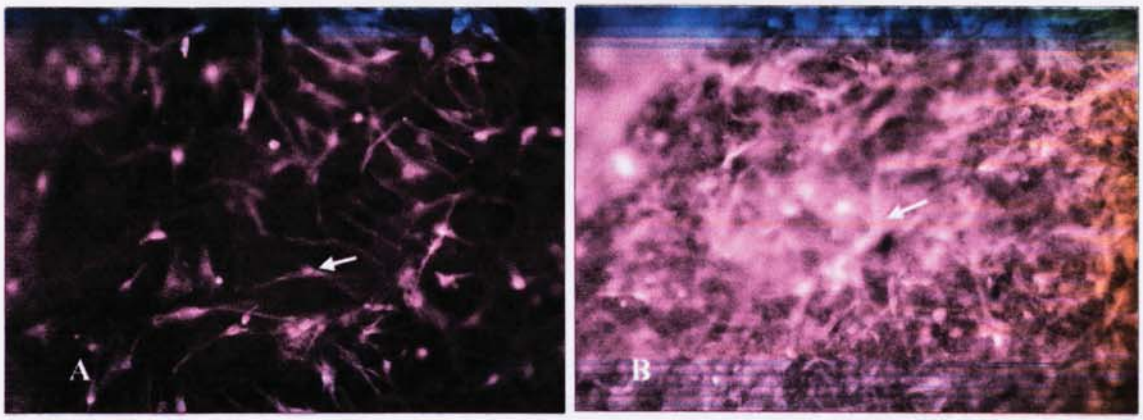

Figure 26: Immunohistochemistry assay of PHDF growth on 1:8 collagen:PCL biocomposites for 1 (A) and 7 (B) days (100x; scale bar: 100μm).

PHDF ($2.0x10^4$ cells per cm^2) were seeded on 1:8 w/w collagen:PCL biocomposite on day 0. The primary antibody used for labeling of α tubulin was monoclonal mouse anti-human α tubulin antibody 1:200, and the secondary antibody used was fluorescein (FITC)-conjugated goat anti-mouse IgG 1:100. Green fluorescence (arrow) indicates the positive cell staining. The appearance of diffuse green color background (B) might indicate an increase in cell numbers or deposition of ECM.

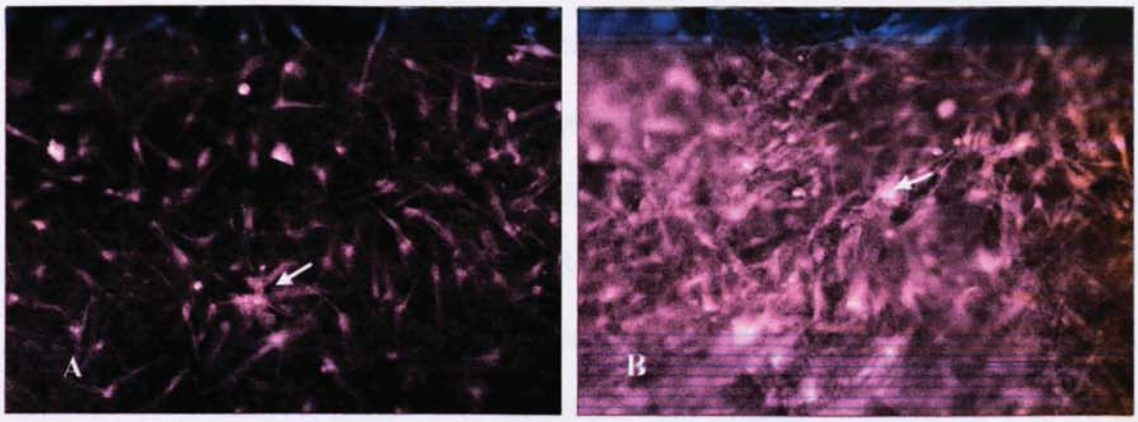

Figure 27: Immunohistochemistry assay of PHDF growth on 1:20 collagen:PCL biocomposites for 1 (A) and 7 (B) days (100x; scale bar: 100μm).

PHDF ($2.0x10^4$ cells per cm^2) were seeded on 1:20 collagen:PCL biocomposite on day 0. The primary antibody used for labeling of α tubulin was monoclonal mouse anti-human α tubulin antibody 1:200, and the secondary antibody used was fluorescein (FITC)-conjugated goat anti-mouse IgG 1:100. Green fluorescence (arrow) indicates the positive cell staining. The appearance of diffuse green color background (B) might indicate an increase in cell numbers or deposition of ECM.

5.2 Study on gelatin:PCL biocomposites

5.2.1 Estimation of gelatin release from gelatin:PCL biocomposites incubated in PBS at 37°C

The BCA total protein assay was used to estimate the amount of gelatin content released from gelatin:PCL biocomposites in PBS at 37°C. Samples having w/w ratios of 1:4, 1:8 and 1:20 gelatin:PCL were prepared from 0.1% w/v gelatin (type B) solution.

The cumulative release of gelatin from the biocomposites is shown in Figure 28. The highest cumulative release of gelatin was revealed for 1:4 gelatin:PCL biocomposite, followed by 1:8 and 1:20. The 1:4 biocomposites exhibited the highest mean gelatin release rate at 6 hours with about 95.5% of the original gelatin content being released into PBS, while 57.3% and 23.2% were released from 1:8 and 1:20 biocomposites respectively. The amount of gelatin released significantly increased within 12 hours for all the biocomposites investigated. After 12 hours, the release of gelatin in 1:4, 1:8 and 1:20 biocomposites reached slow increasing rate resulting in a final mean cumulative release (w/w) of 100%, 72.7% and 44% on day 12 respectively ($P<0.05$). Furthermore, the release rate reached a plateau for 1:4, 1:8 and 1:20 biocomposites at time intervals of day 3, 3 and 6 respectively ($P<0.05$).

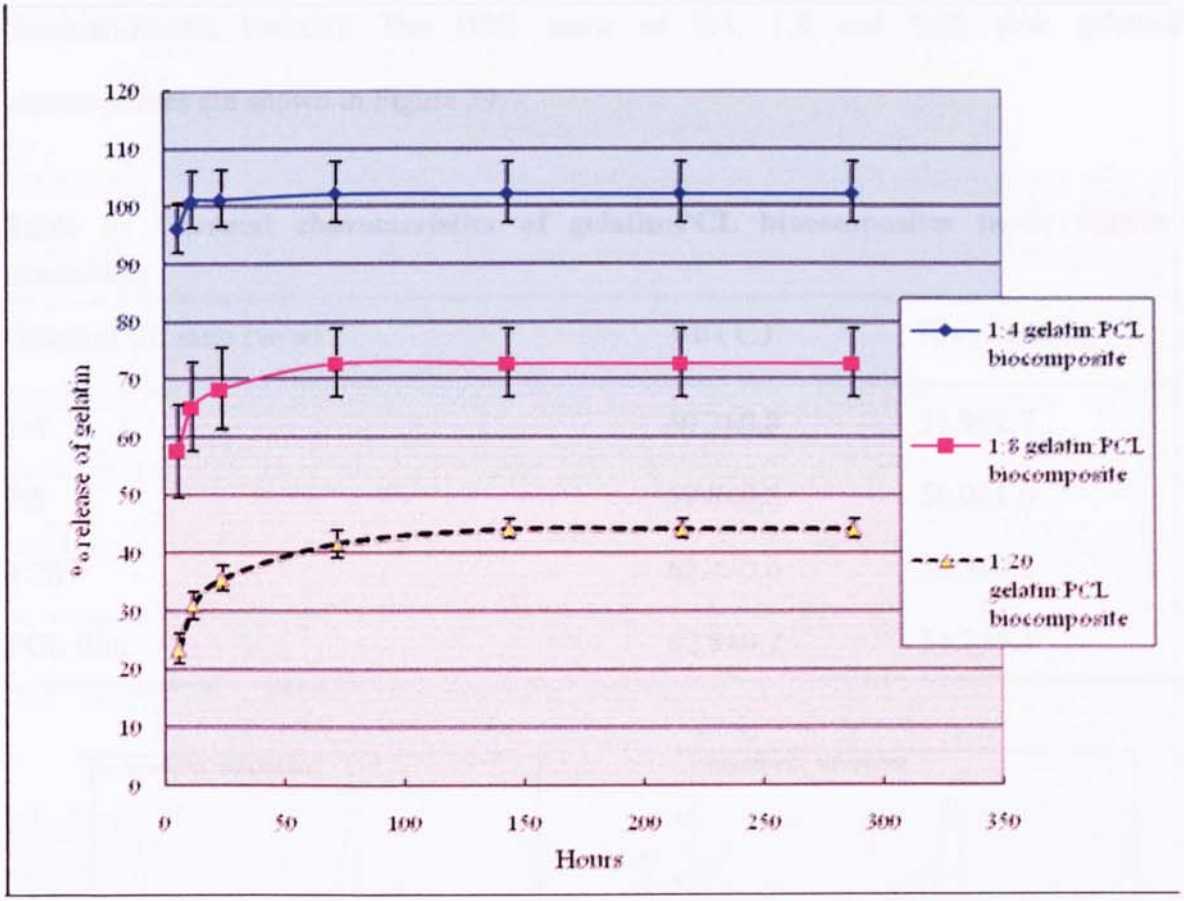

Figure 28: Cumulative release of gelatin from 1:4, 1:8 and 1:20 w/w gelatin:PCL biocomposites in PBS at 37°C.

The BCA total protein assay was used to estimate the amount of gelatin release in 1:4, 1:8 and 1:20 w/w gelatin:PCL biocomposites after incubation in PBS at 37°C for 12 days. The release media were analysed for gelatin content and replaced by fresh PBS periodically (n=3; Values are mean±SE; ANOVA: $P<0.05$; Newman-Keuls: $P<0.05$).

5.2.2 Differential Scanning Calorimetry (DSC) for gelatin:PCL biocomposites

The thermal analysis of gelatin:PCL biocomposites (n=3) is shown in Table 3. The melting point of the PCL phase was close to the value of 60℃ normally quoted for PCL. The mean percentage crystallinity of the PCL phase in the highest gelatin content (1:4 w/w) materials tended to be lower than that of solvent cast films. A reduction in crystallinity of around 4% was measured in the case of the highest collagen loaded (1:4 w/w) materials. In contrast the average % crystallinity of the PCL phase in the lowest gelatin content (1:20 w/w) composite was found to increase by almost 7% relative to the solvent cast films. However, no significant differences were measured between all of these biocomposite groups (ANOVA: P=0.197;

Newman-Keuls: P>0.05). The DSC scans of 1:4, 1:8 and 1:20 w/w gelatin:PCL biocomposites are shown in Figure 29.

Table 3: Thermal characteristics of gelatin:PCL biocomposites (n=3; Values are mean±SE)

Gelatin:PCL ratio (w/w)	Tm (°C)	% cystallinity
1:4	60.2±0.8	51.9±2.7
1:8	59.8±0.8	56.0±1.6
1:20	62.4±0.6	58.3±0.5
PCL film	62.8±0.2	54.2±5.4

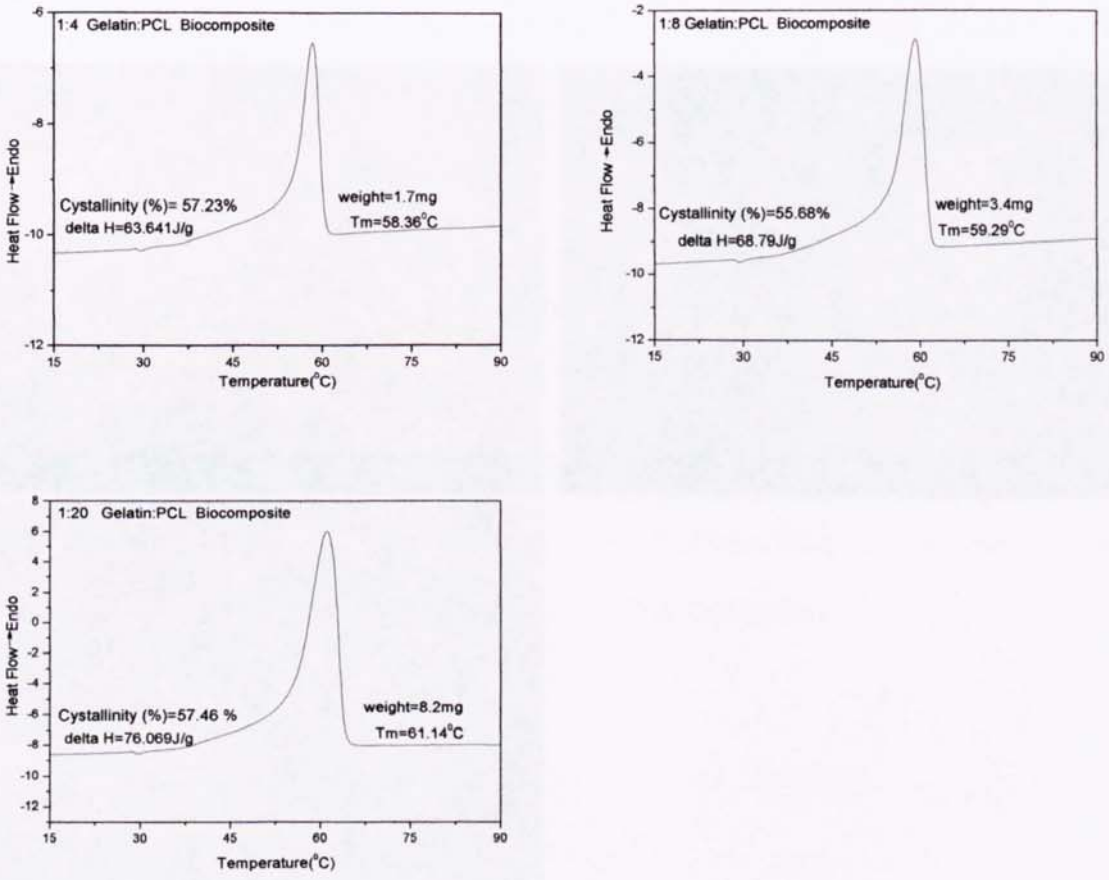

Figure 29: Differential scanning calorimetry scan of 1:4, 1:8 and 1:20 w/w gelatin:PCL biocomposites. (Tm: melting temperature; Endo: endothermic; data H: enthalpy)

5.2.3 Scanning electron microscopy (SEM)

The morphology of 1:4, 1:8 and 1:20 (w/w) gelatin:PCL biocomposites were investigated using SEM (HITACHI® 3000N Scanning Electron Microscope). All of the biocomposite groups exhibit a similar rough, fibrous surface due to the collagen mat structure and smooth overlying areas that could be formed by the PCL phase. Little differences in morphology between 1:4, 1:8 and 1:20 groups were apparent. However, the 1:8 and 1:20 biocomposites exhibited a similar greater masking or coating effect of the fibrous structure by PCL to produce a smoother surface than that of the group of 1:4 biocomposites. The SEM of 1:4, 1:8 and 1:20 (w/w) gelatin:PCL biocomposites were shown in Figure 30.

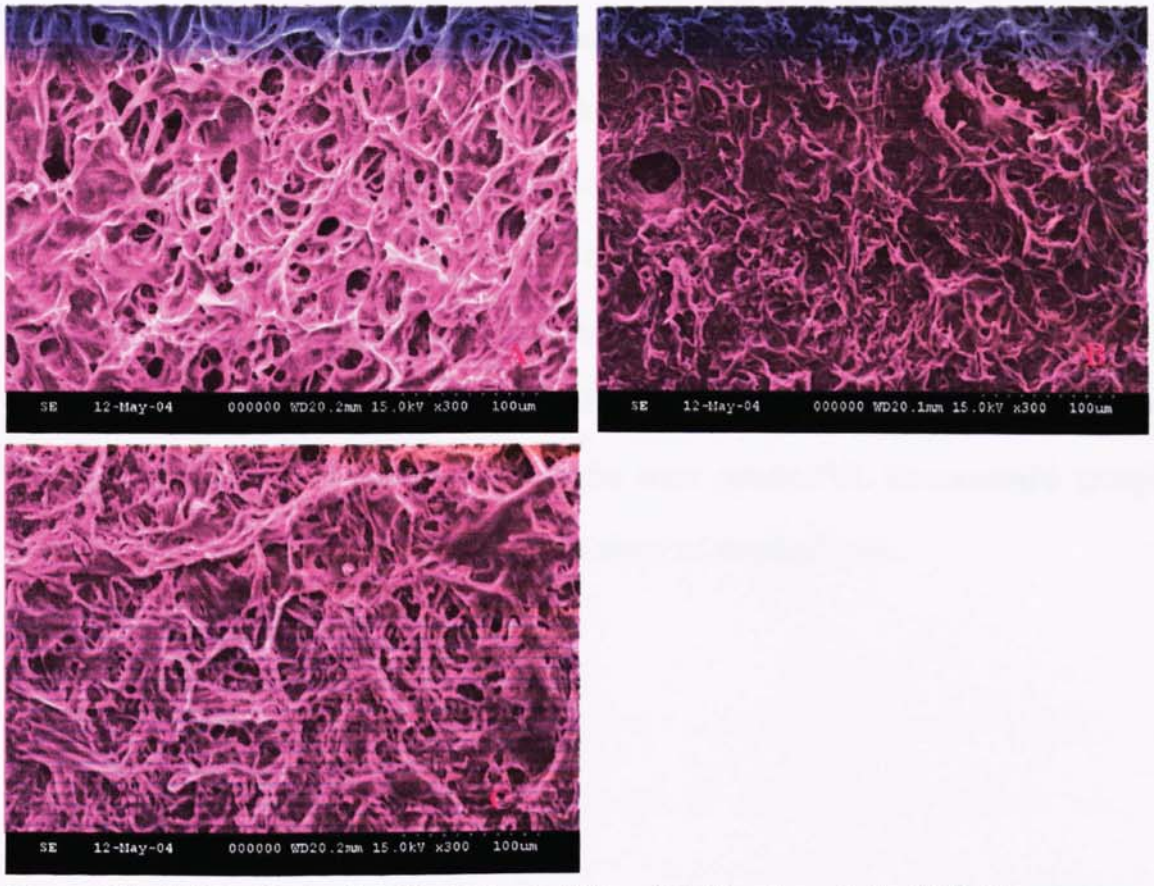

Figure 30: SEM of 1:4 w/w (A), 1:8 w/w (B) and 1:20 w/w gelatin:PCL biocomposites.

5.2.4 Interaction of 3T3 fibroblasts with gelatin:PCL biocomposites

Mouse 3T3 fibroblasts were seeded on the top surface of 1:4, 1:8 and 1:20 w/w gelatin:PCL & type I collagen:PCL biocomposites and TCP (24-well tissue culture plastics) at a cell density of $3.5x10^4$ per cm^2 for time intervals up to 12 days. In order to investigate the differences in cell biocompatibility between gelatin:PCL biocomposites and type I collagen:PCL materials, the collagen:PCL biocomposites were included in this work. The proliferation rates of 3T3 fibroblasts on type I collagen:PCL & gelatin:PCL biocomposites and TCP surfaces are shown in Figure 31. The TCP surface showed the best cell attachment with a cell density of $2.3x10^5$ per cm^2 at time interval of 8 days ($P<0.05$). A better cell growth curve was also apparent in TCP control group compared to all collagen:PCL biocomposite groups ($P<0.05$) on day 12. Furthermore, 1:20 gelatin:PCL biocomposite group has the better cell growth numbers compared to 1:4 and 1:20 collagen:PCL biocomposite groups at time intervals of 8 and 12 days ($P<0.05$). On day 12, TCP control group exhibited the highest number of cells ($3.4x10^5$ per cm^2), followed by 1:20 gelatin:PCL biocomposite group with $2.8x10^5$ per cm^2, 1:8 gelatin:PCL group with $2.4x10^5$ per cm^2,and 1:4 gelatin:PCL group with $2.37x10^5$ per cm^2. However, no significant differences in cell numbers between TCP and 1:20 gelatin:PCL groups, or between 1:20 gelatin:PCL and the other gelatin:PCL biocomposite groups were apparent, the measurements being within the range of standard error.

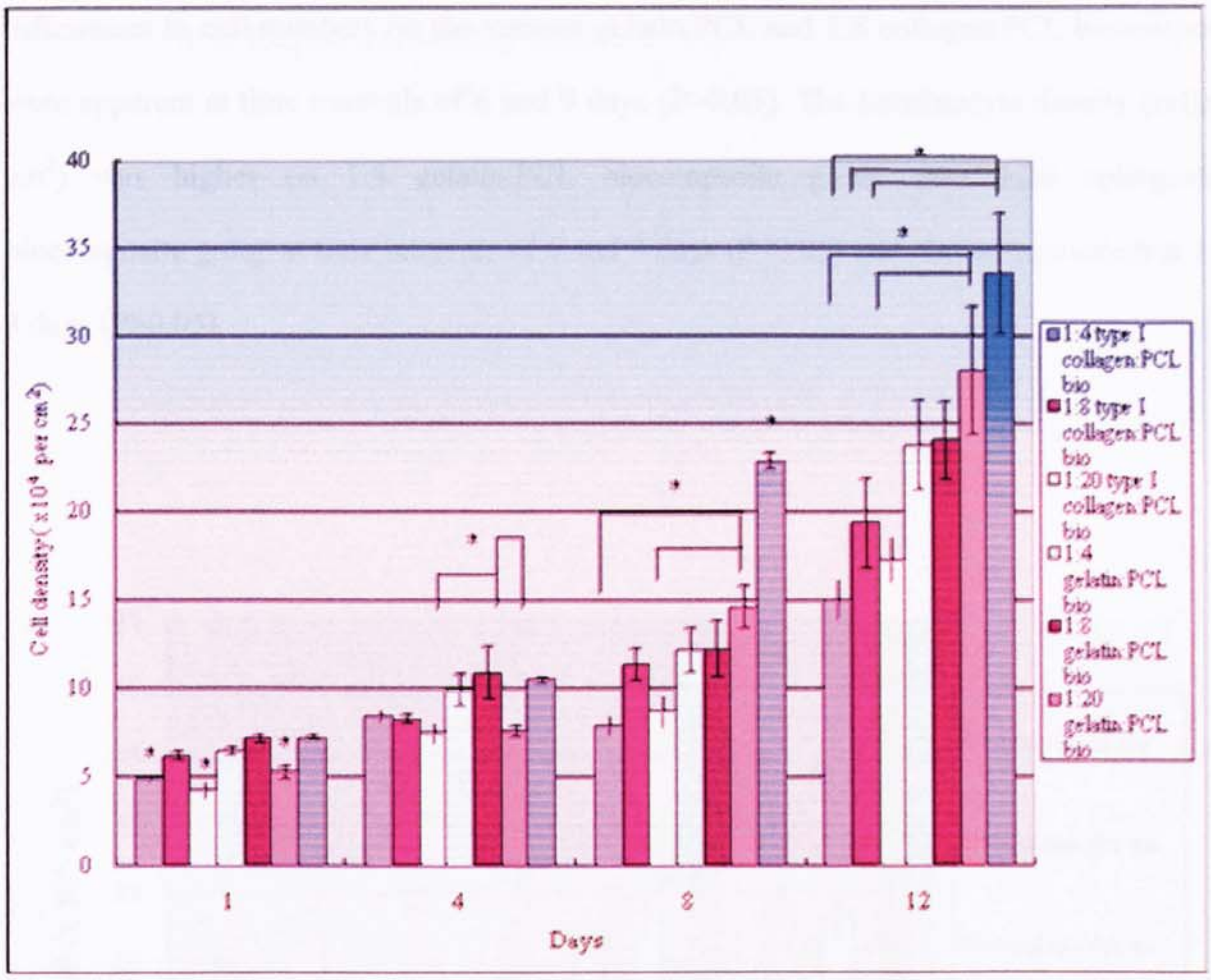

Figure 31: Comparison of 3T3 fibroblast growth on 1:4, 1:8 & 1:20 (w/w) collagen:PCL & gelatin:PCL biocomposites and TCP.

Mouse 3T3 fibroblasts ($3.5x10^4$ per cm^2) were seeded in 7ml glass shell vials containing 1:4, 1:8 and 1:20 gelatin:PCL & collagen:PCL biocomposites. Cells were also seeded in 24-well tissue culture plastics (TCP) as control. (n=4; Values are mean±SE; ANOVA: $P<0.05$; Newman-Keuls: $P<0.05$; Asterisk indicates statistically significant difference).

5.2.5 Interaction of PHEK with gelatin:PCL biocomposites

Primary human epidermal keratinocytes (PHEK; child foreskin; P4) were seeded on the top surface of gelatin:PCL biocomposites (1:8 and 1:20), collagen:PCL biocomposites (1:8 and 1:20) and TCP (24-well tissue culture plastics) at a cell density of $1.7x10^5$ cells per cm^2 for a time intervals up to 9 days. The submerged proliferation rates of PHEK on biocomposites and TCP are shown in Figure 32. Cell confluence and best cell growth curve were observed in TCP control group at a cell density of $4.1x10^5$ cells per cm^2 on day 9. No significant

differences in cell numbers on the various gelatin:PCL and 1:8 collagen:PCL biocomposites were apparent at time intervals of 6 and 9 days ($P>0.05$). The keratinocyte density (cells per cm^2) was higher on 1:8 gelatin:PCL biocomposite group than 1:20 collagen:PCL biocomposite group at time intervals of 6 and 9 days ($P<0.05$) and almost equivalent at 1 and 3 days ($P>0.05$).

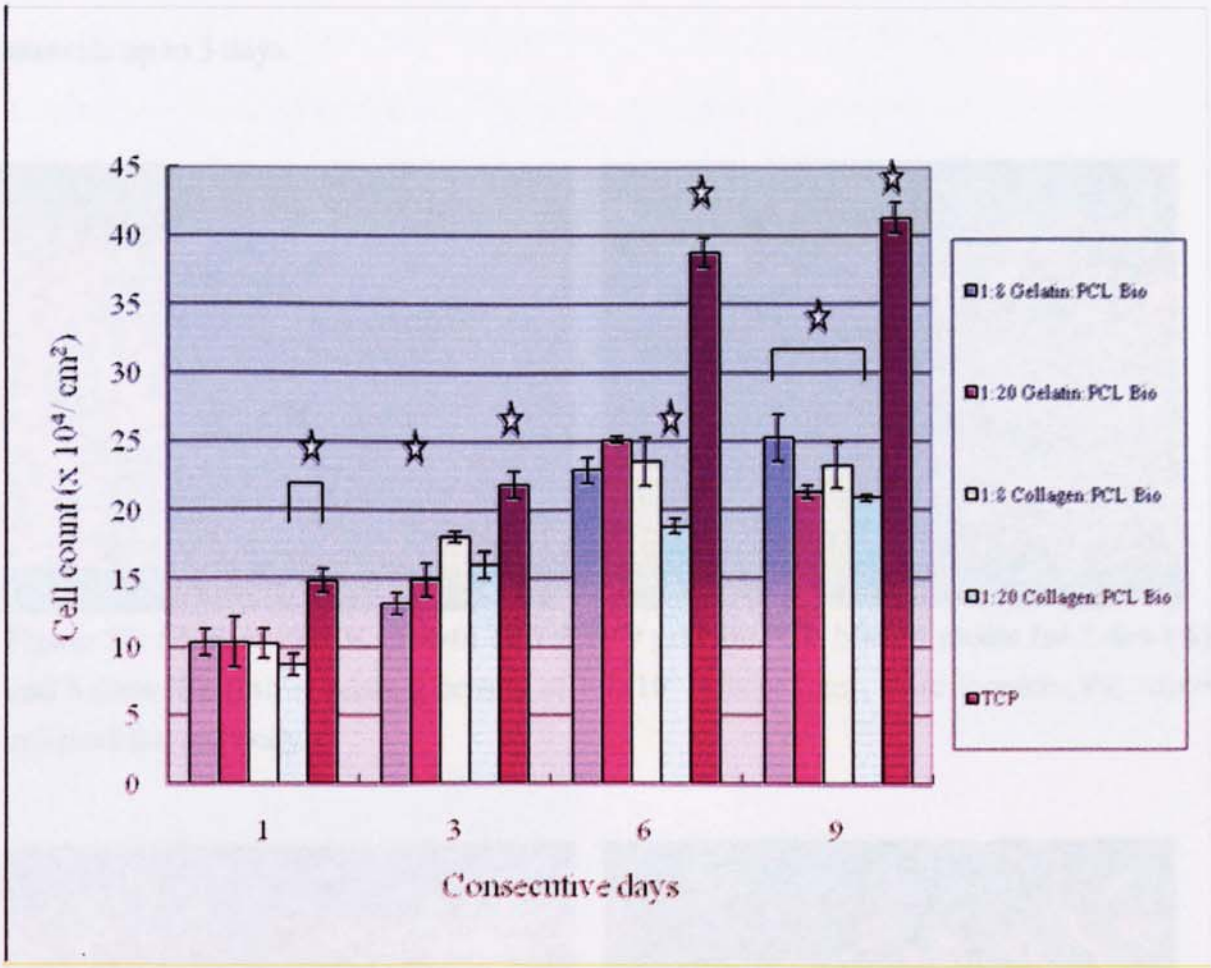

Figure 32: Comparison of primary human epidermal keratinocyte (PHEK) growth on gelatin:PCL & collagen:PCL biocomposites and TCP.

PHEK ($1.7x10^5$ cells per cm^2; child foreskin; P4) were seeded in 7 ml glass shell vials containing biocomposites (1:8 and 1:20) and TCP. Submerged growth of PHEK was allowed for 9 days. Cell confluence was observed in the TCP control group at day 9. Cell counting was performed at day 1, 3, 6 and 9. (n=4; Values are mean±SE; ANOVA: $P<0.05$; Newman-Keuls: $P<0.05$; Asterisk indicates statistically significant difference).

5.2.5.1 Scanning electron microscopy (SEM)

The PHEK ($1.7x10^5$ cells per cm^2; child foreskin; P4) growth on 1:8 and 1:20 w/w gelatin:PCL biocomposites for 1 and 3 days were examined by using SEM (Figure 33 and 34). The pictures revealed good initial cell attachment and growth on various biocomposites at day 1. In addition, increased cell density and diffuse distribution of cells were noted at time intervals up to 3 days.

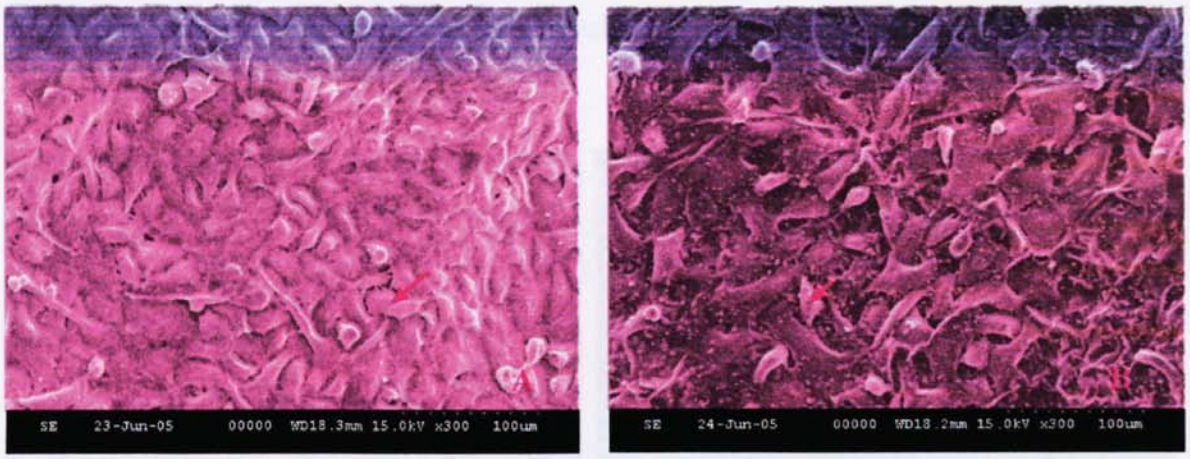

Figure 33: SEM of PHEK growth on 1:8 w/w gelatin:PCL biocomposite for 1 day (A) and 3 days (B). (Initial seeding density of $1.7x10^5$ cells per cm^2; child foreskin; P4; Arrow indicates the cell body.)

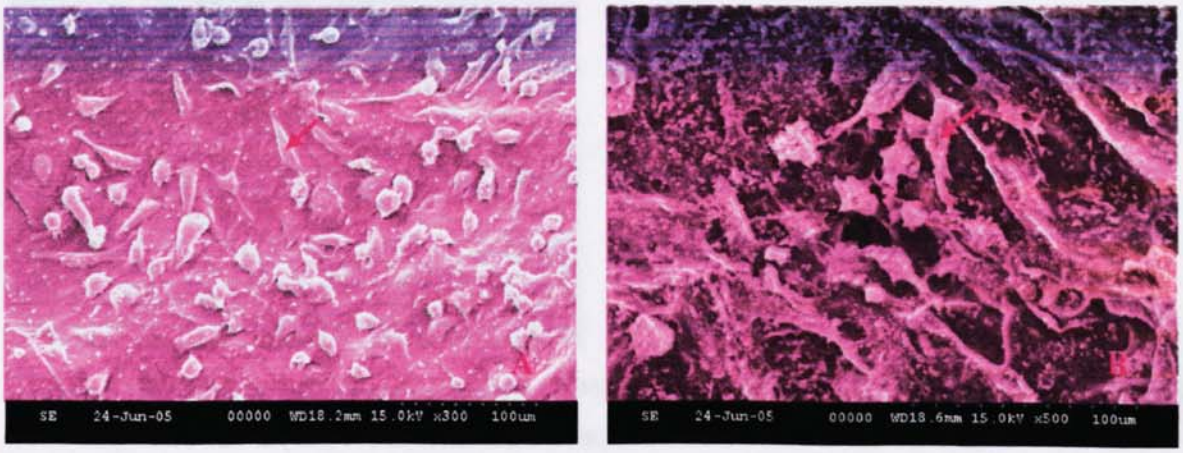

Figure 34: SEM of PHEK growth on 1:20 w/w gelatin:PCL biocomposite for 1 day (A) and 3 days (B). (Initial seeding density of $1.7x10^5$ cells per cm^2; child foreskin; P4; Arrow indicates the cell body.)

5.2.5.2 Immunohistochemistry assay

The growth and distribution of PHEK (seeding density of $1.7x10^5$ cells per cm^2; child foreskin; P4) on the top surface of 1:8 and 1:20 (w/w) gelatin:PCL biocomposites on day 1, 3, 6 and 9 were investigated by immunohistochemistry assay. PHEK were labeled with monoclonal mouse anti-human.involucrin antibody (primary) and goat anti-mouse rhodamine-conjugated antibody (secondary), and then were investigated under fluorescent microscope. Increased keratinocye cell numbers and multiple-layered distribution of cells on biocomposites were apparent at time intervals up to 9 days (Figure 35 and 36).

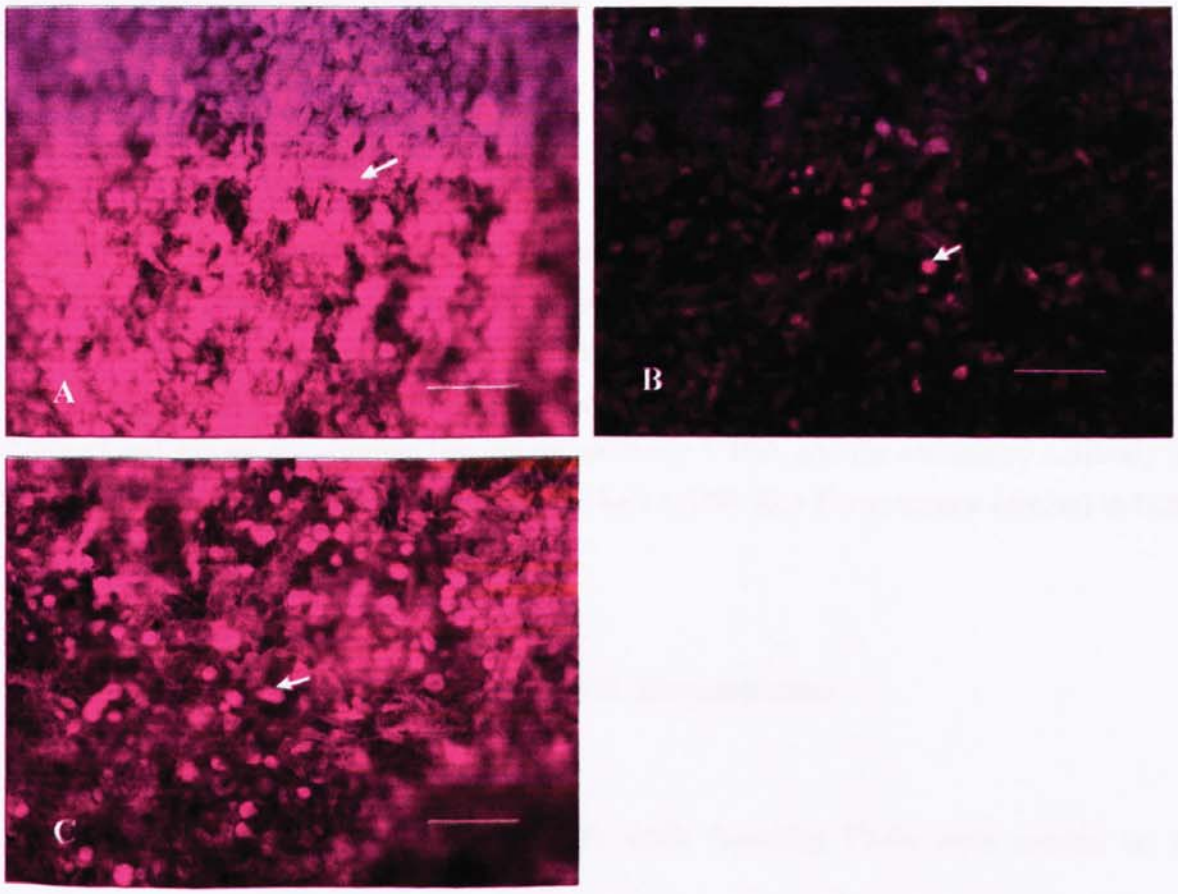

Figure 35: Immunohistochemistry assay of PHEK growth on 1:8 gelatin:PCL biocomposite for 1 (A), 3 (B) and 6 (C) days. (100x; scale bar: 100μm)
PHEK ($1.7x10^5$ cells per cm^2; child foreskin; P4) were seeded on 1:8 gelatin:PCL biocomposites on day 0. The primary antibody used for labeling of involucrin was monoclonal mouse anti-human involucrin antibody 1:100, and the secondary antibody used was rhodamine-conjugated goat anti-mouse IgG 1:100. Red fluorescence (arrow) indicates the positive cell staining.

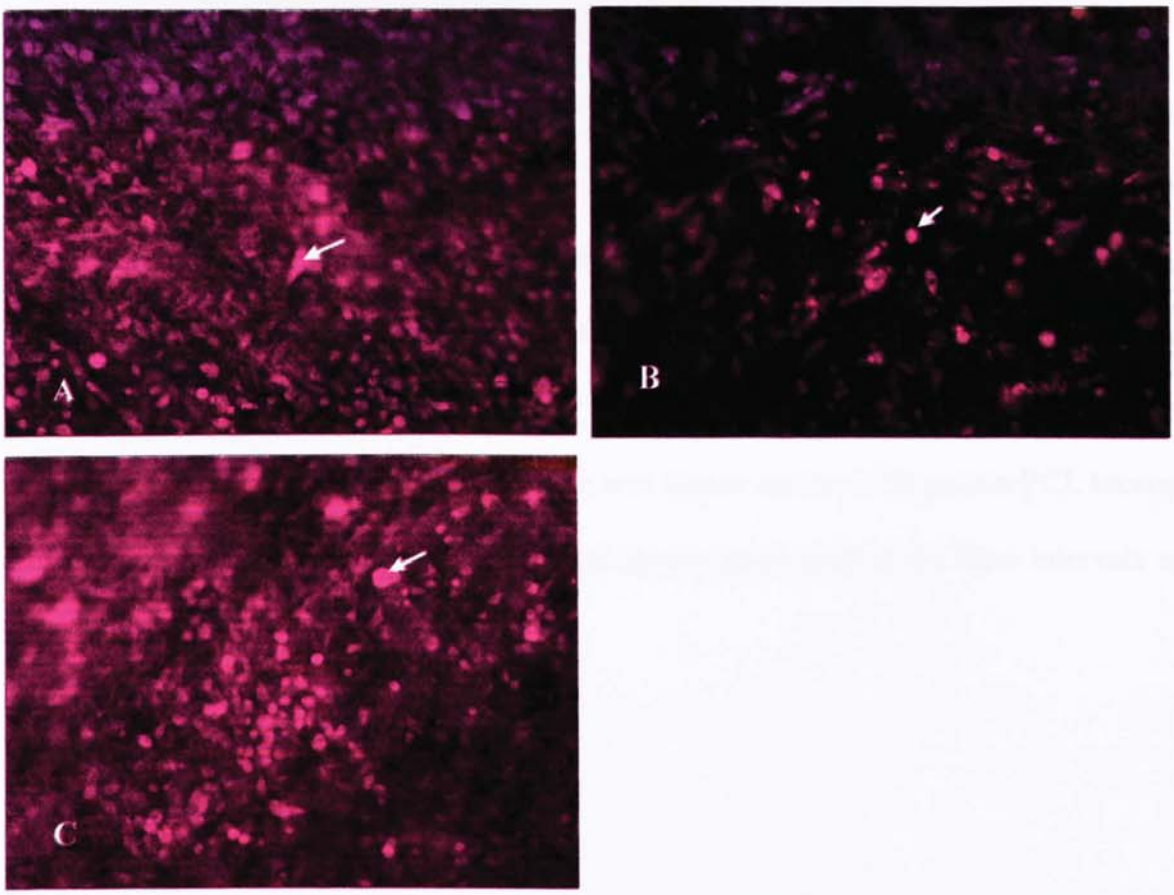

Figure 36: Immunohistochemistry assay of PHEK growth on 1:20 gelatin:PCL biocomposite for 1 (A), 3 (B) and 6 (C) days. (100x; scale bar: 100μm)
PHEK ($1.7x10^5$ cells per cm^2; child foreskin; P4) were seeded on 1:20 gelatin:PCL biocomposites on day 0. The primary antibody used for labeling of involucrin was monoclonal mouse anti-human involucrin antibody 1:100, and the secondary antibody used was rhodamine-conjugated goat anti-mouse IgG 1:100. Red fluorescence (arrow) indicates the positive cell staining.

5.2.6 Interaction of PHDF with gelatin:PCL biocomposites

Primary human dermal fibroblasts (PHDF; adult foreskin; P3-4) were seeded on the top surface of gelatin:PCL and collagen:PCL biocomposites (1:8 and 1:20) and TCP (24-well tissue culture plastics) at a cell density of $2.0x10^4$ cells per cm^2 for time intervals up to 10 days. Trypsin-EDTA solution was used for cell detachment followed by cell counting at day 1, 4, 7 and 10 using a Weber's haemocytometer.

The submerged proliferation rates of PHDF on biocomposites and TCP are shown in Figure 37. Best cell growth was observed in TCP control group at a cell density of $3.4x10^5$ cells per cm^2 on day 10. Both 1:8 and 1:20 gelatin:PCL biocomposite groups have the better cell growth than 1:20 collagen:PCL biocomposite on day 10 ($P<0.05$). No significant differences in cell numbers on the various collagen:PCL biocomposites (1:8 and 1:20) were apparent at time intervals of 1, 4, 7 and 10 days, the measurements being within the range of standard error. The fibroblast density (cells per cm^2) was higher on the 1:20 gelatin:PCL biocomposite group than 1:8 group at day 7 ($P<0.05$) and almost equivalent at the time intervals up to 10 days ($P>0.05$).

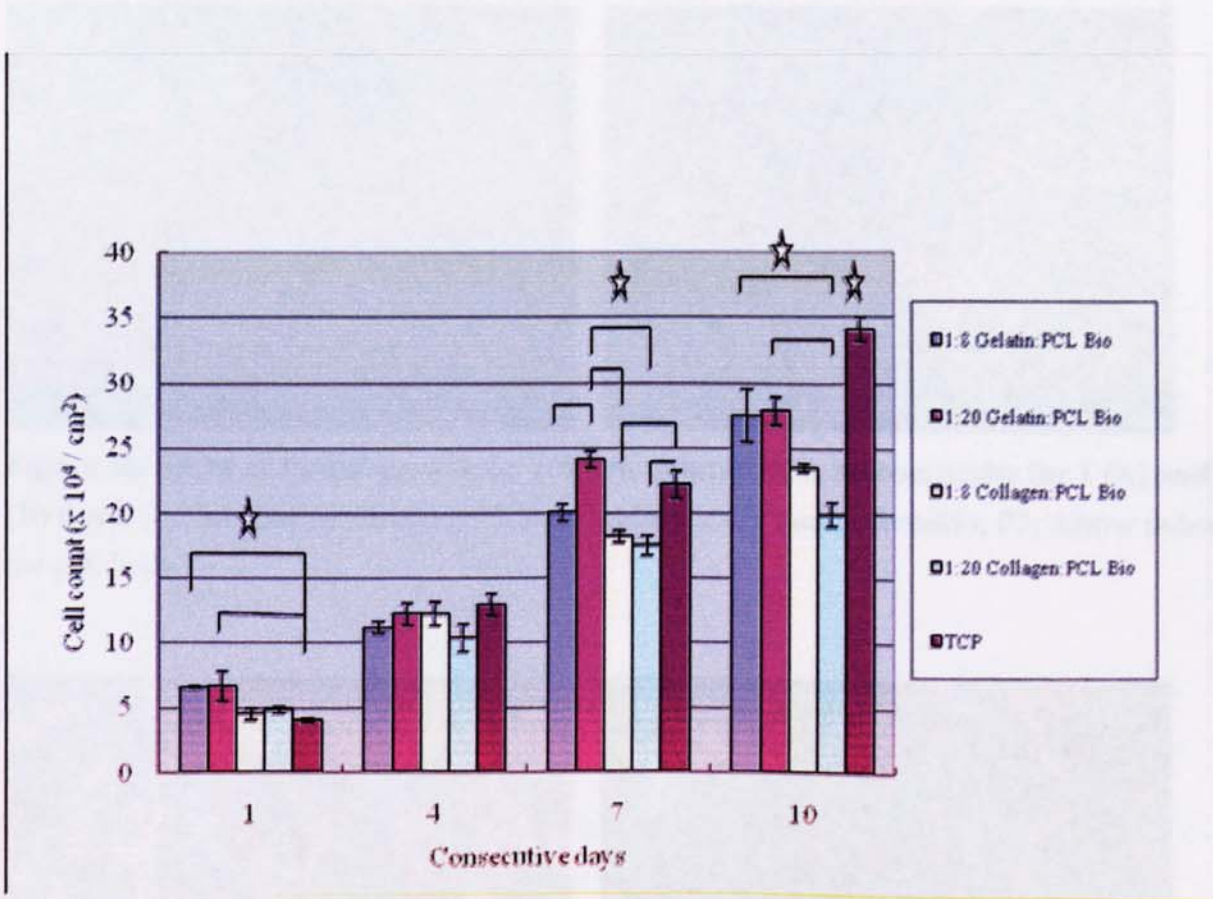

Figure 37: Comparison of primary human dermal fibroblasts (PHDF) growth on gelatin:PCL & collagen:PCL biocomposites and TCP.

PHDF ($2.0x10^4$ cells per cm^2; adult foreskin; P3) were seeded in 7 ml glass shell vials containing gelatin:PCL and collagen:PCL biocomposites (1:8 and 1:20) and TCP. Submerged growth of PHDF was allowed for 10 days. Cell counting was performed at day 1, 4, 7 and 10. (n=4; Values are mean±SE; ANOVA: $P<0.05$ except $P=0.344$ at day 4; Newman-Keuls: $P<0.05$ except at day 4; Asterisk indicates statistically significant difference).

5.2.6.1 Scanning electron microscopy (SEM)

The morphology of growth and distribution of PHDF (seeding density of $2.0x10^4$ cells per cm^2; adult foreskin; P3) on the top surface of 1:8 and 1:20 (w/w) gelatin:PCL biocomposites were investigated by using SEM. Increased fibroblast cell numbers and more diffuse distribution of cells with diffuse ECM deposition on biocomposites were apparent on day 4 compared to that on day 1. The results of SEM of cell growth on 1:8 and 1:20 (w/w) gelatin:PCL biocomposites at day 1 and 4 are shown in Figure 38 and 39.

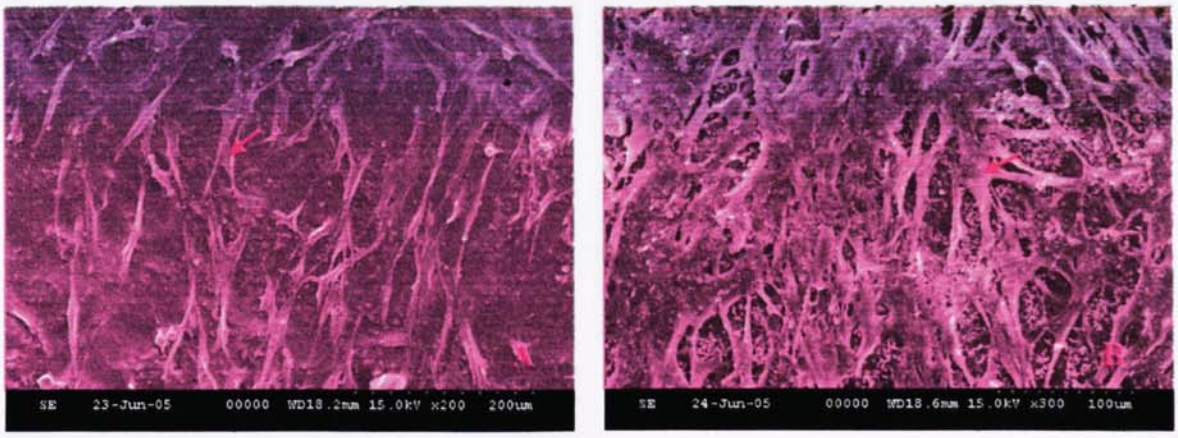

Figure 38: SEM of PHDF growth on 1:8 w/w gelatin:PCL biocomposite for 1 (A) and 4 (B) days. (Initial seeding density of $2.0x10^4$ cells per cm^2; adult foreskin; P3; Arrow indicates the cell body.)

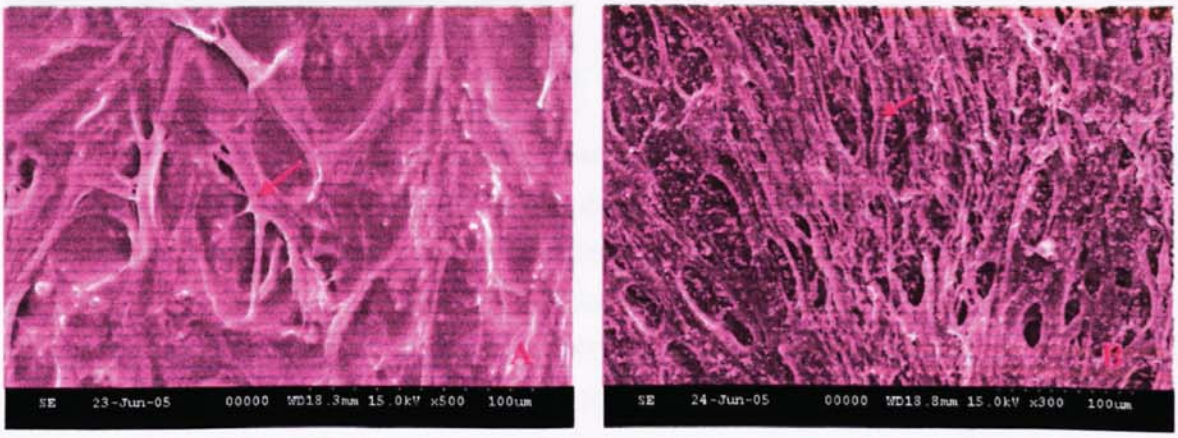

Figure 39: SEM of PHDF growth on 1:20 w/w gelatin:PCL biocomposite for 1 (A) and 4 (B) days. (Initial seeding density of $2.0x10^4$ cells per cm^2; adult foreskin; P3; Arrow indicates the cell body.)

5.2.6.2 Immunohistochemistry assay

The growth and distribution of PHDF (seeding density of $2.0x10^4$ cells per cm^2; adult foreskin; P3) on the top surface of 1:8 and 1:20 (w/w) gelatin:PCL biocomposites on day 1, 7 and 10 were investigated by immunohistochemistry assay. PHDF were labeled with monoclonal mouse anti-human.α tubulin antibody (primary) and goat anti-mouse FITC-conjugated antibody (secondary), and were investigated under fluorescent microscope. Increased fibroblast cell numbers and distribution of cells with diffuse ECM deposition on biocomposites were apparent at time intervals up to 10 days (Figure 40 and 41).

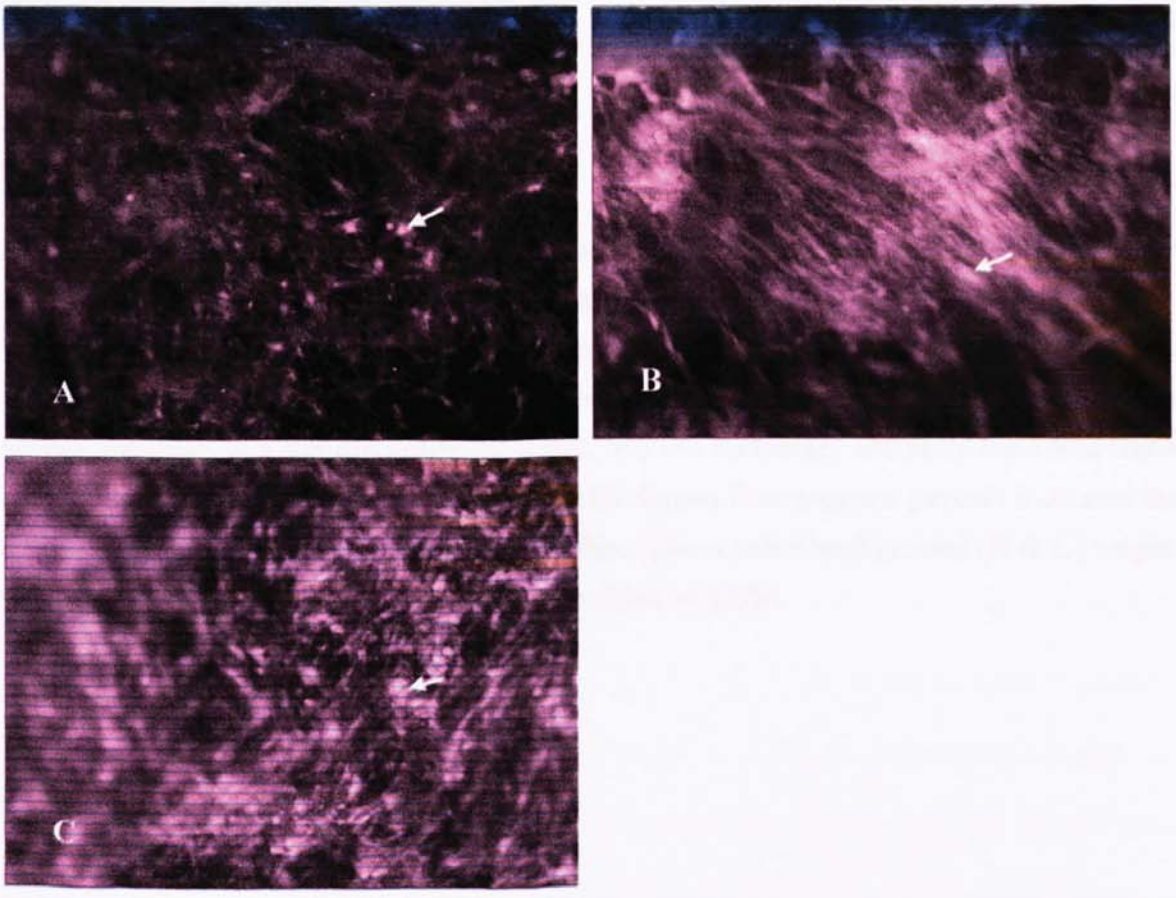

Figure 40: Immunohistochemistry assay of PHDF growth on 1:8 gelatin:PCL biocomposite for 1 (A), 7 (B) and 10 (C) days. (100x; scale bar: 100μm)
PHDF ($2.0x10^4$ cells per cm^2; adult foreskin; P3) were seeded on 1:8 gelatin:PCL biocomposites on day 0. The primary antibody used for labeling of α tubulin was monoclonal mouse anti-human α tubulin antibody 1:100, and the secondary antibody used was fluorescein (FITC)-conjugated goat anti-mouse IgG 1:100. Green fluorescence (arrow) indicates the positive cell staining. The appearance of diffuse green color background (B & C) might indicate an increase in cell numbers or deposition of ECM.

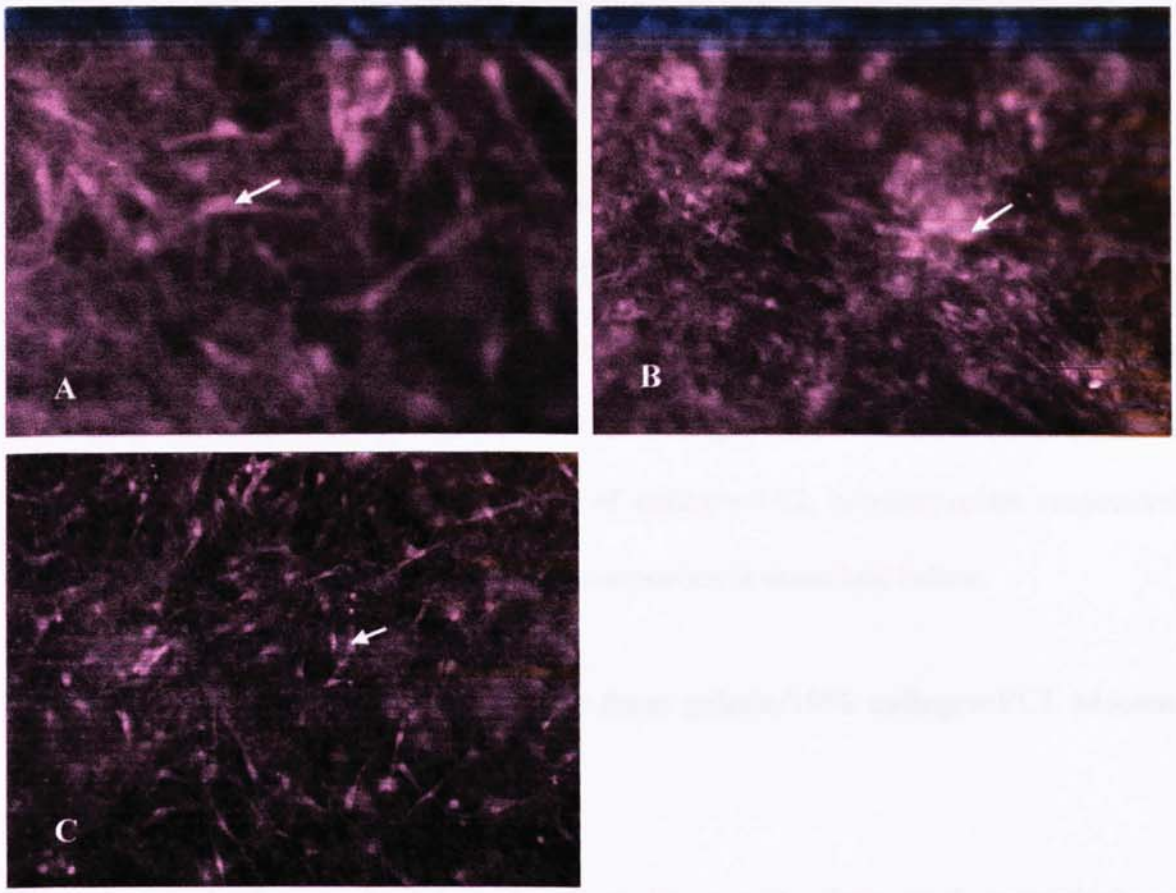

Figure 41: Immunohistochemistry assay of PHDF growth on 1:20 gelatin:PCL biocomposite for 1 (A), 7 (B) and 10 (C) days. (100x; scale bar: 100μm)

PHDF ($2.0x10^4$ cells per cm^2; adult foreskin; P3) were seeded on 1:20 gelatin:PCL biocomposites on day 0. The primary antibody used for labeling of α tubulin was monoclonal mouse anti-human α tubulin antibody 1:100, and the secondary antibody used was fluorescein (FITC)-conjugated goat anti-mouse IgG 1:100. Green fluorescence (arrow) indicates the positive cell staining. The appearance of diffuse green color background (B & C) might indicate an increase in cell numbers or deposition of ECM.

5.3 Study on gelatin/collagen:PCL biocomposites

The BCA total protein assay was used to estimate the amount of protein content released from 1:8 & 1:20 w/w gelatin/10% collagen:PCL and gelatin/25% collagen:PCL biocomposites in PBS at 37°C. The gelatin/10% collagen:PCL and gelatin/25% collagen:PCL biocomposites were prepared from 0.2% gelatin and 0.25% collagen solutions with 10% and 25% of the amount of collagen used for preparation of collagen:PCL biocomposites respectively. The cumulative release of protein from the biocomposites is described below.

5.3.1 Estimation of total protein release from gelatin/10% collagen:PCL biocomposites incubated in PBS at 37°C

Since the standard curves built by using the collagen and gelatin stock respectively revealed the same trend in the pilot study, the protein release from gelatin/collagen:PCL biocomposites was measured on the basis of collagen standard curves in the following study. The cumulative release of protein from the biocomposites is shown in Figure 42. The higher cumulative release of protein content was revealed for 1:8 gelatin/10% collagen:PCL biocomposite, followed by 1:20 group. The 1:8 biocomposites exhibited the higher mean total protein release rate at 6 hours with about 78.3% of the original protein content being released into PBS, while 52.6% was released from 1:20 biocomposites respectively. The amount of protein released significantly increased within 12 hours for all the biocomposites investigated. After 12 hours, the release of protein in 1:8 and 1:20 biocomposites reached a slow increasing rate resulting in a final cumulative release (w/w) of 100%, and 82.6% respectively. The release rate reached a plateau for all biocomposites at the same time on day 3.

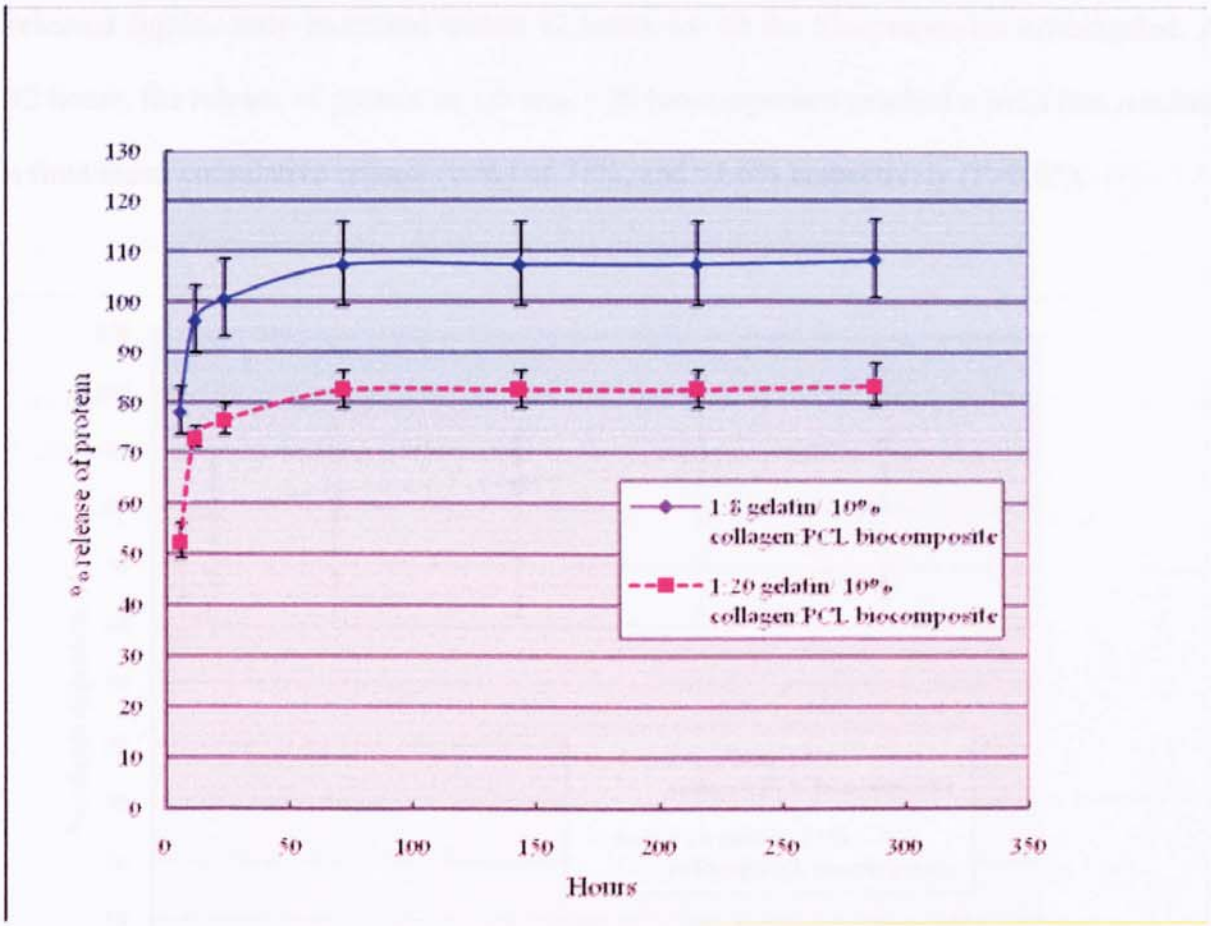

Figure 42: Cumulative release of protein from gelatin/10% collagen:PCL biocomposites in PBS at 37°C.

The BCA total protein assay was used to estimate the amount of total protein release in 1:8 and 1:20 w/w gelatin/10% collagen:PCL biocomposites after incubation in PBS at 37°C for 12 days. The release media were analysed for protein content and replaced by fresh PBS periodically (n=3; Values are mean±SE; Paired t-test: $P<0.05$ except $P=0.05$ at time intervals of day 3, 6 & 9).

5.3.2 Estimation of total protein release from gelatin/25% collagen:PCL biocomposites incubated in PBS at 37°C

The cumulative release of protein from the biocomposites is shown in Figure 43. The higher cumulative release of protein content was revealed for 1:20 gelatin/25% collagen:PCL biocomposite, followed by 1:8 group. The 1:20 biocomposites exhibited the higher mean total protein release rate at 6 hours with about 60.3% of the original protein content being released into PBS, while 52.5% was released from 1:8 biocomposites respectively; however, no significant differences in protein release were apparent ($P>0.05$). The amount of protein

released significantly increased within 12 hours for all the biocomposites investigated. After 12 hours, the release of protein in 1:8 and 1:20 biocomposites reached a mild rate resulting in a final mean cumulative release (w/w) of 71%, and 91.6% respectively (P>0.05).

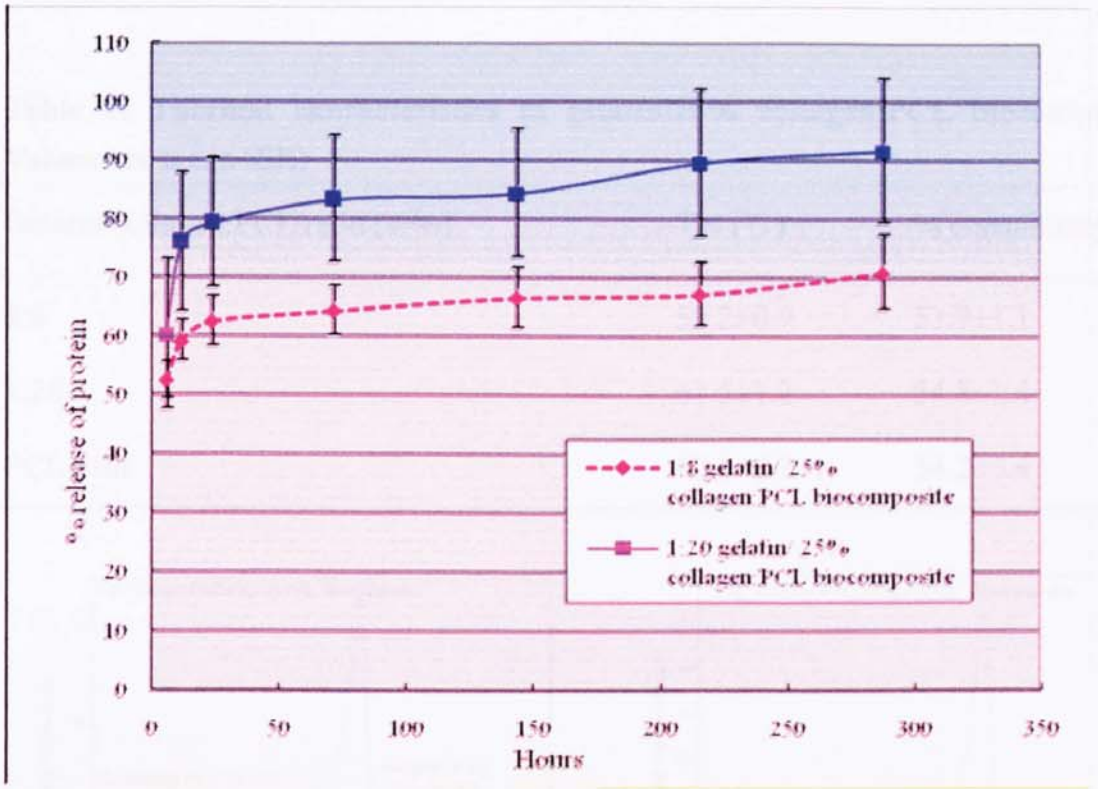

Figure 43: Cumulative release of protein from gelatin/25% collagen:PCL biocomposites in PBS at 37°C.

The BCA total protein assay was used to estimate the amount of total protein release in 1:8 and 1:20 w/w gelatin/25% collagen:PCL biocomposites after incubation in PBS at 37°C for 12 days. The release media were analysed for protein content and replaced by fresh PBS periodically (n=3; Values are mean±SE; Paired t-test: P>0.05).

5.3.3 Differential Scanning Calorimetry (DSC) for gelatin/collagen:PCL biocomposites

The thermal analysis of gelatin/10% collagen:PCL biocomposites (n=3) is shown in Table 4. The melting point of the PCL phase was close to the value of 60℃ normally quoted for PCL. The mean percentage crystallinity of the PCL phase in the higher gelatin/collagen content (1:8 w/w) materials tended to be lower than that of solvent cast films. In contrast the average % crystallinity of the PCL phase in the lower gelatin/collagen content (1:20 w/w) composite was found to increase by almost 1% relative to the solvent cast films. Furthermore, the mean

percentage crystallinity of the PCL phase in the higher gelatin/collagen content (1:8 w/w) materials tended to be lower than that of 1:20 films; however the results were within the standard error (Paired t-test: P=0.683). The DSC scans of 1:8 and 1:20 w/w gelatin/10% collagen:PCL biocomposites are shown in Figure 44.

Table 4: Thermal characteristics of gelatin/10% collagen:PCL biocomposites (n=3; Values are mean±SE)

Gelatin/collagen:PCL ratio (w/w)	Tm (°C)	% crystallinity
1:8	59.2±0.9	53.9±1.1
1:20	61.5±1.2	54.8±1.4
PCL film	62.8±0.2	54.2±5.4

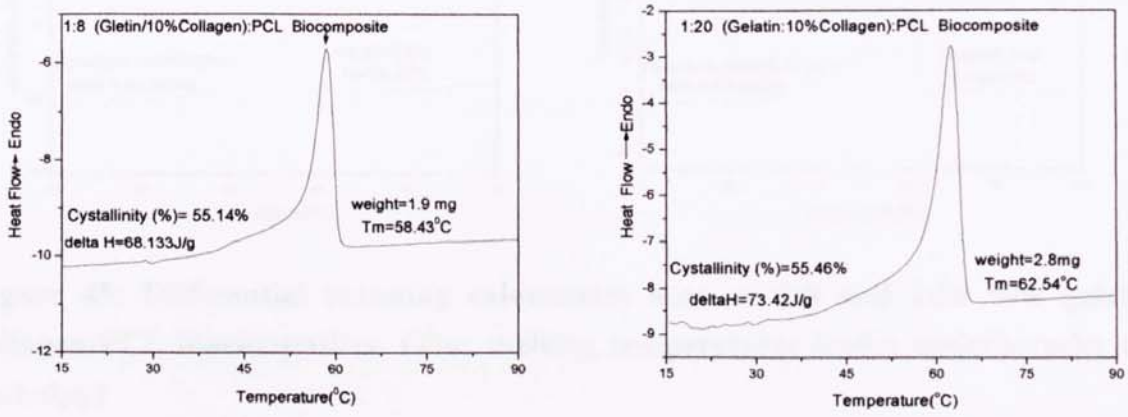

Figure 44: Differential scanning calorimetry scan of 1:8 and 1:20 w/w gelatin/10% collagen:PCL biocomposites. (Tm: melting temperature; Endo: endothermic; data H: enthalpy)

The thermal analysis of gelatin/25% collagen:PCL biocomposites (n=3) is shown in Table 5. The average % crystallinity of the PCL phase in the 1:8 and 1:20 w/w gelatin/collagen content biocomposites were found to increase by almost 1% and 5% relative to the solvent cast films respectively. Furthermore, the mean percentage crystallinity of the PCL phase in the higher gelatin/collagen content (1:8 w/w) materials tended to be lower than that of 1:20 films; however the results were within the standard error (Paired t-test: P=0.173). The DSC scans of

1:8 and 1:20 w/w gelatin/25% collagen:PCL biocomposites are shown in Figure 45.

Table 5: Thermal characteristics of gelatin/25% collagen:PCL biocomposites (n=3; Values are mean±SE)

Gelatin/collagen:PCL ratio (w/w)	Tm (°C)	% crystallinity
1:8	58.3±0.1	55.1±0.7
1:20	59.8±0.2	57.1±0.8
PCL film	62.8±0.2	54.2±5.4

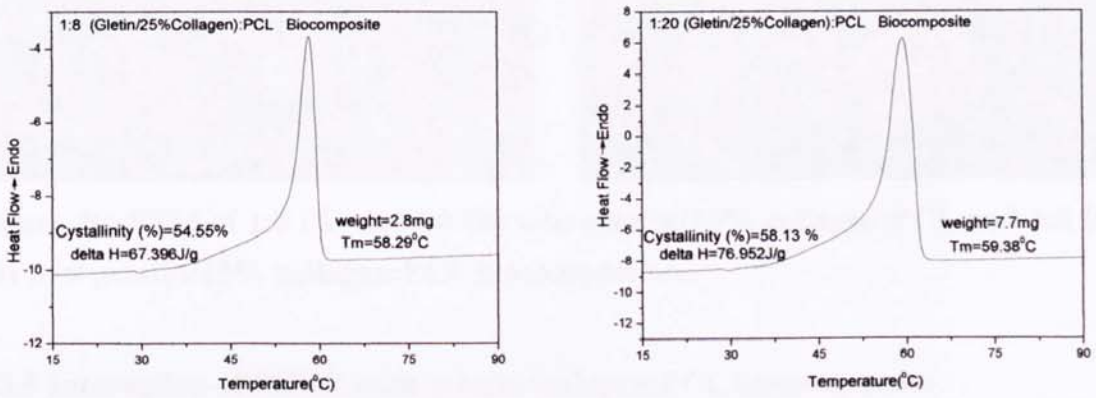

Figure 45: Differential scanning calorimetry scan of 1:8 and 1:20 w/w gelatin/25% collagen:PCL biocomposites. (Tm: melting temperature; Endo: endothermic; data H: enthalpy)

5.3.4 Scanning electron microscopy (SEM) for gelatin/collagen:PCL biocomposites

The morphology of 1:8 and 1:20 (w/w) gelatin/10% collagen:PCL and gelatin/25% collagen:PCL biocomposites were investigated using SEM. The results are shown in Figure 46. All of the biocomposites exhibit a similar rough, fibrous surface due to the collagen mat structure and smooth overlying areas that could be formed by the PCL phase. Little differences in morphology between 1:8 and 1:20 groups were apparent in gelatin/10% collagen:PCL and gelatin/25% collagen:PCL biocomposites respectively.

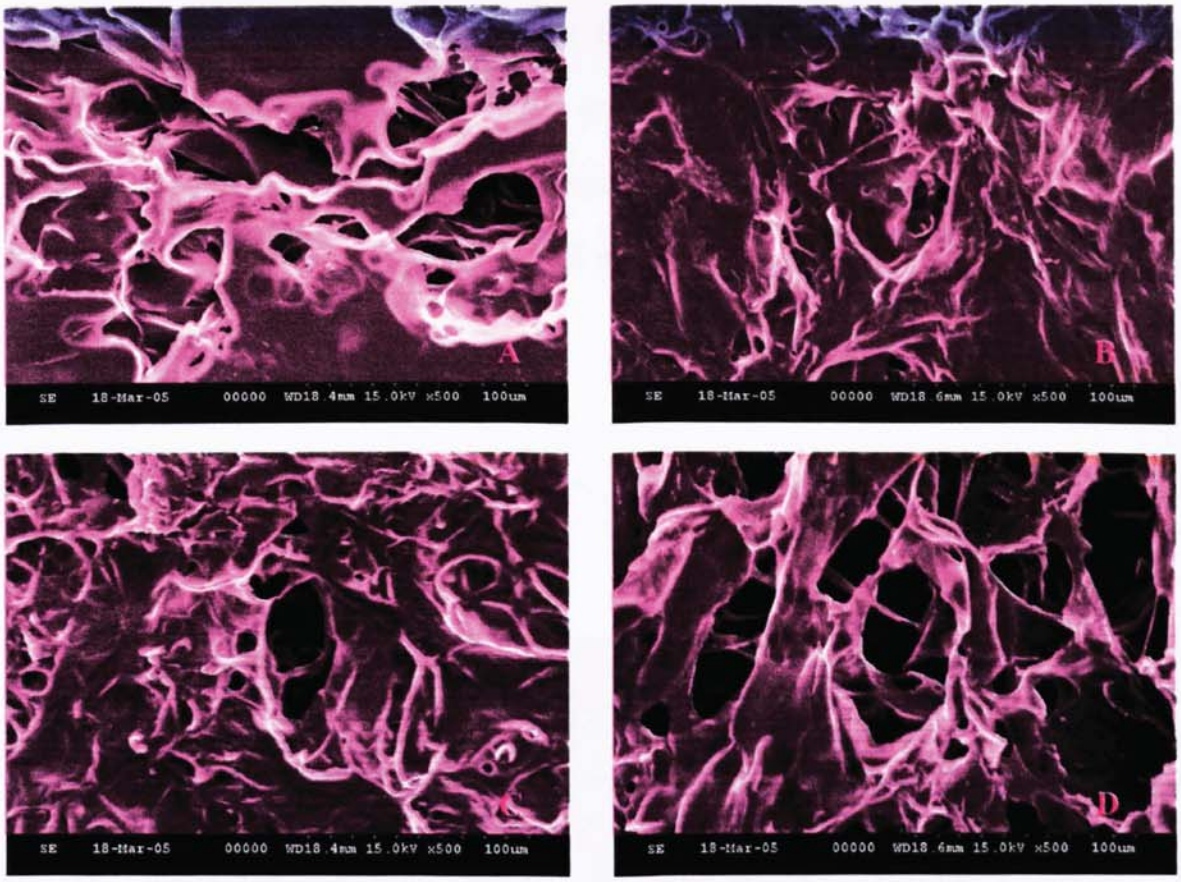

Figure 46: SEM of 1:8 (A) & 1:20 (B) w/w gelatin/10% collagen:PCL and 1:8 (C) & 1:20 (D) w/w gelatin/25% collagen:PCL biocomposites.

5.3.5 Interaction of PHEK with gelatin/collagen:PCL biocomposites

Primary human epidermal keratinocytes (PHEK; child foreskin; P4) were seeded on the top surface of gelatin/10% collagen:PCL biocomposites (1:8 and 1:20), gelatin/25% collagen:PCL biocomposites (1:8 and 1:20), collagen:PCL biocomposites (1:8 and 1:20) and TCP (24-well tissue culture plastics) at a cell density of $1.7x10^5$ cells per cm^2 for time intervals up to 9 days. Trypsin-EDTA solution was used for cell detachment followed by cell counting at day 1, 3, 6 and 9 using a Weber's haemocytometer.

The submerged proliferation rates of PHEK on biocomposites and TCP are shown in Figure 47. Cell confluence and best cell growth curve were observed in TCP control group at a cell density of $4.1x10^5$ cells per cm^2 on day 9. The keratinocyte density (cells per cm^2) was higher on the 1:8 collagen:PCL biocomposite group than the other biocomposite groups at time

intervals of 3 and 6 days ($P<0.05$) and almost equivalent at 9 days ($P<0.05$). The 1:8 gelatin/10% collagen:PCL biocomposite group has the better mean cell growth numbers compared to the other groups of gelatin/collagen:PCL and 1:20 collagen:PCL biocomposite; however, no significant differences in cell numbers were apparent, the measurements being within the range of standard error.

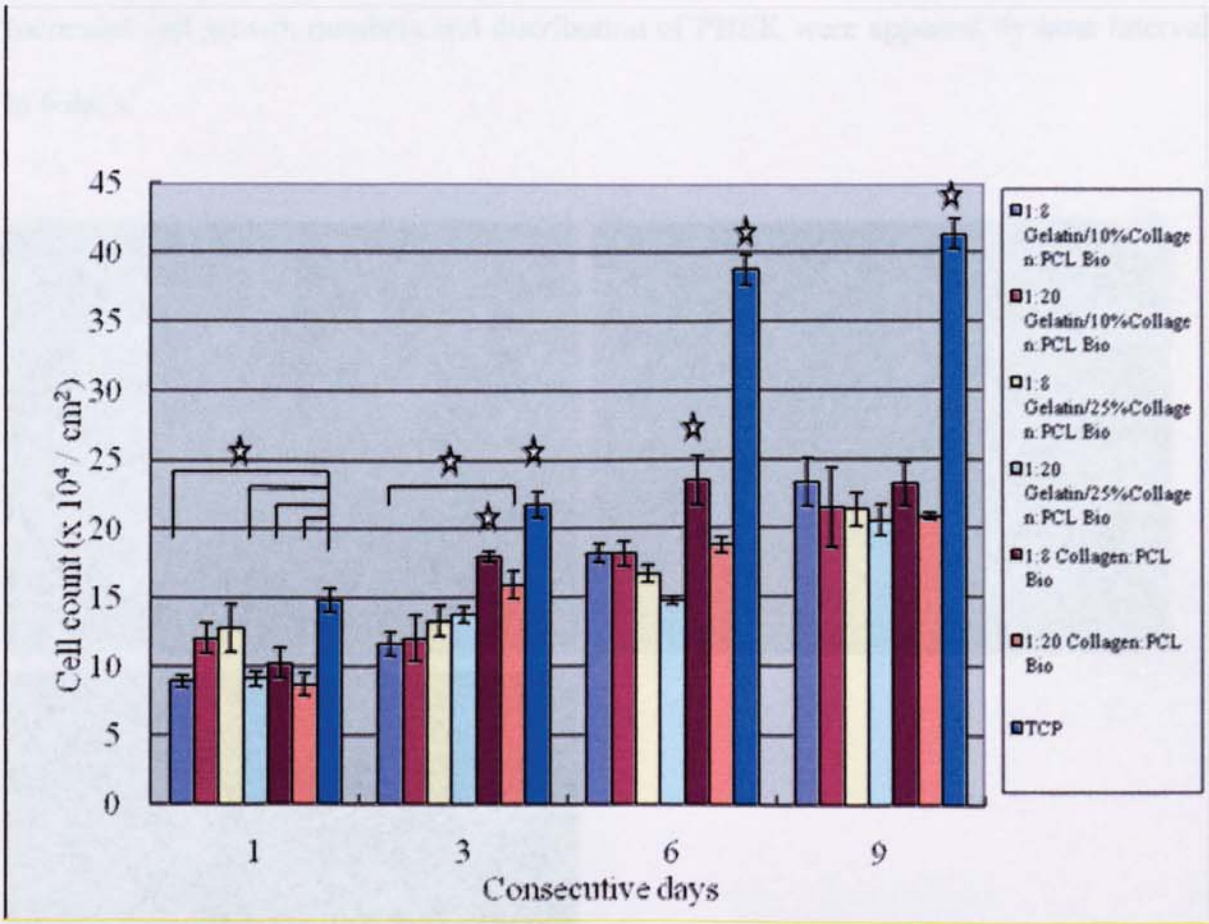

Figure 47: Comparison of primary human epidermal keratinocyte (PHEK) growth on gelatin/collagen:PCL & collagen:PCL biocomposites and TCP.

PHEK ($1.7x10^5$ cells per cm^2; child foreskin; P4) were seeded in 7 ml glass shell vials containing biocomposites (1:8 and 1:20) and TCP. Submerged growth of PHEK was allowed for 9 days. Cell confluence was observed in the TCP control group at day 9. Cell counting was performed at day 1, 3, 6 and 9. (n=4; Values are mean±SE; ANOVA: $P<0.05$; Newman-Keuls: $P<0.05$; Asterisk indicates statistically significant difference).

5.3.5.1 Immunohistochemistry assay

Immunohistochemistry assay of cell growth on the top surface of 1:8 and 1:20 (w/w) gelatin/collagen:PCL biocomposites was performed by labeling of keratinocytes with monoclonal mouse anti-human involucrin antibody 1:100, and the secondary antibodies of rhodamine-conjugated goat anti-mouse IgG 1:100 on day 1, 3 and 6 (Figure 48 to 51). Increased cell growth numbers and distribution of PHEK were apparent by time intervals up to 6 days.

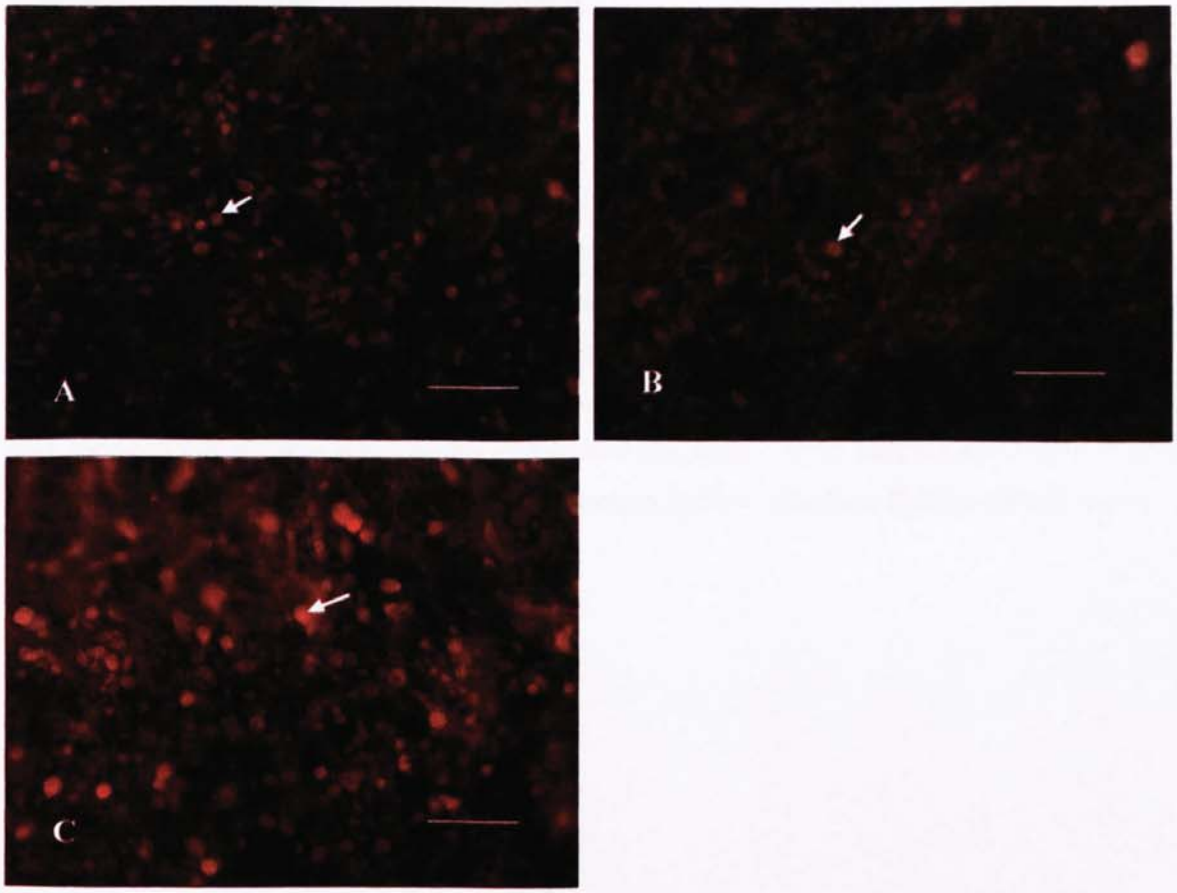

Figure 48: Immunohistochemistry assay of PHEK growth on 1:8 w/w gelatin/10% collagen:PCL biocomposite for 1 (A), 3 (B) and 6 (C) days. (100x; scale bar: 100μm)
PHEK ($1.7x10^5$ cells per cm^2; child foreskin; P4) were seeded on 1:8 gelatin/10% collagen:PCL biocomposites on day 0. The primary antibody used for labeling of involucrin was monoclonal mouse anti-human involucrin antibody 1:100, and the secondary antibody used was rhodamine-conjugated goat anti-mouse IgG 1:100. Red fluorescence (arrow) indicates the positive cell staining.

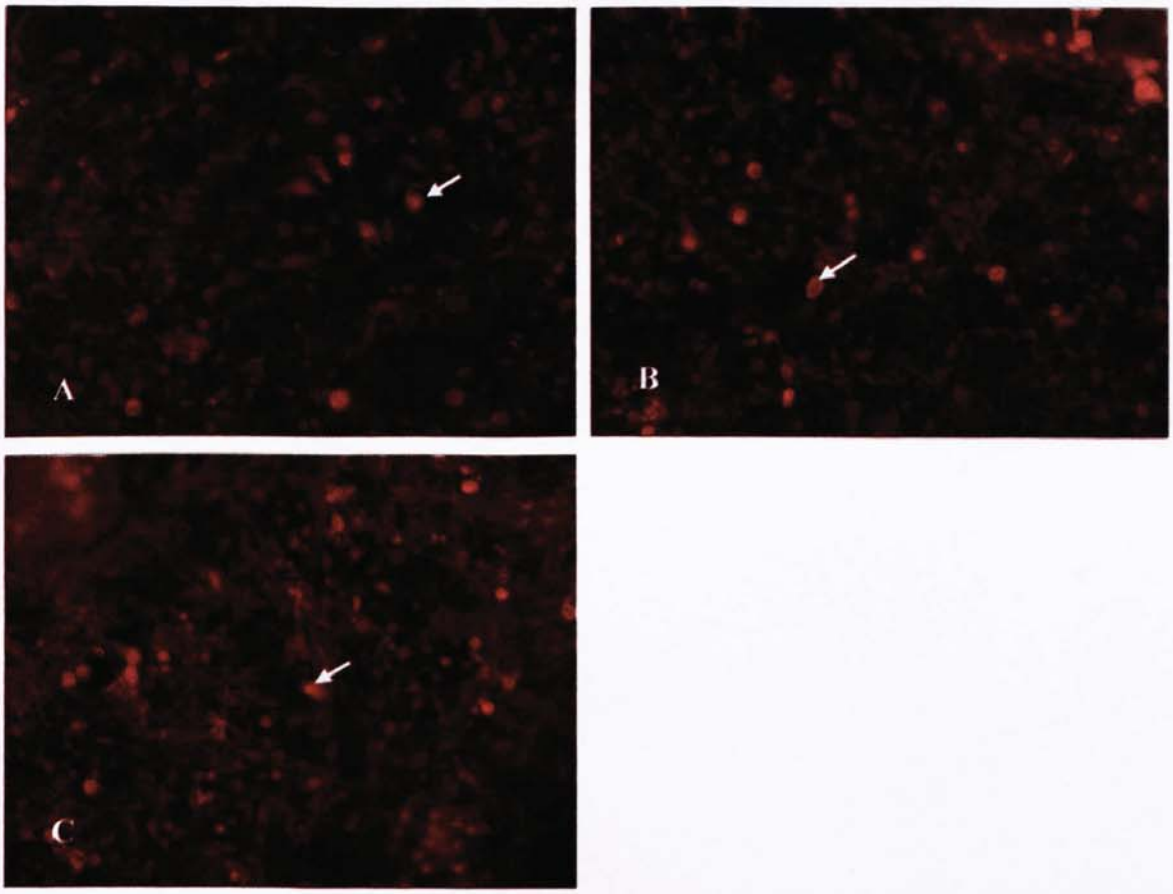

Figure 49: Immunohistochemistry assay of PHEK growth on 1:20 w/w gelatin/10% collagen:PCL biocomposite for 1 (A), 3 (B) and 6 (C) days. (100x; scale bar: 100μm)
PHEK ($1.7x10^5$ cells per cm^2; child foreskin; P4) were seeded on 1:20 gelatin/10% collagen:PCL biocomposites on day 0. The primary antibody used for labeling of involucrin was monoclonal mouse anti-human involucrin antibody 1:100, and the secondary antibody used was rhodamine-conjugated goat anti-mouse IgG 1:100. Red fluorescence (arrow) indicates the positive cell staining.

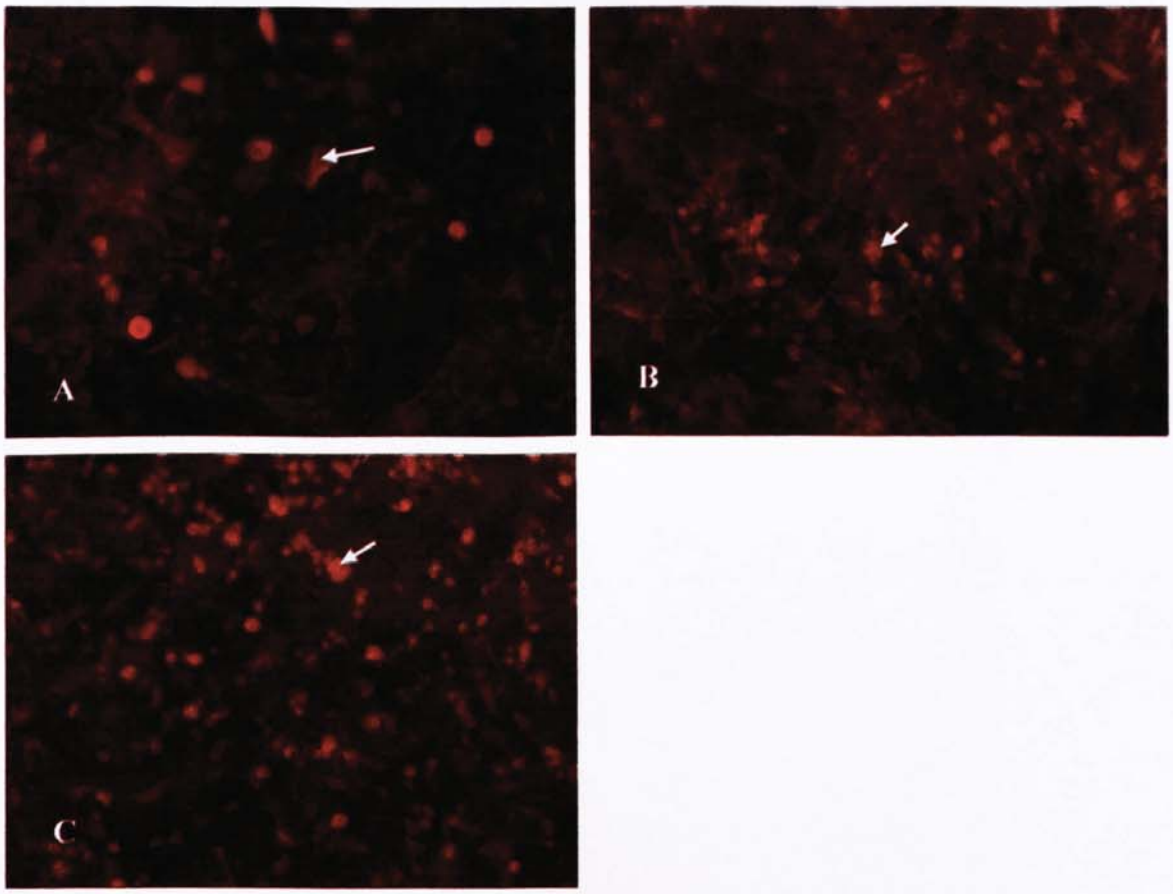

Figure 50: Immunohistochemistry assay of PHEK growth on 1:8 w/w gelatin/25% collagen:PCL biocomposite for 1 (A), 3 (B) and 6 (C) days. (100x; scale bar: 100μm)
PHEK ($1.7x10^5$ cells per cm^2; child foreskin; P4) were seeded on 1:8 gelatin/25% collagen:PCL biocomposites on day 0. The primary antibody used for labeling of involucrin was monoclonal mouse anti-human involucrin antibody 1:100, and the secondary antibody used was rhodamine-conjugated goat anti-mouse IgG 1:100. Red fluorescence (arrow) indicates the positive cell staining.

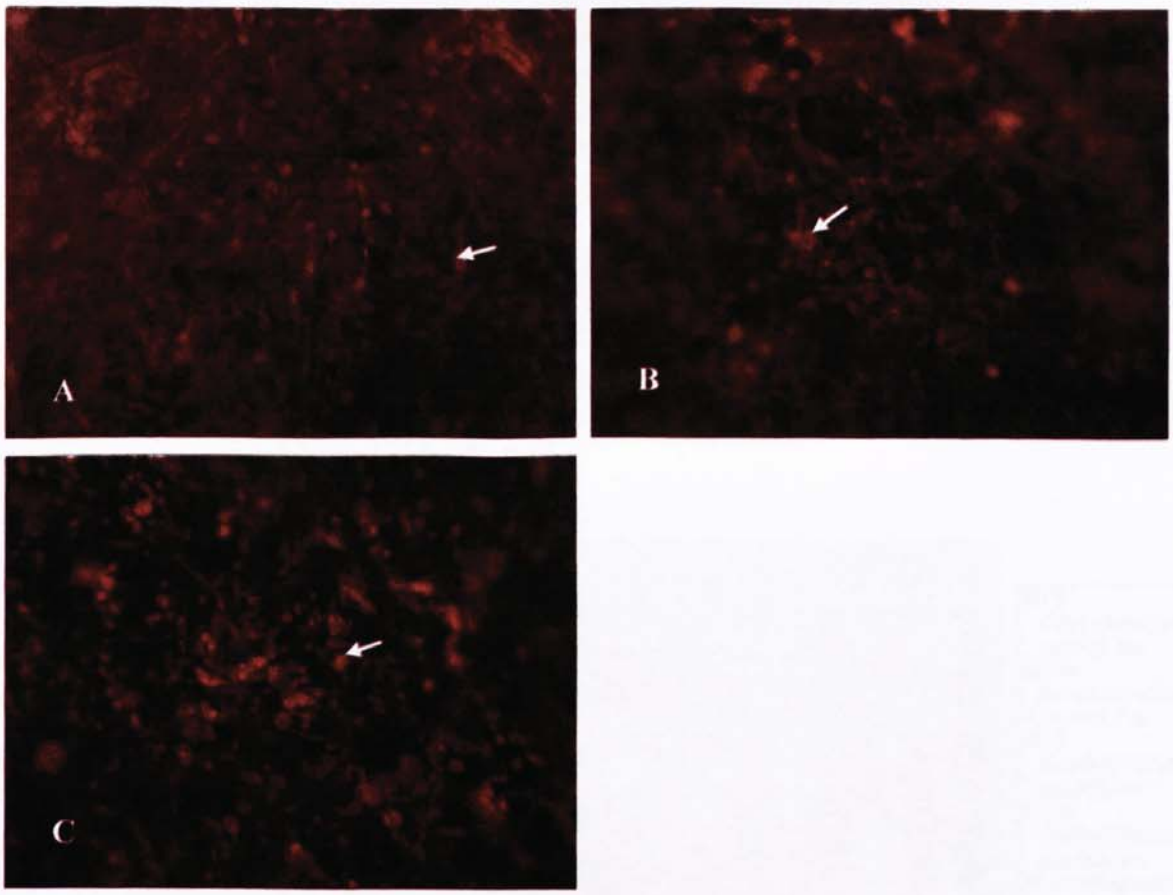

Figure 51: Immunohistochemistry assay of PHEK growth on 1:20 w/w gelatin/25% collagen:PCL biocomposite for 1 (A), 3 (B) and 6 (C) days. (100x; scale bar: 100μm)
PHEK ($1.7x10^5$ cells per cm^2; child foreskin; P4) were seeded on 1:20 gelatin/25% collagen:PCL biocomposites on day 0. The primary antibody used for labeling of involucrin was monoclonal mouse anti-human involucrin antibody 1:100, and the secondary antibody used was rhodamine-conjugated goat anti-mouse IgG 1:100. Red fluorescence (arrow) indicates the positive cell staining.

5.3.6 Interaction of PHDF with gelatin/collagen:PCL biocomposites

Primary human dermal fibroblasts (PHDF; adult foreskin; P3-4) were seeded on the top surface of 1:8 and 1:20 (w/w) gelatin/10% collagen:PCL, gelatin/25% collagen:PCL and collagen:PCL biocomposites and TCP (24-well tissue culture plastics) at a cell density of $2.0x10^4$ cells per cm^2 for time intervals up to 10 days. Trypsin-EDTA solution was used for cell detachment followed by cell counting at day 1, 4, 7 and 10 using a Weber's haemocytometer. The submerged proliferation rates of PHDF on biocomposites and TCP are shown in Figure 52. Best cell growth was shown in TCP control group at time intervals of 7

and 10 days ($P<0.05$). The 1:8 gelatin/25% collagen:PCL biocomposite group has the better cell growth numbers compared to the other groups of gelatin/collagen:PCL and 1:20 collagen:PCL biocomposite on day 1 ($P<0.05$); however, the cell growth numbers became almost equivalent in all biocomposite groups at time intervals up to 10 days ($P>0.05$).

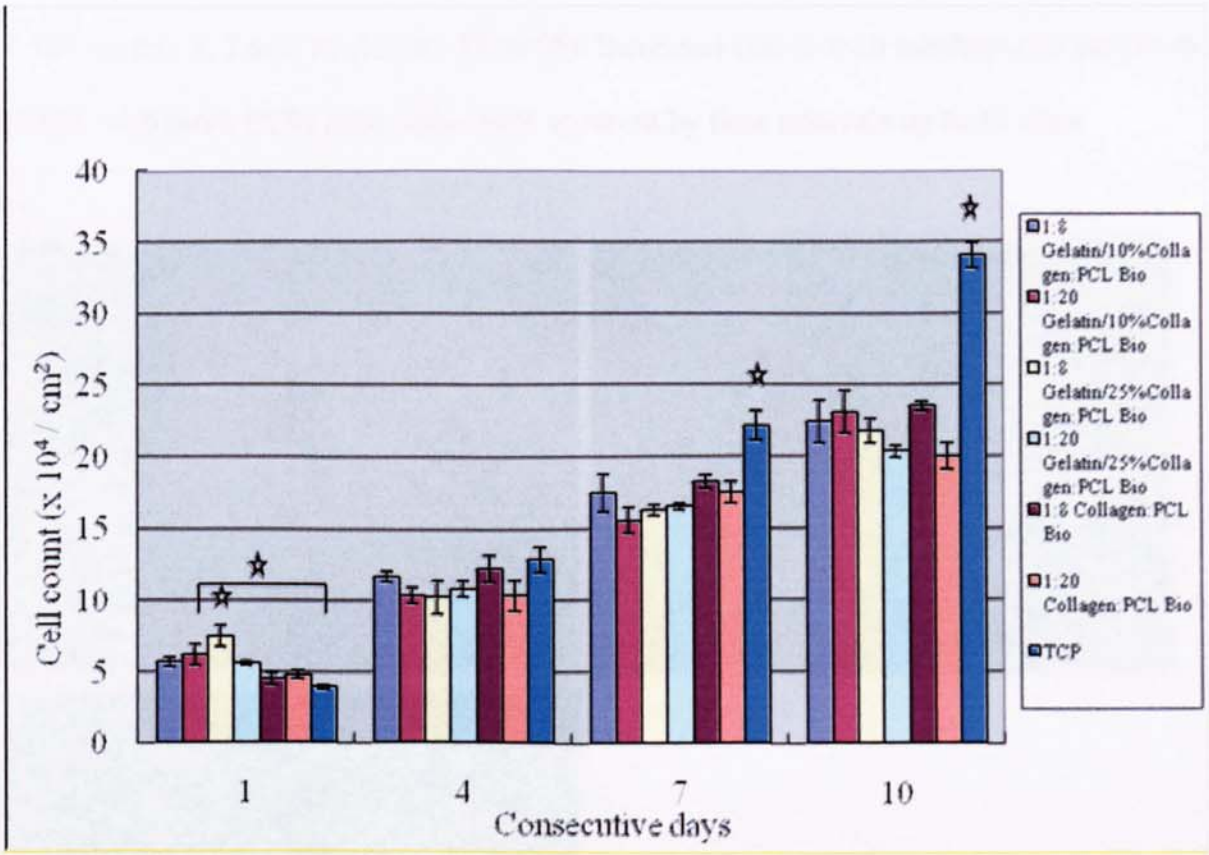

Figure 52: Comparison of primary human dermal fibroblasts (PHDF) growth on gelatin/collagen:PCL & collagen:PCL biocomposites and TCP.

PHDF ($2.0x10^4$ cells per cm^2; adult foreskin; P3) were seeded in 7 ml glass shell vials containing gelatin/collagen:PCL and collagen:PCL biocomposites (1:8 and 1:20) and TCP. Submerged growth of PHDF was allowed for 10 days. Cell counting was performed at day 1, 4, 7 and 10. (n=4; Values are mean±SE; ANOVA: $P<0.05$ except on day 4; Newman-Keuls: $P<0.05$ except on day 4; Asterisk indicates statistically significant difference).

5.3.6.1 Immunohistochemistry assay

Immunohistochemistry assay of cell growth on the top surface of biocomposites was performed by labeling of fibroblasts with monoclonal mouse anti-human α tubulin antibody 1:200, and the secondary antibodies of fluorescein (FITC)-conjugated goat anti-mouse IgG 1:100 on day 1, 7 and 10 (Figure 53 to 56). Increased cell growth numbers and distribution of PHDF with more ECM deposition were apparent by time intervals up to 10 days.

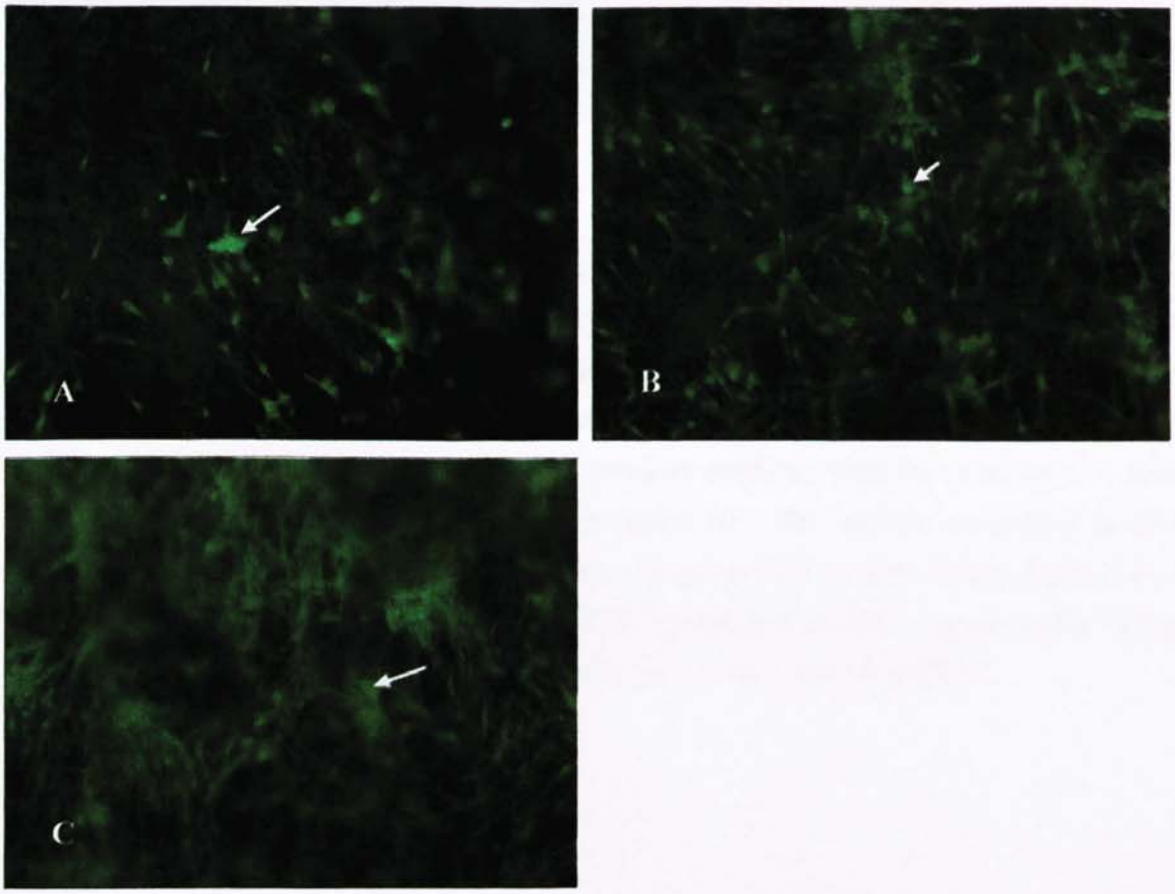

Figure 53: Immunohistochemistry assay of PHDF growth on 1:8 w/w gelatin/10% collagen:PCL biocomposite for 1 (A), 7 (B) and 10 (C) days. (100x; scale bar: 100μm)
PHDF ($2.0x10^4$ cells per cm^2; adult foreskin; P3) were seeded on 1:8 gelatin/10% collagen:PCL biocomposites on day 0. The primary antibody used for labeling of α tubulin was monoclonal mouse anti-human α tubulin antibody 1:100, and the secondary antibody used was fluorescein (FITC)-conjugated goat anti-mouse IgG 1:100. Green fluorescence (arrow) indicates the positive cell staining. The appearance of diffuse green color background (B & C) might indicate an increase in cell numbers or deposition of ECM.

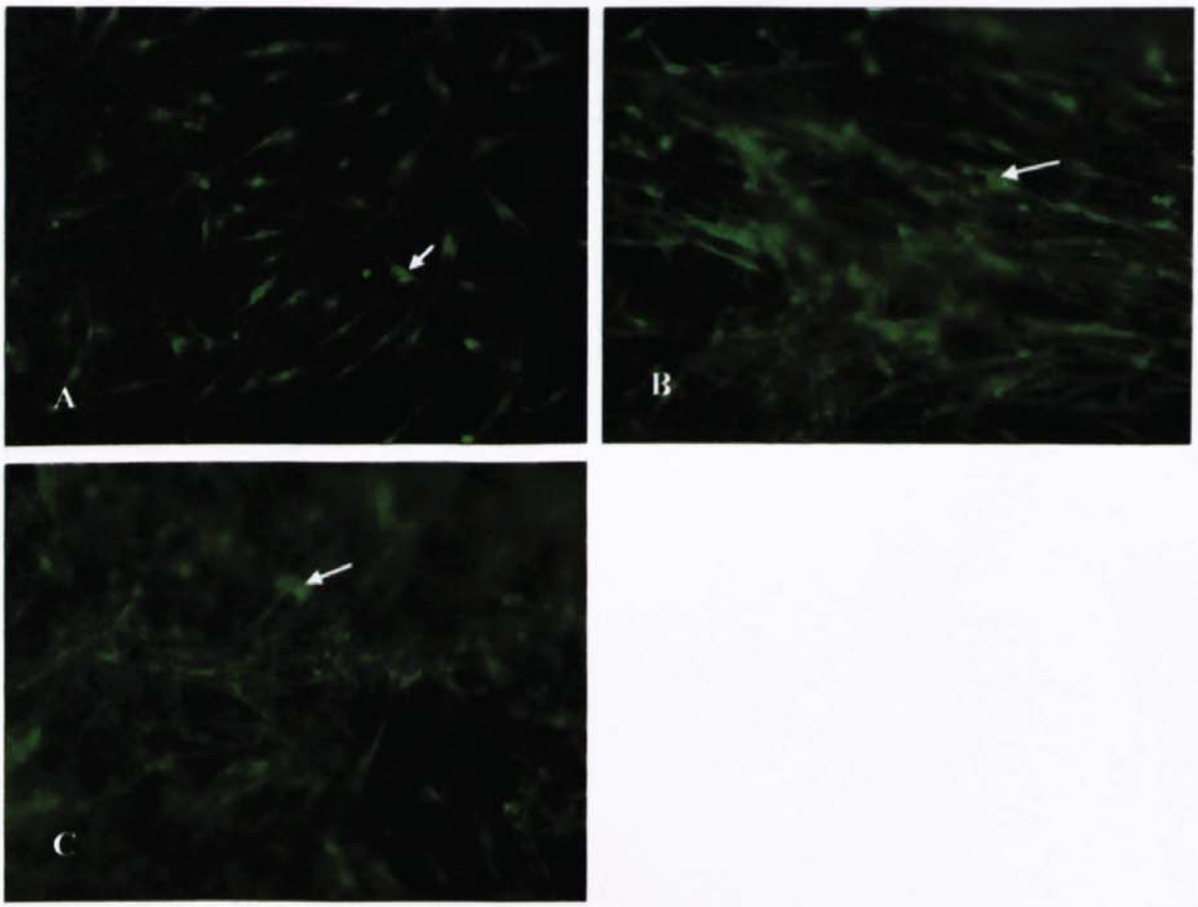

Figure 54: Immunohistochemistry assay of PHDF growth on 1:20 w/w gelatin/10% collagen:PCL biocomposite for 1 (A), 7 (B) and 10 (C) days. (100x; scale bar: 100μm) PHDF ($2.0x10^4$ cells per cm^2; adult foreskin; P3) were seeded on 1:20 gelatin/10% collagen:PCL biocomposites on day 0. The primary antibody used for labeling of α tubulin was monoclonal mouse anti-human α tubulin antibody 1:100, and the secondary antibody used was fluorescein (FITC)-conjugated goat anti-mouse IgG 1:100. Green fluorescence (arrow) indicates the positive cell staining. The appearance of diffuse green color background (B & C) might indicate an increase in cell numbers or deposition of ECM.

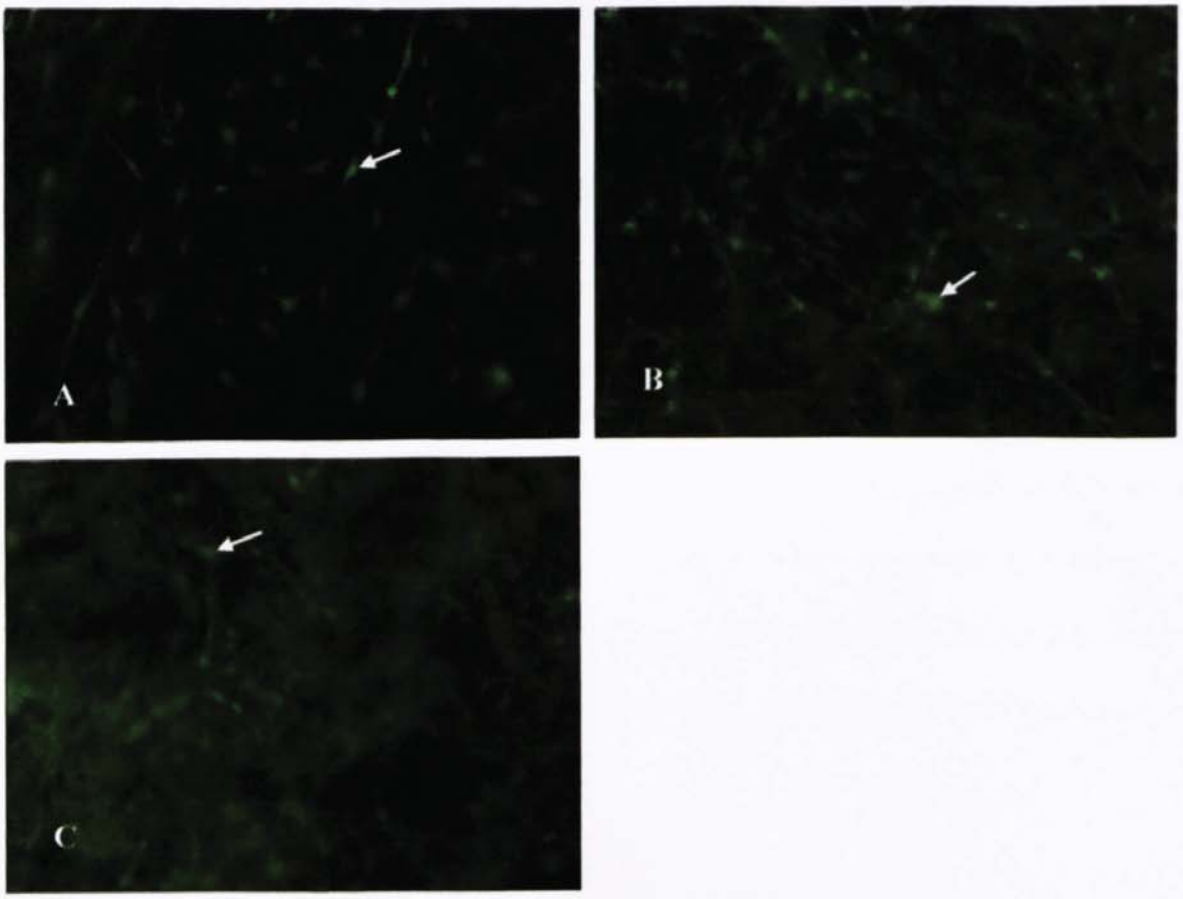

Figure 55: Immunohistochemistry assay of PHDF growth on 1:8 w/w gelatin/25% collagen:PCL biocomposite for 1 (A), 7 (B) and 10 (C) days. (100x; scale bar: 100μm) PHDF ($2.0x10^4$ cells per cm^2; adult foreskin; P3) were seeded on 1:8 gelatin/25% collagen:PCL biocomposites on day 0. The primary antibody used for labeling of α tubulin was monoclonal mouse anti-human α tubulin antibody 1:100, and the secondary antibody used was fluorescein (FITC)-conjugated goat anti-mouse IgG 1:100. Green fluorescence (arrow) indicates the positive cell staining. The appearance of diffuse green color background (B & C) might indicate an increase in cell numbers or deposition of ECM.

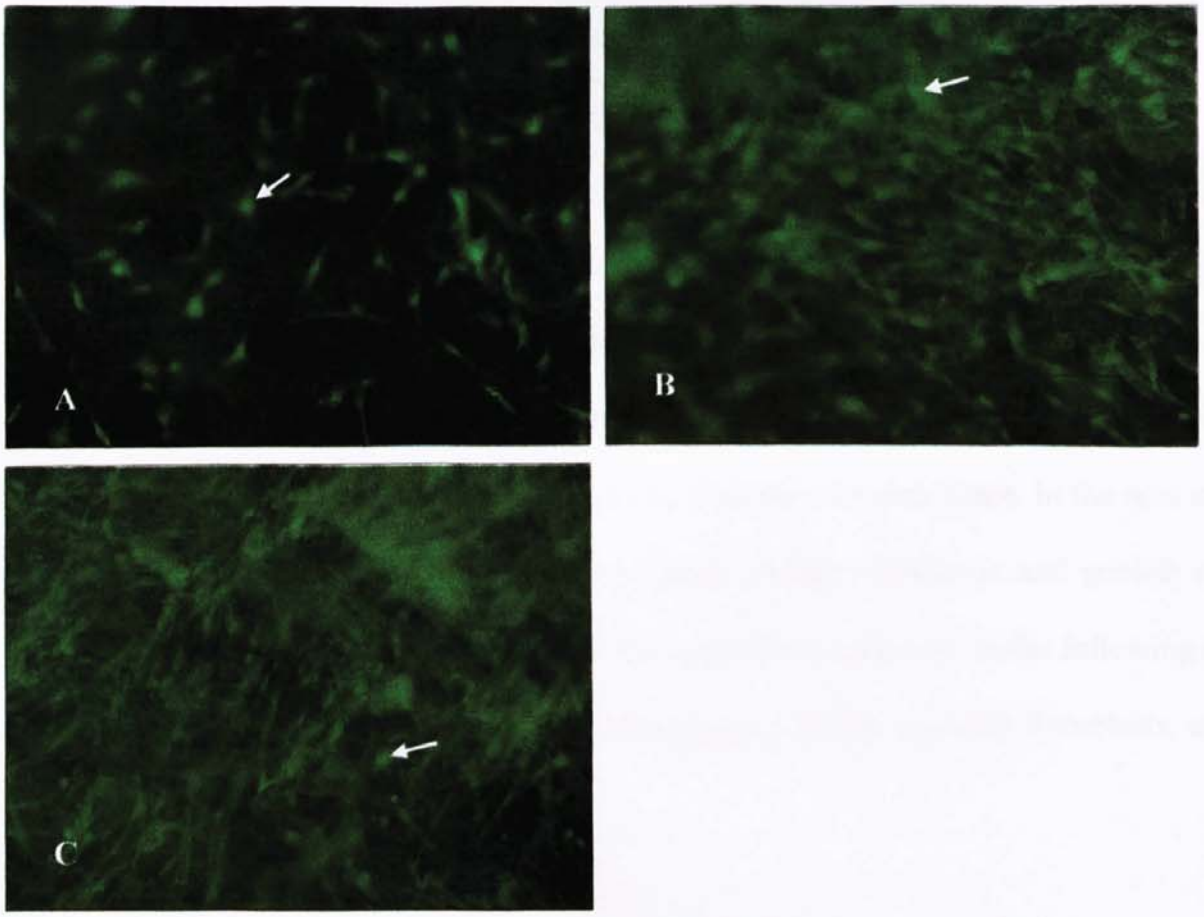

Figure 56: Immunohistochemistry assay of PHDF growth on 1:20 w/w gelatin/25% collagen:PCL biocomposite for 1 (A), 7 (B) and 10 (C) days. (100x; scale bar: 100μm) PHDF ($2.0x10^4$ cells per cm^2; adult foreskin; P3) were seeded on 1:20 gelatin/25% collagen:PCL biocomposites on day 0. The primary antibody used for labeling of α tubulin was monoclonal mouse anti-human α tubulin antibody 1:100, and the secondary antibody used was fluorescein (FITC)-conjugated goat anti-mouse IgG 1:100. Green fluorescence (arrow) indicates the positive cell staining. The appearance of diffuse green color background (B & C) might indicate an increase in cell numbers or deposition of ECM.

5.4 *In vitro* study on co-cultured skin model

The design of a co-cultured skin model in this study was based on the successful seeding, adherence and growth of both epidermal keratinocytes and dermal fibroblasts alone on either side of the membrane. Preliminary investigations carried out to establish the design of the co-culture device and the cell seeding technique were based on two-stage cell seeding of 3T3 fibroblasts on either side of a 1:20 collagen:PCL biocomposite membrane. In the next stage of the study, the design was based on the successful seeding, adherence and growth of both NHEK and 3T3 fibroblasts on either side of the membrane separately. In the following studies, the co-culture designs were based on the cell seeding of PHEK and 3T3 fibroblasts, and that of PHEK and PHDF respectively.

5.4.1 Feasibility study: Co-culture of 3T3 fibroblasts on both surfaces of collagen:PCL biocomposite membranes separately

The results of co-culture of 3T3 fibroblasts on either side of 1:20 collagen:PCL biocomposite films are shown in Figure 57. After seeding 3T3 fibroblasts on the upper surface at a cell density of $1.0x10^5$ cells per cm^2 for 3 days, the cell number was measured as $9.7x10^4$ per cm^2. At day 3, the same density of 3T3 fibroblasts was seeded on the other surface of biocomposites and cultured for a further 3 days. On day 6, the cell density in the control group (cells were only seeded on one surface of the biocomposite film) and the co-cultured group (sum of cell number in both sides of surface) were measured as $1.7x10^5$ and $2.6x10^5$ per cm^2 respectively. A 55.3% increase in cell number was measured in the co-culture system indicating that cell proliferation was sustained on both sides of the biocomposite membrane.

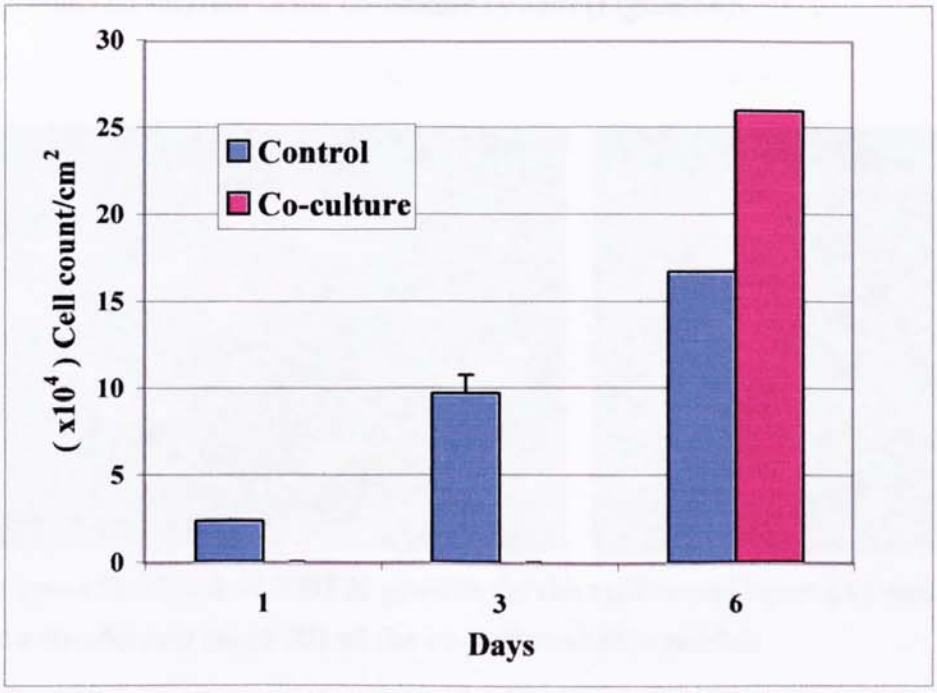

Figure 57: Co-culture of 3T3 fibroblasts on 1:20 collagen:PCL biocomposites.

Preliminary investigations carried out to establish the design of the co-culture device and the two-stage cell seeding technique were based on two-stage cell seeding of 3T3 fibroblasts on either side of a 1:20 collagen:PCL biocomposite membrane. Cells ($1.0x10^5$ cells per cm^2) were seeded on one surface of a biocomposite film in the co-culture device on day 0 (n=8). In control groups, cell counting was performed at day 1 (n=1), day 3 (n=3; Values are mean±SE) and day 6 (n=2). In the co-culture group, cells were also seeded at the same density on the other surface of biocomposite film at day 3 and then the total numbers of attached cells were counted at day 6 (n=2).

5.4.2 Co-culture of NHEK and 3T3 fibroblasts

Co-culture of NHEK and 3T3 fibroblasts on either side of the membrane was subsequently performed using the same co-culture system. In the early stage of the study, the design of a co-cultured skin model was based on the successful seeding, adherence and growth of both NHEK and 3T3 fibroblasts on either side of the membrane separately. 3T3 fibroblasts were seeded on one side of the 1:20 collagen:PCL biocomposite in the co-culture system firstly for 3 days, and then PHEK were seeded on the other side of the biocomposite for another 3 days. The results were proven by SEM and showed that both NHEK and 3T3 fibroblasts, when seeded alone onto one side of the biocomposites, were shown by standard cell culture to

divide and migrate in the co-culture system (Figure 58).

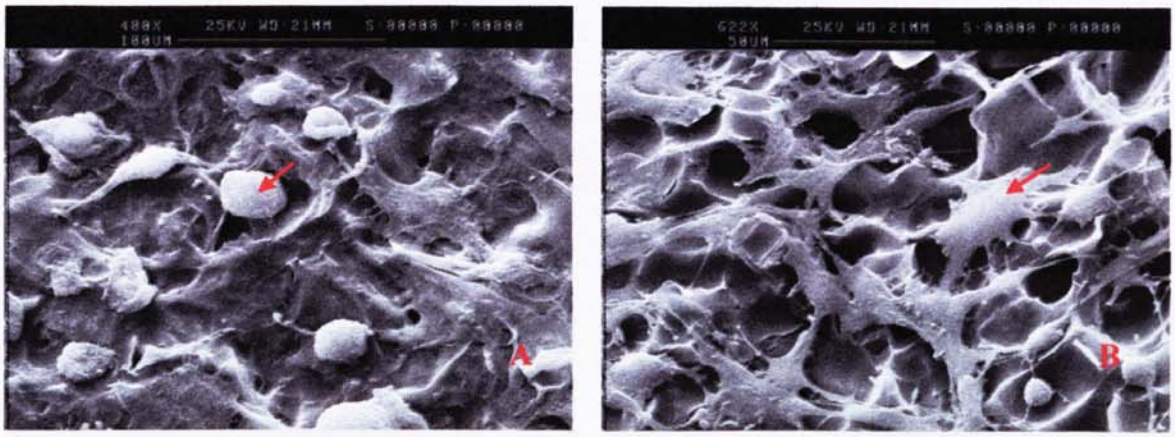

Figure 58: SEM of NHEK growth on the epidermal layer (A) and 3T3 fibroblast growth on the dermal layer (B) of the co-cultured skin model.

The pilot co-culture study was performed by seeding NHEK and 3T3 fibroblasts on either side of 1:20 w/w collagen:PCL biocomposite *in vitro* for 3 and 6 days respectively. Arrow indicates the cell body.

5.4.3 Co-culture of PHEK and 3T3 fibroblasts

To increase the resources of human keratinocyte cells and mimic the normal clinical condition, primary human epidermal keratinocytes (PHEK) were isolated and cultured from the epidermal layer of human foreskin in the this study. Co-culture of PHEK and 3T3 fibroblasts on either side of the membrane was subsequently performed using the same co-culture system. The design of a novel co-cultured skin model was achieved by growing a confluent PHEK sheet on the biocomposite film upwards with a populated 3T3 fibroblast layer underneath followed by lifting the co-cultured membrane onto the air-fluid level for another 10 days to enhance keratinocyte differentiation.

The results were proven by SEM (Figure 59) and immunohistochemistry assays (Figure 60 and 61). SEM revealed a confluent sheet of keratinocytes on the top surface of biocomposite membrane, and good cell attachment and spreading of 3T3 fibroblasts on the other side of the membrane. Immunohistochemistry assay of co-cultured skin model using double labeling of

human keratinocytes and mouse 3T3 fibroblasts with monoclonal mouse anti-cytokeratin 19 IgG 1:200 (Cat No.NCL-CK 19; Novocastra®, Inc.) and mouse anti-vimentin (Cat No.MAB3400; Chemicon® International, Inc.) antibodies respectively showed that a confluent multi-layered keratinocytes in red fluorescent staining, and populated fibroblasts in green fluorescent staining were isolated completely on either side of the membrane.

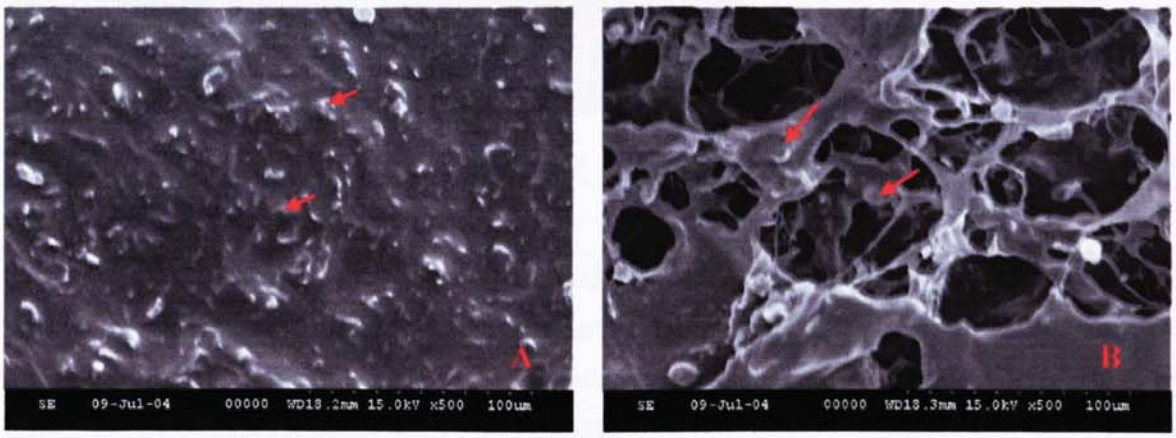

Figure 59: SEM of a co-cultured skin model with a confluent epidermal layer (A) populated with NHEK and a porous dermal layer (B) populated with 3T3 fibroblasts.

SEM revealed a confluent epidermal sheet on the upper surface of 1:20 w/w collagen:PCL biocomposite after seeding PHEK in culture for 28 days, and good attachment and spreading of 3T3 fibroblasts in the underneath dermal layer for 14 days. Arrow indicates the cell body.

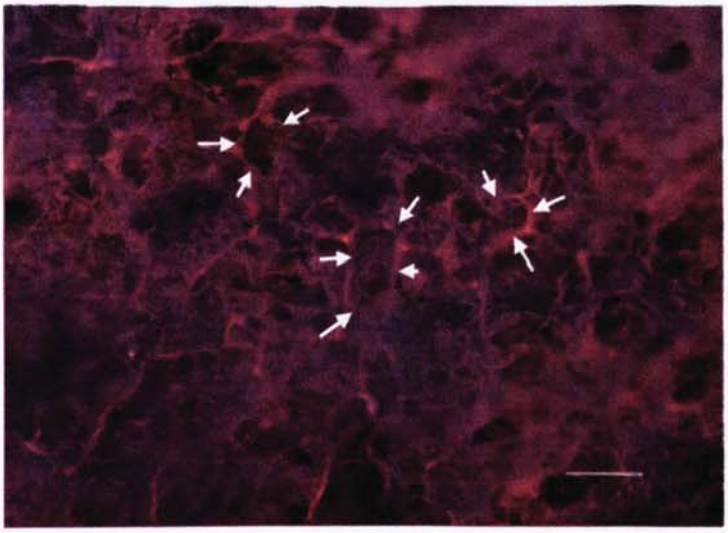

Figure 60: Immunohistochemistry assay of the epidermal layer of the co-cultured skin model (100x; scale bar: 100μm).

Keratinocytes were labeled with monoclonal mouse anti-human cytokeratin 19 antibody 1:200 and the secondary antibody of rhodamine-conjugated goat anti-mouse IgG 1:100 on day 28. It revealed a confluent multi-layered keratinocytes presenting with an upper layer of cornification and underneath keratinocytes (arrow; red fluorescence) on the upper surface of 1:20 collagen:PCL biocomposite in the co-culture system.

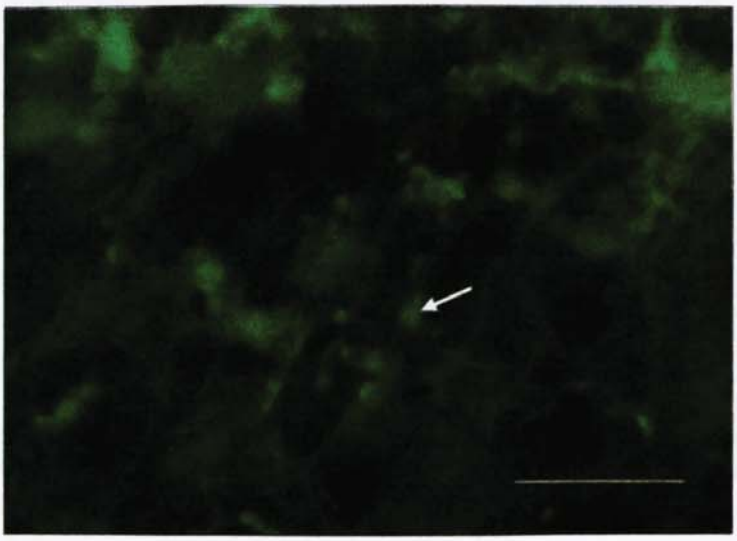

Figure 61: Immunohistochemistry assay of the dermal layer of the co-cultured skin model (200x; scale bar: 100μm).

3T3 fibroblasts were labeled with monoclonal mouse anti-vimentin IgG 1:200 and the secondary antibody of fluorescein (FITC)-conjugated goat anti-mouse IgG 1:100. It revealed good attachment and spreading of 3T3 fibroblasts populated along the porous structure of scaffold in the dermal layer of 1:20 collagen:PCL biocomposite in the co-culture system for 14 days. Green fluorescence (arrow) indicates the positive cell staining. The appearance of diffuse green color background might indicate an increase in cell numbers or deposition of ECM.

5.4.4 Co-culture of single-donor PHEK and PHDF

To increase the resources of human keratinocyte cells and mimic the normal clinical condition, primary human epidermal keratinocytes (PHEK) and primary human dermal fibroblast (PHDF) were isolated and primarily cultured from the epidermal and dermal layers of human foreskin respectively in the this study. Co-culture of PHEK and PHDF on either side of the membrane was subsequently performed using the same co-culture system. The design of a novel co-cultured skin model was achieved by growing a confluent PHEK sheet on the biocomposite film upwards with a populated PHDF layer underneath followed by lifting the co-cultured membrane onto the air-fluid level for another 10 days to enhance keratinocyte differentiation. The results were proven by SEM (Figure 62 and 63) and immunohistochemistry assay (Figure 64 and 65).

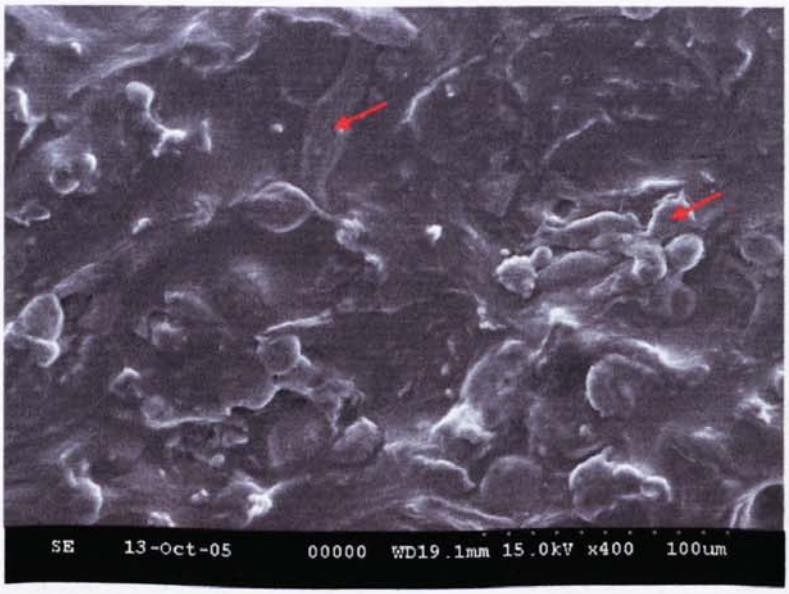

Figure 62: SEM of a confluent PHEK growth on the epidermal layer of the co-cultured skin model.

SEM revealed a confluent sheet of primary human epidermal keratinocytes (PHEK) on the upper surface of 1:20 collagen:PCL biocomposite in the co-culture system for 35 days. Arrow indicates the cell body.

Figure 63: SEM of populated PHDF growth on the dermal layer of the co-cultured skin model.

SEM revealed good attachment and spreading of primary human dermal fibroblasts (PHDF) forming linear fibrous structure on the lower surface of 1:20 collagen:PCL biocomposite in the co-culture system for 35 days. Arrow indicates the cell body.

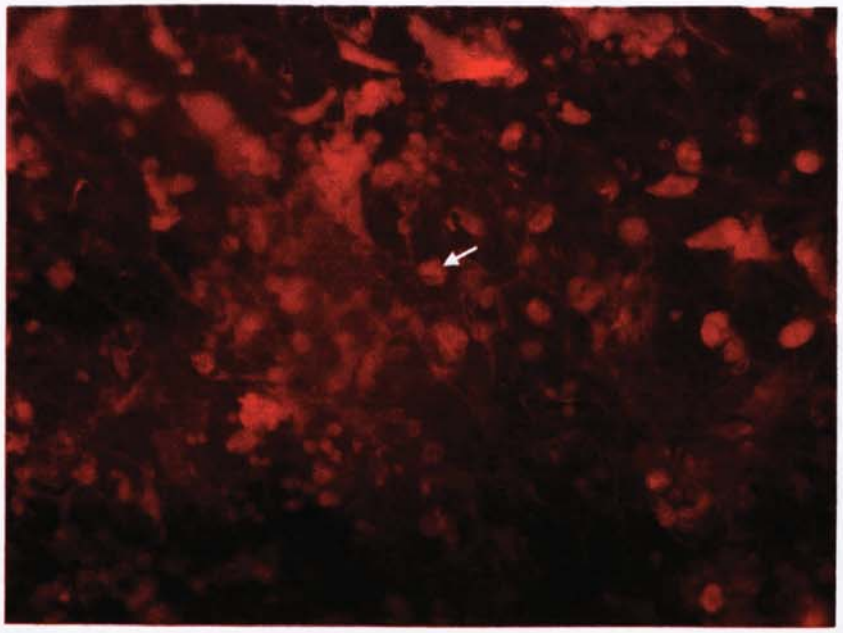

Figure 64: Immunohistochemistry assay of the epidermal layer of the co-cultured skin model (100x; scale bar: 100μm).

PHEK growth on the epidermal layer of 1:20 collagen:PCL biocomposite in the co-culture system was studied by immunohistochemistry assay. Keratinocytes were labeled with monoclonal mouse anti-human involucrin IgG 1:200 and the secondary antibody of rhodamine-conjugated goat anti-mouse IgG 1:100 on day 35. Red fluorescence (arrow) indicates the positive cell staining.

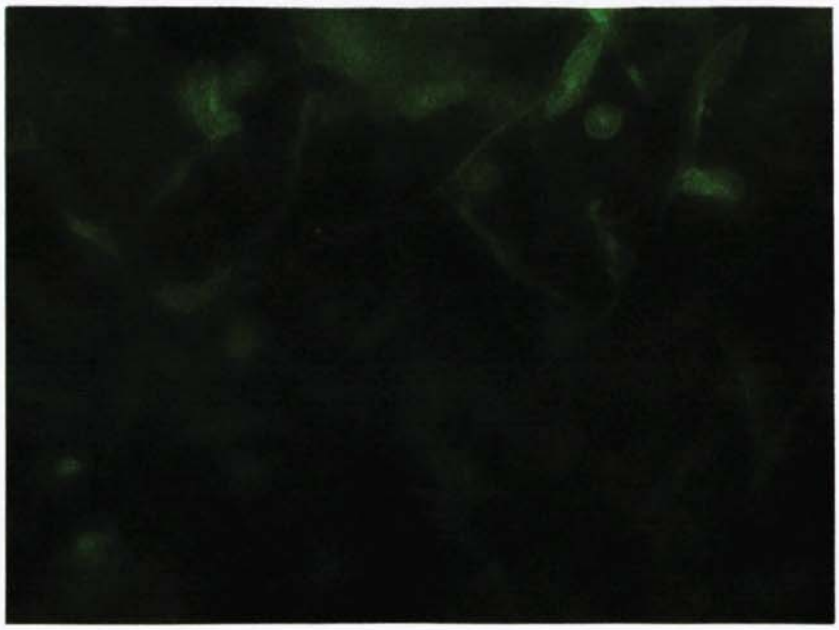

Figure 65: Immunohistochemistry assay of the dermal layer of the co-cultured skin model (200x; scale bar: 100μm).
PHDF growth on the dermal layer of 1:20 collagen:PCL biocomposite in the co-culture study was studied by immunohistochemistry assay. Fibroblasts were labeled with monoclonal mouse anti-human α tubulin antibody 1:200 and the secondary antibody of fluorescein (FITC)-conjugated goat anti-mouse IgG 1:100 on day 35. Green fluorescence (arrow) indicates the positive cell staining.

5.4.5 Interaction of PHEK and PHDF in the co-culture system *in vitro*

To investigate the interaction between skin keratinocytes and fibroblasts in the co-cultured skin mode based on 1:20 collagen:PCL biocomposites, we compared the KGF production of fibroblasts populations after co-culture with keratinocytes and after stimulation with the proinflammatory cytokine IL-1β (10ng/ml). PHDF (adult foreskin) at passage 4-6 were seeded on polystyrene in 24-well plates, on 1:20 collagen:PCL biocomposites in 7 ml glass vials, or in the co-cultured skin model with the same cell seeding number of $2.4x10^4$ cells in 3ml DMEM/0.5% FCS culture medium. The study and control groups were arranged as A to F groups (A: Human fibroblast growth on TCP; B: Human fibroblast growth on TCP with addition of IL-1β; C: Human fibroblast growth on 1:20 collagen:PCL biocomposite; D: Human fibroblast growth on 1:20 collagen:PCL biocomposite with addition of IL-1β; E: Human fibroblasts co-cultured with keratinocytes in co-culture system; F: Human fibroblasts co-cultured with keratinocytes in co-culture system with addition of IL-1β). The results

revealed that the KGF release amount in group B increased significantly compared to that in group A at 24 hour (n=3; Values are mean±SE; P=0.01). The results are shown in Figure 66.

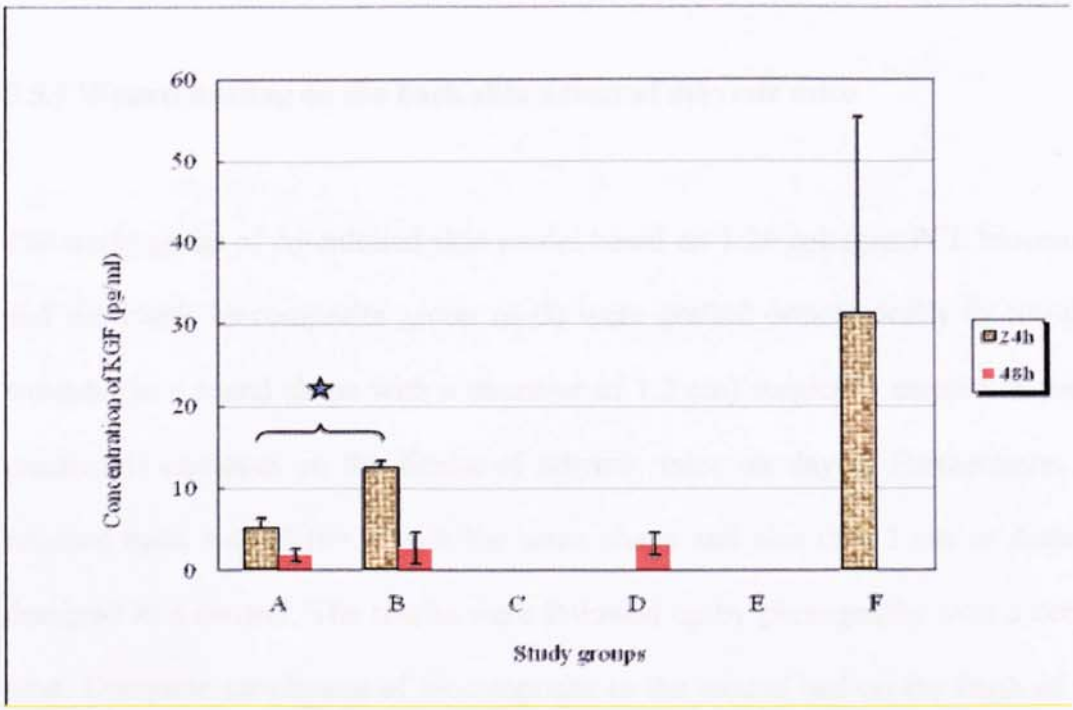

Figure 66: KGF ELISA on 24 and 48 hours.
The comparison of KGF release from human fibroblasts by stimulation of IL-1β (10ng/ml), growth on collagen:PCL biocomposite and co-culture with keratinocytes were measured by ELISA at 24 h and 48 h respectively (A: Fibroblast growth on TCP; B: Fibroblast growth on TCP with addition of IL-1β; C: Fibroblast growth on 1:20 collagen:PCL biocomposite; D: Fibroblast growth on 1:20 collagen:PCL biocomposite with addition of IL-1β; E: Fibroblasts co-cultured with keratinocytes; F: Fibroblasts co-cultured with keratinocytes and addition of IL-1β). (n=3; Values are mean±SE; $P<0.05$ for difference in KGF release from both groups A and B at 24 h by analysis of variance and a paired t-test; ANOVA: $P>0.05$; Asterisk indicates statistically significant difference).

5.5 *In vivo* study on co-cultured skin model

Tissue-engineered skin model based on 1:20 collagen:PCL biocomposites was prepared by co-culture of human single-donor keratinocytes and fibroblasts alone on each side of the membrane. Confluent keratinocyte growth on the epidermal layer and populated fibroblast growth in the dermal layer of the skin model were achieved in culture for 28 to 35 days and

proven by SEM and immunohistochemistry assay. Athymic mice were chosen as the study animal to test the biocompatibility of the tissue-engineered skin model *in vivo*. The results were shown by clinical photography and histological investigation in a certain period of time.

5.5.1 Wound healing on the back skin defect of athymic mice

The study group of co-cultured skin model based on 1:20 collagen:PCL biocomposites (n=3) and the blank biocomposite group (n=3) were grafted orthotopically to full-thickness skin wounds (in a round shape with a diameter of 1.2 cm) surgically created to the depth of the panniculus carnosus on the flanks of athymic mice on day 0. Furthermore, the group of retained open wound (n=3) with the same shape and size of 1.2 cm in diameter was also designed as a control. The results were followed up by photography over a certain period of time. Complete attachment of biocomposite to the wound bed on the flank of athymic mice was observed in the group of co-cultured skin model in one week time. Even though the wound size decreased apparently in all three groups mentioned above due to the rapid skin regeneration pattern of mice, the earlier completely wound coverage and healing were observed in the group of co-cultured skin model at time intervals up to 10 days compared to the other two groups. On the other hand, the blank biocomposite group seemed to exhibit a better wound healing compared to the retained open wound group at time interval up to 19 days. The study procedures including the transferring of membrane to the wound bed, fixation by suturing, and wound coverage with gel-type medium and transparent adhesive film are shown in Figure 67 and 68. All the follow-up photographs are shown in Figure 68 to 76. The characteristics of the wound healing process were summarised in Table 6.

Table 6: Characteristics of wound healing process for *in vivo* animal study

	Co-cultured skin model			Blank biocomposite			Retained open wound		
	S1	S2	S3	S1	S2	S3	S1	S2	S3
Immediate wound coverage	+	+	+	+	+	+	−	−	−
Permanent wound coverage	+	+	+	−	−	−	−	−	−
Times for complete wound healing (days)	7	7	10	19	19^+	19^+	19^+	19^+	22

* S: Sample number; +: positive result; −: Negative result; 19^+: More than 19 days.

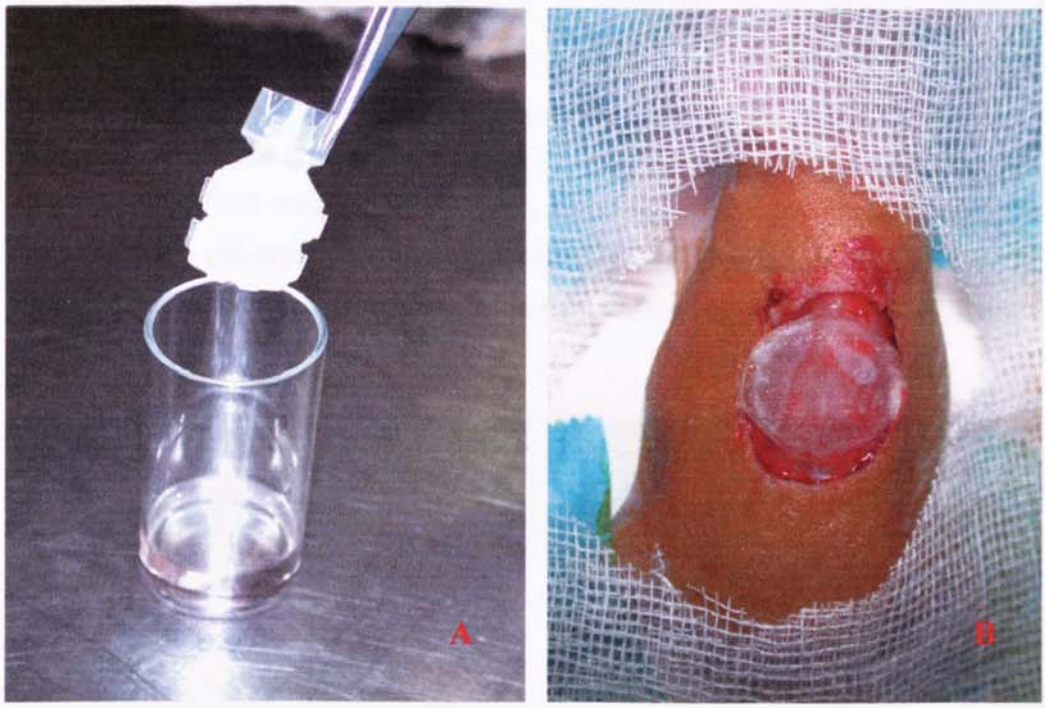

Figure 67: Transplantation of a co-cultured skin model to athymic mice.
The co-cultured skin model based on 1:20 collagen:PCL biocomposite in the co-culture device (A) was transferred to the full-thickness skin wound (B) surgically created to the depth of the panniculus carnosus on the flank of athymic mice.

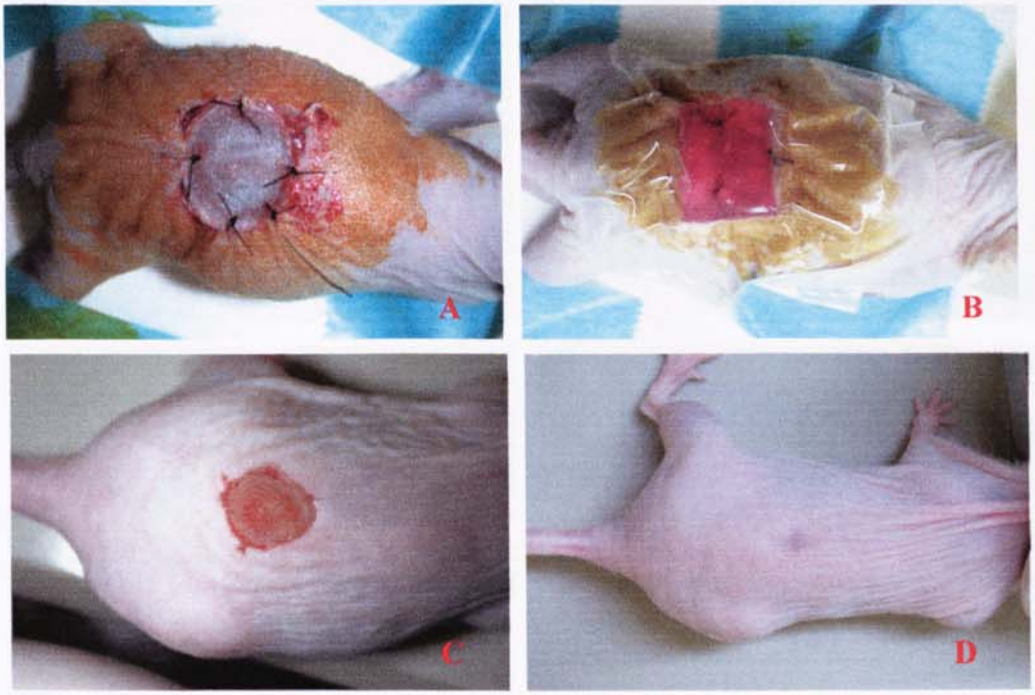

Figure 68: *In vivo* animal study for co-cultured skin model (sample 1).

The skin substitute was grafted orthotopically to full-thickness skin wound on the flank of athymic mice, and was attached with 4 stent-sutures at the wound margin (A), and then was covered with gel-type medium containing DMEM/gelatin/agarose/10% FCS covered with Tagaderm® transparent film (B) on day 0. Following up at day 7 (C) and day 28 (D) were recorded.

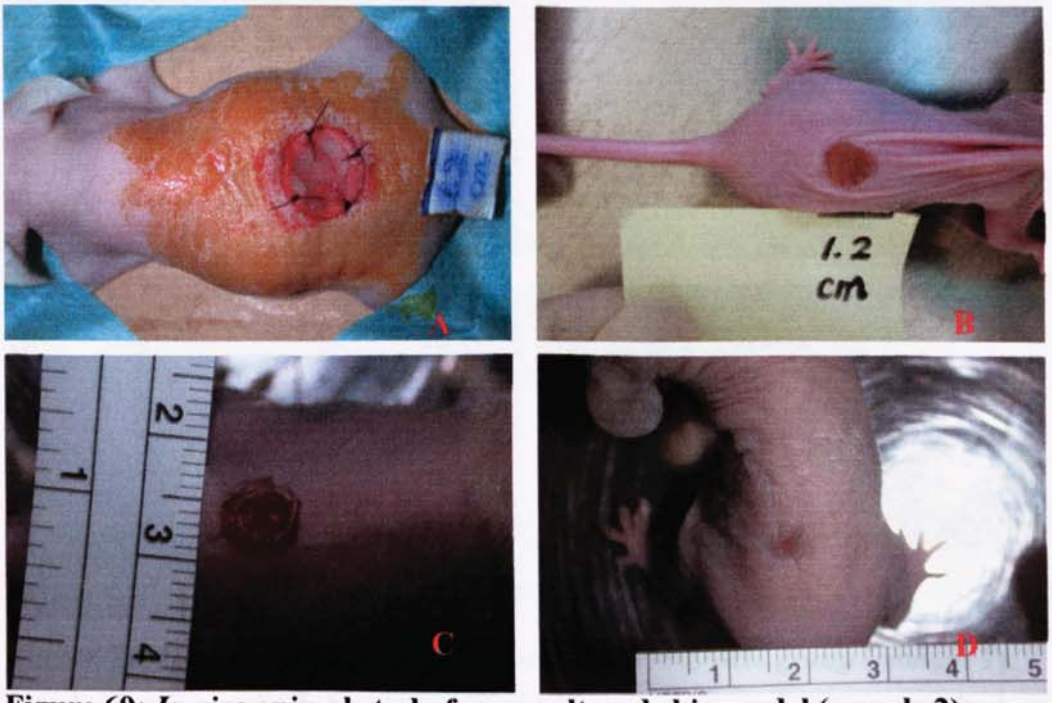

Figure 69: *In vivo* animal study for co-cultured skin model (sample 2).

The skin substitute was grafted orthotopically to full-thickness skin wound on the flank of athymic mice, and was attached with 4 stent-sutures at the wound margin (A) on day 0. Following up at day 7 (B), day 10 (C) and day 19 (D) were recorded.

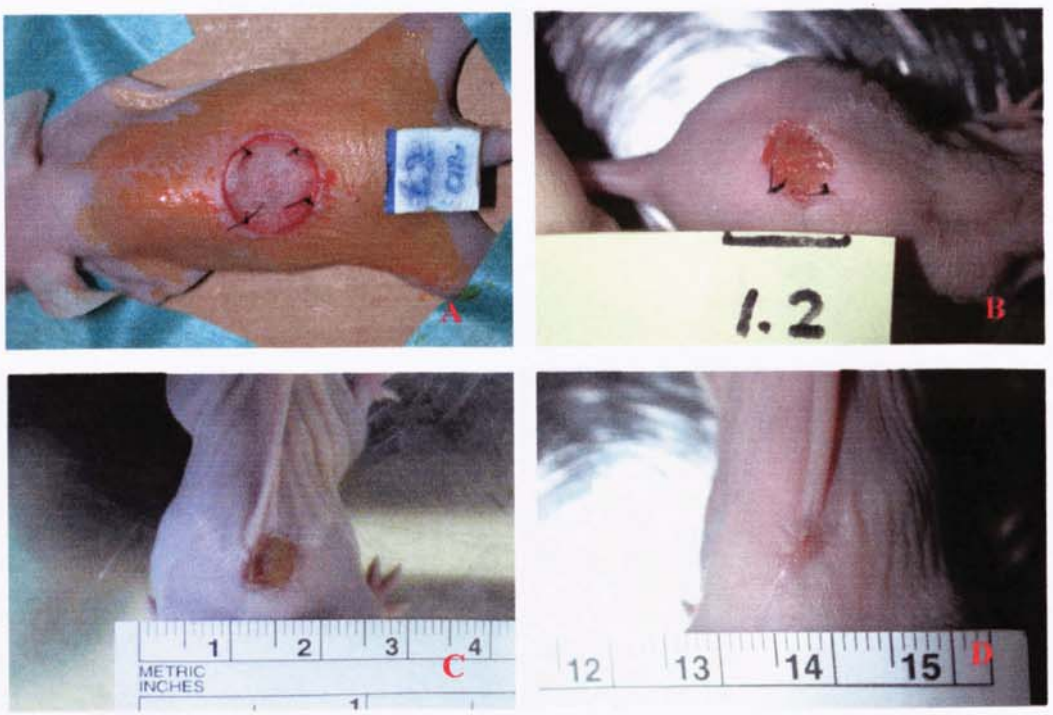

Figure 70: *In vivo* animal study for co-cultured skin model (sample 3).

The skin substitute was grafted orthotopically to full-thickness skin wound on the flank of athymic mice, and was attached with 4 stent-sutures at the wound margin (A) on day 0. Following up at day 7 (B), day 10 (C) and day 19 (D) were recorded.

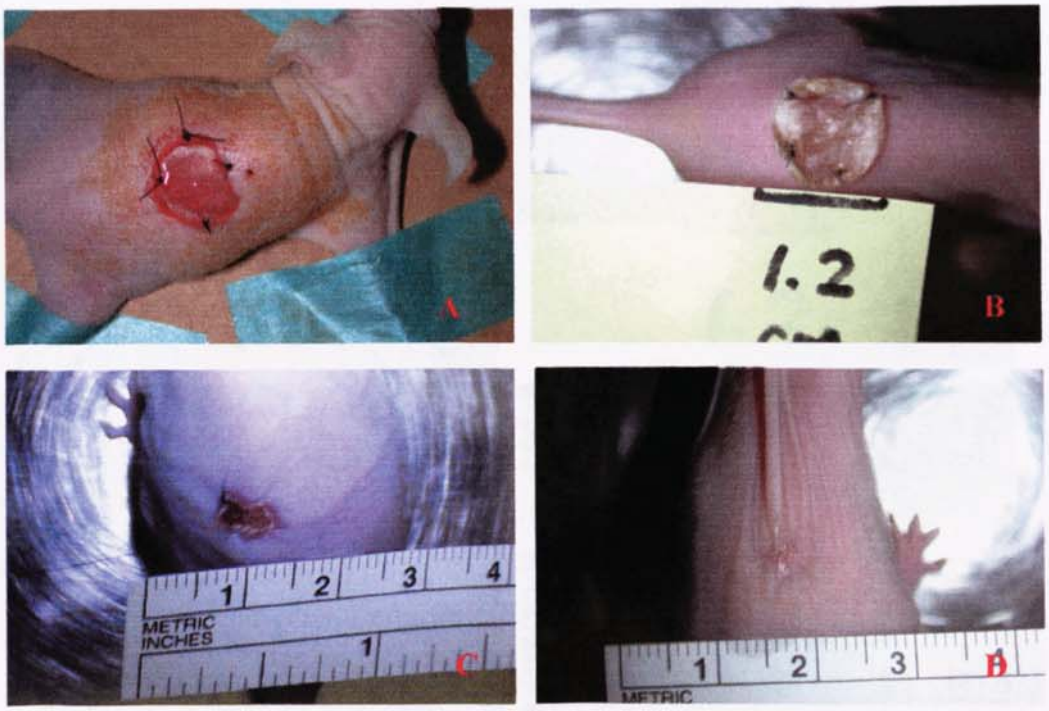

Figure 71: *In vivo* animal study for blank biocomposite group (sample 1).

The 1:20 collagen:PCL biocomposite sample (no cell seeding) was grafted orthotopically to full-thickness skin wound on the flank of athymic mice, and was attached with 4 stent-sutures at the wound margin (A) on day 0. Following up at day 7 (B), day 10 (C) and day 19 (D) were recorded.

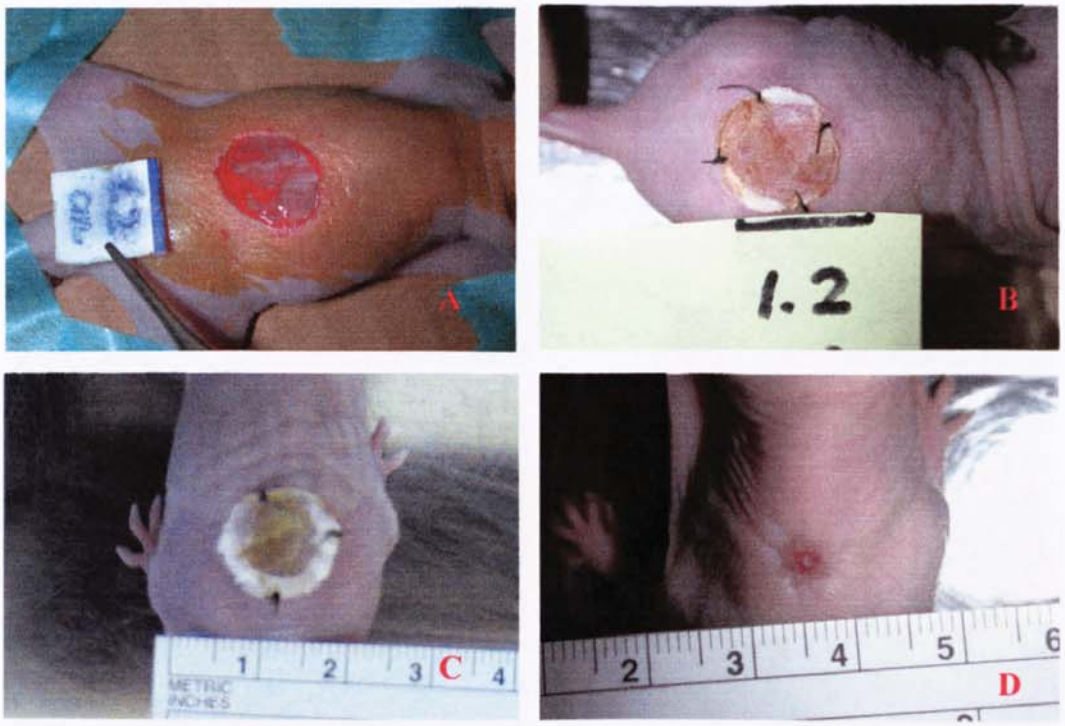

Figure 72: *In vivo* animal study for blank biocomposite group (sample 2).
The 1:20 collagen:PCL biocomposite (no cells) was grafted orthotopically to full-thickness skin wound (A) on the flank of athymic mice, and was attached with 4 stent-sutures at the wound margin on day 0. Following up at day 7 (B), day 10 (C) and day 19 (D) were recorded.

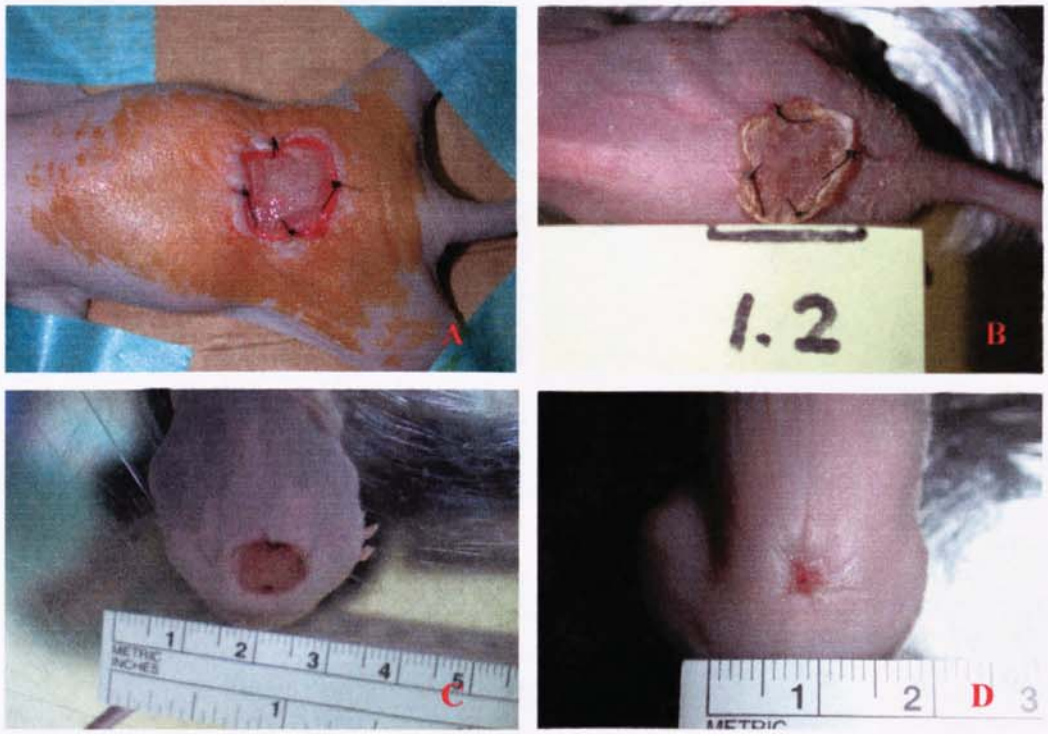

Figure 73: *In vivo* animal study for blank biocomposite group (sample 3).
The 1:20 collagen:PCL biocomposite sample (no cell seeding) was grafted orthotopically to full-thickness skin wound on the flank of athymic mice, and was attached with 4 stent-sutures at the wound margin (A) on day 0. Following up at day 7 (B), day 10 (C) and day 19 (D) were recorded.

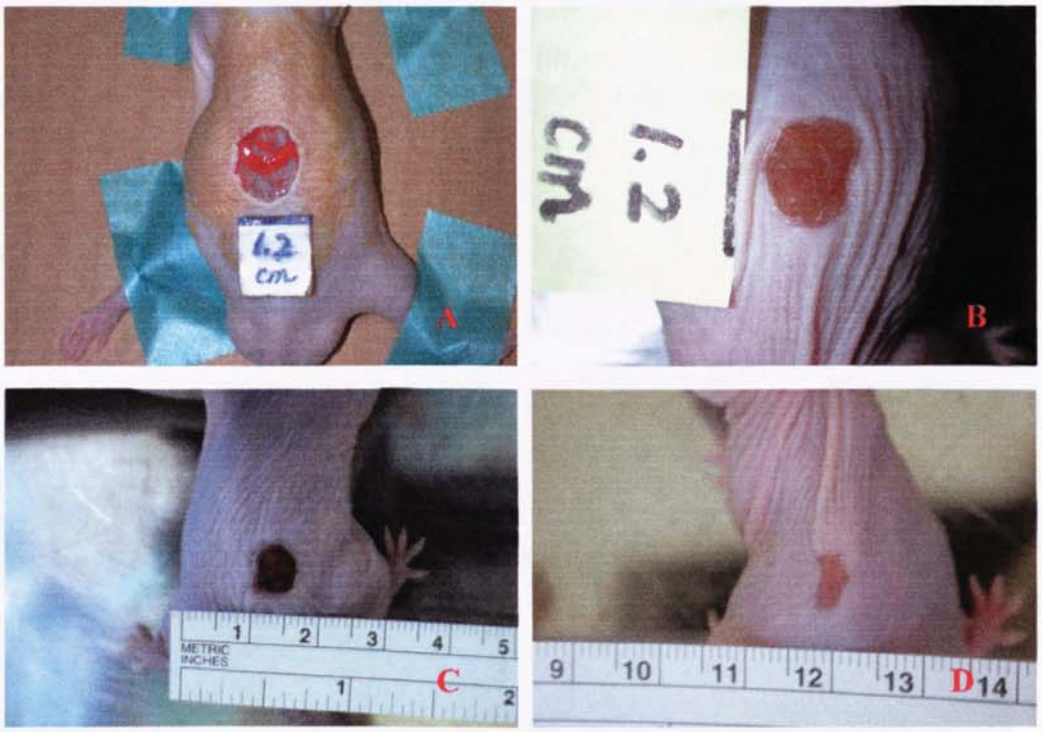

Figure 74: *In vivo* animal study for retained open wound group (sample 1).
The open wound only study group was surgically created to the depth of the panniculus carnosus on the flank of athymic mice (A) on day 0. Following up at day 7 (B), day 10 (C) and day 19 (D) were recorded.

Figure 75: *In vivo* animal study for retained open wound group (sample 2).
The open wound only study group was surgically created to the depth of the panniculus carnosus on the flank of athymic mice (A) on day 0. Following up at day 7 (B), day 10 (C) and day 19 (D) were recorded.

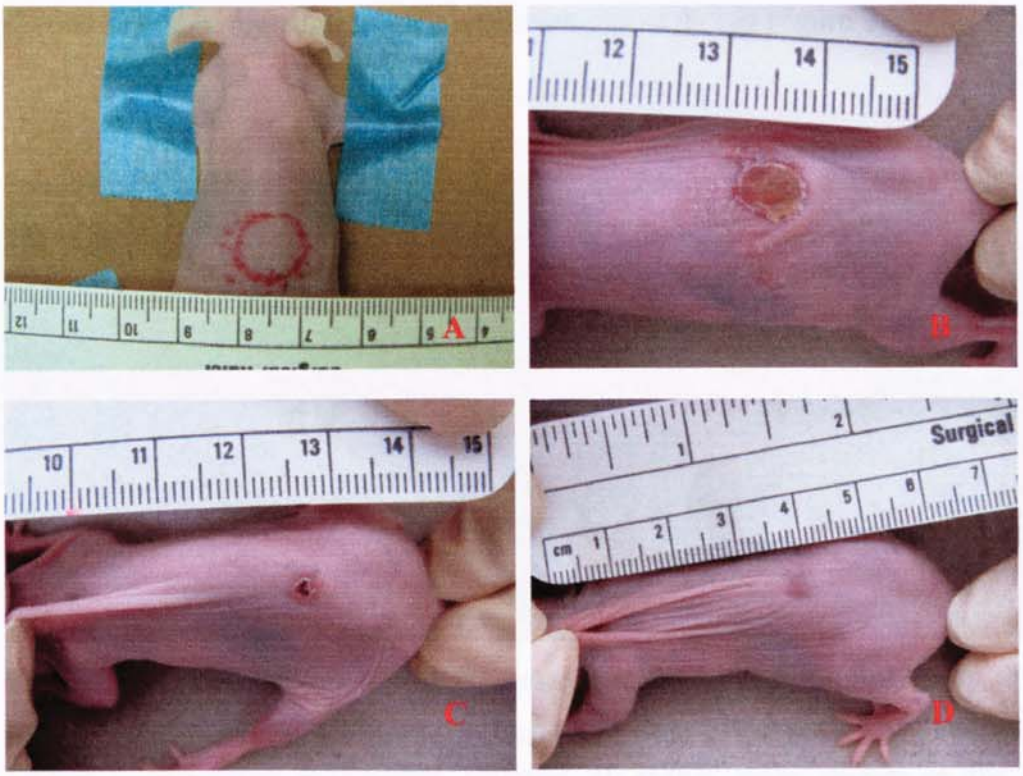

Figure 76: *In vivo* animal study for retained open wound group (sample 3).
The open wound only study group was surgically created to the depth of the panniculus carnosus on the flank of athymic mice (A) on day 0. Following up at day 7 (B), day 14 (C) and day 22 (D) were recorded.

5.5.2 Histological study

A pilot study for the co-cultured skin model *in vivo* was performed by grafting the co-cultured skin model on the back defect of athymic mice. The athymic mice were sacrificed and the specimen including biocomposite and adjacent normal mouse skin tissue were widely excised for histological study periodically in a certain period of time. Frozen section of the specimen was performed and the immunohistochemistry assay was used to evaluate the biocompatibility of grafts. Labeling of PHEK with the (primary) monoclonal mouse anti-human involucrin antibody 1:200 (Cat No.I8447-25; United States Biological, Inc.), and the (secondary) rhodamine-conjugated polyclonal goat anti-mouse IgG 1:100 (Cat No.I1903-08C, United States Biological, Inc.) respectively for detection of involucrin were performed. Successful engrafting of the skin model and strong positive red fluorescent staining of keratinocytes in the transplanted skin substitute embedded in the epidermal and

dermal layers of the athymic skin specimen are shown in Figure 77.

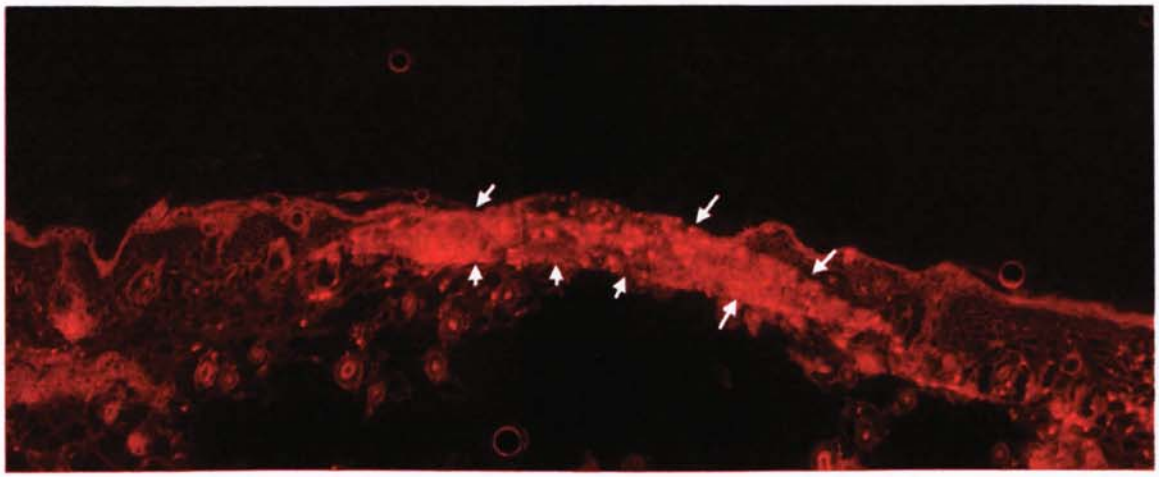

Figure 77: Immunohistochemistry assay for the *in vivo* animal study of co-cultured skin model (pilot study) at time interval up to 43 days (40x; scale bar: 100μm).
Strong positive red fluorescent staining of PHEK were shown in the transplanted skin substitute engrafted on the back skin defect of the athymic mice (arrow). The (primary) monoclonal mouse anti-human involucrin antibody 1:200 and the (secondary) rhodamine-conjugated goat anti-mouse IgG 1:100 were used.

The groups of the co-cultured skin model (n=3), the blank biocomposite (n=3), and the retained open wound (n=3) were included in the following *in vivo* animal study, in which the histological studies based on both frozen and paraffin wax-embedded section methods were performed by using H & E and Gomori's trichrome staining methods, and immunohistochemistry assay. Nevertheless, the survival of human-origin fibroblasts/epithelial cells in graft was further confirmed by labeling PHEK and PHDF with monoclonal mouse anti-human D7-FIB antibody 1:200 (Cat No.NB 600-777; Novus® Biologicals, Inc.) that will not cross-react with mouse or rat, and the secondary antibody of rhodamine-conjugated goat anti-mouse IgG 1:100 (Cat No.I1903-08C, United States Biological, Inc.). Thus, the human-origin fibroblasts/epithelial cells will show in red fluorescent staining alone in the co-cultured skin model *in vivo*. The results are shown in Figure 78 to 89.

In the *in vivo* study group of co-cultured skin models (sample 1 & 2), it showed rapid wound coverage and healing with the formation of differentiated epidermal layer and abundant regular parallel-arranged collagen deposition in the dermal layer (Figure 78 to 83). Furthermore, the survival of human-origin fibroblasts/epithelial cells in grafted skin substitutes at time intervals up to 225 and 34 days respectively was confirmed by labeling PHEK and PHDF with monoclonal mouse anti-human D7-FIB antibody 1:200 (Cat No.NB 600-777; Novus® Biologicals, Inc.) that has been tested not to cross-react with mouse or rat, and the secondary antibody of rhodamine-conjugated goat anti-mouse IgG 1:100 (Cat No.I1903-08C, United States Biological, Inc.). Strong positive red fluorescent staining was shown in the dermal layer of skin substitute (Figure 80 and 83).

However, in the *in vivo* study group of retained open wound, it showed the relatively slower wound healing process with the formation of thin differentiated epidermal layer and the loose collagen/ECM deposition in the dermal layer (Figure 84 to 86). In addition, no existence of human-origin fibroblasts/epithelial cells was found in the surgical site of the back skin defect of athymic mice (Figure 86).

In comparison with the *in vivo* study group of retained open wound, the group of blank biocomposite showed a relative rapid wound healing process with the formation of differentiated epidermal layer and the more deposition of collagen/ECM in the dermal layer (Figure 87 to 89). However, the same as in the group of retained open wound, there was no existence of human-origin fibroblasts/epithelial cells in the surgical site of the back skin defect of athymic mice (Figure 89).

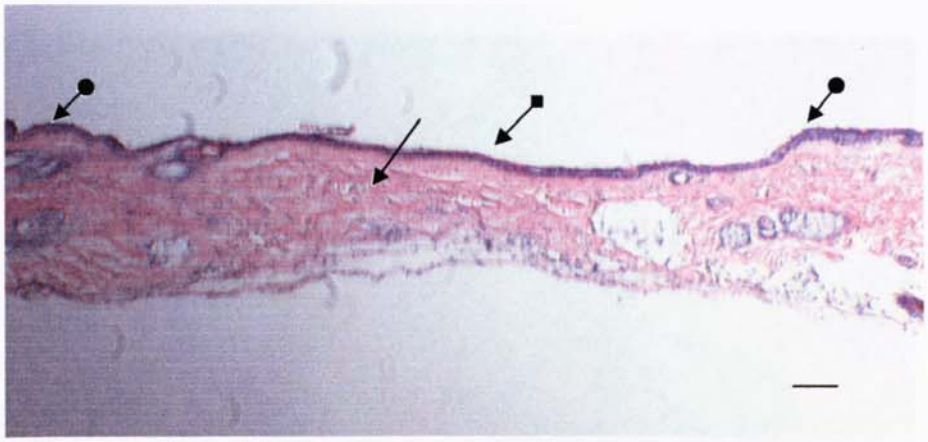

Figure 78: H & E staining for the *in vivo* animal study of co-cultured skin model (sample 1) at time interval up to 225 days (40x; scale bar: 100μm).

The histological study by using the paraffin wax-embedded H & E staining method for co-cultured skin model transplanted on the back skin defect of athymic mice at time interval up to 225 days was investigated. Complete wound healing with differentiated epidermal layer (◆→) and parallel arranged ECM formation (→) were shown in the skin substitute engrafted between the normal skin structures (●→) of athymic mice.

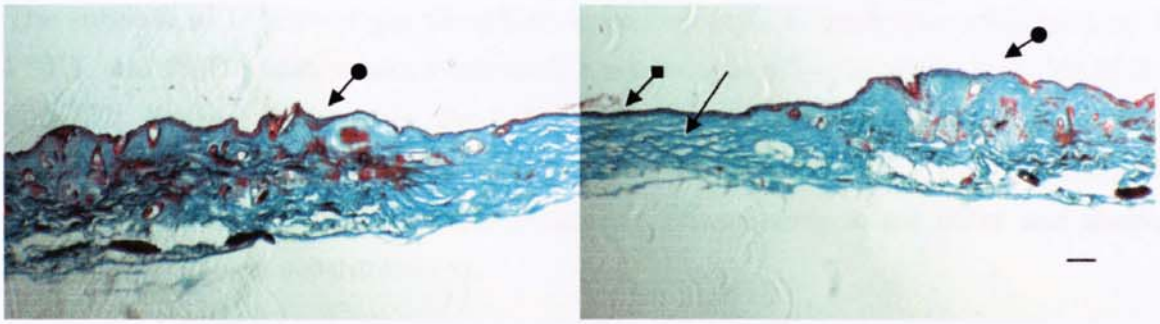

Figure 79: Gomori's trichrome staining for the *in vivo* animal study of co-cultured skin model (sample 1) at time interval up to 225 days (40x; scale bar: 100μm).

The histological study by using the frozen section and Gomori's trichrome staining method for co-cultured skin model transplanted on the back skin defect of athymic mice at time interval up to 225 days was investigated. Complete wound healing with differentiated epidermal layer (◆→) and abundant collagen/ECM deposition (→; green color) were shown in the skin substitute engrafted between the normal skin structures (•→) of athymic mice.

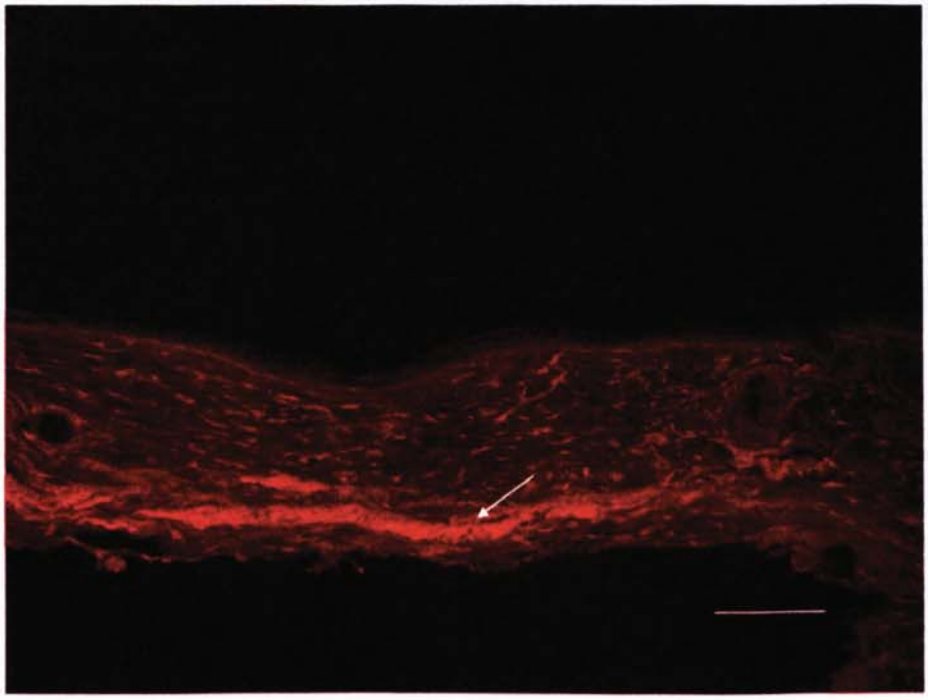

Figure 80: Immunohistochemistry assay for the *in vivo* animal study of co-cultured skin model (sample 1) at time interval up to 225 days (100x; scale bar: 100μm).

The survival of human-origin fibroblasts/epithelial cells in graft was confirmed by labeling PHEK and PHDF with monoclonal mouse anti-human D7-FIB antibody 1:200 (Cat No.NB 600-777; Novus® Biologicals, Inc.) that will not cross-react with mouse or rat, and the secondary antibody of rhodamine-conjugated goat anti-mouse IgG 1:100 (Cat No.I1903-08C, United States Biological, Inc.). Strong positive fluorescence in red color was shown in the dermal layer of skin substitute (→).

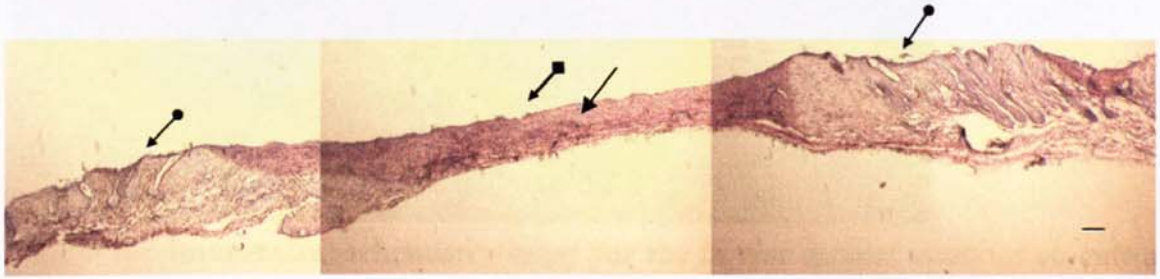

Figure 81: H & E staining for the *in vivo* animal study of co-cultured skin model (sample 2) at time interval up to 34 days (40x; scale bar: 100μm).

The histological study by using the paraffin wax-embedded H & E staining method for co-cultured skin model transplanted on the back skin defect of athymic mice at time interval up to 34 days was investigated. Complete wound healing with differentiated epidermal layer (◆→) and parallel arranged ECM formation (→) were shown in the skin substitute engrafted between the normal skin structures (•→) of athymic mice.

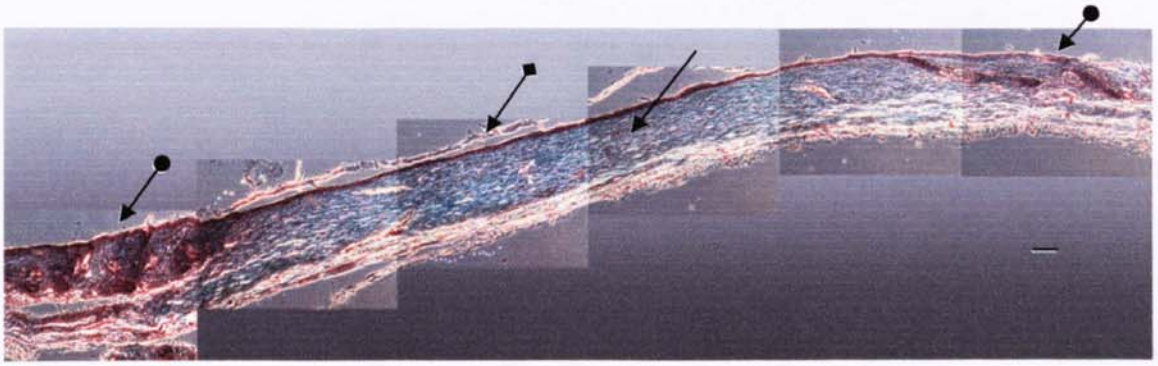

Figure 82: Gomori's trichrome staining for the *in vivo* animal study of co-cultured skin model (sample 2) at time interval up to 34 days (100x; scale bar: 100μm).

The histological study by using the frozen section and Gomori's trichrome staining method for co-cultured skin model transplanted on the back skin defect of athymic mice at time interval up to 34 days was investigated. Complete wound healing with differentiated epidermal layer (◆→) and abundant collagen/ECM deposition (→; green color) were shown in the skin substitute engrafted between the normal skin structures (•→) of athymic mice.

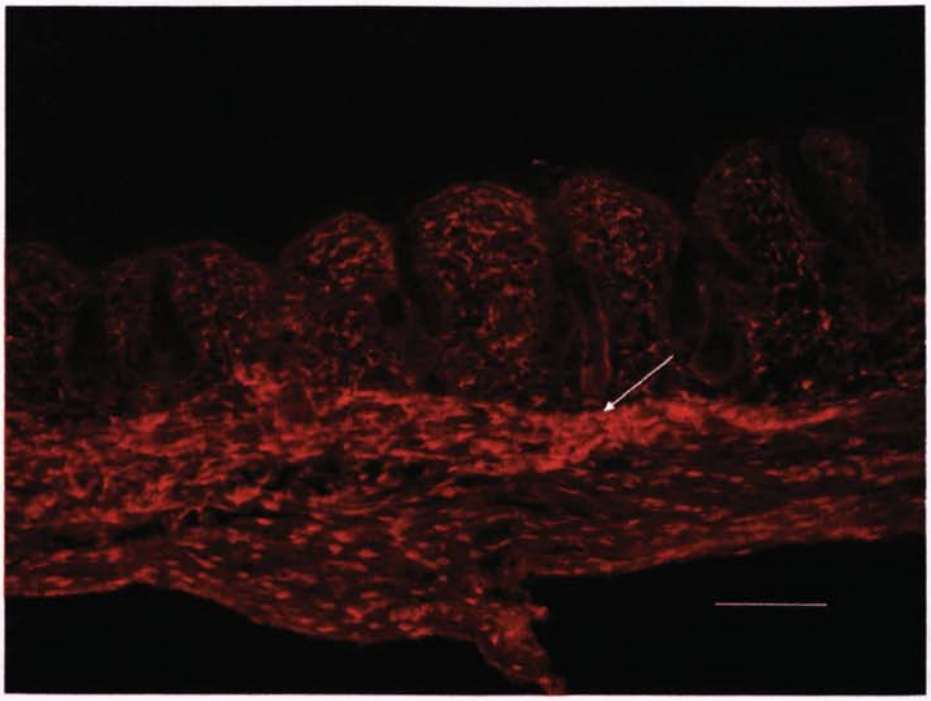

Figure 83: Immunohistochemistry assay for the *in vivo* animal study of co-cultured skin model (sample 2) at time interval up to 34 days (100x; scale bar: 100μm).

The survival of human-origin fibroblasts/epithelial cells in graft was confirmed by frozen section of the specimen of skin substitute engrafted on the back skin defect of athymic mice at time interval up to 34 days and labeling PHEK and PHDF with monoclonal mouse anti-human D7-FIB antibody 1:200 (Cat No.NB 600-777; Novus® Biologicals, Inc.) that will not cross-react with mouse or rat, and the secondary antibody of rhodamine-conjugated goat anti-mouse IgG 1:100 (Cat No.I1903-08C, United States Biological, Inc.). Strong positive fluorescent reaction in red color was shown in the dermal layer of skin substitute (→).

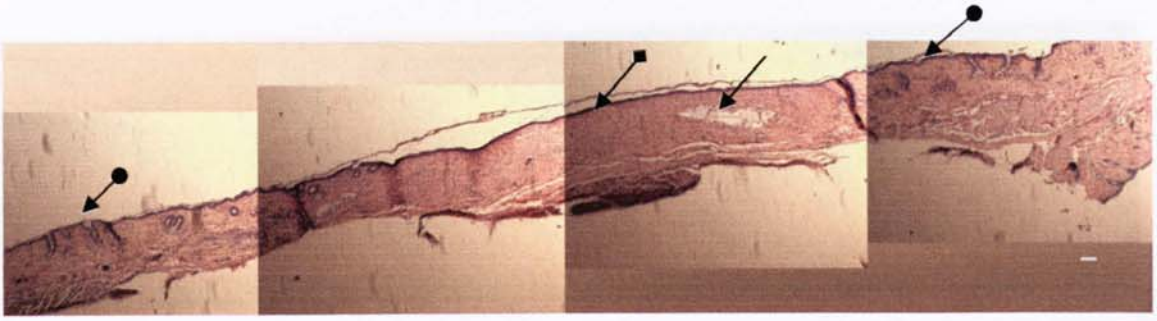

Figure 84: H & E staining for the group of retained open wound in the animal study of co-cultured skin model at time interval up to 34 days (40x; scale bar: 100μm).

The histological study by using the paraffin wax-embedded H & E staining method for the study group of open wound on the back skin defect of athymic mice at time interval up to 34 days was investigated. Complete wound healing with differentiated epidermal layer (◆→) and loose ECM formation (→) were shown in between the normal skin structures (•→) of athymic mice.

Figure 85: Gomori's trichrome staining for the group of retained open wound in the animal study of co-cultured skin model at time interval up to 34 days (40x; scale bar: 100μm).

The histological study by using the frozen section and Gomori's trichrome staining method for co-cultured skin model transplanted on the back skin defect of athymic mice at time interval up to 34 days was investigated. Complete wound healing with differentiated epidermal layer (◆→) and loose collagen deposition (→) were shown in between the normal skin structures (•→) of athymic mice.

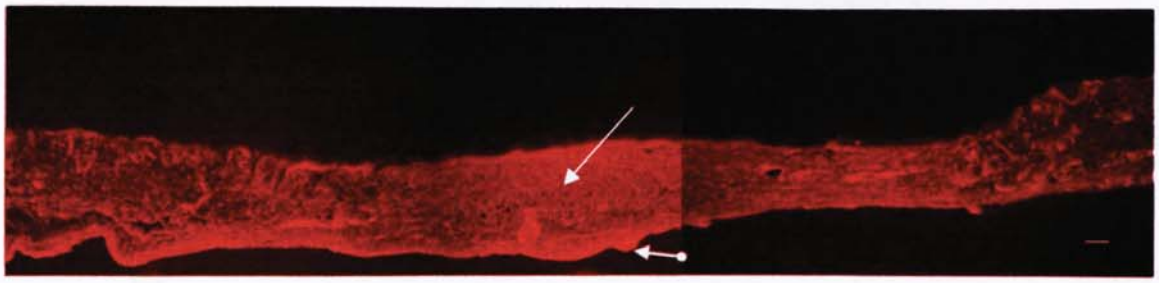

Figure 86: Immunohistochemistry assay for the group of retained open wound in the animal study of co-cultured skin model at time interval up to 34 days (40x; scale bar: 100μm).

The existence of human-origin fibroblasts/epithelial cells in the surgical site was investigated by frozen section of the specimen of the back skin defect of athymic mice at time interval up to 34 days and labeling PHEK and PHDF with monoclonal mouse anti-human D7-FIB antibody 1:200 (Cat No.NB 600-777; Novus® Biologicals, Inc.) that will not cross-react with mouse or rat, and the secondary antibody of rhodamine-conjugated goat anti-mouse IgG 1:100 (Cat No.I1903-08C, United States Biological, Inc.). Negative red fluorescence was shown in the dermal skin layer of surgical site (→). False positive fluorescence (•→)was noted over the lower surface of specimen due to the entrapment of secondary antibody.

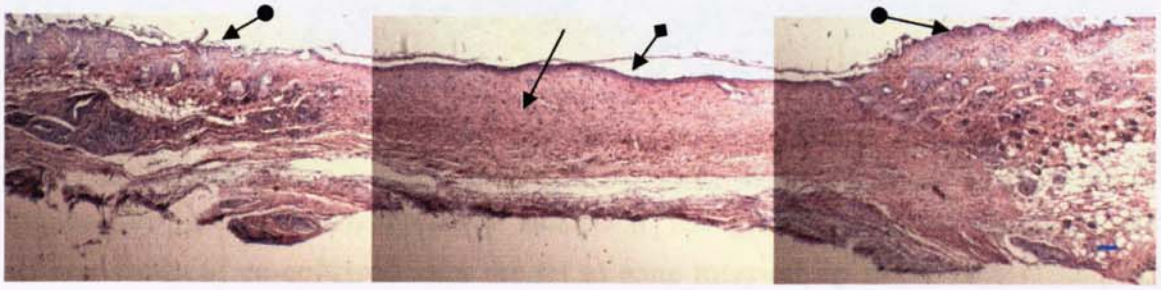

Figure 87: H & E staining for the group of blank biocomposite in the animal study of co-cultured skin model at time interval up to 34 days (40x; scale bar: 100μm).

The histological study by using the paraffin wax-embedded H & E staining method for the study group of blank biocomposite (no cell seeding) on the back skin defect of athymic mice at time interval up to 34 days was investigated. The biocomposite grafted was found to slough in one week time during the study period. Complete wound healing with differentiated epidermal layer (◆→) and loose ECM formation (→) were shown in between the normal skin structures (•→) of athymic mice.

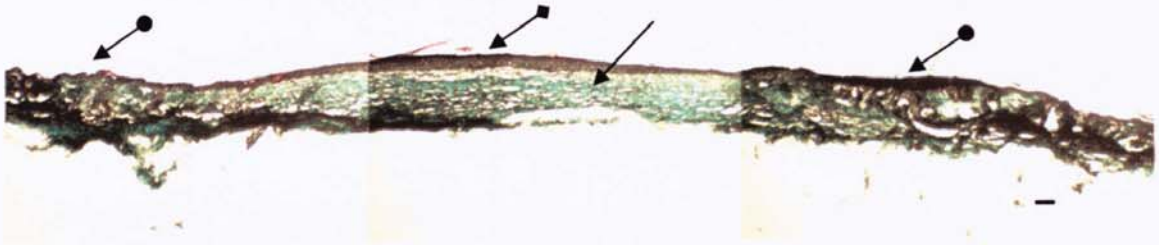

Figure 88: Gomori's trichrome staining for the group of blank biocomposite in the animal study of co-cultured skin model at time interval up to 34 days (100x; scale bar: 100μm).

The histological study by using the frozen section and Gomori's trichrome staining method for the study group of blank biocomposite (no cell seeding) on the back skin defect of athymic mice at time interval up to 34 days was investigated. The biocomposite grafted was found to slough in one week time during the study period. Complete wound healing with differentiated epidermal layer (◆→) and abundant collagen deposition (→) were shown in between the normal skin structures (•→) of athymic mice.

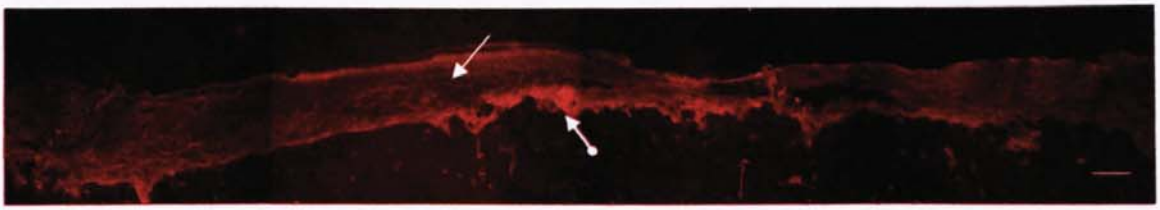

Figure 89: Immunohistochemistry assay for the group of blank biocomposite in the animal study of co-cultured skin model at time interval up to 34 days (100x; scale bar: 100μm).

The existence of human-origin fibroblasts/epithelial cells in the surgical site was investigated by frozen section of the specimen of the back skin defect of athymic mice at time interval up to 34 days and labeling PHEK and PHDF with monoclonal mouse anti-human D7-FIB antibody 1:200 (Cat No.NB 600-777; Novus® Biologicals, Inc.) that will not cross-react with mouse or rat, and the secondary antibody of rhodamine-conjugated goat anti-mouse IgG 1:100 (Cat No.I1903-08C, United States Biological, Inc.). The biocomposite grafted was found to slough in one week time during the study period. Negative red fluorescence was shown in the dermal skin layer of surgical site (→). False positive fluorescence (•→) was noted over the surface of specimen due to the entrapment of secondary antibody.

CHAPTER SIX

DISCUSSION

The materials described here apply physical integration of natural and synthetic polymers to provide a favourable substrate for growth of skin cells. This approach exploits the cell binding properties of natural polymers (collagen, gelatin and gelatin/collagen) and the structural properties of PCL whilst avoiding the toxicological concerns associated with chemical cross-linking of natural polymers to impart stability. The composite films are highly flexible which potentially allows effective draping over the wound site and close proximity with the wound bed to improve the prospects for graft take. Tear resistance is also conferred by the PCL component which facilitates handling and manipulation during surgery. Effective inhibition of wound contraction by contractile fibroblasts has long been considered essential for optimum dermal regeneration in full thickness wounds [133]. The structural stability conferred on the material by the PCL phase is expected to be advantageous in this respect.

Tissue engineering scaffolds (or regeneration templates) are required to exhibit a residence time that is long enough to support tissue development but not compromise complete space filling by new tissue at the wound site. PCL is characterised by a resorption time in excess of 1 year [123] but is known to be susceptible to enzymatic degradation [134]. A variety of collagenase enzymes are secreted by macrophages, epidermal cells and fibroblasts during wound healing, including matrix matalloproteinases (MMP-1), gelatinase A (MMP-2) and stromelysin-1 (MMP-3), which are implicated in the process of cell migration during wound repair [135, 136]. Thus enzymatic breakdown of the PCL phase may play a part in elimination of the composite from the repair site. The notable reduction of PCL crystallinity in high collagen content materials especially in the study group of collagen:PCL biocomposites (Table 2) suggests that the collagen phase is impeding crystallisation of PCL, possibly through an effect on the nucleation of PCL crystals. This behavior may also lead to an increase in matrix resorption rate since fluid ingress and subsequently hydrolytic chain scission is restricted in the crystalline regions of the polymer.

The % crystallinity of the PCL phase in the collagen:PCL, gelatin:PCL and gelatin/collagen:PCL biocomposites was thereby estimated respectively by comparing the heat of fusion of biocomposites with that of a 100% crystalline PCL – 139 J/g. In the DSC study on 1:4, 1:8 and 1:20 w/w collagen:PCL biocomposites, the 1:20 biocomposites displayed the highest crystallinity of 84.7%, followed by 58.7% for 1:8 and 49.4% for 1:4 materials. Interestingly, the degree of crystallinity increased with increasing w/w% content of PCL in the biocomposite, which may indicate that the collagen phase is impeding crystallisation of PCL. PCL is known to exhibit high crystallinity in certain cases up to 80%. However, the % crystallinity of the PCL films produced by solvent casting in this study was unrealistically low with 54.2±5.4% relative to 1:20 w/w collagen:PCL biocomposite of 63.5±3.8% (Table 2). PCL film production by solvent evaporation may be conducive to development of high crystallinity due to the differences of crystal nucleation process between the pellet form (by industry manufacture) and the thin membranous form of PCL prepared by solvent casting.

In the DSC study on 1:4, 1:8 and 1:20 w/w gelatin:PCL biocomposites (Table 3), similar trend of the differences in % crystallinity of the PCL phase was observed compared to that in the study on collagen:PCL groups. The highest % crystallinity of the PCL phase was observed in the 1:20 w/w gelatin:PCL biocomposite followed by 1:8 and 1:4 groups ordinarily. However, there were no statistically significant differences between these study groups (ANOVA: $P=0.197$; Newman-Keuls: $P>0.05$). The characteristics of lower molecular weight and higher fragmentation in the structure of gelatin compared to that of collagen may explain why the crystallinity of the PCL phase in the gelatin:PCL biocomposites was not influenced by the gelatin content significantly. Gelatin prepared by the enzyme-degradation of collagen may not be able to develop a very strong architecture during the process of lyophilisation thereby less impeding on the crystal nucleation of the PCL phase afterwards. The hypothesis could be supported by the facts of more fragile and shrinkage in size of the gelatin mats during the

prepration by lyophilisation process. Furthermore, the refinement of gelatin:PCL biocomposites by preparation of gelatin/collagen:PCL biocomposites showed great improvement in the physical characteristics of protein mats prepared by lyophilisation process due to the addition of large molecular protein – collagen in a less amount compared to that of the collagen:PCL materials. For the DSC study on the 1: 8 and 1:20 w/w gelatin/collagen:PCL groups, almost the same % crystallinity of the PCL phase was measured in the gelatin/10% collagen:PCL groups (Table 4); however, the trend of higher % crystallinity of PCL phase in 1:20 group was observed in gelatin/25% collagen:PCL materials even though the results were still within the standard error (Paired t-test: P=0.173; Table 5). The larger amount of collagen content may play a critical role in the change of the crystal nucleation pattern of PCL and thereby the % crystallinity of the PCL phase in the protein:PCL biocomposites.

The natural polymer phase (collagen) of the biocomposites under investigation for production of tissue engineered skin substitutes is considered to be stabilised due to localised coating by the synthetic polymer component (PCL). Use of a biodegradable synthetic polymer, such as PCL, potentially allows complete replacement of implanted material by repair tissue while compaction of the initial lyophilised collagen mat to a film during the solvent evaporation stage of the process is expected to improve mechanical integrity [117]. However, the degree of exposure of the collagen component, the porous structure, the release/ retention of the collagen phase and the biological stability are all crucial properties of biocomposites, which will influence cell attachment and growth.

A previous report of collagen:PCL biocomposite morphology [117] using SEM showed that 1:4 and 1:8 (w/w) materials were characterised by a more open, porous structure relative to 1:20 (w/w) materials. The exposure of collagen also decreased as the PCL content of the biocomposite increased as evidenced by collagenase digestion. Collagen:PCL biocomposite with a w/w ratio of 1:8 had the highest estimated collagen exposure of 97.3±4.4% , followed

by 1:4 biocomposites with 95.1±1.7% and 1:20 with 50.3±7.9% [117]. In the present work, the SEM of collagen:PCL biocomposite samples before and after incubation in PBS at 37°C revealed the similar characteristics of a fibrous surface structure for 1:4 biocomposites (Figure 10 to 12) and more effective coating of the fibrous component by a smoother surface layer in 1:8 and 1:20 samples (Figure 13 to 18). Although the porosity seemed to increase for 1:8 and 1:20 biocomposites after incubation in PBS, major changes in porosity were not in evidence. This suggests that protein release may be occurring mostly from sub-surface layers of the biocomposites. The SEM of 1:4, 1:8 and 1:20 gelatin:PCL biocomposites revealed a similar fibrous porous surface morphology compared to that of the collagen:PCL materials. However, no significant differences in surface morphology could be distinguished in these gelatin:PCL materials. Furthermore, the similar porous and fibrous surface morphology were shown in 1:8 & 1:20 w/w gelatin/10% collagen:PCL and 1:8 & 1:20 w/w gelatin/25% collagen:PCL biocomposites by SEM as well.

Porous polymer scaffolds are widely used as a carrier of cells in tissue engineering allowing for cellular incorporation and vascular ingrowth. Once porous polymer scaffolds are seeded with cells in vitro and implanted, the infiltration and induction by host tissue will occur via the release of incorporated chemotactic agents that attract the desired cells into the porous scaffold [28]. Cells attached to the polymer scaffold proliferate and secrete matrix and growth factors, while the polymer scaffold provides structural and mechanical form. Fibrovascular inflammatory tissue thereby infiltrates the scaffold pores and cells reorganize into functional tissue as the polymer scaffold degrades [31-33]. An appropriate pore size of scaffold for skin tissue engineering is critical to allow the optimal ingrowth of native fibroblast and endothelial cells from the wound bed, and is optimal to be controlled at 20 to 50μm in diameter [137]. Higher mean bubble point pore size in diameter, in terms of the maximum pore size, was measured as 47.1 ± 11.5μm (n=3) in the 1:8 collagen:PCL biocomposites (ranged from 22.18 to 77.63μm) compared to that of 28.8 ±16.1μm (n=3) in the 1:20 group (ranged from 5.6 to

75.41μm); however, no significant differences were apparent (P=0.391) (Figure 19). Furthermore, both 1:8 and 1:20 collagen:PCL biocomposites exhibited the similar pore size of 9 to 10μm in diameter at the maximum pore size distribution (P=0.739). Therefore, the characteristics of porosity of 1:8 and 1:20 collagen:PCL biocomposites could possibly allow for the ingrowth of fibroblasts and endothelial cells, and isolate keratinocytes and fibroblasts on each side of the membrane simultaneously. Even though the distribution of the pore sizes varied in 1:8 and 1:20 collagen:PCL biocomposite samples respectively, the cell growth curves produced by seeding 3T3 fibroblasts, NHEK, PHEK and PHDF respectively revealed good cell growth and proliferation in this work.

In the protein release study for the group of collagen:PCL materials, 1:4 collagen:PCL biocomposites exhibited the highest collagen release rate (Figure 7) followed by 1:8 and 1:20 materials in line with the higher ratio of PCL polymer in the biocomposite that tends to lock in the collagen component. More than 86% of the collagen content of 1:4 biocomposites was released into PBS in 12 days (Figure 7). However, the residual collagen assay performed on different samples of 1:4 collagen:PCL biocomposites revealed retention of around 28% of the original collagen component at day 11 (Figure 8). A high collagen loading would be expected to promote cell attachment due to integrin binding with cell adhesion domains in collagen such as the RGD sequence *in vitro* and *in vivo* [138-140]. However, the extent of collagen release during cell seeding and proliferation, the actual collagen exposure and distribution in composite, and the deposition of ECM by fibroblasts themselves in culture may all affect the outcome. Furthermore, the differences in retained collagen measured in the present study may indicate formulation based, inter-sample variability. Similar trend for the protein (gelatin) release from gelatin:PCL biocomposite groups was measured compared to that of collagen:PCL materials with the highest release rate on 1:4 group followed by 1:8 and 1:20 groups. However, rapid release of gelatin was shown in all gelatin:PCL groups with almost 100% release rate on 1:4 group in only 6 hours post incubation in PBS at 37℃. On day 3, the

release of protein in 1:8 and 1:20 groups reached a mild rate resulting in a final cumulative release (w/w) of 72.7%, and 41.4% respectively. The characteristics of rapid protein release were shown in all gelatin:PCL materials; however, cell attachment could still be achieved in a shorter period of time and thus allows for the survival of cells and subsequent deposition of ECM by cells themselves. The good biocompatibility of gelatin:PCL biocomposites was proven in the following study of interactions between biocomposite samples with 3T3 fibroblasts, PHEK and PHDF respectively shown in Section 5.2.4, 5.2.5 and 5.2.6.

In the protein release study for the group of 1:8 and 1:20 gelatin/10% collagen:PCL materials, higher cumulative release of protein content was revealed for 1:8 gelatin/10% collagen:PCL biocomposite with about 78.3% of the original protein content being released at only 6 hours post incubation in PBS at 37℃, while 52.6% was released from 1:20 biocomposites at the time point (Figure 79). Almost 100% release of the original protein content was measured for 1:8 samples in only 24 hours ($n=3\pm SE$; Paired t-test: $P<0.05$); however good biocompatibility for gelatin/10% collagen:PCL biocomposites was still observed in the study on PHEK and PHDF cultures shown in Section 5.3.5 and 5.3.6. Similar good biocompatibility for the gelatin/25% collagen:PCL biocomposites was observed in the study on PHEK and PHDF cultures shown in Section 5.3.5 and 5.3.6. Higher mean total protein release rate was measured on 1:20 gelatin/25% collagen:PCL samples; however, there were no statistically significance ($n=3\pm SE$; Paired t-test: $P>0.05$). The differences in protein release rate measured in the present study may indicate formulation based, inter-sample variability.

The results for estimation of retained protein contents in collagen:PCL biocomposites incubated in PBS revealed that all the samples investigated seemed to have similar residual collagen contents at the end of the release study (Section 5.1.3). Differences in residual collagen contents determined from release experiments and the residual collagen assay could be due to formulation effects and inter-sample variability. The results of BCA assay used in

collagen release study may be affected by the acidic properties of both collagen solution (pH 2.7) used for preparation of calibration samples and biocomposite itself following incubation in PBS (pH 7.16 to 7.33). Furthermore, the retained collagen contents were obtained by dissociation of biocomposite samples in an acetone/DCM/PBS solution to allow for dissociation and precipitation of PCL particles from collagen contents after solvent evaporation in the present work. It is possible that re-crystallisation of PCL polymer may occur while solvent evaporating in process, thus some parts of collagen content will be locked in by PCL particles again. Overall the release study indicated that collagen:PCL biocomposites with higher PCL content result in a lower collagen release rate, thereby enhancing biological stability.

Analysis of the amount of retained collagen in collagen:PCL biocomposites following cell culture with 3T3 fibroblasts was also estimated using the BCA assay. All the cells grown on the biocomposites were supposedly detached by the trypsinisation procedure for cell counting. In addition, all the samples were washed three times in PBS before BCA analysis of residual collagen. The results revealed that 1:20 collagen:PCL biocomposite exhibited the highest level of residual collagen (Figure 9) followed by 1:8 and 1:4 materials in line with the retention data obtained in PBS. In the assessment of differences of residual collagen contents between the groups of biocomposites following incubation in PBS and that following cell cultures, both the 1:8 and 1:20 materials display similar collagen retention (Figure 8 and 9). The residual collagen content of 1:4 materials showed the greatest variation between these two studies; however, the measurement of residual collagen (17.3%) in the group of biocomposites following cell cultures matched closely to the amount (86.8%) indicated by the collagen release study (Figure 9 and 7).

A higher PCL content may result in improved and prolonged presentation of collagen for cell adhesion. Furthermore, the ability to vary the release profile of collagen by adjusting the

collagen:PCL ratio of the composite suggests a potential for controlled delivery of growth factors into the wound site. Newly formed tissue in wound repair proceeds via a complex interaction between blood vessel formation, macrophages and migrating fibroblasts modulated by growth factors [135, 141]. PDGF and TGF-β, for example, are both present in wounds and stimulate fibroblasts contraction of collagen matrices while TGF-β is also recognized to be a profibrotic cytokine. IFN-γ has been implicated in the process of down regulation of fibroblast proliferation and matrix synthesis.

Enhanced attachment and growth of human osteoblasts were measured previously on collagen:PCL substrates relative to PCL surfaces, albeit over a limited 24h time span. The collagen:PCL biocomposites were designed to function as matrices and scaffolds for optimising cell attachment, spreading and proliferation. Human fibroblasts are known to proliferate in a bio-absorbable polyglactin acid mesh (Vicryl®, Ethicon, Inc., Somerville, New Jersey) where they secrete dermal collagen, fibronectin (FN), GAGs, growth factors, and other proteins. In effect, a dermal matrix is self-produced even when exogenous collagen is not used [142]. In the present study, the biocomposites were investigated as support matrices for dermal and epidermal skin cells to produce bi-layer skin substrates and models. Cells interaction is expected via cell surface receptor binding with adhesion ligands on the biomaterial. Fibroblasts link to collagen in the ECM through α1β1 and α2β1 integrin receptors [117, 138, 143, 144] and also bind to FN's RGDS cell adhesion domain via the α3β1 and α5β1 integrin receptors. Thus the process for fibroblasts binding to the biocomposite via FN is possible following exposure to biological fluids and the establishment of FN/collagen linkages.

The growth rate of 3T3 fibroblasts on type I and type IV collagen:PCL materials demonstrated favourable cell interaction at time interval up to 12 days (Figure 20); however, no significant differences were observed between the groups of type I and type IV materials.

Since the comparative results of biocompatibility for both type I and type IV collagen:PCL biocomposites, type I collagen was therefore chosen as the material used for tissue engineering of skin due to the cost effect in the following work. On the other hand, the group of TCP exhibited the best cell growth curve in the study. It may be due to the TCP substrate conducive to attachment and growth of 3T3 fibroblasts, and the easier detachment of cells by trypsinisation compared to that in the study groups of biocomposites. The higher collagen content in 1:4 and 1:8 materials relative to 1:20 samples does not translate into higher cell proliferation indicating that the factors of substrate itself and the exposure and/or retention of proteins may not affect the biocompatibility of materials alone. Another explanation is suggested by the pattern of cell attachment to the composites revealed in Figure 22 to 25. Fibroblasts tend to be confined to the ridges of the pore structure indicating a restriction on the number of attached cells due to available substrate area. For the cell growth curve on gelatin:PCL biocomposites, 1:20 materials exhibited the best cell growth at time interval up to 12 days compared to 1:4 and 1:20 collagen:PCL biocomposites ($P<0.05$); however, no significant differences were found in comparison with the other gelatin:PCL and collagen:PCL biocomposite groups. The good biocompatibility of gelatin:PCL biocomposites represented here may show the potential for application in tissue engineering in the future.

The layering of spread fibroblasts following cell culture for 3 days (Figure 23 and 25) is of interest concerning scaffold colonization. It is recognized that cell-scaffold binding can block pores of inadequate size and geometry [145, 146]. Although the cell spreading tendency effectively reduces the cell profile, thereby improving pore access and infiltration, this effect could be offset by multi-layer formation. Cell-cell, cell-matrix and matrix-matrix binding (involving cross-linked collagen bundles) are important for providing a network which permits transmission of fibroblasts contractile stresses across the wound. However, cell-cell coupling between rounded fibroblasts, quickly following cell seeding (Figure 22), is likely to restrict infiltration of the scaffold. Nevertheless, for the design of a tissue-engineered skin

model, no confluence of dermal fibroblasts is needed in culture because fibroblasts could function to produce ECM satisfactorily by communicating *via* the cell signaling systems just like that existing in the normal skin dermal structure. This concept is applied in the design of skin substitutes based on collagen gel seeded with fibroblasts [29]. Although fibroblasts are surrounded completely by contracted collagen gel, they still perform vital functions.

The growth rates of NHEK were similar on 1:4, 1:8 and 1:20 (type I) collagen:PCL biocomposites investigated and higher than TCP up to 4 days (Figures 29 and 30). Wound keratinocytes express integrin cell surface receptors for fibronectin (FN), vitronectin (VN) and in particular the integrin $\alpha 2\beta 1$ receptor which binds to type I collagen fibers of the dermis and assists migration of the epidermis over viable dermis [135]. Thus collagen:PCL biocomposites are expected to present integral binding sites for both keratinocytes and fibroblasts which could be advantageous for preparation of co-cultured skin models and substitutes. Furthermore, the incorporation of chemoattractants and growth factors in the natural polymer phase, to further modulate skin cells behavior, may present a logical extension of the composite technology presented here in the future.

Good biocompatibility has been shown in all of the study groups including collagen:PCL, gelatin:PCL and gelatin/collagen:PCL biocomposites *in vitro*. However, the cost effect and the quality of materials in terms of the successful preparation rate are critical for development of a tissue-engineered skin model to be applicable in practice. The collagen:PCL materials have the best quality and successful preparation rate in the present work; however, the price of type I collagen is much higher than that of gelatin (type B). Therefore, the replacement of collagen by gelatin or other biomaterials with a cheaper price might be a good choice for the development of tissue engineering in the future. However, gelatin prepared by enzyme degradation of collagen has a lower molecular structure compared to that of collagen. Relatively fragile and weaken in pure gelatin mats formation were observed during the

lyophilisation procedure causing one-third failure preparation rate in this work. To improve the quality and the successful preparation rate of biocomposites, the mixture of gelatin and collagen in less amount than that used for collagen:PCL biocomposites was designed and used for preparation of gelatin/10% collagen:PCL and gelatin/25% collagen:PCL materials in the following study. Good biocompatibility of gelatin/10% collagen:PCL materials has been proven here *in vitro*, and the price for them is measured just one-tenth of that for collagen:PCL samples. Gelatin/10% collagen:PCL biocomposites have shown their potential for application in the field of tissue engineering in the future.

It has been shown that epidermal homeostasis, growth, and differentiation are controlled by epithelial-mesenchymal interactions [147-149]. Epidermal morphogenesis is modulated by cell-cell interactions via diffusible factors including cytokines and growth factors, as well as by cell-matrix interactions via cellular adhesion molecules [150-152]. On the other hand, dermal fibroblast collagen synthesis appears to be regulated by keratinocytes via diffusible factors in an *in vitro* skin model [153]. Moreover, the fact that fibroblast proliferation is increased in an *in vitro* co-culture model, compared with a fibroblast monolayer alone, implicates that the keratinocytes regulate fibroblast growth and proliferation [124]. These facts indicate that keratinocytes and fibroblasts are not isolated in the skin tissue but their activity is influenced by each other. Therefore, an *in vitro* skin model designed by the co-culture of keratinocytes and fibroblasts to mimic the normal skin tissue would be more realistic for not only pharmaceutical screening, but also for possible clinical applications.

On the other hand, *in vitro* organotypic co-culture systems have been proposed and developed not only to simplify the complex *in vivo* situation but also mimic the natural tissue architecture. The basic principle of organotypic co-cultured skin models is to culture mesenchymal and epithelial cells spatially separated by seeding epithelial cells on the top surface of a matrix consisting of type I collagen, which is populated with fibroblasts [154,

155]. Moreover, many other *in vitro* models have been established for the study of keratinocyte secretion [3, 156]. Katz and Taichman introduced a two-chamber co-culture model [157] to study keratinocyte protein secretion [158], which was then modified by Chang and colleagues to study epidermal-fibroblast interactions [125]. In this system (Transwell®, Corning Costar Corporation), epithelial and mesenchymal cells are kept physically separated in a lower chamber of culture dish and an upper chamber of permeable bottom insert within the same conditioned medium. A reconstructed skin substitute was also developed by co-culture of keratinocytes and fibroblasts simultaneously onto the papillary surface of a terminally sterilized acellular de-epidermized dermis (DED) harvested from allogenic skin tissue for clinical use [159]. Furthermore, a kind of cultured skin substitute (CSS) was prepared by use of the type I collagen-glycosaminoglycan (C-GAG) biopolymer substrate [110]. In this co-culture CSS model, fibroblasts were inoculated into the porous surface of the C-GAG substrate and allowed to incubate for one day, at which time the substrates were inverted and keratinocytes inoculated onto the nonporous laminated surface [160]. Conceptually, the co-cultured skin substitutes developed in this work were based on the basic principle of organotypic co-cultures; however, the distinct co-culture procedure of seeding keratinocytes and fibrobalsts on either side of the scaffold is different from the others mentioned above.

Available permanent skin substitutes could be classified as three types: [A] cultured epidermal equivalent base on processed skin dermal layer or fabricated biomaterials containing collagen and/or other matrix proteins, [B] cultured dermal substitutes based on processed skin dermal layer or fabricated biomaterials, and [C] possessing distinct dermal and epidermal components, which are popularly referred to as composite skin. Dermal tissue is proven to contribute to durability, elasticity and cosmetic appearance of normal skin. Recognition of the necessity of attachment to the wound bed for keratinocytes to survive, proliferate and differentiate, and the fragility of wounds closed with epithelial cells alone has lead to several

attempts to develop a functional dermal layer. AlloDerm® is a freeze-dried, acellular dermal allograft to act as a template and to regenerate into a viable dermis when grafted into a full thickness burn [114,161]. Integra® artificial skin is a bi-layered construct consisting of a dermal replacement layer and covered with a silicon sheet as an outer layer. The dermal layer is made of a porous matrix of fibers of cross-linked bovine tendon collagen and a glycosaminoglycan (chondroitin-6-sulfate) [162-164]. The temporary outer layer is medical grade silicone 100 μm thick to be replaced in 14 to 21 days with an ultra thin autologous epidermal graft or cultured keratinocytes [165]. Comp Cult Skin® is a type of composite cultured skin consisting of neonatal keratinocytes and fibroblasts cultured in distinct layers of a bovine type-I collagen scaffold. The clinical trials approved by FDA are ongoing in burns patients [166]. Apligraf® is a bi-layered living skin consisting an epidermal layer formed from neonatal keratinocytes, and a dermal layer composed of neonatal fibroblasts interspersed in a type I bovine collagen gel. Cornified epidermis develops by incubation at the air-liquid interface for 7 to10 days [115,167,168]. Most of these update co-cultured skin constructs were developed using dermal components in gel formulation or matrices consisting with mainly collagen contents, and thereby they prone to shrink somehow by the natural force generated by fibroblasts later on. A stronger biodegradable scaffold may be needed to allow for cell transfer and also function to resist the contraction force generated from fibroblasts to prevent possible scar formation in clinical application. The collagen:PCL biocomposites developed in this work represent all the beneficial characteristics mentioned above; however, the *in vivo* animal study on athymic mice revealed that the wound size decreased in all study groups in the late stage of wound healing process. It is considered to be caused by the rapid growing of epidermal layer in mice. Nevertheless, the effects on prevention of scar formation by using tissue-engineered skin substitutes could be only verified by clinical evaluation and further histologic studies.

The ultimate goal of the present work was to develop a tissue-engineered skin substitute by

the co-culture of keratinocytes and fibroblasts onto a non-crosslinking collagen:PCL biocomposite. To enable seeding these two distinct cell types on either side of a biocomposite membrane to mimic the normal skin structure, a specific co-culture device was designed for this purpose (Figure 3). To investigate the technical and biological possibilities of the new design of a co-culture system, a feasibility study was carried out by seeding 3T3 fibroblasts on each side of a biocomposite film. The 1:20 collagen:PCL biocomposites were chosen for this study as they exhibited good cell growth curves by seeding 3T3 fibroblasts and NHEK in the early stage of this work as well as the higher mechanical strength in comparison with the other types of biocomposite due to higher composition of PCL in 1:20 materials, which facilitates handling.

Co-culture of 3T3 fibroblasts on both surfaces of 1:20 collagen:PCL biocomposite films was achieved in this study by using a specially designed co-culture device (Figure 113). Due to the limitation of the numbers of the designed co-culture devices, only 7 samples could test in the preliminary study. In the co-culture technique, 3T3 fibroblasts growth on the upper surface of biocomposite films (n=7) was allowed for three days, and three in seven samples were trypsinised for cell counting on day 3 with the cell number of 9.7±1.07 ($x10^4$) per cm^2 (mean±SE). Two in seven samples were allowed for growth for another 3 days, and another two in seven samples of the co-culture devices were turned upside down to enable cell seeding on the other surface of the biocomposite film for 3 days. Total cell numbers on both surfaces in the co-culture system on day 6 were $2.6x10^5$ per cm^2 (n=2). On day 6, in the single culture system the cell density on one surface of the biocomposite was $1.7x10^5$ per cm^2 (n=2). An estimated 55.3% increase in cell number was measured in the co-culture system indicating that cell proliferation was sustained on both sides of the biocomposite membrane even though no statistical significance presented. Thus the co-culture technique and device designed in this study proved to be work to allow 3T3 fibroblasts to grow on both side of surface of 1:20 collagen:PCL biocomposites theoretically. Therefore, co-culture of human keratinocytes and

3T3 fibroblasts on either side of the membrane was subsequently performed using the same co-culture system. The preliminary study on co-culture of NHEK and 3T3 fibroblasts alone on either side of the membrane was thereby performed using the same co-culture system, and the SEM revealed good cell attachment and growth for both NHEK and 3T3 fibroblasts alone on each side of the composite film in culture for up to 6 days (Figure 114 and 115). The feasibility of the co-culture system developed by our own was further proven in principle at this stage.

In consideration of the difficulty in judgment of the confluence of epidermal layer on the biocomposite membrane, the co-culture technique was modified to simplify the technique. The human keratinocytes were seeded on the top surface of biocomposite film firstly with the control group of cell growth on the 24-well TCP to monitor the confluence of keratinocytes. It took about 14 days in this study to achieve 90% to 95% confluence of keratinocytes in the TCP indicating that a near confluent sheet of epidermal cells grown on the top surface of biocomposite has been developed as well. To mimic the normal dermal structure of skin, fibroblasts seeded on the other side of biocomposite membrane were thought to be populated on the surface of membrane and ingrow the porous scaffold structure, thus cell confluence was not needed for the design of a co-cultured skin model. Therefore, a co-cultured skin model with a confluent differentiated epidermal sheet of PHEK on the upper surface of biocomposite membrane and a layer of populated 3T3 fibroblasts underneath the membrane was firstly developed using the designed co-culture system in 28 days. The results were proven by SEM and immunohistochemistry assay. SEM revealed a confluent sheet of PHEK on the top surface of biocomposite membrane, and good cell attachment and spreading of 3T3 fibroblasts on the other side of the membrane (Figure 116 and 117) indicating the establishment of focal contacts of both types of cells with the collagen:PCL substrate respectively. Immunohistochemistry assay of co-cultured skin model showed that a confluent differentiated sheet of keratinocytes in red-brown fluorescent staining and underneath

populated fibroblasts in green fluorescent staining were isolated completely on either side of the membrane indicating a successful design of a bi-layer skin model (Figure 118 and 119).

To increase the resources of human keratinocyte cells and mimic the normal clinical condition, primary human epidermal keratinocytes (PHEK) and primary human dermal fibroblast (PHDF) were isolated and primarily cultured from the epidermal and dermal layers of human foreskin respectively in the this study. Co-culture of PHEK and PHDF on either side of the membrane was subsequently performed using the same co-culture system. The design of a novel co-cultured skin model was achieved by growing a confluent PHEK sheet on the biocomposite film upwards with a populated PHDF layer underneath followed by lifting the co-cultured membrane onto the air-fluid level for another 10 days to enhance keratinocyte differentiation. The results were proven by SEM (Figure 120 and 121) and immunohistochemistry assay (Figure 122 and 123).

In vitro studies have shown that subepidermal fibroblasts can stimulate keratinocyte growth via diffusible factors [169] and that keratinocytes can induce expression of fibroblast genes [151]. Subepithelial fibroblasts in adult tissues, such as the oral mucosa and the skin, express the paracrine growth factors including keratinocyte growth factor (KGF) and hepatocyte growth factor (HGF), which are primarily synthesized by fibroblasts and have their respective receptors on epithelial cells [127, 170], and may thus influence both normal epithelial growth and regeneration during wound healing [127-131]. The oral fibroblasts were further proved to produce more KGF than skin fibroblasts in response to co-culture with keratinocytes and the stimulation of pro-inflammatory cytokine IL-1β. Furthermore, the cell culture environment such as the collagen-contained materials was found to interfere the production of KGF [171]. To investigate the interaction between single-donor PHEK and PHDF in the co-culture system based on 1:20 collagen:PCL biocomposites, we compared the KGF production from PHDF populations either co-cultured with PHEK or stimulated by cytokine IL-1β alone. The results

revealed that the KGF release amount in group B of human fibroblast growth on TCP with addition of IL-1β increased significantly compared to that in group A of human fibroblast growth on TCP alone at time interval of 24 hours (n=3±SE; P=0.01); however, no significant differences were measured in the other paired study groups. The effect of cytokine IL-1β was proved to induce the production of KGF from PHDF grown on TCP at time interval of 24 hours in this study; however, the effect might be unapparent due to the change of cell-cell and/or cell-matrix interactions by co-culture of skin keratinocyte and fibroblast cells from a single donor therefore eliminating the pro-inflammatory cytokine stimulations, and/or the specific cell culture environment, i.e. the collagen:PCL biocomposite membrane.

Cultured skin substitutes (CSS) provide therapeutic alternatives for the closure of massive burn wounds and chronic ulcerations caused by poor wound healing ability of the host [172, 173]. However, current models of CSS have anatomical and physiologic deficiencies compared with the grafts of native skin. These limitations include lack of a vascular plexus, functional appendages such as sweat glands, and incomplete barrier function at the time of grafting [92,174]. Furthermore, some CSS are too thick to be engrafted easily on wound bed, too fragile to be manipulated, or too weak and would be degraded in a very short period of time. To develop a more promising skin substitute, a newly designed tissue-engineered skin model based on collagen:PCL biocomposites was investigated in this work. Even though the tissue-engineered skin model we developed did not comprise functional appendages and vessels, successful engrafting on athymic mice was achieved due to adequate thickness, porous structure and tensile strength of biocomposites allowing for imbibition (tissue fluid infiltration), vascular ingrowth, and suturing fixation. Furthermore, the skin substitutes with the existence of living cells showed a good engrafting rate and permanent wound coverage in the *in vivo* animal study. On the other hand, the blank biocomposite was observed to slough from the wound bed of athymic mice in about 2 weeks time. In consideration of the characteristics of good wound adhesion and protection, 1:20 w/w collagen:PCL materials may

function as a temporary wound dressing for wound care in clinical application in the future.

CHAPTER SEVEN

CONCLUSIONS

The preparation and characterisation of 1:4, 1:8 and 1:20 w/w collagen:PCL biocomposites for manufacture of tissue engineered skin substitutes have been reported here. Good biocompatibility was proven in the *in vitro* study for 1:4, 1:8 and 1:20 collagen:PCL materials, as well as in the *in vivo* study for 1:20 materials. Co-cultured skin model developed by seeding keratinocytes and fibroblasts alone on either side of the composite film showed a bi-layer structure of differentiated epidermal and dermal layers *in vitro* and *in vivo* mimicking the normal skin structures in this work. The results of successful engrafting of the co-cultured skin substitute on the back skin defect of athymic mice in 10 days showed the potential for development of an optimal tissue-engineered skin substitute for clinical application in the future. In exploration of brand new biomaterials by modification of the formulation and preparation methods for collagen:PCL substrates, gelatin:PCL and gelatin/collagen:PCL biocomposites were prepared and the results were also presented in this work. Good physical characteristics and biocompatibility *in vitro* were shown in the gelatin/10% collagen:PCL materials indicating the potential refinement of the collagen:PCL biocomposites and the possibility for mass manufacture for clinical use or study purpose in the future due to the much lower costs of the composition used for preparation of protein:PCL biocomposites.

REFERENCES

1. Robson MC, Barnett RA, Leitch IO, Hayward PG. Prevention and treatment of postburn scars and contracture. *World J Surg* 1992;16(1):87-96.
2. McHugh AA, Fowlkes BJ, Maevsky EI, Smith Dr DJ, Rodriguez JL, Garner WL. Biomechanical alterations in normal skin and hypertrophic scar after thermal injury. *J Burn Care Rehabil* 1997;18(2):104-8.
3. Rheinwald JG and Green H. Serial cultivation of strains of human epidermal keratinocytes: the formation of keratinizing colonies from single cells. *Cell* 1975;6:331-44.
4. Green H, Kehinde O, Thomas J. Growth of cultured human epidermal cells into multiple epithelia suitable for grafting. *Proc Natl Acad Sci USA* 1979;76:5665-8.
5. Munster AM, Weiner SH, Spence RJ. Cultured epidermis for the coverage of massive burn wounds: a single-center experience. *Ann Surg* 1990;211:676-9.
6. Gallico III GG, O'Connor NE, Compton CC, Kehinde O, Green H. Permanent coverage of large burn wounds with autologous cultured human epithelium. *N Engl J Med* 1984;311:448-51.
7. Sheridan RL, Hegarty M, Tompkins RG, Burke JF. Artificial skin in massive burns-result to ten years. *Eur J Plast Surg* 1994;17:91.
8. Compton CC. Wound healing potential of cultured epithelium. *Wounds* 1993;5(2):97-111.
9. Cuono C, Langdon R, McGuire J. Use of cultured epidermal autografts and dermal allografts as skin replacement after burn injury. *Lancet* 1986;1:1123-4.
10. Woodley DT, Peterson HD, Herzog SR, Stricklin GP, Burgeson RE, Briggaman RA, Cronce DJ, O'Keefe EJ. Burn wounds resurfaced by cultured epidermal autografts show abnormal reconstitution of anchoring fibrils. *JAMA* 1988;259:2566-71.
11. Cuono CB, Langdon R, Birchall N, Barttelbort S, McGuire J. Composite autologous-allogenic skin replacements: development and clinical application. *Plast Reconstr Surg* 1987;80:626-35.
12. Elias PM. Stratum corneum architecture, metabolic activity and interactivity with subjacent cell layers. *Exp Dermatol* 1996;5:191-201.
13. Goldsmith LA. My organ is bigger than your organ. *Arch Dermatol* 1990;126:301-2.
14. Arndt K, Bigby M. Skin Disorders. In: Levy BS, Wegman DH, ed. Occupational. Health. Boston, MA: Little, Brown and Company, 1988:371-85.
15. Watt FM. Terminal differentiation of epidermal keratinocytes. *Cell Biol* 1989;1:1107-15.
16. Pringle JH, Ruprai, A. K., Primrose L, Keyte J, Potter L, Close P, Lauder I. In situ hybridization of immunoglobulin light chain mRNA in paraffin sections using biotinylated or hapten-labelled oligonucleotide probes. *J Pathol* 1990;162:197-207.
17. Hotchin NA, Kovach NL, Watt FM. Functional down-regulation of integrins is reversible but commitment to terminal differentiation is not. *J Cell Science* 1993;106:1131-8.
18. Jones PH, Watt FM. Separation of human epidermal stem cells from transit amplifying cells on the basis of differences in integrin function and expression. *Cell* 1993;73:713-24.

19. Reichert U, Michel S, Smidt R. The cornified envelope: A key structure of terminally differentiating keratinocytes. In: Darmon M, Blumenberg M, ed. Molecular Biology of the Skin: The Keratinocyte. San Diego: Academic Press, 1993:107-40.
20. Urmacher C. Normal skin. In: Sternberg SS, ed. Histology for pathology. New York: Raven Press, 1992:381-97.
21. Eckert RL. Structure, function and differentiation of the keratinocyte. *Physiol Rev* 1989;69:1316-46.
22. Woodcock-Mitchell J, Eichner R, Nelson WG, Sun TT. Immunolocalization of keratin polypeptides in human epidermis using monoclonal antibodies. *J Cell Biol* 1982;95:580-8.
23. Hohl D, Roop DL. The keratinocyte. In: Darmon M, Blumenberg M, ed. Molecular Biology of the Skin. San Diego: Academic Press, 1993:151-72.
24. White Jr. CR, Bigby M, Sangueza OP. What is normal skin? In: Arndt KA, Robinson JK, Leboit PE, Wintroub BU, ed. Cutaneous Medicine and Surgery: An Integrated Program in Dermatology. Philadelphia: W. B. Saunders, 1996: 3-41.
25. Clark RAF, Henson PM. Molecular and Cellular Biology of Wound Repair. New York: Plenum, 1988:3-33.
26. Ross R. Wound healing. *Sci Am* 1969;220:40-50.
27. Shakespeare P. Burn wound healing and skin substitutes. *Burns* 2001;27:517-22.
28. Mikos AG, McIntire LV, Anderson JM, Babensee JE. Host response to tissue engineered devices. *Advanced Drug Delivery Reviews* 1998;33:111-39.
29. Kemp PD, ed. Extracellular Matrix Protocols: Tissue engineering and cell-populated collagen matrices Totowa, NJ: Humana Press Inc.
30. Anderson JM, ed. Biocompatibility of tissue-engineered implants. Oxford, UK: Elsevier Science Inc., 1998.
31. Barrera DA, Zylastra E, Lansbury Jr. PT, Langer R. Synthesis and RGD peptide modification of a new bio-degradable copolymer: poly(lactic acid-co-lysine). *J Am Chem Soc* 1993;115:11010-1.
32. Cook AD, Hrkach JS, Gao NN, Johnson IM, Pajvani UB, Cannizzaro SM, Langer R. Characterization and development of RGD-peptide-modified poly(lactic acid-co-lysine) as an interactive, resorbable biomaterial. *J Biomed Mater Res* 1997;35:513-23.
33. In't Veld PJA, Shen ZR, Takens GAJ, Dijkstra PJ, Feijen J. Glycine/glycolic acid based copolymers. *J Polym Sci Poly Chem* 1994;32:1063-9.
34. Pachence JM. Collagen-based devices for soft tissue repair. *J Biomed Mater Res* 1996:3335-40.
35. Nehrer S, Breinan HA, Ramappa A, Young G, Shortkroff S, Louie LK, Sledge CB, Yannas IV, Spector M. Matrix collagen type and pore size influence behavior of seeded canine chondrocytes. *Biomaterials* 1997;18(11):769-76.
36. Shibata H, Shioy N, Kuroyanagi Y. Development of new wound dressing composed of spongy collagen sheet containing dibutyryl cyclic AMP. *J Biomater Sci polym (Edn)* 1997;8:601-21.

37. van Luyn MJA, Verheul J, van Wachem PB. Regeneration of full-thickness wounds using collagen split grafts. *J Biomed Mater Res* 1995;29:1425-36.
38. Spilker MH, Yannas IV, Hsu HP, Norregaard TV, Kostyk SK, Spector M. The effect of collagen-based implants on early healing of the adult rat spinal cord. *Tissue Eng* 1997;3:309-17.
39. Ellis DL, Yannas IV. Recent advances in tissue synthesis in vivo by use of collagen-glycosaminoglycan copolymers. *Biomaterials* 1996;17(3):291-9.
40. Louie LK, Yannas IV, Hsu HP, Spector M. Healing of tendon defects implanted with a porous collagen-GAG martrix: histological evaluation. *Tissue Eng* 1997;3:187-95.
41. Tong XJ, Hirai K, Shimada H, Mizutani Y, Izumi T, Toda N, Yu P. Sciatic nerve regeneration navigated by laminin-fibronectin double-coated biodegradable collagen grafts in rats. *Brain Res* 1994;663(1):155-62.
42. Sickel BR, Jones D, Hekimian KJ, Wong KK, Chakalis DP, Costas PD. Hyaluronic acid through a new injectable nerve guide delivery system enhances peripheral nerve regeneration in the rat. *J Neurosci Res* 1995;40:318-24.
43. Byrne DJ, Hardy J, Wood RA, McIntosh R, Cushieri A. Effect of fibrin glues on the mechanical properties of healing wounds. *Br J Surg* 1991;78(7):841-3.
44. Mikos AG, Thorsen AJ, Czerwonka LA, Bao Y, Langer R, Winslow DN, Vacanti JP. Preparation and characterization of poly(L-lactic acid) foams. *Polymer* 1994;35:1068-77.
45. Ishaug SL, Yaszemski MJ, Bizios R, Mikos AG. Osteoblast function on synthetic biodegradable polymers. *J Biomed Mater Res* 1994;28:1445-53.
46. Freed LE, Marquis JC, Nohria A, Emmanual J, Mikos AG, Langer R. Neocartilage formation in vitro and in vivo using cells cultured on synthetic biodegradable polymers. *J Biomed Res* 1993;27:11-23.
47. Freed LE, Grande DS, Lingbin Z, Emmanual J, Marquis JC, Langer R. Joint resurfacing using allograft chondrocytes and synthetic biodegradable polymer scaffolds. *J Biomed Mater Res* 1994;28:891-9.
48. Grande DS, Southerland SS, Manji R, Pate DW, Schwartz RE, Lucas PA. Repair of articular cartilage defects using mesenchymal stem cells. *Tissue Eng* 1995;1:345-53.
49. Cao Y, Vacanti JP, Ma X, Paige KT, Upton J, Chowanski Z, Schloo B, Langer R, Vacanti CA. Generation of neo-tendon using synthetic polymers seeded with tenocytes. *Transplant Proc* 1994;26:3390-2.
50. Atala A, Vacanti JP, Peters CA, Mandell J, Retick AB, Freeman MR. Formation of urothelial structure in vivo from disassociated cells attached to biodegradable polymer scaffolds in vitro. *J Urol* 1992;148:658-62.
51. Organ GM, Mooney D, Hansen LK, Schloo BL, Vacanti JP. Enterocyte transplantation using cell-polymer devices to create intestinal epithelial-lined tubes. *Transplant Proc* 1993;25:998-1001.
52. Johnson LB, Aiken J, Mooney D, Schloo BL, Griffith-Cima L, Langer R, Vacanti JP. The mesentery as a laminated vascular bed for hepatocyte transplantation. *Cell Transplant* 1994;3:273-81.

53. Vancanti CA, Kim W, Upton J, Mooney D, Vacanti JP. The efficacy of periosteal cells compared to chondrocytes in the tissue engineered repair of bone defects. *Tissue Eng* 1995;1:301-8.
54. Juang JH, Bonner-Weir S, Ogawa Y, Vacanti JP, Weir GC. Outcome of subcutaneous islet transplantation improved by polymer device. *Transplantation* 1996;61:1557-61.
55. Gilbert JC, Takada T, Stern SE, Langer R, Vacanti JP. Cell Transplantation of genetically altered cells on biodegradable polymer scaffolds in syngeneic rats. *Transplantation* 1993;56:423-7.
56. Thomson RC, Yaszemski MJ, Powers JM, Mikos AG. Fabrication of biodegradable polymer scaffolds to engineer trabecular bone. *J Biomater Sci Polym (Edn)* 1995;7:23-28.
57. Ishaug-Riley SL, Crane GM, Gurlek A, Miller MJ, Yasko AW, Yaszemski MJ, Mikos AG. Ectopic bone formation by marrow stromal osteoblast transplantation using poly(DL-lactic-co-glycolic) foams implanted into the rat mesentery. *J Biomed Mater Res* 1997;36(1):1-8.
58. Ishaug-Riley SL, Crane GM, Miller MJ, Yasko AW, Yaszemski MJ, Mikos AG. Bone formation by three-dimensional stromal osteoblast culture in biodegradable polymer scaffolds. *J Biomed Mater Res* 1997;36(1):17-28.
59. Vacanti CA, Ishuang-Riley SL, Schloo BL, Vacanti JP. Synthetic polymers seeded with chondrocytes provide a template for new cartilage formation. *Plast Reconstr Surg* 1991;88:753-9.
60. Mooney DJ, Organ GM, Vacanti JP, Langer R. Design and fabrication of biodegradable polymer devices to engineer tubular tissues. *Cell Transplant* 1994;3:203-10.
61. Mooney DJ, Park S, Kaufmann PM, Sano K, McNamara, Vacanti JP, Langer R. Biodegradable sponges for hepatocyte transplantation. *J Biomed Mater Res* 1995;29:959-65.
62. Kaufmann PM, Heimrath S, Kim BS, Mooney DJ. Highly porous polymer matrices as a three-dimensional culture system for hepatocytes. *Cell Transplant* 1997;6(5):463-8.
63. Wake MC, Gupta PK, Mikos AG. Fabrication of pliable biodegradable polymer foams to engineer soft tissues. *Cell Transplant* 1996;5(4):465-73.
64. de Groot JH, Zijlstra FM, Kuipers HW, Pennings AJ, Klompmaker J, Veth RP, Jansen HW. Meniscal tissue regeneration in porous 50/50 copoly(L-lactide/ε-caprolactone) implants. *Biomaterials* 1997;18:613-22.
65. den Dunnen WF, Stokroos I, Blaauw EH, Holwerda A, Pennings AJ, Robinson PH, Schakenraad JM. Light-microscopic and electron-microscopic evaluation of short term nerve regeneration using a biodegradable poly(DL-lactitude-ε-caprolactone) nerve guide. *J Biomed Mater Res* 1996;31:105-15.
66. Laurencin CT, El-Amin SF, Ibim SE, Willoughby DA, Attawia M, Allcock HR, Ambrosio AA. A highly porous 3-dimensional polyphosphazene polymer matrix for skeletal tissue regeneration. *J Biomed Mater Res* 1996;30:133-8.
67. Langone F, Lora S, Veronese FM, Caliceti P, Parrigotto PP, Valenti F, Palma G.

Peripheral nerve repair using a poly(organo)phosphazene tubular prosthesis. *Biomaterials* 1995;16:347-53.

68. Yaszemski MJ, Payne RG, Hayes WC, Langer RS, Aufdemorte TB, Mikos AG. The ingrowth of new bone tissue and initial mechanical properties of a degrading polymeric composite scaffold. *Tissue Eng* 1995;1:41-52.
69. Suggs LJ, Payne RG, Yaszemski MJ, Alemany LB, Mikos AG. Synthesis and characterization of a block consisting of poly(proplylene fumarate) and poly(ethylene glycol). *Macromolecules* 1997;30:4318-23.
70. Beumer GJ, van Blitterswijk CA, Bakker D, Ponec MA. A new biodegradable matrix as part of a cell seeded skin substitute for the treatment of deep dermal skin defects: a physico-chemical characterization. *Clin Mater* 1993;14:21-7.
71. Beumer GJ, van Blitterswijk CA, Bakker D, Ponec MA. Cell-seeding and in vitro biocompatibility evaluation of polymeric matrices of PEO/PBT copolymers and PLLA. *Biomaterials* 1993;14:598-604.
72. Ennker IC, Ennker J, Schoon D, Schoon HA, Rimpler M, Hetzer R. Formaldehyde-free collagen glue in experimental lung gluing. *Ann Thorac Surg* 1994;57(6):1622-7.
73. Baum J, Brodsky B. Folding of peptide models of collagen and misfolding in disease. *Curr Opin Struct Biol* 1999;9(1):122-8.
74. Bella J, Eaton M, Brodsky B, Berman HM. Crystal and molecular structure of a collagen-like peptide at 1.9 A resolution. *Science* 1994;266: 75-81.
75. Brodsky B, Ramshaw JA. The collagen triple-helix structure. *Matrix Biol* 1997;15:545-554.
76. Rich A, Crick FH. The molecular structure of collagen. *J Mol Biol* 1961;3:483-506.
77. Polycaprolactone. (2006, July 8). In: Wikipedia, The Free Encyclopedia. Retrieved 00:04, August 9, 2006, from http://en.wikipedia.org/wiki/Collagen.
78. Gelatin. (2006, July 30). In: Wikipedia, The Free Encyclopedia. Retrieved 00:10, August 9, 2006, from http://en.wikipedia.org/wiki/Gelatin.
79. Stevens PV, Wijaya IMS, Paterson JL. Modeling of physical properties of gelatin: gel strength. *Food Australia* 1995:47(4):167-172.
80. Grobben AH, Steele PJ, Somerville RA, Taylor DM. Inactivation of the bovine-spongiform-encephalopathy (BSE) agent by the acid and alkali processes used in the manufacture of bone gelatine. *Biotechnol Appl Biochem* 2004;39:329-338.
81. Sinha VR, Bansal K, Kaushik R, Kumria R and Trehan A. Poly-ε-caprolactone microspheres and nanospheres: an overview. *Int J Pharm* 2004;278(1):1-23.
82. Polycaprolactone. (2006, July 8). In: Wikipedia, The Free Encyclopedia. Retrieved 00:12, August 9, 2006, from http://en.wikipedia.org/wiki/Polycaprolactone.
83. Boyce ST. Design principles for composition and performance of cultured skin substitutes. *Burns* 2001;27(5):523-33.
84. Boyce ST. Skin repair with the cultured cells and biopolymers. In: Wise D, ed. Human Biomedical Applications. Totowa, NJ: Humana Press, Inc., 1997:347-377.
85. Boyce ST. Cultured skin substitutes: a review. *Tissue Eng* 1996;2(4):255-66.

86. Elias PM. Epidermal lipids, barrier function, and desquamation. *J Invest Dermatol* 1983;80:44s-9s.
87. Compton CC, Gill JM, Bradford DA, Regaur S, Gallico GG, O'Conner NE. Skin regenerated from cultured epithelial autografts on full-thickness burn wounds from 6 days to 5 years after grafting. *Lab Invest* 1989;60(5):600-12.
88. Clugson PA, Snelling CF, Macdonald IB, Maledy HL, Boyle JC, Germann E, Courtemanche AD, Wirtz P, Fitzpatrick DJ, Kester DA. Cultured epithelial autografts: three years experience with eighteen patients. *J Burn Care Rehabil* 1991;12(6):533-9.
89. Herndon DN, Rutan RL. Comparison of cultured epidermal autograft and massive excision with serial autografting plus homograft overlay. *J Burn Care Rehabil* 1992;13(1):154-7.
90. Coleman JJ, Siwy BK. Cultured epidermal autografts: a life-saving and skin-saving technique in children. *J Pediatr Surg* 1992;27(8):1029-32.
91. Desai MH, Mlakar JM, McCanley RL, Abdullah KM, Rutan RL, Waymack JP, Robson MC, Herdon DN. Lack of long term durability of cultured keratinocyte burn-wound coverage: a case report. *J Burn Care Rehabil* 1991;12(6):540-5.
92. Boyce ST, Greenhalgh DG, Kagan RJ, Housinger T, Sorrel JM, Childress CP, Rieman M, Warden GD. Skin anatomy and antigen expression after burn wound closure with composite grafts of cultured skin cells and biopolymers. *Plast Reconstr Surg* 1993;91:632-41.
93. Hansbrough JF, Dore C, Hansbrough WB. Clinical trials of a living dermal tissue replacement placed beneath meshed, split-thickness skin grafts on excised wounds. *J Burn Care Rehabil* 1992;13(5):519-29.
94. Parenteau NL, Bilbo P, Nolte CJ, Mason VS, Rosemberg M. The organotypic culture of human skin keratinocytes and fibroblasts to achieve form and function. *Cytotechnology* 1992;9(1-3):163-71.
95. Wang CK, Nelson CF, Birnkman AM, Miller AC, Hoeffler WK. Spontaneous cell sorting of fibroblasts and keratinocytes creates an organotypic human skin equivalent. *J Invest Dermatol* 2000;114:674-80.
96. Lerner AB, Halaban R, Klaus SN, Moellmann GE. Transplantation of human melanocytes. *J Invest Dermatol* 1987;89(3):219-24.
97. Stoner ML, Wood FM. The treatment of hypopigmented lesions with cultured epithelial autograft. *J Burn Care Rehabil* 2000;21:50-4.
98. Boyce ST, Medrano EE, Abdel-Malek Z, Supp AP, Dodick JM, Nordlund JJ, Warden GD. Pigmentation and inhibition of wound contraction by cultured skin substitutes with adult melanocytes after transplantation to athymic mice. *J Invest Dermatol* 1993;100:360-5.
99. Swope VB, Supp AP, Cornelius JR, Babcock GF, Boyce ST. Regulation of pigmentation in cultured skin substitutes by cytometric sorting of melanocytes and keratinocytes. *J Invest Dermatol* 1997;109:289-95.
100. Ward RS, Tuckett RP. Quantitative threshold changes in cutaneous sensation of patients with burns. *J burn Care Rehabil* 1991;12(6):569-75.

101. Ward RS, Saffle JR, Schnebly WA, Hayes–Lundy C, Reddy R. Sensory loss over grafted areas in patients with burns. *J Burn Care Rehabil* 1989;10(6):536-8.
102. Jahoda CA, Oliver RF, Reynold AJ, Forrester JC, Horne KA. Human hair follicle regeneration following amputation and grafting into the nude mouse. *J Invest Dermatol* 1996;10:804-7.
103. Michel M, L'Heureux N, Pouliot R, Xu W, Auger FA, Germain L. Characterisation of a new tissue-engineered human skin equivalent with hair. *In Vitro Cell Dev Biol* 1999;35:318-26.
104. Anderson JM. Mechanisms of inflammation and infection with implanted devices. *Cardiovasc Pathol* 1993;2:33S-41S.
105. Anderson JM. Inflammatory response to implants. *Trans Am Soc Intern Organs* 1988;24:101-7.
106. Anderson JM, ed. Perspectives on the in vivo responses of biodegradable polymers. Boca Raton: CRC Press, 1995.
107. Lam KH, Schakenraad JM, Esselbrugge H, Feijen J, Nieuwenhuis P. The effect of phagocytosis of poly(L-lactic acid) fragments on cellular morphology and viability. *J Biomed Mater Res* 1993;27:1569-77.
108. Nakaoka R, TabataY, Ikada Y. Production of interleukin I from macrophages incubated with poly(DL-lactic acid) granules containing albumin. *Biomaterials* 1996;17(23):2253-8.
109. Rowling PJ, Raxworthy MJ, Wood EJ, Kearney JN, Cunliffe WJ. Fabrication and reorganization of dermal equivalents suitable for skin grafting after major cutaneous injury. *Biomaterials* 1990;11(3):181-5.
110. Boyce ST, Hansbrough JF. Biologic attachment, growth and differentiation of cultured human epidermal keratinocytes on a graftable collagen and chondroitin-6-sulfate substrate. *Surgery* 1988;103(4):421-31.
111. Monafo WW, West MA. Current treatment recommendations for topical burn therapy. *Drugs* 1990;40(3):364-73.
112. Nyberg SL, Shirabe K, Peshwa MV, Sielaff TD, Crotty PL, Mann HJ, Remmel RP, Payne WD, Hu WS, Cerra FB. Extracorpeal application of a gel-entrapment, bioartificial liver: demonstration of drug metabolism and other biochemical functions. *Cell Transplant* 1993;2(6):441-452.
113. Heimbach D, Luterman A, Burke J, Cram A, Herdon D, Hunt J, Jordan M, McManus W, Solem L, Warden G. Artificial dermis for major burns: a multi-center randomized clinical trial. *Ann Surg* 1988;208(3):313-20.
114. Wainwright D, Madden M, Luterman A, Hunt J, Monafo W, Heimbach D, Kagan R, Sitting K, Dimick A, Herdon D. Clinical evaluation of an acellular allografts dermal matrix in full-thickness burns. *J Burn Care Rehabil* 1996;17(2):124-36.
115. Bell E, Ehrlich HP, Buttle DJ, Nakatsuji T. Living tissue formed in vitro and accepted as skin-equivalent tissue of full thickness. *Science* 1981;211:1052-4.
116. Parenteau N, ed. Skin equivalents: Cambridge University Press, 1994.

117. Coombes AGA, Verderio E, Shaw B, Li X, Griffin M, Downes S. Biocomposites of non-crosslinked natural and synthetic polymers. *Biomaterials* 2002;23(10):2113-8.
118. Asmursen PD, ed. The skin. Hamburg, Biersdorf: Compendium Medical, Berlin, 1986.
119. Wiechelman K, Braun R and Fitzpatrick J. Investigation of the bicinchoninic acid protein assay identification of the groups responsible for color formation. *Anal Biochem* 1988;175:231-237.
120. Smith PK, Krohn RI, Hermanson GT, Mallia AK, Gartner FH, Provenzano MD, Fujimoto EK, Goeke NM, Olson BJ and Klenk DC. Measurement of protein using bicinchoninic acid. *Anal Biochem* 1985;150:76-85.
121. Turi EA. Thermal characterization of polymeric materials. 2nd ed. San Diego, CA, USA: Academic Press, 1997.
122. Clas SD, Dalton CR, Hancock BC. Differential scanning calorimetry: applications in drug development. *PSTT* 1999;2(8):311-20.
123. Pitt CG, Chasalow FJ, Hibionada YM, Kilmas DM, Schindler A. Aliphatic polyesters 1. The degradation of poly(ε-caprolactone) in vivo. *J Appl Polym Sci* 1981;26:3779-87.
124. Freshney R. Culture of animal cells: A manual of basic technique. New York: Wiley-Liss, Inc., 1987:117.
125. Chang CC, Kuo YF, Chiu HC, Lee JL, Wong TW and Jee SH. Hydration, not silicone, modulates the effects of keratinocytes on fibroblasts. *J Surg Res* 1995;59(6):705-11.
126. Boyce ST, Ham R G. Calcium-regulated differentiation of normal human epidermal keratinocytes in chemically defined clonal culture and serum-free serial culture. *J Invest Dermatol* 1983;81(1 Suppl):33s-40s.
127. Jian WG, Hiscox S. Hepatocyte growth factor/ scatter factor, a cytokine playing multiple and converse roles. *Histol Histopathol* 1997;12:537-55.
128. Finch PW, Rubin JS, Miki T, Ron D, Aaronson SA. Human KGF is FGF-related with properties of a paracrine effector of epithelial cell growth. *Science* 1989;245:752-5.
129. Dabelsteen S, Wandall H, Gron B, Dabelsteen E. Keratinocyte growth factor mRNA expression in periodontal ligament fibroblasts. *Eur J Oral Sci* 1997;105:593-8.
130. Watanabe S, Hirose M, Wang XE, Maehiro K, Murai T, Kobayashi O, Nagahara A, Sato N. Hepatocyte growth factor accelerates the wound repair of cultured gastric mucosal cells. *Biochem Biophys Res Commun* 1994;199:1453-60.
131. Werner S, Smola H, Liao X, Longaker MT, Krieg T, Hofschneider PH, Williams LT. The function of KGF in morphogenesis of epithelium and reepithelialization of wounds. *Science* 1994;266:819-22.
132. Leffler CC, Muller BW. Influence of the acid type on the physical and drug liberation properties of chitosan-gelatin sponges. *Internat J Pharma* 2000;194:229-37.
133. Yannas IV. Studies on the biological activity of the dermal regeneration template. *Wound repair regeneration* 1998;6:518-24.
134. Mochizuki M, Hirami M, Kanmuri Y, Kudo K, Tokiwa Y. Hydrolysis of polycaprolactone fibers by lipase: effects of draw ratio on enzymatic degradation. *J App Polym Sci* 1995;55:289-96.

135. Clark RAF, Singer AJ: Wound repair: basic biology to tissue engineering. In: Principles of Tissue Engineering. 2nd Edition, Lanza RP, Langer R, Chick WL, ed. San Diego: Academic Press, 2000:857-78.
136. Mignatti P, Rifkin DB, Welgus HG and Parks WC. Proteinases and tissue remodeling. In: The Molecular Biology of Wound Repair. 2nd Edition, Clark RAF, ed. New York, USA: Plenum Press, 1996:427–474.
137. Yannas IV, Burke JF, Gordon PL, Huang C, Rubenstein RH. Design of an artificial skin. II. Control of chemical composition. *J Biomed Mater Res* 1980;14:107-32.
138. Hubbel JA. Biomaterials in tissue engineering. *Biotechnology* 1995;13:565-6.
139. Lebaron RG, Athanasiou KA. Extracellular matrix cell adhesion peptides: functional applications in orthopedic materials. *Tissue Eng* 2000;6:85-103.
140. LeBarron RG, Athanasiou KA. Extracellular matrix cell adhesion peptides: functional application in orthopaedic materials. *Tissue Eng* 2000;6:85-103.
141. Martin P. Wound healing-aiming for perfect skin regeneration. *Science* 1997;276:75-81.
142. Gentzkow GD, Iwasaki SD, Hershon KS. Use of Dermagraft, a cultured human dermis, to treat diabetic foot ulcers. *Diabetes Care* 1996;19:350-4.
143. Welch MP, Odland GF, Clark RAF. Temporal relationships of F-actin bundle formation, collagen and fibronectin matrix assembly and fibronectin receptor expression to wound contraction. *J Cell Biol* 1990;110(1):133-45.
144. Hynes RO. Integrins: versalitility, modulation and signaling in cell adhesion. *Cell* 1992;69:11-25.
145. Yannas IV, ed. In vivo synthesis of tissues and organs. San Diego: Academic Press, 2000.
146. Freed LE, Vunjak-Novakovic G. Culture of organized cell communities. *Adv Drug Delivery Rev* 1998;33:15-30.
147. Fusenig NE, ed. Epithelial-mesenchymal interactions regulate keratinocyte growth and differentiation in vitro. Cambridge: Cambridge University Press, 1994.
148. Mackenzie IC, ed. Epithelial-mesenchymal interactions in the development and maintenance of epithelial tissues. Cambridge: Cambridge University Press, 1994.
149. Mass-Szabowski N, Shimotoyodome A and Fusenig NE. Keratinocyte growth regulation in fibroblast co-culture via a double paracrine mechanism. *J cell Sci* 1999;112:1843-53.
150. Werner S, Peters KG, Longaker MT, Fuller-Pace F, Banda MJ, and Williams LT. Large induction of keratinocyte growth factor expression in the dermis during wound healing. *Proc Natl Acad Sci U.S.A.* 1992;89(15):6896-900.
151. Smola HG, Thiekotter G, and Fusenig NE. Mutual induction of growth factor gene expression by epidermal-dermal cell interaction. *J Cell Biol* 1993;122(2):417-29.
152. Smola HG, Thiekotter G, Baur M, Stark H-J, Breitkreutz D, and Fusenig NE. Organotypic and epidermal-dermal co-cultures of normal human keratinocytes and dermal cells: Regulations of transforming growth factor alpha, beta 1 and beta 2 mRNA levels. *Toxicol In Vitro* 1994;8:641-50.
153. Warren LG. Epidermal regulation of dermal fibroblast activity. *Plast Reconstr Surg* 1998;102:135-139.

154. Fusenig NE, Breitkreutz D, Boukamp P, Bohnert A, Mackenzie IC, ed. Epithelial-mesenchymal interactions in tissue homeostasis and malignant transformation. New York: Cambridge University Press, 1991.
155. Fusenig NE. Cell interaction and epithelial differentiation. In: Freshney RJ, ed. Culture of Epithelial Cells. New York: Wiley-Liss, Inc., 1992: 25-57.
156. Bell E, Sher S, Hull B, Merrill C, Rosen S, Chamson A, Asselineau D, Dubertret L, Coulomb B, Lapiere C, Nusgens B, Neveux Y. The reconstitution of living skin. *J Invest Dermatol* 1983;81 (1 Suppl):2s-10s.
157. Katz AB and Taichman LB. Epidermis as a secretory tissue: An in vitro tissue model to study keratinocyte secretion. *J Invest Dermatol* 1994;102(1):55-60.
158. Katz AB and Taichman LB. A partial catalog of proteins secreted by epidermal keratinocytes in culture. *J Invest Dermatol* 1999;112(5):818-21.
159. Chakrabarty KH, Dawson RA, Harris P, Layton C, Babu M, Gould L, Phillips J, Leigh I, Green C, Freedlander E, MacNeil S. Development of autologous human dermal-epidermal composites based on sterilized human allodermis for clinical use. *Br J Dermatol* 1999;141(5):811-23.
160. Boyce ST, Williams ML. Lipid supplemented medium induces lamellar bodies and precursors of barrier lipids in cultured analogues of human skin. *J Invest Dermatol* 1993;101(2):180-4.
161. Wainwright DJ. Use of an acellular allografts dermal matrix (AlloDerm) in the management of full-thickness burns. *Burns* 1995;21:243-8.
162. Burke JF, Yannas IV, Jr. Quinby WC, Bondoc CC, Jung WK. Successful use of a physiologically acceptable artificial skin in the treatment of extensive burn injury. *Ann Surg* 1981;194(4):413-28..
163. Burke JF. Observations on the development and clinical use of artificil skin - an attempt to employ regeneration rather than scar formation in wound healing. *Jpn J Surg* 1987;17:431-8..
164. Burke JF. The effects of the configuration of an artificial extracellular matrix on the development of a functional dermis. In: Trelstad R, ed. The role of extracellular matrix in development. New York: Liss, 1984: 351-5.
165. Yannas IV, Burke JF. Design of an artificial skin. I. Basic design principles. *J Biomed Mater Res* 1980;14:65-81.
166. Schwartz S. A new composite cultured skin product for treatment of burns and other deep dermal injuries. Bioengineering of Skin Substitutes Conference 1997, Boston.
167. Wilkine LM, Watson S, Prosky SJ, Meunier S, Parenteua NL. Development of a bilayered living skin construct for clinical applications. *Biotechnol Bioeng* 1994;43:747-56.
168. Trent JF, Kirsner RS. Tissue engineered skin: Apligraf, a bi-layered living skin equivalent. *Int J Clin Pract* 1998;52(6):408-13.
169. Boukamp P, Breitkreutz D, Stark HJ and Fusenig NE. Mesenchyme-mediated and endogenous regulation of growth and differentiation of human skin keratinocytes derived

from different body sites. *Differentiation* 1990;44:150-61.

170. Chedid M, Rubin JS, Csaky KG, Aaronson SA. Regulation of keratinocyte growth factor gene expression by interleukin 1. *J Biol Chem* 1994;269(14):10753-7.
171. Grøn B, Stoltze K, Andersson A, Dabelsteen E. Oral fibroblasts produce more HGF and KGF than skin fibroblasts in response to co-culture with keratinocytes. *APMIS* 2002;110(12):892-8.
172. Boyce ST, Kagan RJ, Yakuboff KP, Meyer NA, Rieman MT, Greenhalgh DG, Warden GD. Cultured skin substitutes reduce donor skin harvesting for closure of excised, full-thickness burns. *Ann Surg* 2002;235(2):269–79.
173. Boyce ST, Kagan RJ, Meyer NA, Yakuboff KP, Warden GD. The 1999 Clinical Research Award. Cultured skin substitutes combined with Integra Artificial Skin to replace native skin autograft and allograft for the closure of excised full-thickness burns. *J Burn Care Rehabil* 1999;20(6):453–61.
174. Boyce ST, Goretsky MJ, Greenhalgh DG, Kagan RJ, Rieman MT, Warden GD. Comparative assessment of cultured skin substitutes and native skin autograft for treatment of fullthickness burns. *Ann Surg* 1995;222(6):743–52.